ЖУРНАЛ
ПРИКЛАДНОЙ ХИМИИ

JOURNAL OF
APPLIED CHEMISTRY
OF THE USSR

(ZHURNAL PRIKLADNOI KHIMY)

IN ENGLISH TRANSLATION

VOL. 30 NO. 4

CONSULTANTS BUREAU, INC.
227 WEST 17TH STREET, NEW YORK 11, N. Y.

an agency for the interpretation of international knowledge

JOURNAL OF APPLIED CHEMISTRY OF THE U.S.S.R.

(ZHURNAL PRIKLADNOI KHIMY)

Volume 30, No. 4

April, 1957

(A Publication of the Academy of Sciences of the U.S.S.R.)

IN ENGLISH TRANSLATION

CONSULTANTS BUREAU, INC.
227 West 17th Street
New York 11, N.Y.

Printed in the United States

Annual subscription $80.00
Single issue $20.00

SIGNIFICANCE OF ABBREVIATIONS MOST FREQUENTLY ENCOUNTERED IN SOVIET PERIODICALS

FIAN	Phys. Inst. Acad. Sci. USSR.
GDI	Water Power Inst.
GITI	State Sci.-Tech. Press
GITTL	State Tech. and Theor. Lit. Press
GONTI	State United Sci.-Tech. Press
Gosenergoizdat	State Power Press
Goskhimizdat	State Chem. Press
GOST	All-Union State Standard
GTTI	State Tech. and Theor. Lit. Press
IL	Foreign Lit. Press
ISN (Izd. Sov. Nauk)	Soviet Science Press
Izd. AN SSSR	Acad. Sci. USSR Press
Izd. MGU	Moscow State Univ. Press
LEIIZhT	Leningrad Power Inst. of Railroad Engineering
LET	Leningrad Elec. Engr. School
LETI	Leningrad Electrotechnical Inst.
LETIIZhT	Leningrad Electrical Engineering Research Inst. of Railroad Engr.
Mashgiz	State Sci.-Tech. Press for Machine Construction Lit.
MEP	Ministry of Electrical Industry
MES	Ministry of Electrical Power Plants
MESEP	Ministry of Electrical Power Plants and the Electrical Industry
MGU	Moscow State Univ.
MKhTI	Moscow Inst. Chem. Tech.
MOPI	Moscow Regional Pedagogical Inst.
MSP	Ministry of Industrial Construction
NII ZVUKSZAPIOI	Scientific Research Inst. of Sound Recording
NIKFI	Sci. Inst. of Modern Motion Picture Photography
ONTI	United Sci.-Tech. Press
OTI	Division of Technical Information
OTN	Div. Tech. Sci.
Stroiizdat	Construction Press
TOE	Association of Power Engineers
TsKTI	Central Research Inst. for Boilers and Turbines
TsNIEL	Central Scientific Research Elec. Engr. Lab.
TsNIEL-MES	Central Scientific Research Elec. Engr. Lab.–Ministry of Electric Power Plants
TsVTI	Central Office of Economic Information
UF	Ural Branch
VIESKh	All-Union Inst. of Rural Elec. Power Stations
VNIIM	All-Union Scientific Research Inst. of Meteorology
VNIIZhDT	All-Union Scientific Research Inst. of Railroad Engineering
VTI	All-Union Thermotech. Inst.
VZEI	All-Union Power Correspondence Inst.

Note: Abbreviations not on this list and not explained in the translation have been transliterated, no further information about their significance being available to us. – Publisher.

A NEW TYPE OF HEAT-RESISTING GLASSES FOR CHEMICAL LABORATORY WARE

S.K. Dubrovo and Yu. A. Shmidt

Institute of Silicate Chemistry, Academy of Sciences USSR

The main requirements in laboratory ware are high chemical and thermal endurance. The commonest glass for mass-produced laboratory ware and apparatus in the Soviet Union has been glass No. 23, developed over fifty years ago by Academician V.E. Tishchenko. In recent years new types of laboratory glass – No. 29 and TsL – have replaced glass No. 23. Glass of the No. 23 type has high chemical resistance but is not highly heat-resisting.

As is known, heat-resistant ware is able to withstand considerable changes of temperature. The thermal endurance is largely determined by the coefficient of expansion. Although there is no generally accepted classification of glasses by their thermal endurance, it is possible to divide them arbitrarily into several groups on a basis of the practical behavior of wares on abrupt changes of temperature, and of the coefficients of expansion of the glasses.

The first group includes glasses of moderate thermal endurance (90–120° in tests for thin-walled ware according to GOST 3184-46) with linear expansion coefficients of $90 \cdot 10^{-7} \cdot 1$/degree in the 20–400° temperature range.

The second group comprises semi-heat resisting glasses, with higher thermal endurance of the order of 120–160°. The coefficient of expansion of these glasses is in the range of $50–65 \cdot 10^{-7} \cdot 1$/degree.

The third group includes glasses of high thermal endurance, with linear expansion coefficients of $35–50 \cdot 10^{-7} \cdot 1$/degree; thin-walled wares of such glasses must withstand temperature changes of 170–210°.

Quartz glass, and the similar quartzoid glass, have exceptional thermal endurance. Their linear coefficient of thermal expansion is less than $10 \cdot 10^{-7} \cdot 1$/degree.

Typical representatives of the first group are glasses used for making laboratory ware for routine analytical operations — No 23, No 29, TsL, and others [1]. Their composition includes 67–69% SiO_2 and 12–16% alkali oxides. They are made at temperatures of 1440–1470°, so that the partial use of low-grade fuel (peat, wood) is possible. Their softening temperature is in the range 560–590°. These glasses are relatively easy to work in the blowpipe flame without the use of oxygen.

Glasses of the second group are characterized by a higher silica content, from 72 to 76%, with a lower alkali oxide content (6–10%). Industrial glasses of this type as a rule contain 3 to 8% of boric anhydride. They must be made at higher temperatures — up to 1500°. They start to soften at 620–645°. Examples of commercial glasses of this group are glass No. 846, ampoule glass, neutral glass, Schott apparatus glasses G-20 and G-44, the Czechoslovakian "Sial" glass, and others.

The third group contains the high-silica borosilicate glasses: pyrex, Duran Resista, etc. They contain 75–82% silica, 12–14% boric anhydride, and 4–5% alkali oxides. They are made at temperatures above 1500°. Glass of the pyrex type, used for the production of laboratory ware at the "Pobeda Truda" Works, is made at 1660–1680° in order to ensure better removal of bubbles from the melt.

Quartz glass, which is a representative of the fourth group has, in addition to exceptional thermal endurance, a high softening temperature (of the order of 1600°) and high-resistance to acids. These and certain

other valuable properties of quartz glass determine its range of applications. However, the production of transparent quartz glass is still very complex and costly. Quartz glass fines badly even at temperatures above 2000° owing to its high viscosity. Laboratory ware made from quartz glass is inferior to ware made from other laboratory glasses in transparency and external appearance.

Compositions of some chemical laboratory semiheat-resisting and heat-resisting glasses are given in Table 1. The composition of the pyrex-type glass corresponds to the formulation used at the "Pobeda Truda" Works [2].

TABLE 1

Compositions of Certain Glasses

Glass	Contents (%):										
	SiO_2	B_2O_3	Al_2O_3	BaO	ZnO	CaO	MgO	Na_2O	K_2O	CaF_2	As_2O_3
"Pyrex" heat-resisting	81.0	12.0	2.26	—	—	0.3	0.6	3.4	1.0	—	—
"Duran"	74.5	14.0	3.5	3.0	—	—	—	4.5	—	—	0.3
No. 846	74.0	3.0	3.0	—	—	6.0	4.0	10.0	—	—	—
Ampoule, neutral	72.5	6.0	4.0	—	—	7.0	—	8.5	2.0	—	—
Schott G-20	76.4	8.0	4.0	4.0	—	—	—	6.5	—	0.75	0.35
Schott G-44	76.2	3.0	5.0	5.0	3.0	—	—	6.5	—	1.0	0.6
Quartz	99.95	—	0.01	—	—	0.028	0.012	0.041	—	—	—

Apart from thermal endurance, the most important physicochemical properties of laboratory glasses are chemical resistance to various reagents, crystallization tendency, softening temperature, and viscosity. We have determined these properties in a number of commercial glasses [3]. It was found that all laboratory glasses have relatively high chemical resistance to water and acid solutions. TsL glass has somewhat lower resistance to water and acids. Alkali resistance (in 2 N caustic soda solution) is worst in pyrex-type glass, while TsL glass is somewhat better than the others.

Crystallization tendency is most pronounced in heat-resisting glasses. While glasses No. 23 and No. 29 show almost no crystallization during prolonged exposure in the 700–1200° temperature range, pyrex crystallizes appreciably in this range. At 1020° a layer of crystallized glass about 0.5 mm thick is formed on its surface. The viscosity of semiheat resisting and heat-resisting glasses is considerably greater than that of the first group, which makes them difficult to work.

It is thus clear from the foregoing that there is no single universal chemical laboratory glass with all the optimum physicochemical properties.

In connection with the recent extension of the fields of application of glass in various branches of industry, in particular as a substitute for metal, investigations to find new glass compositions based on cheap and available raw materials have commenced. During the war and postwar years research has been carried out in a number of countries (Germany, Czechoslovakia, Japan, etc.) aimed at the elimination of boric anhydride from the composition of technical glasses, owing to the shortage of this material in these countries. It follows from the data presented above that boric anhydride is an indispensable constituent of most heat-resisting glasses. The role of boric anhydride in the technology of glass production, and its influence on the properties of glass, have been investigated [4, 5]. The use of boric anhydride confers favorable technological and physicochemical properties to glass. Attempts at mere replacement of boric anhydride by some other oxide do not solve the problem of creating a new glass, not inferior in properties to the original boron-containing glass. It is necessary to develop glass compositions on a new basis. Alkaline earth–aluminosilicate systems have been used for this purpose. Investigations of this type were carried out by Kalsing and Thomas on the basis of the system $CaO–MgO–Al_2O_3–SiO_2$;

the eutectic composition α-tridymite–anorthite–clinoenstatite with m.p. 1222° was used. A glass of this composition was made, containing (in %): 61.9 SiO_2, 18.5 Al_2O_3, 9.4 MgO and 10.2 CaO [6]. Other work on the development of boronless heat-resisting glasses was also largely based on compositions in the same system [7, 8]. Of other aluminosilicate systems without alkali metals, the systems BaO–MgO–Al_2O_3–SiO_2 and BaO–CaO–Al_2O_3-SiO_2 were studied. However, these investigations were not duly developed.

The glasses of this type which have been developed by various workers are a new kind of aluminosilicate glasses with a linear expansion coefficient of the order of $50 \cdot 10^{-7}$·1/degree and over in the 20–400° range, an initial softening temperature of 680–850°, and a crystallization range of 900–1250°.

Investigations carried out in various countries on aluminosilicate glasses were directed toward the development of heat-resisting and thermally durable glasses for various purposes: for high-pressure and high-voltage tubes or lamps, glass pipes, heat-resisting ware, etc. The least work was done on compositions for chemical laboratory ware. Therefore not enough attention was paid in these researches to chemical resistance, especially to acids.

The purpose of our investigation was to determine the main principles of formation of a new type of heat-resisting and chemically durable glasses, suitable for chemical laboratory ware.

EXPERIMENTAL*

Our searches for new heat-resisting glass compositions for chemical laboratory ware were based mainly on alkali-free aluminosilicate systems. We were guided in the first instance by available data on the influence of individual oxides on the expansion coefficient of glass [9]. Alkali oxides have the highest partial coefficients of expansion, while oxides of bivalent metals, especially of magnesium and zinc, have considerably lower values. Zirconium dioxide and aluminum oxide are the most effective in decreasing the coefficient of thermal expansion.

However, the development of new glass compositions cannot be based only on the selection of a suitable coefficient of expansion; it is necessary to take into account all the required technological and other physicochemical properties. Favorable glass-making properties are determined by the location of the composition in the region of low-melting eutectics on the phase diagram. Among the alkali-free aluminosilicate systems, systems containing calcium oxide have the most easily fusible eutectics. Therefore, although calcium oxide increases the coefficient of expansion more than magnesium oxide or zinc oxide, it is nevertheless a usual component of aluminosilicate glasses.

Our experiments on the synthesis and properties of alkali-free boronless aluminosilicate glasses showed that such glasses are extremely viscous and have high softening temperatures (above 700°), which makes them difficult to use for making laboratory ware. Because of this, we used calcium fluoride, and later also small amounts of alkalies, as fluxes. Special experiments were carried out to study the effects of lithium oxide and calcium fluoride on the physicochemical properties of aluminosilicate glasses. It was shown that addition of these components up to a certain limit has a favorable effect on a number of physicochemical properties of these glasses [10]. Our glass compositions were based on the system CaO–MgO–Al_2O_3–SiO_2 with additions of lithium oxide and sodium oxide (up to 2–3%), and with a part of the calcium oxide replaced by equimolar amounts of calcium fluoride. Low-boron glasses, containing 2–3% of boric anydride, were developed on the same basis.

The softening temperature, chemical resistance, and the coefficient of linear expansion in the 20–400° range were determined for all the glasses studied. The viscosity of a number of the glasses was also measured by means of an automatically recording torsion viscosimeter, and the crystallizing tendency was studied. The softening temperature was determined as the temperature at which glass rods about 2 mm in diameter and 125 mm long began to bend when heated in a muffle furnace at a rate of 1 degree per minute. The coefficient of linear expansion was determined by means of the dilatometer designed by the State Ceramic Research Institute [11]. The chemical resistance was determined mainly by the powder method, and in some cases also by the GOST method for chemical laboratory ware. The powder method was used to determine the resistance of

*S.S. Kayalova, L.A. Kuznetsov, and S.D. Spirina took part in the experimental work.

the glasses to water and acids. The acid resistance was determined from the loss in weight when 4 g of glass powder was heated with 50 ml of 1 N sulfuric acid in a quartz beaker on the water bath for 3 hours, and also from the amounts of SiO_2 and Al_2O_3, determined colorimetrically, which were dissolved in the process. The resistance to water was determined from the amount of 0.01 N HCl required for titration after 2 g of glass powder had been boiled in 50 ml of water for 1 hour. Glass powder sifted between sieves of 40 and 70 mesh, washed with alcohol to remove the dust fraction, and dried at 110°, was used for the experiments.

We had shown earlier that, if aluminum oxide is added beyond a certain limit to glassy sodium silicates, their acid resistance deteriorates [12]. This was taken into account when we were working out the compositions of the new aluminosilicate glasses: their silica contents were at least seven times their alumina contents (calculated as molecular percentages).

The glasses were first made in small lots (200 g) from active materials in platinum crucibles, and their physicochemical properties were then studied. The glasses with the best properties were tested in large-scale meltings (in 3-liter and 100-liter pots). The following raw materials were used for the latter experiments: silver sand or marshalite, hydrated alumina, magnesium oxide, fluorspar, soda, and spodumene concentrate, used for introducing lithium oxide, which contained 4–4.2% Li_2O.

The starting glass in these experiments was glass T-7 of the following composition (in mole %): SiO_2 71, Al_2O_3 10, CaO 4, CaF_2 7, MgO 6, Li_2O 2. This was used as the basis for other compositions, by variations of the $CaO-CaF_2$ ratio, replacement of part of the lithium oxide by sodium oxide, or addition of boric oxide in place of some of the alumina or calcium fluoride. This gave rise to a series of heat-resisting aluminosilicate glasses. The compositions of some of these glasses, presenting the greatest interest from the point of view of practical utilization, are given in Table 2.

TABLE 2

Compositions of Heat-Resisting Aluminosilicate Glasses

Components	Composition by synthesis (in molar %) of glasses					
	T-7	T-16$_1$	T-16$_2$	T-12	T-31	T-28
SiO_2 . . .	71	71	71	71	71	72
Al_2O_3 . . .	10	10	9	8	9	9
B_2O_3 . . .	—	—	—	3	2	3
CaO	4	4	6	8	6	5
CaF_2 . . .	7	7	5	2	4	4
MgO . . .	6	6	6	6	6	4
Na_2O . . .	—	1	2	—	—	1
Li_2O . . .	2	1	1	2	2	2

Glasses T-7 and T-31 were melted in 3-liter pots at 1480–1490° for 14–16 hours after the batch had been put in. Glasses T-16$_1$ and T-12 were melted in 100-liter fireclay pots at the same temperatures. These meltings were continued for 20-22 hours. Glasses T-16$_1$ and T-12 were used for making a few pieces of experimental ware: flasks and crucibles. Trial meltings of glasses T-16$_2$ and T-28 were carried out in a small tank furnace, 2.5 tons in capacity, at the "Pobeda Truda" Works, and an experimental batch of ware was made. Tables 3 and 4 give the physicochemical properties of these glasses and of "Pyrex" glass. The data show that our aluminosilicate glasses have higher softening temperatures than pyrex glass. They are somewhat inferior to pyrex in heat resistance, but nevertheless, as they have a coefficient of expansion less than $50 \cdot 10^{-7}$ 1/degree in the 20–400° range, these aluminosilicate glasses can be classified as having high heat resistance. This was confirmed in thermal endurance tests of a large number of the experimental pieces by GOST standards for pyrex glass, and also by trials of their use in various chemical laboratories. The aluminosilicate glasses are not inferior to pyrex in chemical resistance. In comparison with borosilicate glasses, of which pyrex is a typical representative, aluminosilicate glasses show peculiar changes of viscosity with temperature. In the high-temperature region they have a considerably

TABLE 3

Physicochemical Properties of Aluminosilicate Glasses

Properties studied	Glasses						
	7-7	T-16$_1$	T-16$_2$	T-12	T-31	T-28	"Pyrex"
Softening temperature (in degrees)	660	680	680	680	670	645	620
Cofficient of linear expansion $\alpha \cdot 10^{-7}$	44.6	45.6	50.4	44.2	43.6	46.3	36.0
Density	2.474	2.497	—	2.455	—	2.41	2.25
Chemical resistance by the powder method							
Acid resistance (in 1 N H_2SO_4)							
weight loss (in mg)	2.0	2.4	—	—	1.9	1.6	—
mg SiO_2 in solution	0.81	0.90	—	0.69	0.66	0.6	—
mg Al_2O_3 in solution	1.03	1.5	—	1.9	0.99	0.75	—
Water resistance (in ml 0.01 N HCl)	—	0.02	—	0.14	0.11	0.16	—
Chemical resistance by GOST (weight loss in mg/100 cm^2) on boiling:							
in distilled water	—	0.7—0.9	0.6—0.9	0.2	—	0.4	0.5—1.0
in 1 N H_2SO_4	—	0.7	0.5—1.0	0.4	0.8	0.3—0.6	0.3—0.5
in 2 N NaOH	73—75	—	75—79	88	86	79—83	89—93

TABLE 4

Viscosities of Glasses in Poises

Temperature (degree)	Glasses						
	T-7	T-16$_1$	T-16$_2$	T-12	T-31	T-28	"Pyrex"
1480	425	437	380	450	—	540	740
1460	515	538	445	570	630	630	870
1400	870	978	615	1050	1000	1080	1450
1360	1340	1520	1050	1660	1480	1550	2050
1300	2700	3170	1890	3240	2950	3100	3480
1260	4360	5250	3170	5250	4900	4900	5130
1200	9770	12600	7250	12400	12300	10800	10300
1180	13200	17400	9780	17800	17000	14200	13500
1160	17800	24000	13900	—	23400	19100	18200

lower viscosity than pyrex but at relatively low temperature their viscosity rises more rapidly than that of pyrex. This makes the production melting of aluminosilicate glasses easier, but hinders working in the blowpipe flame.

In addition to the above properties, the crystallization tendency of the aluminosilicate glasses and of pyrex glass was determined in a temperature-gradient furnace in the 750—1300° range during 6-hour exposures. The following results were obtained: in glasses T-12 and T-28 the start of crystallization in the form of a weak surface film is found at 850—870°. In the 950—1150° range the film thickens to 0.1—0.2 mm, after which it becomes scarcely noticeable. At 1180° and upward the glass has a bright surface. Glasses with high

fluorine contents (T-7, T-16, etc.) become opalescent in the 725–750° range, but above 1180° they are quite transparent. The crystallization tendency of pyrex glass can be described as follows: from 650° a crystalline film appears on the surface of the specimen; this attains a thickness of ~0.5 mm in the 700–1020° range, after which the thickness of the film decreases up to 1130°; in the 1130–1280° range the film becomes scarcely noticeable, and above 1280° the glass is quite transparent. Thus, pyrex glass crystallizes over a wider temperature range then the aluminosilicate glasses described above.

Comparison of the physicochemical properties of our aluminosilicate glasses with the properties of pyrex borosilicate glass leads to the following conclusion. Low-alkali boronless or low-boron aluminosilicate glasses belong to the highly heat-resisting class. They are not inferior to pyrex glass in chemical resistance. The viscosity variations of aluminosilicate glasses with temperature indicate that these glasses may be made and worked into ware under the same conditions as pyrex glass; this was confirmed in large-scale trials with glasses T-16 and T-28.

Aluminosilicate glasses cannot yet replace pyrex glass for apparatus. However, they are quite suitable as substitutes for pyrex for production of various articles which do not require repeated working in the blowpipe flame, such as flasks, beakers, etc.

SUMMARY

Aluminosilicate glasses based on the system $CaO-MgO-Al_2O_3-SiO_2$, with calcium fluoride and up to 3 molar% of alkali oxides (sodium oxide and lithium oxide) as fluxes, have softening temperatures between 645 and 680°, linear expansion coefficients of $44-50\cdot10^{-7}$.1/degree in the 20–400° range, and crystallize in the 800–1200° temperature range.

These glasses have high chemical resistance, which conforms to the requirements for glasses used for the production of chemical laboratory glassware.

LITERATURE CITED

[1] V.D. Shevlyagin, Factory Labs. 20, 4, 507 (1954).

[2] A.S. Pryanishnikov, Glass and Ceramics 7, 11, 10 (1950).

[3] S.K. Dubrovo, S.S. Kayalova, and Yu. A. Shmidt, Glass and Ceramics 12, 10, 9 (1955).

[4] W.A. Weyl, Glass Industry 29, 3–11 (1948).

[5] N.N. Kachalov, K.S. Evstropiev et al., Glass and Ceramics 11, 7, 20 (1954).

[6] H. Kalsing, M. Thomas, Glasstechn. Ber., 18, 8, 210 (1940).

[7] N.M. Pavlushkin, Glass and Ceramics 11, 3, 10 (1954).

[8] LE. Shapiro, Sci.-Tech. Bull. Inst. Glass 7–8, 24 (1953).

[9] A.A.Appen, J. Appl. Chem. 28, 2, 121 (1954).

[10] S.K. Dubrovo and Yu. A. Shmidt, J. Appl. Chem. 29, 4, 557 (1956).*

[11] A.A. Appen, Doctorate Dissertation (Leningrad, 1953).

[12] S.K. Dubrovo, Bull. Acad. Sci. USSR, Div. Chem. Sci. 2, 244 (1954).*

Received March 23, 1956

*Original Russian pagination. See C.B. Translation.

THE MECHANISM OF SILICATE SCALE FORMATION

M.S. Ostrikov and V.G. Gleim

State University, Rostov-on-Don and Institute of Railroad Transport Engineers

During the spring and summer seasons, instances of warping (bulging) of locomotive boiler walls occur in some water supply regions. This effect, which is very harmful to the transport economy, is usually associated with the presence of stable clay suspensions in the boiler feed water. The boiler walls are found to be coated with a very dense layer of silicate scale, which reduces heat transfer and creates favorable conditions for breakdowns and overheating.

It was thought that formation of this scale involves silicic acid, formed in the aqueous medium in a state of true solution and colloidal dispersion by hydrolysis of the silicate suspensions. The object of the experimental investigation described below was to study the kinetics of silicic acid formation in systems similar to boiler water, and its sorption of aluminum and iron hydroxides.

It should be pointed out that the whole question of silicic acid in aqueous media is of special importance at the present time in connection with the problem of silica removal from feed waters [1 - 5] and the role of silicic acid in clarification of natural waters [6].

EXPERIMENTAL

Formation of silicic acid from clay suspensions. In order to simulate operating conditions, all the experiments were carried out in steel beakers (height 12 cm, diameter 5 cm, and wall thickness 1 mm) cut from the fire tube of a locomotive boiler.

Experiments with Chasov Yar kaolin which had been carefully washed free from electrolytes and suspended in distilled and in river water showed that no appreciable amounts of silicic acid were formed in solution at room temperature, even on prolonged standing. On the other hand, if the suspensions were boiled, silicic acid always appeared in detectable amounts within an hour, and the amount increased with time. Curves for the variations of the amount of silicic acid with boiling time and with the amount of suspended purified kaolin show a regularity, with the amount of silicic acid tending to a limit. It follows from these results that clay is the actual source of silicic acid and that the temperature is the most important factor.

When the solutions are cooled to room temperature, the silicic acid disappears almost entirely, but reappears in increasing amounts when boiling is resumed.

The subsequent experiments were carried out with clays taken from the water supply settling tanks, from the river shore, and from the river bottom. The results were all in good agreement, irrespective of the origin of the clay.

Figure 1 shows that the silicic acid content of the aqueous medium increases steadily during boiling. The accumulation of silicic acid is more rapid with higher clay contents and with more rapid approach of the systems to equilibrium. Curves 1, 2, 3 and 4, represent aqueous suspensions containing 0.15, 0.5, 0.8, and 1.5% of clay respectively.

Data for the variation of the silicic acid concentration in the solution after 4 hours of boiling, as a function of the amount of clay in the suspension are given in Fig. 2. This clearly confirms the tendency of the systems to reach equilibrium during boiling.

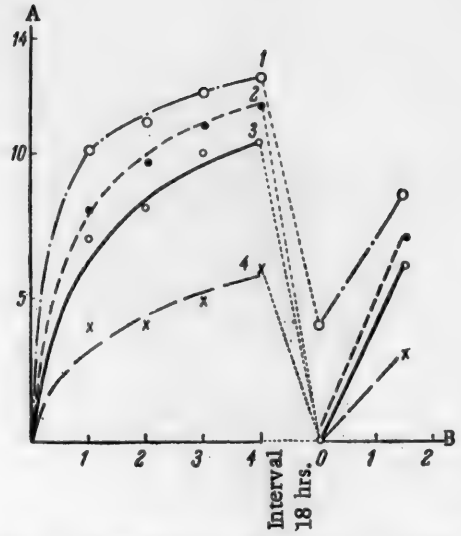

Fig. 1. Accumulation of silicic acid in solutions during boiling of river water with different clay contents.
A) SiO_2 content (in mg/liter), B) time (hours).
Clay contents (in %): 1) 1.5, 2) 0.8, 3) 0.5, 4) 0.15.

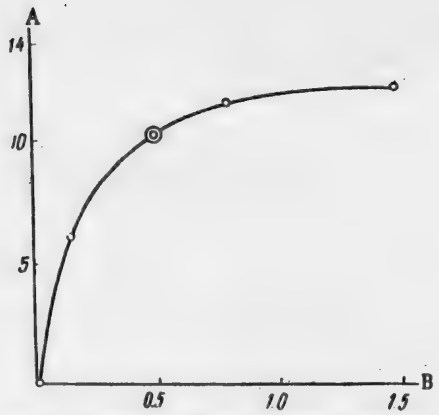

Fig. 2. Variation of the amount of silicic acid accumulated in solution with silicate suspension (clay) content, after 4 hours of boiling.
A) SiO_2 content (in mg/liter),
B) clay content (in %).

The subsequent experiments were carried out with a constant clay content, 0.5%. Significance of this amount of clay is seen from the position of the corresponding point marked by a large circle in Fig. 2. The suspensions were made from river water and clay taken from the bottom of the water supply settling tank.

Effect of an alkaline medium. From the practical standpoint it was of considerable interest to study the the effects of small amounts of caustic soda and sodium carbonate on the formation of silicic acid from clay on boiling. Parallel comparative experiments were carried out with the following 0.5% suspensions: control, without alkali; with 100 mg NaOH per liter; and with 100 mg NaOH and 100 mg Na_2CO_3 per liter. The results illustrated in Fig. 3 indicate that the amount of silicic acid formed in solution increases considerably in presence of alkali.

It should be noted that in suspensions 2 and 3, in contrast to the control suspension 1, the amount of silicic acid did not fall to zero after cooling and an interval of 18 hours.

The nature of the effect of alkali on the process may be judged from the pH decrease in the systems during boiling.

It is evident that this action of an alkaline medium in working boilers may play a very important part in the accumulation of dissolved silicic acid, as boiler water always contains certain amounts of sludge with highly dispersed clay silicates.

Under certain conditions silicic acid may be deposited on the boiler walls in the form of silicates, such as magnesium silicate [7], or it may serve as a cementing material for settling particles of a different composition. The silicic acid and the silicates formed from it first pass into the colloidal state, and are then coagulated on the heated boiler wall surfaces.

It seems likely that a high boiler wall temperature plays an important part in the mechanism of the coagulative accumulation of these colloidal products. When a sol particle collides with the heated surface, the parts of the stabilizing hydrate and ionic diffuse layers facing the latter disintegrate (by a kind of "melting"). The exposed part of the colloidal particle surface can then come into direct contact with the heated boiler wall and adhere to it as the result of collision in the course of its thermal motion. Under certain conditions this unilateral action on the particle may cause the rest of the solvate layer of the micelle to act as a factor favoring even closer contact. This interpretation may be applied to a number of other effects in analogous conditions.

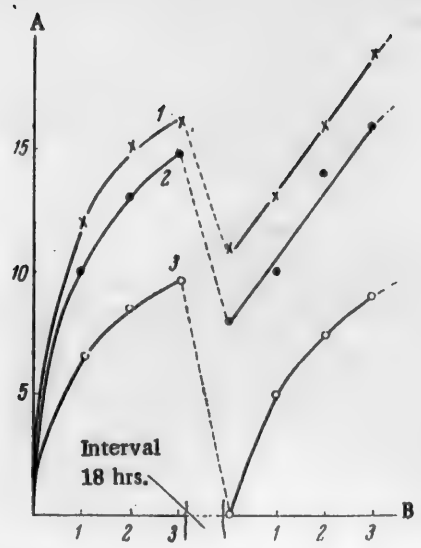

Fig. 3. Effect of caustic soda on the rate of accumulation of silicic acid in the aqueous medium during boiling of 0.5% clay suspensions with additions of alkali.
A) SiO_2 content (in mg/liter), B) boiling time (hours). NaOH contents (in mg/liter): 1) 100 + 100 Na_2CO_3, 2) 100, 3) without alkali (control).

It was thought that this process might be prevented by the use of readily available sorbents which could remove, physically or chemically, as much silicic acid as possible from the solution. All the experiments described below were carried out in order to examine this possibility.

Sorption of silicic acid by aluminum and ferric hydroxides. Hydrolyzing aluminum salts are used most widely for clarification of natural waters. It was therefore appropriate to investigate aluminum hydroxide as a sorbent for silicic acid. The hydroxide was prepared by precipitation with soda from potash alum solution, and used in the moist state after being washed to remove SO''_4 ions.

The suspensions were boiled in steel beakers, with addition of boiling distilled water to make up for evaporation losses. Aluminum hydroxide was added in amounts from 0.01 to 0.2% to suspensions containing 5% clay, 50 mg/liter NaOH, and 50 mg/liter Na_2CO_3. It was found that the amount of silicic acid taken up by aluminum hydroxide from boiling solutions increases with the amount of sorbent used.

When the boiled systems were left to stand in the cold, silicic acid was entirely absent in the solutions containing 0.1 and 0.2% sorbent. However, when the boiling was recommenced, the silicic acid reappeared in increasing amounts. Some of the results of these experiments, relating to systems boiled for 4 hours, are given in Fig. 4, Curve 1, which shows the decrease of silicic acid concentration with increasing amounts of aluminum hydroxide added as sorbent.

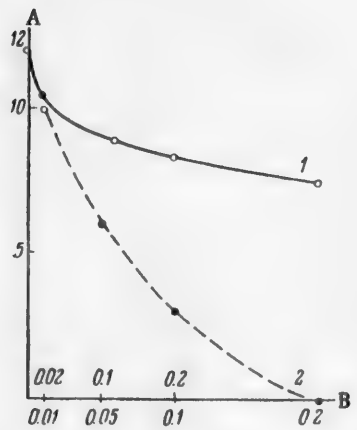

Fig. 4. Variation of the amount of silicic acid remaining in solution with the amount of sorbent.
A) SiO_2 content (in mg/liter), B) content of sorbent (in %). Curves: 1) for $Al(OH)_3$, 2) for $Fe(OH)_3$.

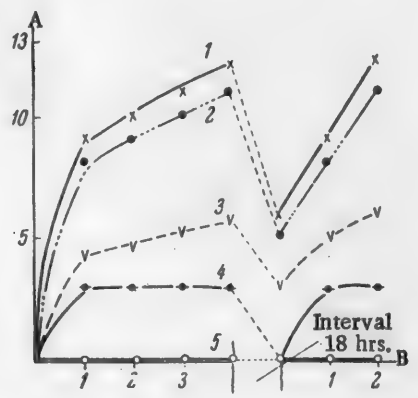

Fig. 5. Effect of $Fe(OH)_3$ as sorbent.
A) SiO_2 content (in mg/liter), B) boiling time (hours). $Fe(OH)_3$ contents (in %): 1) 0, 2) 0.02, 3) 0.1, 4) 0.2, 5) 0.4.

The same suspensions were used for testing the effects of magnesium sulfate and magnesium hydroxide as additives for silica removal from water. Here again the silicic acid concentration in the solutions clearly decreased, and the curves were of the same characteristic form, but the silica-removing effect was less.

The highest sorptive capacity was found for ferric hydroxide, which was added in the form of freshly prepared and throughly washed moist precipitate. The results of these experiments are given in Fig. 5 in the form of curves representing the different increases of silicic acid content during boiling in presence of different amounts of added $Fe(OH)_3$.

In systems containing 0.4% ferric hydroxide, silicic acid is completely removed from solution and its appearance on boiling is prevented. In systems with additions of 0.2% $Fe(OH)_3$ if silicic acid is formed at all, the amount is very small, and does not increase on prolonged boiling but falls to zero on cooling. These results show good reproducibility if the experiments are repeated. Curve 2, Fig. 4, represents the variations of the amount of silicic acid remaining on solution (after 4 hours of boiling) with the amount of ferric hydroxide used as sorbent. Comparison of these results with the results for $Al(OH)_3$, discussed above and plotted in the same Fig. 4 (Curve 1) shows that ferric hydroxide is greatly preferable as sorbent for silicic acid. It is quite possible that ferric hydroxide is important not only as a sorbent for silicic acid. Its highly dispersed colloidal fraction may coagulate on the surface of the clay silicate particles to form a protective film which prevents further silicate hydrolysis. This may explain why in the systems containing 0.2% of ferric hydroxide the amount of silicic acid in solution does not increase on prolonged boiling.

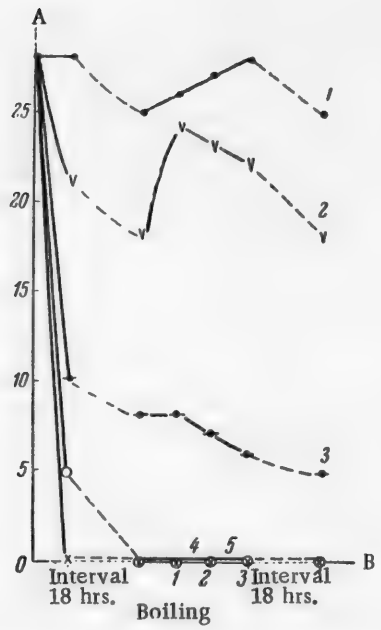

Fig. 6. Variation of silicate ion concentration with time of boiling of suspensions containing various amounts of $Fe(OH)_3$ as sorbent. Experiments in quartz flasks. A) SiO_2 content (in mg/liter), B) boiling time (hours). $Fe(OH)_3$ contents (in %): 1) 0, 2) 0.02, 3) 0.1, 4) 0.2, 5) 0.4

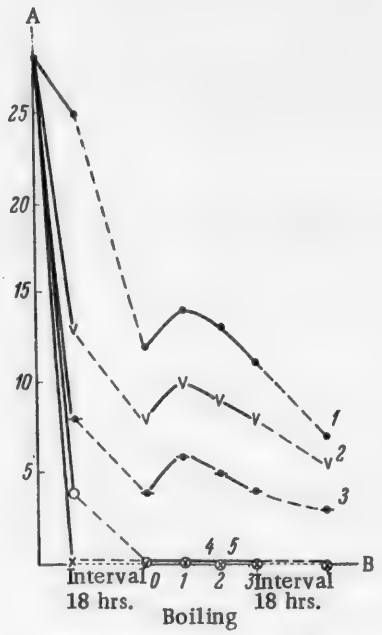

Fig. 7. Designations as in Fig. 6. Experiments in steel beakers.

In view of the possibility of using metallurgical wastes for the production of technical ferric hydroxide, these results suggest that this sorbent is quite suitable as a simple and cheap means for removal of silica from water.

The high and stable sorption capacity which was found in ferric hydroxide first of all accounts for the formation of silicate scale on boiler walls. If the wall surface becomes covered with a fairly dense, even if

thin, layer of silicate scale, its further accumulation is retarded, as the factor of the reaction of silicic acid with ferric hydroxide gradually loses its significance owing to the shielding of the boiler walls.

In order to determine the extent to which the steel beaker walls are involved in the sorption of silicic acid, parallel experiments were carried out in steel beakers and quartz flasks with sodium silicate solution (28 mg/liter) containing the same amounts of ferric hydroxide (from 0.02 to 0.4%) as before.

The results of these experiments are given in Fig. 6 for systems in quartz flasks, and in Fig. 7 for systems in steel beakers.

Comparison of these results reveals significant differences only between the curves (Fig. 6) for small amounts of sorbent. In the presence of 0.2% ferric hydroxide the influence of the walls is only slight, and is manifested only during the first stages of boiling. The distinction disappears entirely in systems with 0.4% sorbent.

It is interesting to note that in systems with smaller amounts of sorbent the amount of silicic acid rises during the first hour when boiling is renewed after an interval, and then begins to fall regularly. It seems likely that two sorption mechanisms operate here: chemical (irreversible), and physical (reversible). The latter prevails in the cold systems.

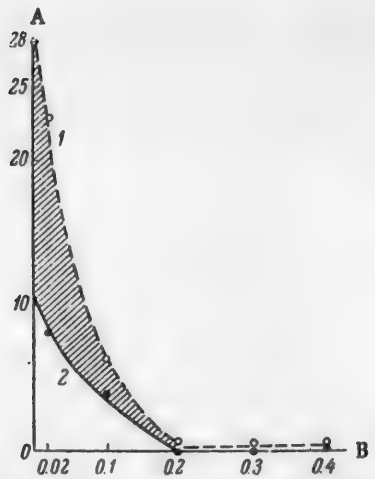

Fig. 8. Variation of silicate ion concentration with the amount of added sorbent.
A) SiO_2 content (in mg/liter), B) content of $Fe(OH)_3$ sorbent (in %). For systems: 1) in quartz flasks, and 2) in steel beakers.

Variations of silicic acid concentration with the amount of sorbent added in systems boiled 3 hours (after an interval of 18 hours) in quartz flasks and steel beakers are plotted in Fig. 8.

It is seen that the divergence between the curves in the region of low sorbent contents gradually diminishes with increasing amount of sorbent. The two curves meet strictly in one point on the abscissa axis. This shows that the effect of the vessel walls can be reduced to zero in this way. Evidently this role of the glass beaker walls (or of the boiler walls) is determined, at a given temperature, by the quantitative ratios between the true adsorbent surface and wall area on the one hand, and the amount of silicic acid or of the silicate suspension acting as the source of it, on the other.

In order to study these relationships in conditions of continuous formation of silicic acid from silicate suspensions on boiling, the same 0.5% clay suspensions with alkaline additions (50 mg NaOH and 50 mg Na_2CO_3 per liter) were boiled simultaneously with different amounts of ferric hydroxide in quartz flasks and steel beakers (the latter were cleaned internally with a steel brush to remove rust and scale before each experiment).

The results for systems in quartz flasks are given in Fig. 9, and for steel beakers, in Fig. 10.

The curves in these two figures are of the same nature as before but, as in the previous experiment, the influence of the steel vessel walls is very pronounced, and again only in systems with low sorbent contents.

Variations of the silicic acid content with the amount of sorbent, after 3 hours of boiling in quartz flasks (Curve 1) and in steel beakers (Curve 2) are plotted in Fig. 11. The two curves meet at a point in the abscissa axis corresponding to 0.4% $Fe(OH)_3$, where the influence of the walls is completely suppressed by the sorbent.

In the next experiments the sorption of silicate ions from sodium silicate solutions by ferric and aluminum hydroxides without heat (i.e., at room temperature) during prolonged periods was studied. The experiments were performed simultaneously in steel beakers and quartz flasks, as before. Some of the results, representing the state of the systems after 42 hours, are given in Fig. 12 in the form of plots of the amount of H_2SiO_3 in solution against the amount of sorbent.

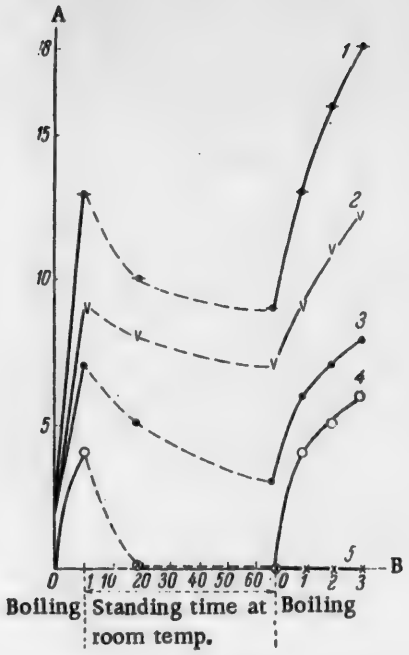

Fig. 9. Effect of $Fe(OH)_3$ sorbent on the yield of dissolved silicic acid in boiling clay suspensions. Experiments in quartz flasks.
A) SiO_2 contents (in mg/liter), B) boiling time (hours). $Fe(OH)_3$ contents (in %): 1) 0, 2) 0.02, 3) 0.1, 4) 0.2, 5) 0.4.

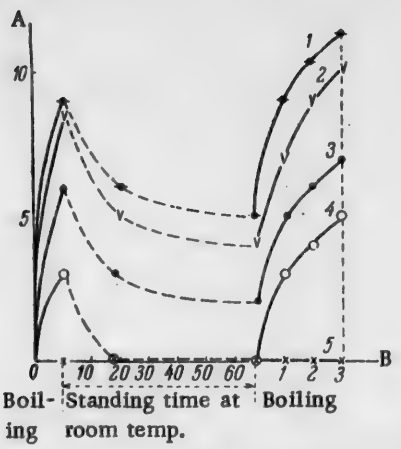

Fig. 10. As in Fig. 9, with the same designations. Experiments in steel beakers.

These results show that, in contrast to the effects found at the boiling point, ferric hydroxide in this case has a considerably lower sorbent power than aluminum hydroxide. However, on further interaction (up to 115 hours) the difference in favor of aluminum hydroxide disappears almost entirely.

This positive influence of increased temperatures on the sorption capacity of ferric hydroxide must be regarded as indicating that the sorption process in this instance is an example of activated adsorption.

From all the foregoing experimental results it may be concluded that silicic acid, formed by the action of water on highly dispersed silicate suspensions in systems of the type of boiler water, gradually accumulates at relatively high temperatures and elevated pressures in the form of true solutions, which then pass into colloidal solutions. This process depends on the temperature, the pH of the medium, and the compositions of the suspension and system. In these conditions new silicate compounds are gradually formed, and these are deposited together with silicic acid on the boiler walls, as stated above.

The following general conclusions may be drawn from the above results. Silicic acid in an aqueous medium behaves as a semicolloid. Most of it is present in the undissociated state in the form of microaggregates of various sizes down to molecular, and a little is present in the ionized state. The equilibrium is shifted (reversibly) in the direction of ionization with increase of temperature, and is influenced by the pH. Confirmation of this is provided by the well-known method of silicate block production by hydrothermal treatment of a mixture of quartz sand and lime [8, 9], and in particular from mixtures of clay and lime [10].

This also accounts for the high contents of silicic acid in hot springs (at pH values close to 7), and for the formation of tuff deposits of the so-called "geyserite." At great depths and at high temperatures and pressures, the water which penetrates through cracks hydrolyzes silicates with formation of free silicic acid, which passes into solution. These solutions are in a state of supersaturation when ejected to the surface, and colloidal silicic acid is therefore precipitated. It is also quite likely that weak solutions of silicic acid, soil waters, play a very considerable part in the processes taking place in the layers of sedimentary rocks through which they migrate.

It is interesting to note that the laterite soils typical of the tropics are devoid of silicic acid, apart from residual quartz. In high temperature and humidity conditions the matrix aluminosilicates are hydrolyzed more rapidly and completely, and the silicic acid, which does not have time to form aqueous silicates (such as are formed in temperate climatic conditions), is leached out, leaving only the hydroxides. Probably the origin of laterites and bauxites themselves can be explained in this way.

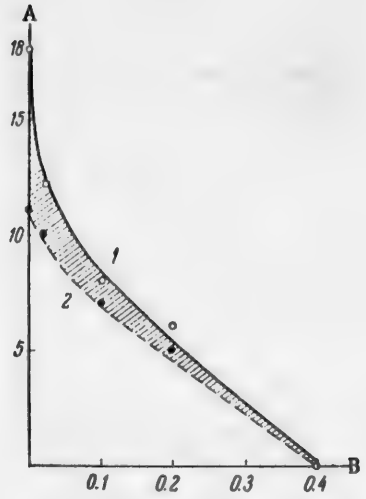

Fig. 11. Variations of the silicic acid yield in solutions with the amount of sorbent. Experiments with the usual suspensions.
A) SiO_2 content (in mg/liter), B) sorbent content (in %). 1) In quartz flasks, 2) in steel beakers.

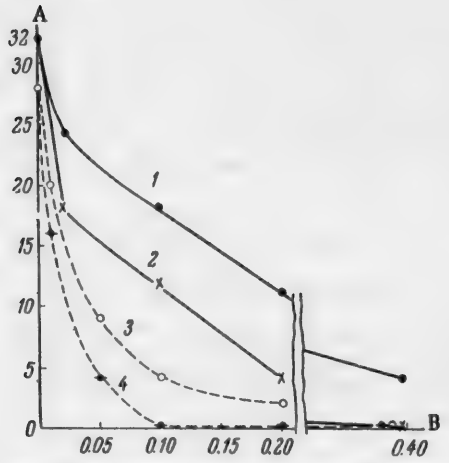

Fig. 12. Variations of the silicate ion concentration with the standing time of systems at room temperature in quartz flasks (1.3) and steel beakers (2.4).
A) SiO_2 content (in mg/liter), B) contents of $Al(OH)_3$ and $Fe(OH)_3$ (in %). Sorbents: 1), 2) $Fe(OH)_3$; 3), 4) $Al(OH)_3$.

SUMMARY

1. It has been shown in a study of the kinetics of formation of dissolved silicic acid from purified kaolin and native clays when their suspensions are boiled that as these systems are cooled their silicic acid contents gradually fall to the initial level.

2. The relationship between the accumulation of silicic acid in solution and the amount of highly dispersed silicate suspensions has been determined and it is shown that the former tends to a limit, which is raised by the presence of small amounts of alkali, which are usually present in boiler water.

3. The sorption of silicic acid from solution by aluminum and ferric hydroxide has been studied in relation to the contents of the latter and the boiling time. It was found that ferric hydroxide is considerably better as a sorbent; it extracts silicic acid completely or prevents its appearance in the solution. The fact that increase of temperature has a positive influence on this process indicates that it is chemisorptive in character.

4. A mechanism is suggested for the adhesion of colloidal particles to the surface of the heated boiler walls in scale formation.

5. The participation of the walls of the steel vessels used for the experiments on the sorption of silicic acid has been investigated. The conditions in which this effect is completely suppressed by additions of ferric hydroxide as a sorbent have been determined.

6. It is concluded from the experimental results that ferric hydroxide can be used for removal of silica from water at elevated temperatures.

7. The sorption of silicic acid from solutions by aluminum and ferric hydroxide during 42 hours at room temperature has been studied. In these conditions aluminum hydroxide is the better sorbent.

LITERATURE CITED

[1] M.S. Shkrob, Water Treatment (1950) pp.351-360.*

[2] L.A. Kulsky, Chemistry and Technology of Water Treatment (1954).*

[3] V.M. Kvyatkovsky and L.M. Zhivilova, Bull. All-Union Heat Engineering Inst. 6 and 10 (1951).

[4] A.M. Spiridonova, Bull. All-Union Heat Engineering Inst. 9 (1951).

[5] A.M. Prokhorova, Ibid., 4, 1 (1953).

[6] J.R. Baylis, Water and Sewerage, 83, 469, (1936).*

[7] L.A. Kulsky, A.M. Koganovsky, I.G. Gornovsky, and M.V. Shevchenko, Physicochemical Principles of Water Purification by Coagulation (1950).*

[8] A. Volzhensky, Hydrothermal Treatment of Building Materials (1944).*

[9] I.P. Gvozdarev, Production of Silicate Blocks (1951).*

[10] N.P. Remezov, Soils, their Properties and Distribution (1952).*

Received March 28, 1955

* In Russian.

STUDY OF THE CONDITIONS OF STRONTIUM SILICATE FORMATION

V.B. Glushkova and E.K. Keler

Institute of Silicate Chemistry, Academy of Sciences USSR

Silicates of the alkaline earth elements are extensively used in many branches of chemical industry. There have been many investigations of calcium, magnesium, and barium silicates. There are also published papers on strontium silicate, but these mainly deal either with the phase diagram for the system $SrO - SiO_2$, or with the preparation of individual silicates from the melt and studies of their properties.

In 1922 Eskola [1] determined the phase diagram for the $SrO - SiO_2$ system. Only two chemical compounds were found in the system: the orthosilicate Sr_2SiO_4 and the metasilicate $SrSiO_3$. Phase diagrams for compositions with high SiO_2 contents were also studied by Greig [2] and Olshansky [3]. Reports of the preparation of strontium ortho- and metasilicates are found in papers by Stein [4], Wallace [5], Jander and Wuhrer [6], and Jander and Klooster [7]. The densities [4, 8], melting points [1, 4], heats of formation [8, 9], optical properties [1, 10], and x-ray diffraction patterns [10, 11] of these compounds have been determined. However, there are considerable discrepancies between the results of different authors.

In 1952 Nurse [12] obtained a new silicate of strontium, Sr_3SiO_5, and studied its crystallographic optical properties.

No information is available in the literature as to how and under what conditions strontium silicates are formed in the solid phase.

The purpose of the present investigation was to study the interaction of strontium oxide and silica on heating, in mixtures with different proportions of the reacting oxides.

The mixtures were made from strontium carbonate, and amorphous silica previously heated at 1400°. Silicate formation was studied both when the temperature was raised uniformly, and in mixtures held at various temperatures, up to 1400°, for 4 hours. Mixtures corresponding to the known strontium compounds (Sr_3SiO_5, Sr_2SiO_4 and $SrSiO_3$) were studied, and also mixtures of the following compositions (in molar %):

$80SrCO_3 + 20SiO_2$, $60SrCO_3 + 40SiO_2$, $40SrCO_3 + 60SiO_2$, $33.3SrCO_3 + 66.7SiO_2$,

$20SrCO_3 + 80SiO_2$, $10SrCO_3 + 90SiO_2$.

Pure silicates of the compositions Sr_3SiO_5, Sr_2SiO_4 and $SrSiO_3$ were synthesized. The x-ray diffraction patterns of these compounds, and also of SiO_2, $SrCO_{3\,orthorhombic}$, and $SrCO_{3\,hexagonal}$ (the low- and high-temperature modifications of strontium carbonate) were obtained, for interpretation of the x-ray patterns for the oxide mixtures heated to different temperatures.

EXPERIMENTAL

Methods of investigation. a)Combined thermal analysis was carried out by means of the apparatus designed by Keler and Kuznetsov [13, 14]. The combined thermal analysis apparatus is used for simultaneous determinations of temperature, heat effects (differential thermal analysis), weight changes (weight loss), and volume (shrinkage) of the test specimen in absolutely identical conditions. The materials to be investigated were molded into cylindrical specimens 33 mm high and 12 mm in diameter, under a pressure of 460 kg/cm^2. The rate of temperature increase was the same in all the experiments, 6 - 7 degrees/minute.

The x-ray structure analysis was carried out by the powder method with copper radiation ($Cu_{k\alpha}$ = 1.542 A). The photographs were taken both at room temperature (in RKD cameras) after quenching of the specimens, and

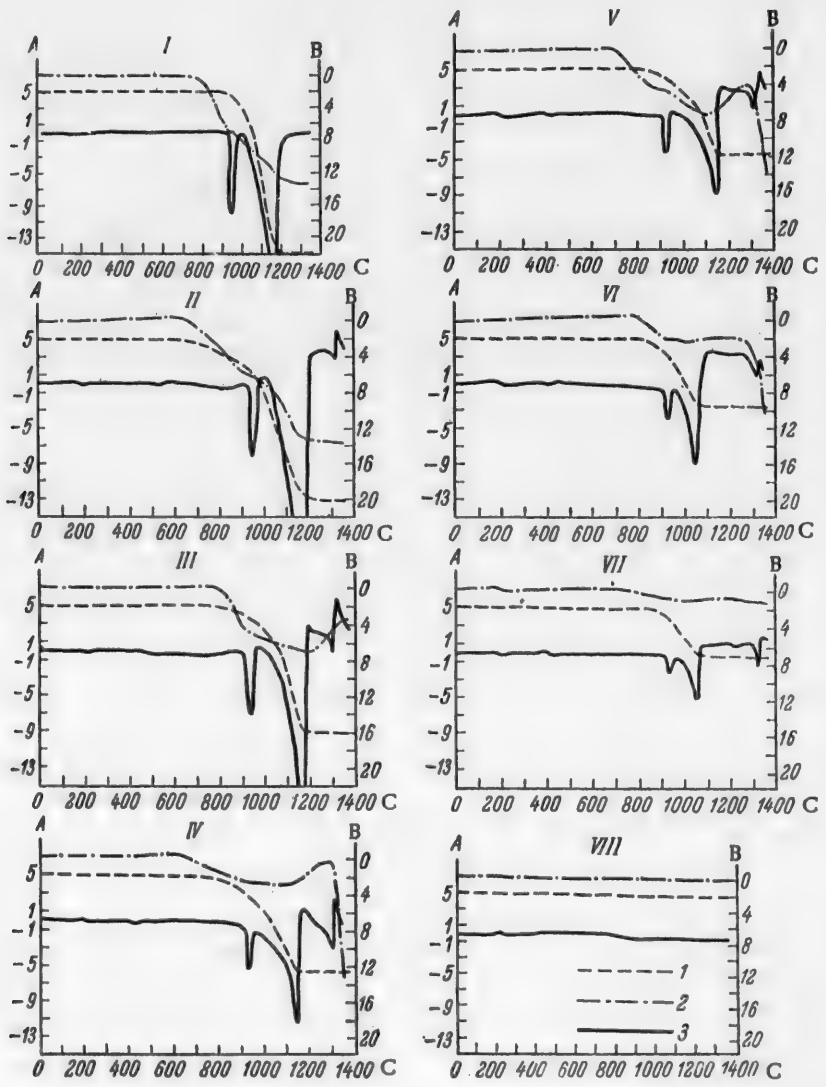

Fig. 1. Heating curves for mixtures made from strontium carbonate and silica. A) Temperature difference between specimen and standard (in arbitrary units), B) changes in weight and length of the specimen (in arbitrary units), C) temperature (in degrees). I) 100% $SrCO_3$, II) 80% $SrCO_3$ + 20% SiO_2, III) 60% $SrCO_3$ + 40% SiO_2, IV) 40% $SrCO_3$ + 60% SiO_2, V) 33% $SrCO_3$ + 67% CiO_2, VI) 20% $SrCO_3$ + 80% SiO_2, VII) 10% $SrCO_3$ + 90% SiO_2, VIII) 100% SiO_2. Weight changes 1 and volume changes 2 with the temperature 3—differential recordings of the thermal effects.

during heating (up to 1400°) in a high-temperature ionization x-ray unit. The principal lines for the strontium compounds, used for the semiquantitative interpretation of the x-ray patterns, are given below:

SrO	$SrCO_3$ rhomb.	$SrCO_3$ hex.	$SrSiO_3$	Sr_2SiO_4	Sr_3SiO_5
2.97	3.53	3.67	3. 57	3.293	2.900
2.58	2.45	3.61	2. 93	2. 85	2.337
1.82	2.05	2.11	2. 06	2. 29	1.808
1.55	1.98	–	1.914	2. 04	1.661

Chemical analysis. The following were determined in the course of the chemical phase analysis: free strontium oxide (by the ethyl glycerate method [15], CO_2 (by gas analysis), SrO combined as strontium metasilicate, unreacted SiO_2, and total amounts of SiO_2 and SrO in the mixture (by the method developed by Jander and Wuhrer [6]).

Preparation and properties of pure strontium compounds. Strontium ortho- and metasilicate were prepared by heating of mixtures of $SrCO_3$ and SiO_2 of the appropriate compositions at 1350° for 180 hours, while tristrontium silicate was prepared by heating at 1400°. After every 50 hours of heating the mixtures were reground, mixed, and heated again until homogeneous products were obtained. The reactions were tested for completion by chemical phase analysis.

Heating curves were plotted for all the strontium compounds. No thermal effects were detected on the heating curves for strontium silicates (at high temperatures), indicating the absence of polymorphic transitions. This is in agreement with the data of Eskola [1] and of Carlson and Wells [10] on strontium silicates.

The heating curve for stontium carbonate is given in Fig. 1. Strontium carbonate shows an endothermic effect at 925°, corresponding to transition of the orthorhombic into the hexagonal modification. At the transition temperature, decomposition of $SrCO_3$ into SrO and CO_2 begins; this develops especially rapidly above 1000° and is complete at 1200°. Shrinkage of strontium carbonate begins at 750°, and at 920° (before the transition) it reaches about 11%; in the region of the transition point the volume change is somewhat retarded and subsequent shrinkage between 930° and 1200° is probably caused by decomposition of strontium carbonate.

To determine the causes of shrinkage in the 750–920° range, the density and porosity were determined, the x-ray diffraction patterns were taken, and the grain size was determined microscopically both in specimens before heating, and in specimens heated at 920°. The results are given below and in Fig. 2.

Linear shrinkage of specimen (in %)	10.8
Volume shrinkage of specimen (in %)	29.4
Sp. gr. of substance before heating	3.71
Porosity of specimen before heating (in %)	39.1
Sp. gr. of substance after heating	3.71
Porosity of substance after heating (in %)	9.1
Decrease of porosity (in %)	30.0

The above data suggest that the volume decrease in the 750–920° temperature range is caused by a decrease of the porosity of the specimen owing to recrystallization of the substance, producing a compaction effect. This conclusion is confirmed by micrographs.

Study of $SrCO_3$ – SiO_2 mixtures on heating

Mixtures with the composition $3SrCO_3 + SiO_2$. Combined heating curves for a mixture of a composition corresponding to 75% $SrCO_3$ and 25% SiO_2 (in molar %) are given in Fig. 3. In addition to the heat effect of $SrCO_3$ transition and the endothermic effect of its decomposition, another endothermic effect is found, immediately followed by an exothermic effect at 1330°. The loss of weight ceases at 1200°. The volume change of the specimen is the result of the presence of strontium carbonate, which undergoes this volume change (Fig. 1), and of its subsequent decomposition into SrO and CO_2. The shrinkage stops at 1150°, and subsequently the volume of the specimen remains unchanged.

The results of chemical and x-ray structure analysis showed that the strontium oxide formed by decomposition of the carbonate reacts with silica, forming the orthosilicate Sr_2SiO_4. The amount of orthosilicate increases with temperature, and tristrontium silicate also appears. At about 1320° the eutectic mixture melts, and this sharply increases the rate of formation of the final product – tristrontium silicate.

To confirm this explanation, mixtures of the same composition ($SrCO_3 : SiO_2 = 3:1$) were held for 4 hours at 900, 1000, 1100, 1200, 1300, 1350 and 1400°, quenched, and analyzed. The analytical data are given in Fig. 4,I. They show good agreement with the above explanation.

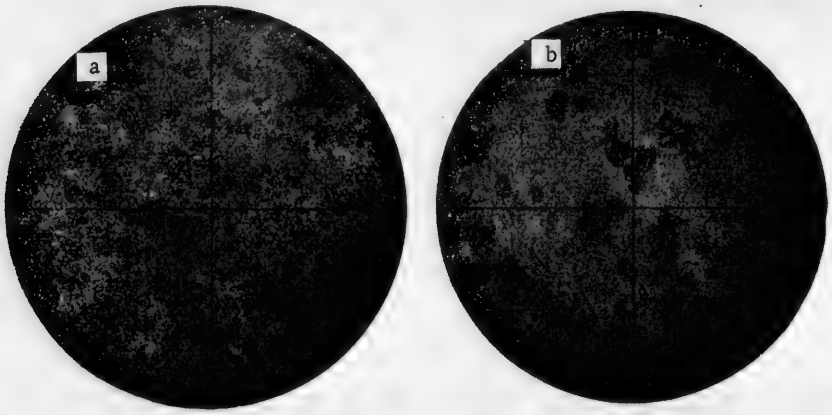

Fig. 2. Micrographs of strontium carbonate before heating (a) and after heating (b).

Mixtures with the composition $2SrCO_3 + SiO_2$. Heating curves for a mixture with the composition 66.7% $SrCO_3$ and 33.3% SiO_2 are given in Fig. 3. They differ from the curves in the preceding diagram mainly by the magnitude of the heat effects, while the nature of these effects remains as before, as shown by the results of x-ray structure analysis at rising temperatures (Fig. 4, IV) and chemical analysis of specimens held for 4 hours at various temperatures (Fig. 4, II). Formation of strontium orthosilicate begins at about 900°. The amounts of SrO and Sr_2SiO_4 increase with temperature. At about 1100°, in addition to Sr_2SiO_4, Sr_3SiO_5 starts to form, its maximum content being reached at 1300 -1320°. Fusion of the eutectic mixture (at 1320°) increases the formation rate of the orthosilicate, both from the mixture of strontium oxide and silica, and from tristrontium silicate by the reaction

$$2Sr_3SiO_5 + SiO_2 \longrightarrow 3Sr_2SiO_4.$$

At about 1400° the product is almost pure orthosilicate.

Mixtures with the composition $SrCO_3 + SiO_2$. Heating curves for a mixture with the composition 50% $SrCO_3$ and 50% SiO_2 are given in Fig. 3. A characteristic feature of the diagram is an increase in the volume of the specimen at about 1150°, with a maximum rate of increase at 1280° followed by slight shrinkage. To determine the causes of the volume increase, and also to study the sequence in which the compounds are formed, x-ray and chemical analyses were carried out both on specimens quenched at different temperatures in the course of a continuous temperature increase, and on specimens held at 1000, 1100, 1200, 1300 and 1400° for 4 hours (Fig. 4, III). The densities of all the specimens were also determined. It was found that, as before, strontium orthosilicate is formed first, and this is subsequently converted into strontium metasilicate by the reaction

$$Sr_2SiO_4 + SiO_2 \longrightarrow 2SrSiO_3.$$

The rate of this reaction is very low, so that only 10% of the metasilicate was found after 4 hours at 1280°. On further increase of the temperature somewhat above 1300° the eutectic mixture melts, as is clear from the diagrams. The appearance of the liquid phase sharply raises the rate of metasilicate formation, and this is shown in the heating curve in the form of an exothermic effect at 1320°. Increase of the size of the specimen at about 1300° is accompanied by an increase of porosity. If the temperature is raised (or if the specimen is held at the same temperature) the specimen shrinks again, probably as the crystal lattice formation of the strontium metasilicate, and subsequent sintering of the latter.

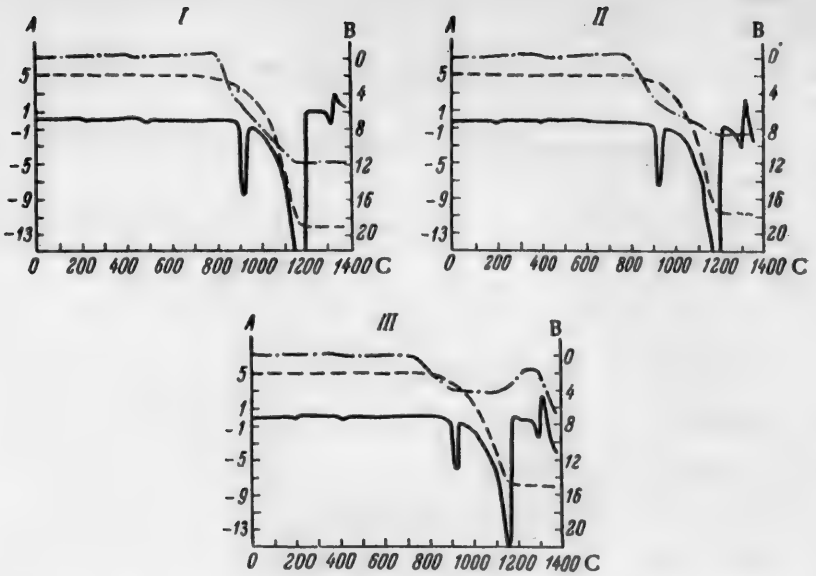

Fig. 3. Heating curves for mixtures made from strontium carbonate and silica. I) 75% $SrCO_3$ + 25% SiO_2, II) 67% $SrCO_3$ + 33% SiO_2, III) 50% $SrCO_3$ + 50% SiO_2. The remaining designations are the same as in Fig. 1.

Mixtures with compositions which do not correspond to known compounds. For complete characterization of the $SrCO_3$ — SiO_2 system, mixtures of other compositions, given above, were also studied. Heating curves for these mixtures are given in Fig. 1. It was found that strontium orthosilicate is formed first in all mixtures, irrespective of composition. In mixtures richer than the orthosilicate in silica, the orthosilicate subsequently reacts with excess silica, forming the metasilicate. The formation of metasilicate is always accompanied by a volume increase. All the mixtures rich in silica melted at about 1350° (the eutectic point for $SrSiO_3$ — SiO_2, according to Eskola [1], is 1358°. In mixtures richer than the orthosilicate in strontium oxide, tristrontium silicate is formed at high temperatures; the amount formed, and amount of the orthosilicate or strontium oxide present with it in the final product, depends on the composition of the original mixture.

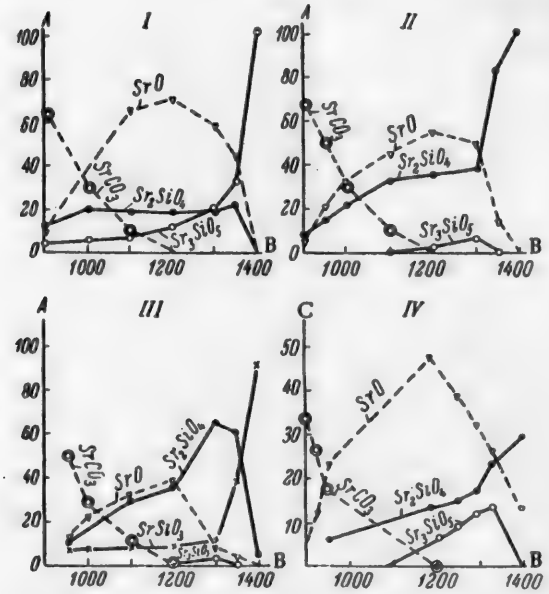

Fig. 4. Variation of phase composition with the burning temperature for mixtures with different proportions of $SrCO_3$:SiO_2. A) Phase composition by chemical analysis of samples (in %), B) temperature (degrees), C) relative intensity I of the characteristic lines. I) 75% $SrCO_3$ + 25% SiO_2, II, IV) 67% $SrCO_3$ + 33% SiO_2, III) 50% $SrCO_3$ + 50% SiO_2.

SUMMARY

1. It was found by means of combined thermal analysis and by chemical and x-ray structure analysis of heated mixtures of various compositions in the system $SrCO_3$ — SiO_2 that the orthosilicate is first formed in mixtures made from strontium carbonate and silica, irrespective of the proportions of the original components.

2. Formation of orthosilicate (from $SrCO_3$ and SiO_2) begins at about 900°.

3. When a 1:1 mixture of $SrCO_3$ and SiO_2 is heated, Sr_2SiO_4 is again formed first, and rapid formation of metasilicate occurs only at 1300° and higher.

4. In mixtures rich in strontium carbonate, formation of tristontium silicate in addition to the orthosilicate begins at about 1100°.

5. The volume is unchanged by formation of the orthosilicate or the tristrontium silicate, whereas formation of the metasilicate results in a volume increase.

6. It was found that the volume changes in $SrCO_3$ specimens in the 750– 920° range are not the result of polymorphic transitions of $SrCO_3$, but are caused by a decrease of porosity resulting from compactive recrystallization of the substance.

LITERATURE CITED

[1] P. Eskola, Am. Journ. Sci., 4, 331 (1922).

[2] I.W. Greig, Am. Journ. Sci., 5, 1 (1927).

[3] Ya. I. Olshansky, Proc. Acad. Sci. USSR 76, 1, 93 (1951).

[4] G. Stein, Z. anorg. Chem., 55, 159 (1907).

[5] R. Wallace, Z. anorg. Chem., 63, 1 (1909).

[6] W. Jander, I. Wuhrer Z. anorg. u allgem. Chem., 226, 225 (1936).

[7] F. Jander, H.S. Klooster, Proc. Konink. Ned. Akad. Wetenschap., 18, 896 (1916).

[8] R. Nacken, Zement, 19, 818 (1930).

[9] M.D. Tschernobaeff, Revue de Metallurgie, 2, 733 (1905).

[10] E.T. Carlson, L.S. Wells, J. Research Nat. Bur. Standards, 51, 2, 73 (1953).

[11] O'Daniel, L. Tscheischwili, Z. Krist., 104, 348 (1942).

[12] R.W. Nurse, J. Applied Chem., 2, 144 (1952).

[13] E.K. Keler and A.K. Kuznetsov, Proc. Acad. Sci. USSR 88, 6, 1031 (1953).

[14] E.K. Keler and A.K. Kuznetsov, Proceedings of the First Conference on Thermography (Izd. AN SSR, 1955) p. 239.

[15] H. Zellner, Z. anal. Ch., 138, 160 (1953).

Received February 11, 1956

CORROSION OF IRON IN HYDROCHLORIC ACID IN THE PRESENCE OF INHIBITORS AT VARIOUS TEMPERATURES*

I.P. Anoshchenko

The preceding paper gave the results of a study of the corrosion of iron in hydrochloric acid in presence of certain inhibitors at various temperatures, obtained by means of polarization curves [1].

The polarization curve method is very helpful for understanding electrode processes which occur in electrochemical corrosion. However, this method (like any other) is not all-embracing in the sense that it can yield all the data necessary for complete evaluation of corrosion phenomena. Other methods, including the gravimetric and the volumetric, substantially augment the polarization curve method. The gravimetric method is a direct and at the same time the simplest method for quantitative determination of corrosion. The volumetric method provides a measure of corrosion by the amount of hydrogen evolved, and in conjunction with the gravimetric method it gives an indication of the degree of hydrogen and oxygen depolarization.

The gravimetric and volumetric methods were used in this study.

EXPERIMENTAL

The gravimetric method was used for studying the effect of additives on corrosion at different temperatures (20, 40, 60 and 80°), and the volumetric method was used only for 20°. Burets of the eudiometer type, described in one of the author's papers [2], were used for work by these two methods. The specimens studied were made from the same iron that was used for the electrodes for determination of the polarization curves [1]. The specimens were in the form of cylinders 10 mm in diameter and 7 mm high.

Before the tests the specimens were cleaned with fine emery paper, degreased with vienna caustic, rinsed in distilled and redistilled water, dried with filter paper, weighted, and then used in the tests. Three specimens were tested in parallel. Most of the tests were carried out with access of air, and the depolarization was therefore of the mixed or hydrogen—oxygen type.

Investigations in pure 6 N hydrochloric acid solution, and in acid containing combinations of such additives as acridine, urotropine, and potassium bromide, were also carried out by the gravimetric method in an atmosphere of hydrogen (with hydrogen depolarization only). For this, the specimens were placed in the apparatus previously used for determination of the polarization curves. A strong stream of electrolytic hydrogen was first blown through the apparatus (before the specimens were put in), and the apparatus was then filled with the test solution, through which a similar stream of hydrogen had been blown previously. During the whole time that the specimens were in the apparatus, i.e., during the entire testing period, hydrogen was passed into the solution. The electrolytic hydrogen was passed through solutions of potassium permanganate, sodium plumbite, and sulfuric acid before entering the test solution. The current strength in the electrolytic cell was 5 amp. It may therefore be assumed that the test solution was saturated with hydrogen and did not contain oxygen.

In all the investigations chemically pure hydrochloric acid was taken and diluted with water to 6 N concentration.

*Communication II.

TABLE 1

Results of a Study of the Effects of Additives on Iron Corrosion

Solution	Temperature (degree)	Gravimetric method: corrosion rate g/m²·hour	Gravimetric method: corrosion rate amp/cm²·sec	Gravimetric method: temperature coefficient (ratio of the corrosion rate at the higher temperature to the corrosion rate at 20°)	Volumetric method Corrosion rate (in g/m²·hour)	Difference between gravimetric and volumetric data (in g/m²·hour)	Oxygen depolarization as % of total depolarization (ratio of the difference and the gravimetric data, multiplied by 100)
6 N HCl	20	9.74	$0.93 \cdot 10^{-3}$	—	9.27	0.47	4.83
	40	48.12	$4.60 \cdot 10^{-3}$	4.95	—	—	—
	60	131.33	$12.50 \cdot 10^{-3}$	14.50	—	—	—
	80	414.90	$39.7 \cdot 10^{-3}$	42.50	—	—	—
6 N HCl + urotropine (3.0 millimoles/liter)	20	0.84	$0.03 \cdot 10^{-3}$	—	0.98	0.14	—
	40	4.07	$0.39 \cdot 10^{-3}$	4.85	—	—	—
	60	21.75	$2.10 \cdot 10^{-3}$	25.90	—	—	—
	80	83.64	$8.00 \cdot 10^{-3}$	99.50	—	—	—
6 N HCl + potassium bromide (0.05 N, 5.95 g/liter)	20	7.26	$0.69 \cdot 10^{-3}$	—	4.0	3.26	45.0
	40	25.40	$2.44 \cdot 10^{-3}$	3.50	—	—	—
	60	119.75	$11.40 \cdot 10^{-3}$	16.50	—	—	—
	80	208.20	$19.90 \cdot 10^{-3}$	28.60	—	—	—
6 N HCl + urotropine (3.0 millimoles/liter) + potassium bromide (0.05 N)	20	0.74	$0.71 \cdot 10^{-3}$	—	0.00	0.74	100.00
	40	3.70	$0.36 \cdot 10^{-3}$	5.00	—	—	—
	60	13.60	$1.30 \cdot 10^{-3}$	18.40	—	—	—
	80	50.16	$4.80 \cdot 10^{-3}$	67.50	—	—	—
6 N HCl + acridine (3.0 millimoles/liter)	20	0.75	$0.07 \cdot 10^{-3}$	—	0.08	0.67	90.0
	40	8.30	$0.79 \cdot 10^{-3}$	11.10	—	—	—
	60	59.20	$5.58 \cdot 10^{-3}$	78.80	—	—	—
	80	205.90	$19.8 \cdot 10^{-3}$	275.00	—	—	—
6 N HCl + acridine (3.0 millimoles/liter) + urotropine (3.0 millimoles/liter)	20	0.58	$0.056 \cdot 10^{-3}$	—	0.10	0.48	82.7
	40	1.03	$0.10 \cdot 10^{-3}$	1.78	—	—	—
	60	8.20	$0.78 \cdot 10^{-3}$	14.10	—	—	—
	80	29.20	$2.80 \cdot 10^{-3}$	50.04	—	—	—
6 N HCl + urotropine (3.0 millimoles/liter) + acridine (3.0 millimoles/liter) + methyl alcohol (0.125 millimole/liter) + potassium bromide (0.10 N)	80	24.1	$2.80 \cdot 10^{-3}$	—	—	—	—

RESULTS AND DISCUSSION

The results of tests in an atmosphere of air are given in Table 1.

It is seen that in pure 6 N hydrochloric acid solution at 20° more than 95.0% of the depolarization is effected by discharge of hydrogen ions. Only 4.83% of the total depolarization is effected by ionization of oxygen. This is to be expected, as the acid is relatively highly concentrated and the solution was not agitated during the corrosion process.

As before, we assume that the difference between the data obtained by the gravimetric and volumetric methods represents oxygen depolarization. It is evident that this assumption is only valid if the depolarization is of the hydrogen—oxygen type (in the practical absence of other depolarizers), if the hydrogen losses are negligibly small, if no gaseous products (apart from hydrogen) are liberated during the corrosion process, and if the metallic corrosion products are easily soluble in the given medium.

The rate of iron corrosion in pure 6 N hydrochloric acid solution increases in geometrical progression with the temperature (in the temperature range studied), the value of the ratio being 3.

In presence of 3.0 millimoles of urotropine per liter the corrosion rate at 20° falls to 0.84 g/m²·hour. At this concentration the volumetric method gives a higher value than the gravimetric. This may be because other gases in addition to hydrogen are evolved during corrosion. It is known from the literature that urotropine decomposes in acid media to give formaldehyde, ammonia, carbon dioxide, and methylamine [3]. Therefore the hydrogen contains the gaseous products of urotropine decomposition.

Increase of the urotropine content to 5.0 millimoles per liter raises the corrosion rate at 20°, and the corrosion rate increases with temperature, but the temperature coefficient is severalfold less than at a concentration of 3.0 millimoles per liter.

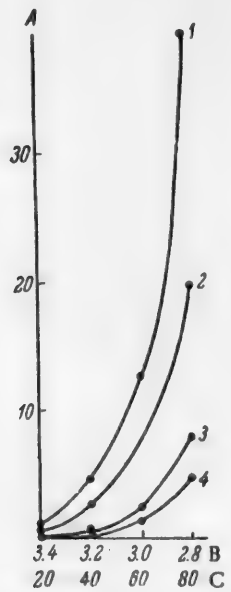

Fig. 1. Iron corrosion rate as a function of the reciprocal of the solution temperature. A) Corrosion rate 10^{-3} (in amp/cm²·sec.), B) $\frac{1}{T} \cdot 10^3$, C) temperature (in degrees). 6 N HCl solution with additives: 1) no additive, 2) potassium bromide (0.05 N), 3) urotropine (3.0 millimoles/liter), 4) urotropine (3.0 millimoles/liter) + potassium bromide (0.05 N).

Fig. 2. Logarithm of the corrosion rate (gravimetric method) as a function of the reciprocal of the solution temperature. 6 N HCl solution with additives: 1) no additive, 2) potassium bromide (0.05 N), 3) urotropine (3.0 millimoles/liter), 4) potassium bromide (0.05 N) + urotropine (3.0 millimoles/liter).

Potassium bromide in 0.01 N concentration, i.e., 1.19 g/liter, intensifies corrosion, especially at elevated temperatures. At a concentration of 0.05 N (5.95 g/liter) the corrosion rate is less at all temperatures (the temperature coefficient decreases).

When the potassium bromide content is raised to 0.1 N (11.9 g/liter), the corrosion is almost halved at 20°, while the participation of oxygen in the depolarization decreases to 0.98%. The rate of solution of the iron rises steeply as the temperature is increased to 80°. The temperature coefficient reaches 68, but the absolute rate is 84% of the rate in pure acid at the same temperature (80°).

Potassium thiocyanate, aniline, camphor, and methyl alcohol have relatively little effect on the solution of iron in 6 N hydrochloric acid solution.

Of all the additives studied, acridine has the greatest inhibiting effect at 20°. However, this inhibitor is unstable at elevated temperatures, especially at 80°. A very important fact is that acridine and urotropine intensify the effects of each other at all the temperatures investigated. The highest inhibiting effect at 80° is produced by a combination of urotropine (3.0 millimoles/liter), acridine (3.0 millimoles/liter), methyl alcohol (0.125 millimole/liter), and potassium bromide (0.1 N, or 11.9 g/liter). The corrosion rate of iron in the presence of this combination of additives is 24.1 g/m^2·hour.

Figure 1 is a plot of the corrosion rates, determined gravimetrically and expressed in current units (amp /cm^2·sec.), against the reciprocal of the temperature, for the pure acid, and acid containing potassium bromide, urotropine, and combinations of these. It is seen that the curves rise exponentially.

TABLE 2

Influence of Additives on the Activation Energy

Solution	Effective activation energy (in cal.)	Difference between activation energy in solution with additive and in pure solution (in cal.)	Increase of activation energy with additive (in %)
6 N HCl	12080	–	–
6 N HCl + bromide (0.05 N)	12300	220	1.825
6 N HCl + urotropine (3.0 millimoles/liter)	12250	3170	26.23
6 N HCl + potassium bromide (0.05 N) + urotropine (3.0 millimoles/liter)	15450	3370	27.95

TABLE 3

Effects of Additives on Corrosion Determined Gravimetrically

Solution	Temperature (degrees)	Corrosion rate		Temperature coefficient (ratio of the corrosion rate at the higher temperature to the corrosion rate at 20°)
		g/m^2·hour	amp./cm^2·sec.	
6 N HCl	20	9.3	$0.89 \cdot 10^{-3}$	–
	40	43.3	$4.14 \cdot 10^{-3}$	4.65
	60	87.4	$7.78 \cdot 10^{-3}$	8.75
	80	416.4	$39.90 \cdot 10^{-3}$	44.80
6 N HCl + acridine (3.0 millimoles/liter) + urotropine (3.0 millimoles/liter) + potassium bromide (0.1 N)	20	0.49	$0.048 \cdot 10^{-3}$	–
	80	26.80	$2.56 \cdot 10^{-3}$	54.60

The negative logarithms of the corrosion rates (determined gravimetrically and expressed in current units) are plotted against the reciprocal of the temperature in Fig. 2. This relationship is linear. The slopes of these lines were used to calculate, with the aid of the equation given previously. The total effective activation energy for the solution of iron in 6 N hydrochloric acid solution. The influence of the additives on the activation energy is given in Table 2.

It is seen that the effective activation energy increases with increasing inhibiting effect of the given additive (or combination of additives).

The results of gravimetric determinations in a hydrogen atmosphere are given in Table 3.

Comparison of the data in Table 3 with the values for the corresponding solutions given in Table 1 shows that the data in the two tables are similar. This is quite understandable, as depolarization in 6 N hydrochloric solution in air under the given experimental conditions (no agitation of the solution, and considerable immersion of the specimens) occurs mainly by way of hydrogen-ion discharge.

SUMMARY

1. It is shown that depolarization in pure 6 N hydrochloric acid solution at 20° is effected by more than 95% by discharge of hydrogen ions. The solution rate of iron in pure acid rises with the temperature in geometrical progression.

2. The fact established previously, that the participation of oxygen in depolarization increases with increasing inhibiting action of additives, has been confirmed.

3. It was found that the greatest inhibiting effect at 80° is produced by a combination of urotropine, acridine, potassium bromide, and methyl alcohol.

4. It is shown that the corrosion rate of iron in acid increases exponentially with the reciprocal of the temperature.

LITERATURE CITED

[1] I.P. Anoshchenko, J. Appl. Chem. 30, 3, 393 (1957).*

[2] I.P. Anoshchenko, Trans. S. Ordzhonikidze Polytechnic Inst. Novocherkassk 25(39), 1 (1954).

[3] S.A. Balezin and S.K. Novikov, J. Appl. Chem. 24, 3 (1951).

Received March 27, 1956

*Original Russian pagination. See C.B. Translation.

THE MECHANISM OF THE ELECTROCHEMICAL POLISHING OF METALS

S.Ya. Grilikhes and N.P. Fedotyev

In our previous communications [1, 2] we gave the results of studies of anode processes taking place during the electrochemical polishing of steel in an electrolyte containing H_3PO_4, H_2SO_4, CrO_3 and H_2O. For elucidation of the state of the metal surface during polishing, the capacity and contact resistance of the electric double layer at the metal–solution boundary were measured and the anode potentials under different conditions of electrolysis were studied.

These investigations showed that an oxide film is formed on the anode surface during electrochemical polishing. The anode potential curves have two critical current regions. The oxide film is formed in the conditions determining the second critical current region.

The presence of CrO_3 in the electrolyte has a significant influence on the course of electrochemical polishing.

Anodic treatment of carbon steel (St 45) in an electrolyte without CrO_3 is characterized by periodic passivity effects. At over 3% of CrO_3 in the electrolyte the periodic effects disappear and two critical current regions appear on the anode potential curve.

Similar investigations were carried out in relation to the electrochemical polishing of copper and nickel [3]. Analysis of the anode potential curve, and data on the capacity and contact resistance of the electric double layer, indicate that the anode processes in the electrochemical polishing of steel, copper, and nickel have much in common.

This is manifested principally in the fact that the metal surface acquires a luster when the electrolyte composition and electrolysis conditions result in the formation of an oxide film of definite composition and thickness on the anode.

These experiments provide new data on anode passivity effects and demonstrate a connection between these effects and the polishing process.

Many authors, in discussing the mechanism of electrochemical polishing, devote considerable attention to the question of smoothing of microirregularities of the metal surface during anodic dissolution, and regard luster as the result of this smoothing. It is known, however, that smoothing of the anode surface need not be accompanied by increased luster. An example is provided by anodic treatment of carbon steel in dilute sulfuric or phosphoric acid. Increase of luster does not always accompany smoothing of surface roughness, and the two processes may have different mechanisms.

It is therefore desirable to distinguish between smoothing of microirregularities, which might be described as electrochemical grinding, and the electrochemical polishing process, a distinctive feature of which is the appearance of luster in the metal.

Some ideas on the mechanisms of these processes can be formulated from the results of our experimental investigations.

Smoothing of the anode surface in electrochemical grinding is the consequence of the difference between the rates at which the metal is dissolved at the projections and pits in the surface. This difference is found when the current density at the projections of the microrelief exceeds the current density in the pits. One consequence

of the anode process is that the anolyte layer becomes enriched with the anodic dissolution products. This layer has a higher specific gravity and lower conductivity than the main bulk of the electrolyte. If this layer surrounds the anode surface it is found that the resistance to the passage of current to the projections is appreciably less than the resistance to the pits, and this leads to a redistribution of the current density over the anode surface.

Saturation of the anolyte layer with the dissolution products of the metal may lead, under certain conditions, to formation of a salt film on the anode surface. If this film is continuous, current ceases to pass through the cell. If the salt film is porous, the current strength decreases and the cell voltage increases. Local heating of the electrolyte caused by increases of the contact resistance raises the solubility of the salts, leading to breakdown of the film. The current strength in the circuit increases, and conditions for repetition of the cycle are created. We observed such periodic processes at the anode in the treatment of carbon steel in a mixture of sulfuric and orthophosphoric acids. These processes were accompanied by leveling of the surface microrelief without any appreciable increase of its reflecting power.

Smoothing of the anode surface in electrochemical grinding is associated with the initial heights of the surface microprojections. In Fig. 1 the rate of smoothing is plotted against the duration of electrolysis for specimens of steel St 45 of different degrees of surface smoothness. The electrolyte was a mixture of 65% H_3PO_4 and 15% H_2SO_4. The specimens were treated at anode current density 40 amp./dm^2 and 70° solution temperature.

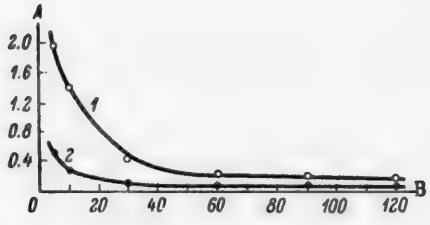

Fig. 1. Effect of duration of electrolysis on the leveling rate. A) smoothing rate (in μ/minute), B) duration of electrolysis (in minutes). Initial surface state: 1) w4, 2) w6.

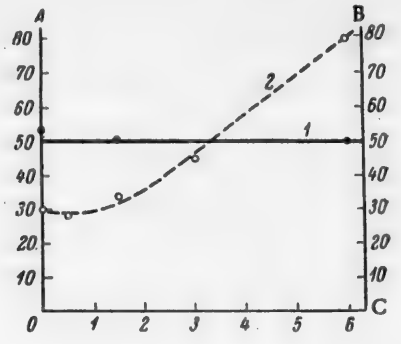

Fig. 2. Effect of CrO_3 content in the electrolyte on smoothing and reflecting power of the metal surface. A) Relative smoothing (in %), B) relative reflecting power (in %), C) CrO_3 content in the electrolyte (in wt.%). Curves: 1) relative smoothing, 2) relative reflecting power.

Figure 1 shows that the most rapid smoothing and the highest solution rate of the microprojections are found for the first 10 minutes of electrolysis. After this the rate of smoothing drops sharply and the subsequent changes of surface smoothness are slight. This effect is more pronounced with increasing original height of the microprojections.

It must be pointed out that in these cases we are concerned with smoothing of microprojections the height of which can be determined by the usual methods for determination of surface smoothness. As their height diminishes, the rates of metal solution at the projections and in the pits approach closer together, the smoothing is retarded, and eventually stops almost entirely.

It may be assumed that the mechanism of electrochemical grinding is determined to a considerable extent by concentrational polarization and is associated with the microgeometry of the anode surface.

These factors are not decisive in electrochemical polishing, as they are not directly related to appearance of luster in the anode. In the latter case it is necessary to consider the role of the oxide film formed on the anode during electrochemical polishing. We studied the effect of the CrO_3 content in the electrolyte on the smoothing and reflecting power of specimens of St 45 carbon steel. The electrolyte used for treatment of the specimens

contained 65% H_3PO_4, 15% H_2SO_4 and CrO_3 in amounts up to 6%. The anode current density was 40 amp./dm^2, the electrolyte temperature was 80°, and the duration of electrolysis was 10 minutes. The surface smoothness of the specimens before electrolysis corresponded to class 6. The surface smoothness was determined by means of a binocular microscope. The results of the determinations were used to calculate the relative smoothing—the ratio of the difference between the initial and final height of the microprojections to their initial height. The reflecting power was determined relative to the reflecting power of a silver mirror, taken as 100%.

The results of these experiments, plotted in Fig. 2, show that addition of CrO_3 to the electrolyte has practically no effect on the surface smoothing, but has an appreciable influence on changes in the reflecting power of the metal. A plot of the relative reflecting power against the CrO_3 concentration ascends steeply when the latter is about 3%, which is just the concentration at which an oxide film appears on the metal surface and the anode potential curve changes sharply [2].

With the same degree of smoothing, the reflecting power rises sharply when an oxide film is formed on the metal. This observation is confirmed by our determinations of the capacity and contact resistance of the electric double layer [1].

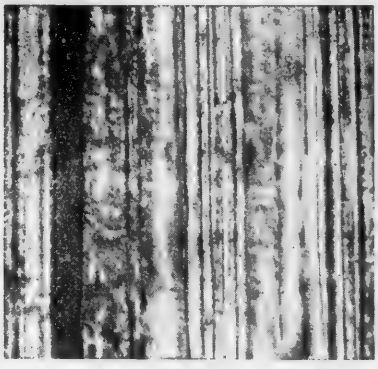

Fig. 3. Steel surface before electrochemical treatment.

Fig. 4. Steel surface after electrochemical treatment in an electrolyte without CrO_3.

The role of the passive oxide film in the anode dissolution process becomes clearer on investigation of the surface of specimens treated under different conditions of electrolysis. This investigation was carried out with the same steel specimen (St 45) the surface of which had been cleaned with No. 100 emery paper. One end of the specimen was treated in an electrolyte containing 65% H_3PO_4, 15% H_2SO_4, 20% H_2O, and the other end in an electrolyte containing 65% H_3PO_4, 15% H_2SO_4, 6% CrO_3, 14% H_2O. In both cases the anode current density was 40 amp./dm^2, the solution temperature was 70°, and the duration of electrolysis was 5 minutes.

Thus, under these experimental conditions the surface texture and chemical composition of the metal was the same in both cases, and differences in the course of the anode process would be determined by the presence or absence of the passivating agent, CrO_3, in the electrolyte.

The original surface of the specimen showed signs of mechanical treatment (Fig. 3). The surface irregularities were largely smoothed out as the result of electrolysis, but the course of this process depended on the composition of the electrolyte used. In the electrolyte free from CrO_3 it was accompanied by etching—grain boundaries can be seen in the micrograph (Fig. 4). The specimen surface became smooth but did not acquire a luster. Electrolysis in a solution containing CrO_3 was accompanied by the formation of a passive anode film, which prevented etching of the metal (Fig. 5). In this case the surface of the specimen not only became smooth, but acquired a luster.

Literature data indicate that etching of the metal cannot always be avoided in electrochemical polishing. For example, microscopic examination of the surface of two-phase brass polished in orthophosphoric acid

solution reveals grain boundaries, whereas no etching is observed on the surface of electropolished one-phase brass. As a result the luster of electropolished two-phase brass is less than that of one-phase brass.

It may be noted that the polishing electrolytes contain two types of ions. Some cause oxidation of the metal, and the others cause solution of the oxide film. For example, in the polishing of aluminum, oxidation occurs under the action of SO_4'' ions, and solution under the action of F' and OH' ions. In the electrolytes used by us for polishing steel, copper, and nickel, passivation of the metal depends on the presence of CrO_3, and solution of the film, on the presence of H_3PO_4 and H_2SO_4 in the solution. In the electropolishing of copper in orthophosphoric acid, conditions also arise for the formation and anodic dissolution of an oxide film [4].

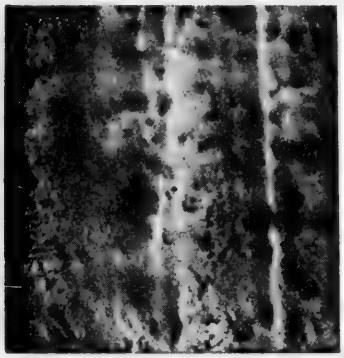

Fig. 5. Steel surface after electrochemical treatment in an electrolyte containing CrO_3.

Complete passivation of the anode does not occur in electrolytic polishing. Evolution of oxygen is accompanied by solution of the metal. Passage of the metal, coated with the oxide film, into solution is affected by its conversion into the oxide and interaction of the latter with the electrolyte.

Formation and solution of the passive anode film take place simultaneously on the anode surface. If the formation rate is greater than the solution rate, and if the film formed is nonporous and nonconducting, the film interrupts the normal course of electrolysis even when it is still thin. If the film is porous and transmits current, it may reach an appreciable thickness, as is the case in anodic oxidation of aluminum. If the solution rate exceeds the formation rate of the film, the latter cannot protect the anode surface, which becomes etched. Electrochemical polishing occurs only when the rates of the two processes are in a certain ratio, giving rise to an oxide film of definite composition and porosity on the anode.

The improvement of the optical properties of the metal surface by electrochemical polishing does not depend only on restriction of the etching action of the electrolyte on the anode. An important part is also played by smoothing of the smallest irregularities, which cannot be measured by the usual methods for determination of surface smoothness.

The factors which determine the smoothing of anode projections in electrochemical grinding have no decisive effects on irregularities of a lower order. In the latter case the smoothing will depend on the presence of an oxide film, the thickness of which is comparable to the height of these projections.

The results of these experiments show that whereas the electrochemical grinding process, accompanied by increased surface smoothness, is determined to a considerable extent by concentrational polarization effects, the luster characteristic of electrochemical polishing is produced when a passive film is formed on the metal surface during electrolysis.

The difference between the mechanisms of the two processes shows them to be distinct. In practice, the two processes sometimes occur simultaneously. It may be noted in this connection that when a metal is treated in a polishing electrolyte an increase of its reflecting power is accompanied by an improvement of its surface smoothness. Conversely, treatment of a metal in a "grinding" electrolyte (for example, steel in dilute mineral acids) does not usually lead to any significant increase of the reflecting power. This is because the two processes have different mechanisms. The formation of a salt layer with increased electrical resistance at the anode causes redistribution of the current over the anode surface, but cannot lead to formation of an oxide film on it.

The foregoing experimental results demonstrate the role and influence of certain factors in smoothing and increase of the reflecting power of a metal during anodic dissolution. In electrochemical polishing the formation of a passive oxide film on the anode during electrolysis plays an important part. Further investigations may reveal the relationship of these factors to other conditions of the process, and this will help to solve practical problems in electrochemical grinding and polishing of metals.

SUMMARY

1. The results of a study of electrochemical polishing show that it is necessary to distinguish between electrochemical grinding, accompanied by smoothing of the metal surface, and electrochemical polishing, accompanied by an increase of the reflecting power of the metal.

2. Smoothing of the microroughnesses of the metal surface in electrochemical grinding is the result of formation of a viscous salt layer near the anode, or a salt film on its surface.

3. The reflecting power of a metal surface subjected to anode treatment is appreciably increased if this treatment is accompanied by the formation of an oxide film on the metal.

LITERATURE CITED

[1] V.L. Kheifets, N.P. Fedotyev, and S. Ya. Grilikhes, J. Appl. Chem. 29, 12 (1956).*

[2] N.P. Fedotyev and S. Ya. Grilikhes, J. Appl. Chem. 30, 2 (1957).*

[3] N.P. Fedotyev and S. Ya. Grilikhes, J. Appl. Chem. 30, 4, 463 (1957).*

[4] A.V. Fortunatov and A.V. Finkelshtein, Proc. Acad. Sci. USSR 5 (1953).

Received September 16, 1955

*Original Russian pagination. See C.B. Translation.

CAUSES OF DIFFICULT STRIPPING OF CATHODE ZINC DEPOSITS

V.L. Klimenko

The term "difficult stripping" in the industrial electrolysis of zinc sulfate solution refers to the abnormal increase of the force required to separate the cathodic zinc deposit from the aluminum cathodes owing to adhesion between them.

Difficult stripping of zinc results in serious disorganization of the electrolytic process, and therefore many scientists and practical engineers have attempted to determine its causes.

Most of those who investigated this effect reached the same conclusion that adhesion of zinc to aluminum is caused by removal of the protective Al_2O_3 film. However, different authors give different interpretations of the causes of the disappearance of the film.

Baimakov [1] considers that coalescence of the zinc with aluminum is the result of penetration of the cathode deposit into deep pits of the cathode sheet, which occurs if copper, zinc, or iron are present as impurities in the aluminum; it is also caused by excessive etching of the cathodes in acid electrolytes, by the presence of fluorine or chlorine in the electrolyte, and by careless handling of the cathodes. He also notes the effect of roughness of the aluminum sheet resulting from incorrect heating and rolling procedures.

Zosimovich and Ilyenko [2] consider that fluoride ions destroy the Al_2O_3 film, and this creates conditions for the formation of a surface alloy of zinc and aluminum.

Levin, Pomosov, and Tkachenko [3] believe that, in difficult stripping, the oxide film on the aluminum cathode has cracks, dents, scratches, and other defects which assist etching of the film in acid zinc sulfate solution, and result in exposure of the crystalline structure of aluminum. This leads to formation of "occluding layers" and "locks" and to coalescence of the zinc with the aluminum.

Shteingart [4] denies that fluoride has any effect, but assumes "possible disturbance of the aluminum surface." He was the first to advance the hypothesis that the zinc structure may influence difficult stripping.

Without dealing with the views of Pletenev and Rozov [5], Baimakov, Lubchenko [6], Shteingart, and Klimenko [7], who did not support their reasons for difficult stripping by laboratory investigations, let us consider why others, who studied this question experimentally, reached contradictory and incorrect conclusions.

Zosimovich and Ilyenko, who studied the effect of fluoride, removed the Al_2O_3 film from the cathode by caustic alkali, soda, and sulfuric acid, and thus artificially created the necessary conditions for difficult stripping.

Levin, Pomosov, and Tkachenko, and also Shteingart, who experimented with industrial concentrations of fluoride, evaluated the adhesion process from the results of a single stripping of the cathode deposit after electrolysis in presence of a given fluoride concentration.

In such cases the fluoride acted on the oxide film once, during the time between immersion of the cathode in the electrolyte and complete protection of the cathode surface by the deposited zinc.

However, the degree of destruction of the oxide film at constant fluoride concentration depends on the time of contact between the film and the fluoride ions, and it is probable that at low fluoride ion concentration appreciable destruction of the film can only occur as the result of repeated deposition and stripping of the zinc.

It must be remembered that restoration of the destroyed oxide film to a definite thickness in air during stripping is also a function of time.

In our opinion, difficult stripping in daily removal of zinc from the same cathode should occur when the fluoride concentration in the electrolyte becomes high enough to cause destruction of the oxide film (from the time of immersion of the cathode in the electrolyte to the time when it is completely coated with zinc) at a rate greater than the rate of its restoration (during the time from the separation of the cathode deposit to immersion of the cathode in the electrolyte).

The above-named authors only studied the influence of fluoride concentration, and did not take these factors into account. Evidently, in Zosimovich and Ilyenko's experiments the oxide film on the cathode was so thin, because of the preliminary etching, that even 20 mg of fluoride per liter was enough to cause partial destruction of the film; in the experimental conditions used by the other authors the film was considerably thicker and higher fluoride concentrations were needed for its destruction.

The workers who studied the conditions for the occurrence of difficult stripping did not use such objective methods as metallography or x-ray structure analysis. All this led to a state of affairs in which correct hypotheses and deductions were found side by side with confused and at times erroneous interpretations of the causes for coalescence of zinc and aluminum.

EXPERIMENTAL

Metallographic Analysis of Industrial Cathode Specimens

Our studies of the causes of difficult stripping started with metallographic analysis (by means of the MIK-5 microscope) of specimens of aluminum cathodes with zinc deposits formed on them. Specimens of cathodes which gave difficult and easy stripping were studied. The former were taken from zinc dust tanks with an electrolyte containing 150 mg each of chloride and fluoride per liter, and the latter from the calcine leach cycle tanks containing only 30 mg of these elements per liter in the electrolyte. It should be noted that in the grinding and polishing of the easy-stripping specimens it was necessary to take special care and use special devices to prevent separation of the zinc.

Fig. 1. Micrographs of polished sections with easy (a) and difficult (b) stripping of zinc. 1) Zinc, 2) aluminum.

Photographs of sections with easy and difficult stripping are given in Fig. 1.

In the first section (Fig. 1, a) there is a distinct, relatively level separation line between the zinc and aluminum, in the form of a dark band from 0.02 to 0.01 mm thick. The separation line is in places penetrated by thin needlelike crystals of zinc, which as a rule do not reach the aluminum surface. This dark band is formed by the oxide film, which prevents penetration of the zinc crystals to the aluminum, and cavities between the needlelike bases of the zinc crystals.

No such clearly defined line of separation between the zinc and aluminum is seen in the second section (Fig.1,b). Here the aluminum surface is less smooth, it is etched, and zinc is embedded between the aluminum crystals.

The presence of crystal nuclei in the interstices between the exposed aluminum crystals is seen especially clearly under 1260-fold magnification with the use of an immersion objective.

To verify the view that difficult stripping is the result of mechanical damage to the cathode surface, leading to formation of "locks" and "occluding layers" [3], we took cathodes with the surfaces damaged artificially to different extents, carried out repeated electrolysis without any fluoride in the solution, and made polished sections (Fig. 2). When the number of pits did not exceed one per 1 cm^2 of the cathode surface, no appreciable changes in the stripping behavior were found; when the number of deep small pits was greater, the stripping deteriorated progressively with increasing number of pits.

Cathodes with extensive damage of this type are not found to any extent under production conditions, not only because such damage is not caused artificially, but also because the surface of each cathode is periodically subjected to mechanical cleaning.

Consequently, extensive pitting, "locks", and "occluding layers" can only result from chemical destruction of the protective film and aluminum crystals. In such cases the number of pits per 1 cm^2 of the sheet surface may run into hundreds.

It also follows from Fig. 2 and from examination of a number of sections with damaged cathode sheet surfaces that zinc fills almost all the pits, and this gives rise to "occluding layers."

Fig. 2. Micrograph of section with artifically damaged surface. 1) Zinc, 2) aluminum.

In our view, this may be explained as follows. The current passing through the cell is, by Ohm's law, given by the equation

$$I = \frac{E}{R_{con} + R_{el} + R_{met}} \quad [8],$$

where R_{con} is the contact resistance at the electrode–solution interface, R_{el} is the resistance of the electrolyte, and R_{met} is the resistance of the metal electrodes. If it is considered that in this equation R_{met} is small, it is seen that the microrelief of the electrode surface cannot significantly influence the uniform distribution of electrons over the electrode surface if the electrodes are parallel to each other.

With an aluminum cathode, the oxide film offers the main resistance, but this film covers the cathode surface in a relatively even layer if the micropores in it are relatively uniformly distributed.

Therefore it may be assumed that the current density and potential gradient will be greater in the pits, owing to the greater surface, than on projections, and therefore zinc will be deposited at a higher rate in the former.

Otherwise zinc would not become embedded in the pits, as the rapidly growing crystals on the projections would cover all the small pits.

The subsequent investigations were aimed at elucidation of the destruction of the film and aluminum cathode surface by fluoride ions.

Effect of Fluoride on the Occurrence of Difficult Stripping

The experiments on electrolysis of zinc sulfate solution were carried out at current density 500 amp/m^2 in 4 laboratory 1.5- liter cells with two cathodes (4.3 × 8.5 cm) in each. The solution was prepared from TsO grade zinc and chemically pure sulfuric acid. The acidity of the electrolyte was maintained in the limits of

98- 102 g/liter. Fluorine was introduced into the electrolyte in the form of sodium fluoride. A 2.5 kg spring balance was used for measuring the force required to detach the zinc from the cathode. In order to obtain a fairly strong zinc deposit, the duration of electrolysis was 3 hours.

TABLE 1

Effect of Fluoride Concentration on the Stripping of Zinc

Stripping No.	Stripping force (in kg) for fluoride concentrations in the electrolyte (in mg/liter)			
	50	100	200	500
1	0.25	0.35	0.5	0.6
2	0.4	0.5	0.8	1.5
3	0.5	0.8	1.5	2.5
4	0.7	1.0	2.0	–
5	0.8	1.25	2.5	–
6	1.0	1.5	–	–
7	1.25	2.0	–	–
8	1.5	2.5	–	–
9	1.75	–	–	–
10	2.0	–	–	–
11	2.2	–	–	–
12	2.5	–	–	–

Stripping of the zinc was carried out in the same way as in production conditions, i.e., one cathode was removed and top right-hand corner of the deposit was turned over by a knife. The bent corner was joined to the spring balance by a special clamp, and the zinc was stripped at an angle of 80°. The maximum stripping force was read off on the balance scale. After the zinc had been stripped the cathode was immediately returned to the cell and the next cathode was stripped.

In our conditions, easy stripping corresponded to a force of 0.25–0.5 kg. moderately difficult, to a force of 0.5 - 1.0 kg, and difficult, to a force of 1.2–2.5 kg; stripping was practically impossible if the force was to be greater than 2.5 kg.

Since in the laboratory experiments these forces corresponded to 4.3 cm of cathode width, the following forces (in kg) would have to be used for stripping zinc from industrial cathodes: easy stripping 35 - 70, moderately difficult 70 - 140, difficult 140–280, practically impossible over 300.

The cathodes were made from a single new sheet of aluminum and thoroughly cleaned with a metal scraper 0.5–1 hour before being put into the cells.

To determine the effect of fluoride concentration on stripping of zinc, prolonged electrolysis experiments were carried out with repeated stripping of the zinc, with different concentrations of fluoride in the electrolyte.

The average experimental results are given in Table 1.

It is seen that difficult stripping, corresponding to a force of 2.5 kg, begins at the 12th stripping with 50 mg fluoride per liter, and at the 3rd with 500 mg/liter.

It must be pointed out that the relationship between the onset of difficult stripping and the number of strippings and the fluoride concentration was not discovered at once, as in the earlier experiments due attention was not paid to the time during which the stripped cathodes remained exposed to the air.

The following example illustrates the influence of the time of exposure of the cathode to air on the onset of difficult stripping: with 100 mg of fluoride per liter, after the stripping force had increased from 0.25 kg to 2 kg, the stripped cathode was exposed to the air for 15 hours, and then zinc was again deposited on it; stripping of this required a force of only 0.7 kg; it only reached 2 kg again after two strippings.

This example from numerous experiments, and experiments on the effects of artificial damage to the cathode surfaces, shows that adhesion of zinc to aluminum occurs both by the action of molecular forces between the zinc and aluminum molecules, and by means of "locks."

After the stripped cathode had been exposed to air for some time, the oxide film formed acts as an obstacle to molecular adherence, but the pits formed on the cathode surface give rise to adherence owing to "locks".

In our example, adherence due to molecular forces comprises 1.3 kg, and that due to "locks" 0.7 kg, if we ignore molecular adherence which arises during the first immersion of the cathode in the tank after its oxidation in air.

Residual increased adherence of the etched cathode due to "locks" is also found if a cathode which was in a cell with fluoride ions is placed in a cell without fluoride after difficult stripping.

Experiments were also carried out on preliminary etching of the cathode in spent electrolyte containing 200 mg of fluoride per liter in an idle cell for 24 hours, followed by electrolysis (without removal of the etched cathodes from the cell).

It was expected that this treatment of the cathodes should immediately result in difficult stripping, as it was found experimentally that in spent electrolyte containing 200 mg fluoride per liter, 50 g of zinc per liter, and 100 g H_2SO_4 per liter at 20° the cathode is corroded at a rate of 2.2 mg/cm^2, which should ensure removal of the oxide film.

However, the expected result was not obtained—the stripping was easy; moreover, for several days the zinc deposit bulged spontaneously and came away from the cathode; so-called "blisters" formed.

The explanation for this effect is that during prolonged etching of the cathode in the electrolyte the aluminum sulfate which is formed is retained in its pits and pores.

It was shown by Mendeleev [9] and established in laboratory experiments that aqueous aluminum sulfate solution interacts with zinc according to the equation:

$$2Al^{\cdots} + SO_4'' + 2H^{\cdot} + 4OH' + Zn = Al_2(OH)_4SO_4 + Zn^{\cdot\cdot} + H_2.$$

The rate of this reaction is low. For example, 1 g of zinc dust lost 520 mg in weight in 16 hours at 25° in 20% aluminum sulfate solution without stirring. Consequently, when a current is passed through the electrolyte, formation of a dense film of zinc on the cathode is more rapid than dissolution of zinc nuclei deposited on the aluminum sulfate. This hinders the free exit of hydrogen bubbles, and thus gives rise to conditions for blistering and peeling of the cathode deposit.

If the electrolyte contains such impurities as cobalt, which gives rise to holes through the zinc after some time, the electrolyte enters into the space between the cathode and the bulged part of the zinc, thus accelerating dissolution of the zinc and its peeling from the aluminum.

To prevent the so-called "blisters" it is necessary to remove the acid film of aluminum sulfate by careful cleaning of the surface with a steel brush, or by drying of the cathode in air.

Fig. 3. Micrograph of a section after mechanical cleaning. 1) Stripe caused by wire, 2) pits.

To determine the effect of cleaning of the cathodes with steel brushes, after a stripping force of 2.0 kg had been reached the cathodes were cleaned with a steel brush for 5 minutes and again used for electrolysis. The force required for stripping then decreased to 0.25 kg, but the time before the value of 2.0 kg for the stripping force was again reached decreased.

This experiment shows that, as the result of mechanical cleaning of the cathodes in air, adherence both by molecular forces and by "locks" was eliminated almost entirely.

To illustrate the changes in the cathode surface by the action of fluoride and by mechanical cleaning, a stripe (Fig. 3,1) was scratched on the cathode surface (after the zinc had been stripped with a force of 2 kg) by a wire from a steel brush (i.e., mechanical cleaning was reproduced), and a micrograph of the cathode surface was then taken. The photograph shows that fluoride, in removing the protective film, exposes the aluminum crystals and attacks them, forming a large number of pits (Fig. 3,2). In the scratch made by the wire, on the other hand, all the irregularities caused by fluoride etching are smoothed out. This substantiates the recommendations made by a number of authors, as the result of practical observations, concerning the necessity for thorough cleaning of the cathodes if difficult stripping occurs.

However, this is not a radical method for prevention of difficult stripping, as with a fluoride concentration of the order of 100 mg/liter it would be necessary to clean the cathodes every other day, which is not practicable under normal conditions.

To summarize the foregoing, the origin of difficult stripping may be represented as follows. Fluoride ions interact with the protective film of $Al_2O_3 \cdot nH_2O$; the destruction of this film is increasingly rapid and complete with increasing fluoride concentration and decreasing film thickness; the latter may vary within wide limits [10]. The time of action of the fluoride is confined to the interval between immersion of the cathode in the electrolyte and complete coating of the cathode with a layer of zinc; only partial destruction of the film occurs during this time.

The attacked places in the film immediately become filled with small nuclei of zinc crystals. If a potential is applied to the cathode, molecular cohesion forces arise between the aluminum and zinc.

Alternate immersion of the cathode in the electrolyte and stripping operations result in further attack on the film and the exposed aluminum, which leads to formation of pits between the etched aluminum crystals and to adherence not only due to molecular forces, but also to "locks," if a part of the aluminum crystals remains protected by a film impenetrable to zinc ions.

After a definite number of stripping operations, which depends on the fluoride concentration and the film thickness, if the cathodes are not cleaned the adherence becomes so strong that stripping of the zinc becomes practically impossible. If the cathodes are cleaned in air with steel brushes, the pits caused by fluoride on the cathode surfaces are eliminated and the thin oxide film is restored.

If the time spent by the cathode in the electrolyte without passage of current, and therefore without protection against the action of fluoride and acid, is increased, an acid aqueous solution of aluminum sulfate may be formed; in such cases difficult stripping does not occur but, on the contrary, so-called "blisters" may be formed.

Effect of Impurities on Difficult Stripping of Zinc and on the Current Efficiency

Effect of antimony. Industrial trials of the electrolysis of solutions formed by leaching dust and oxides, and containing 100 - 150 mg F and 0.1 - 0.5 mg Sb per liter, showed that the microstructure of the zinc, and with it the nature of the stripping, change sharply with increasing antimony concentration.

Thus, if the antimony concentration was increased to 0.25 mg/liter and over, difficult stripping was eliminated entirely. The cathode deposit had a compact structure, but dendrites were formed, the size and configuration of which depended on the antimony concentration. This suggested that modification of the zinc structure by addition of antimony to the electrolyte may be a means of eliminating difficult stripping.

At the Ust-Kamenogorsk lead- zinc combine, additions of antimony under production conditions were first tested, at Shteingart's suggestion, in May 1953. Antimony was fed into 3 cells at half-hourly intervals for 24 hours to give a concentration of 0.1- 0.3 mg/liter.

Although this method of adding antimony made stripping easier, it led to "antimonious" dissolution of the zinc and to an increase of the electric energy consumption.

Since the stripping of zinc depends only on the structure of the part of it which is in direct contact with the cathode, the author has tested and proposed a method for adding antimony only during the initial period of cathodic deposition. Antimony is now fed into each cell once a day, a few minutes before stripping of the zinc.

Single additions of antimony before stripping have been used in the Ust-Kamenogorsk zinc works for over two years, and during this time there have not been any cases of difficult stripping.

Levin [11] attributes the decrease of adherence in presence of added antimony to formation of a monomolecular $Sb(OH)_3$ film, which is actively adsorbed by the exposed aluminum crystals.

He confirmed the increased adsorption of antimony on mechanically exposed aluminum crystals by the use of tagged antimony atoms; the formation of $Sb(OH)_3$ was confirmed by physicochemical data.

In our opinion, a stable film of $Sb(OH)_3$ cannot exist on the surface of aluminum, which has a potential of 1.66 v. The increased concentration of antimony on aluminum from which the oxide film has been removed is attributable to an increased rate of precipitation of antimony in these regions.

Experiments on the precipitation of antimony in a pure, artificial, spent industrial electrolyte in presence of fluoride fully confirm the above view.

At antimony concentrations from hundredths of a milligram to some tens of milligrams per liter, antimony was precipitated by aluminum almost completely in presence of fluoride ions in our experiments (it could not be detected by the appropriate analytical methods). The precipitation of the most electropositive impurities, at low concentrations, on aluminum and other metals is confirmed by our experiments with sparingly soluble salts such as lead sulfate (solubility $1.8 \cdot 10^{-8}$), cuprous chloride (solubility $1.8 \cdot 10^{-7}$), salts of bismuth and tin, etc.

Fig. 4. Micrographs of sections made from zinc deposits with additions of antimony. 1) Zinc with antimony, 2) pure zinc.

In our opinion, the influence of antimony and other impurities in decreasing the adherence of zinc to aluminum can be attributed to changes in the microstructure of zinc, both with regard to crystal size, and to crystal orientation.

Internal stresses, in their turn, make adherence worse, and sometimes even lead to spontaneous peeling of the deposit from the support [12].

Comparison of micrographs of sections (Fig. 4) made from zinc deposits with additions of antimony, in the case of easy stripping in presence of 200 mg of fluoride per liter, with Figs. 1 and 2, which are micrographs of sections obtained without additions of antimony, confirms our views concerning the adherence of zinc to aluminum, and the conclusions drawn by the authors cited above on the causes of adherence in other metals.

While crystals of zinc deposited without addition of antimony are of elongated needlelike shape and are oriented perpendicular to the cathode surface, zinc crystals with additions of antimony are rounded and either have no definite orientation (Fig. 4,a) or weak orientation (Fig. 4,b).

The laboratory experiments on deposition of zinc from an electrolyte containing 200 mg fluoride per liter were carried out as follows. By continuous electrolysis and repeated stripping, difficult stripping requiring a force of 2 kg was attained. After this, antimony was added in the form of $Sb_2(SO_4)_3$, to give 0.27 mg/liter, to the electrolyte before the next stripping. During this stripping the zinc was removed from only one side of the cathodes.

At the end of three hours of electrolysis in the presence of antimony the stripping was repeated; it was found that on the side of the cathodes from which zinc had been removed after addition of antimony the newly formed deposit was easy to strip (with a force of 0.5 - 0.25 kg) whereas on the other sides of the cathodes the stripping was difficult (with a force of 2 kg).

Effect of chloride. Chloride was introduced into the electrolyte in the form of hydrochloric acid.

The current efficiency was determined together with the stripping force. The results of the experiments are given in Table 2.

Each line in Table 2 represents the average result of 18 experiments.

TABLE 2

Effect of Chloride on the Stripping of Zinc

Chloride concentration in electrolyte (in mg/liter)	Current efficiency (%)	Type of stripping
0	95.0	Easy (0.25 -0.5 kg)
100	93.7	
200	93.4	
300	93.2	
400	92.4	
800	91.7	
1200	90.4	

The results confirm the earlier findings of Zosimovich, Ilyenko, et al. concerning the decrease of current efficiency with increasing chloride concentration in the electrolyte. The stripping of zinc remained easy at all chloride concentrations.

It was noted that at chloride concentrations of 300 mg/liter and over the zinc deposit acquires a silvery luster. Analysis of this zinc revealed a considerably increased lead content.

Fig. 5 illustrates the difference between the microstructure of pure zinc, obtained from an electrolyte in absence of chloride ions, and that of zinc obtained in presence of 1 g chloride per liter (the chloride was introduced in the form of $AlCl_3$).

This shows a transition from the usual needlelike structure of the zinc crystals, oriented perpendicular to the cathode surface, to small crystals with weak orientation.

A similar zinc structure is obtained if the lead content in the zinc deposit is increased by continuous introduction of Pb^{++} into the interelectrode space.

Fig. 5. Micrograph of a section obtained from a deposit formed with 1000 mg Cl per liter in the solution. 1)Pure zinc, 2)zinc in presence of Cl.

Fig. 6. Microstructure of zinc with addition of lead. 1)With addition of 0.2% Pb; 2)pure zinc.

Figure 6 is a micrograph of a section which represents the change produced in the structure of the zinc by 0.2% of lead. The needlelike form of the zinc crystals deposited before addition of Pb^{++} to the solution was replaced by a fine crystalline structure characteristic of zinc containing lead. The above clearly reveals the role of chloride, which consists of the transfer of lead from the anodes to the solution and its deposition together with zinc.

In evaluation of the influence of chloride on the adherence of zinc to aluminum it should be remembered that, apart from changes in the structure of the zinc caused by increases in the amount of lead present, fluoride and chloride ions have different corrosive effects on aluminum.

Our experiments on the dissolution of aluminum in spent works zinc electrolyte in presence of fluoride and chloride ions show that the rate of solution of aluminum in presence of up to 2 g chloride ions per liter is the same as in spent electrolyte without chloride, and is several times less than the rate resulting from the action of fluoride ions.

For example, with 660 mg of fluoride or chloride per liter in the spent electrolyte, the amount of aluminum dissolved in 1 hour by the action of fluoride is 0.3 g per 1 m^2 of metal area, while under the action of chloride or in the "pure" spent electrolyte the amount is 0.03 g per 1 m^2.

Consequently, the presence of chloride in the electrolytic deposition of zinc does not cause destruction of the aluminum cathodes, but it results in destruction of the lead anodes, increases the lead content of the zinc, with corresponding changes in the structure of the zinc and a decrease of current efficiency.

Effect of cobalt. As was reported earlier [7], cobalt favors the occurrence of difficult stripping of zinc.

This was confirmed by laboratory experiments. Thus, if the electrolyte contains 15 mg Co and 50 mg F per liter, difficult stripping requiring a force of 2.5 kg commences three strippings earlier than if cobalt is absent. The possibility is not excluded that cobalt forms a microcell with aluminum, in which the latter acts as a corroding anode. It is also possible that cobalt dissolves the zinc and thus makes it possible for fluoride and sulfate ions to penetrate to the aluminum surface, where they can exert prolonged action on the protective film on the aluminum, leading to formation of pits and sites where the zinc can become embedded in the aluminum.

We have not as yet succeeded in finally establishing the mechanism of the action of cobalt on the type of stripping. We are inclined to believe that the second hypothesis is more probable.

In Fig. 3, two "cobalt" pits can be seen on the cathode surface, coinciding in position and diameter with the holes through the zinc. It was found that the depth of these pits increases with increasing time during which fluoride and sulfuric acid act.

It is known that cobalt greatly lowers current efficiency. However, in presence of low concentrations of antimony or other metals, leading to formation of dense finely crystalline zinc deposits, microcouples of zinc and cobalt are not formed. With increasing antimony concentration and the formation of finely crystalline but loose zinc deposits, the dissolution due to cobalt is greater for the same concentration of it in the solution. In our opinion, the explanation for this is as follows. Metallic impurities which are more electropositive than zinc and which do not form solid solutions or chemical compounds with zinc in electrolysis (for example, Cu, Co, and Ni) form microcouples with it.

For the formation of a microcouple the crystal nucleus of a given impurity must reach a critical mass when it can form a microcell with zinc.

Concentration of the molecules of the impurity up to the critical mass is possible only when their ions have enough time for free penetration to the crystallization center of the particular impurity. If the zinc is deposited in the form of densely packed fine crystals, the deposited impurity is rapidly covered over by newly forming and growing zinc crystals, without reaching the critical mass.

If the zinc is deposited in large crystals (pure zinc), the growth of which takes a considerable time, or, conversely, in small crystals which are loosely packed or separate, concentration of molecules of the impurity up to the critical mass is possible. Knowing the influence of impurities on the microstructure of the zinc, we can to some extent prevent the dissolution of zinc resulting from the action of microcouples.

Naturally, attainment of the critical mass by the impurity forming microcells with zinc depends on its concentration, potential, polarization, etc.

Effect of tin. Spectroscopic analysis of the zinc dusts and sublimates showed them to contain tin and bismuth. Small amounts of these metals were at times detected also in the electrolytes. It was found in laboratory experiments that tin, even at low concentrations, decreases the current efficiency. For example, a single addition of 2 mg Sn per liter decreases the current efficiency during deposition by 6.4%; in prolonged electrolysis at a constant concentration of 0.1 mg tin per liter, without addition of glue, the current efficiency decreases by 4%.

In investigations of the influence of tin on the structure and stripping of zinc it was found that additions of tin alter the structure of the zinc and prevent difficult stripping. Fig. 7 represents the structure of zinc obtained after a single addition of 2 mg tin per liter at the start of electrolysis.

It is seen from Fig. 7, that the zinc has a finely crystalline structure and loses the crystal orientation and needlelike form completely, so that internal stresses arise and adherence to aluminum is prevented. Tin, like lead, confers a silvery luster to zinc and makes it brittle when bent.

Since tin greatly decreases current efficiency and has an adverse effect on the zinc quality, it cannot be used for prevention of difficult stripping.

Effects of bismuth, lead, and other impurities. At high concentrations in the electrolyte, bismuth prevents difficult stripping of zinc.

For example, in presence of 500 mg of fluoride per liter, difficult stripping requiring a force of 2.5 kg decreases to 0.5 kg after a single addition of 30 mg of bismuth per liter.

By paralyzing the harmful action of cobalt and other impurities, bismuth increases the current efficiency somewhat.

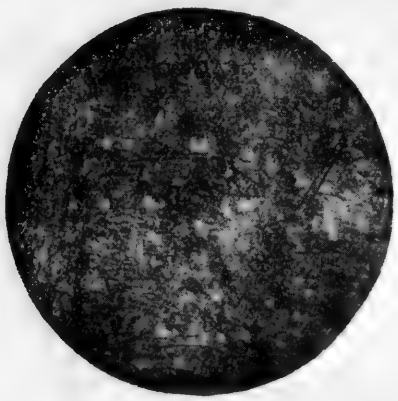

Fig. 7. Microstructure of zinc with addition of tin.

The effects of iron, vanadium, molybdenum, chrominum, and cadmium on stripping were tested; these were added in the following amounts (in mg/liter): iron up to 200, vanadium 4-8, molybdenum up to 4, chromium up to 50, cadmium up to 20. With the exception of iron, these impurities in the concentrations tested did not have any significant effects on the zinc structure or current efficiency.

Iron in amounts up to 200 mg/liter causes some changes in the zinc structure and a decrease of current efficiency; this is in agreement with the findings of Turamshina and Stender [13]. Neither iron nor any of the other impurities mentioned above prevent difficult stripping.

Variations of current density between 200 and 1100 amp./m^2 have no significant effects on the stripping.

The structure of the zinc is changed on increase of the current density: the zinc crystals retain their orientation and needlelike form only at the start of electrolysis if the current density is increased.

SUMMARY

1. Difficult stripping of zinc in its electrolytic production is caused by molecular and mechanical forces of adhesion between the aluminum and the zinc.

2. The adherence due to molecular forces is determined by the extent of the aluminum surface free from protective film; the mechanical adherence depends on the degree of corrosion of the cathode surface.

3. The extent of removal of the oxide film and corrosion of the cathode surface directly depend on the fluoride concentration in the solution and the total time of action of the fluoride between the stripping of the zinc and complete coating of the cathode with a new layer of zinc.

4. The microstructure of the zinc, and therefore the ease of stripping, and also the current efficiency, are influenced by a number of impurities, which can be divided into three groups: a) impurities which cause changes in the microstructure of the zinc, occurrence of internal stresses, and decreased adherence, and which affect the current efficiency (Sb, Sn, Bi, Pb, and others); b) impurities which do not affect the microstructure of the zinc but form microcells with it and favor difficult stripping (Co, Ni, Cu, and others); c) impurities which do not affect the microstructure of the zinc or the current efficiency (Cr, Mo, V, etc.). The classification of these impurities applies to concentrations in the electrolyte which are possible in practice.

5. The degree of the influence of an impurity on the adherence of the zinc deposit is determined by the degree to which it affects the form, dimensions, and orientation of the zinc crystals.

6. Variations of current efficiency are inevitably connected with changes of the zinc microstructure.

LITERATURE CITED

[1] Yu. V. Baimakov, Electrolysis in Metallurgy, 1 (1939) p. 339.

[2] D.P. Zosimovich and N.O. Ilyenko, Nonferrous Metals 2 (1949).

[3] A.I. Levin, A.V. Pomosov, and T.A. Tkachenko, Nonferrous Metals 1 (1952).

[4] G.M. Shteingart, Nonferrous Metals 5 (1954).

[5] S. Pletnev and G. Rozov, Nonferrous Metals 11 (1938).

[6] V.A. Lyubchenko, Nonferrous Metals 9 (1938).

[7] V.L. Kilmenko, Nonferrous Metals 5 (1952).

[8] A.T. Vagramyan and Z.A. Solovyeva, Methods of Investigation of the Electrodeposition of Metals (1947).*

[9] D.I. Mendeleev, Principles of Chemistry, II.*

[10] G.V. Akimov, Bull. Acad. Sci. USSR (1945).

[11] L.I. Levin, "Effect of Antimony on Difficult Stripping of Zinc" Paper at Conference of U.K.S.Ts.K and All-Union Scientific Research Institute for Nonferrous Metals (1956).

[12] K.M. Gorbunova and O.S. Popova, J. Phys. Chem. 30 (1955).

[13] U.F. Turamshina and V.V. Stender, J. Appl. Chem. 27, 4 (1955).

Received January 2, 1956

*In Russian.

KINETICS OF REACTIONS ON AGING CATALYSTS

D.P. Dobychin

The question of the dynamics of processes on aging catalysts has been examined and a general solution has been found. It was shown by Todes [1] that the concentration of the original substance C(x, t) at the exit from the reactor and the initial concentration C_0 at the entry into the reactor are connected by an exponential relationship of the type

$$C_{(x,\ t)} = C_0 \cdot \exp\left\{-\frac{1}{u}\int_0^x a\left((y,\ t-\frac{x-y}{u}\right)dy\right\} =$$

$$= C_0 \cdot \exp\left\{-\int_{t-\frac{x}{u}}^{t} a\,[x-u\,(t-\theta),\ \theta]\,d\theta\right\} \qquad (1)$$

when $t > \frac{x}{u}$. Here x is the length of the catalyst layer, y is its running coordinate (from y = 0 to y = x), t is the time, and u is the linear speed of the gas stream. Consequently, $\frac{x}{u} = \tau$ is the contact time. A portion of gas moving uniformly with velocity u passes across the section y in time $\theta = t - \frac{x-y}{u}$, and the activity of the catalyst at time θ in the section y is

$$a_{\theta,\ y} = a\left(y,\ t-\frac{x-y}{u}\right) = a\,[x-u\,(t-\theta),\ \theta]. \qquad (2)$$

This is the general expression for the variation of catalyst activity with time (t) and position in the reactor (y). The litature contains no solutions for actual particular cases.

In a stationary layer with the whole material aging simultaneously, the activity of the catalyst is a function of the time only:

$$a = a\,(t-\frac{x-y}{u}). \qquad (3)$$

We shall examine the two most typical cases of kinetics of reactions on aging stationary catalysts, namely: 1) the activity falls at a constant rate with time until a certain constant final value a_f is reached; 2) the activity decreases exponentially with time and tends to zero.

In the first case

$$a_t = a_f - \alpha\,(t-t_0) = a_0 - \alpha t \qquad (4)$$

until $t = t_0$ is reached, after which $a_t = a_f$. Here t_0 is the time needed for the activity of the catalyst to decrease from the initial value a_0 to a_f.

From Equation (1), with Equations (3) and (4) taken into account, we have:

$$C_{(x,\ t)} = C_0 \cdot \exp\left\{-\frac{1}{u}\int_0^x \left[a_0 - \alpha\left(t - \frac{x-y}{u}\right)\right] dy\right\}$$

and

$$C_{(x,\ t)} = C_0 \cdot e^{-\left(a_0 - \alpha t + \frac{\alpha\tau}{2}\right)\tau} \tag{5}$$

Equation (5) is valid until time $t = t_0$ is reached, after which $a_t = a_f$ and

$$C(x, t) = C_0 \cdot e^{-a_f \tau}.$$

If the catalytic activity decreases exponentially with time

$$a_t = a_0 \cdot e^{-\alpha t}. \tag{6}$$

Then

$$C_{(x,\ t)} = C_0 \cdot \exp\left\{-\frac{1}{u}\int_0^x a_0 \cdot e^{-\alpha\left(t - \frac{x-y}{u}\right)} dy\right\}$$

and

$$C_{(x,\ t)} = C_0 \cdot e^{-\frac{a_0}{\alpha}\left(e^{-\alpha(t-\tau)} - e^{-\alpha t}\right)}$$

or

$$C_{(x,\ t)} = C_0 \cdot e^{-\frac{a_0}{\alpha} \cdot e^{-\alpha t}\left(e^{\alpha\tau} - 1\right)} \tag{7}$$

A case of special interest is the performance of a rapidly poisoned catalyst in a system with a moving catalyst layer. Suppose that, in a reactor with a catalyst layer of volume $V = L \cdot S$ (where L is the height of the catalyst layer and S is its cross section) the catalyst moves downward, while the reacting substances are blown upward, countercurrent to the catalyst (Fig. 1), at a catalyst feed rate $\underline{v}$ (in m^3/minute) the time it remains in the reactor (ϑ) will be:

$$\vartheta = \frac{V}{v} = \frac{L}{w} \text{ (in min.)} \tag{8}$$

where $\underline{w}$ is the linear speed of the catalyst charge, given by $\underline{w} = \frac{v}{S}$ m/minute.

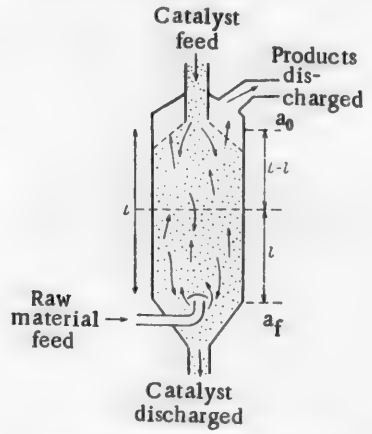

Fig. 1. Diagram of countercurrent reactor with a moving catalyst.

The activity of the fresh catalyst, which is a_0 at entry into the reaction zone, falls during the process according to the exponential law

$$a_t = a_0 \cdot e^{-\alpha t},$$

where $\underline{t}$ is the time during which the catalyst acts and α is its deactivation rate constant.

When the catalyst has traversed a distance $L-\underline{l}$ and reached the cross section $\underline{l}$ of the reactor, its activity will therefore be:

$$a_l = a_0 \cdot e^{-\alpha\frac{L-l}{w}} \tag{9}$$

The activity of the catalyst leaving the reactor will be

$$a_f = a_0 \cdot e^{-\alpha\frac{L}{w}} = a_0 \cdot e^{-\alpha\vartheta} \tag{10}$$

We assume that the reaction taking place on the catalyst conforms to a first-order kinetic law

$$-\frac{dC}{dt} = a \cdot C. \tag{11}$$

Here C is the existing concentration of the starting substance and a is the activity of the catalyst (the rate constant). The reaction time is the contact time $\tau = \frac{L}{u}$, where u is the linear speed of the reaction mixture in the reactor. Consequently,

$$-\frac{dC}{d\tau} = a \cdot C$$

or

$$-u\frac{dC}{dl} = a \cdot C$$

and

$$-\frac{dC}{C} = \frac{a}{u}\, dl. \tag{12}$$

From Equations (10) and (12) we have

$$-\frac{dC}{C} = \frac{a_0}{u} \cdot e^{-\alpha \frac{L-l}{w}} \cdot dl. \tag{13}$$

Integration between C_0 and C_L and between l = 0 and l = L gives

$$C_L = C_0 \cdot e^{-\frac{a_0 \cdot w}{\alpha \cdot u}\left(1 - e^{-\frac{\alpha L}{w}}\right)} \tag{14}$$

or

$$C_L = C_0 \cdot e^{-\frac{a_0 \tau}{\alpha \vartheta}\left(1 - e^{-\alpha \vartheta}\right)}, \tag{15}$$

where C_L is the concentration of the starting substance at the exit from the reactor, τ is the contact time of the reaction mixture, and ϑ is the time spent by the catalyst in the reactor.

Let us analyze this expression.

1. $\vartheta \to 0$; the speed at which the catalyst falls through the reactor is high in comparison with its aging speed. From the indeterminate term we have:

$$\left|\frac{1 - e^{-\alpha\vartheta}}{\vartheta}\right|_{\vartheta \to 0} = \alpha,$$

and hence

$$C_{L_{\vartheta \to 0}} = C_0 \cdot e^{-a_0 \tau}. \tag{16}$$

This is the usual expression for a reaction of the first order taking place on a stable catalyst.

2. $\vartheta \to \infty$; the time spent by the catalyst in the reactor is large compared with its characteristic aging time ($\frac{1}{\alpha}$).

$$\left|\frac{1 - e^{-\alpha\vartheta}}{\vartheta}\right|_{\vartheta \to \infty} = 0$$

and

$$C_{L_{\vartheta \to 0}} = C_0, \tag{17}$$

i.e., the catalyst is deactivated and the reaction does not proceed.

Verification and application of Equations (14) and (15) involve no difficulties. The value of α for a given catalyst can be easily determined in experiments with stationary, catalysts in laboratory conditions.

As regards τ and Θ, these may be calculated from the feed rates of the catalyst and the reacting substance (raw material) (8):

$$\tau = \frac{\varphi \cdot V}{m}. \tag{18}$$

By the accepted notation, V is the volume of the reactor (m^3); $\underline{v}$ is the catalyst feed rate (m^3/minute); m is the raw material feed rate (kg/minute); φ is a term which takes into account the free part of the catalyst volume (δ) and the volume change when the raw material passes into the gas phase:

$$\varphi = \frac{\delta}{v_0}, \tag{19}$$

where v_0 is the volume occupied by 1 kg of the raw material in the gas phase in the conditions of the particular process.

From Equations (8), (15), and (18) we have:

$$C_L = C_0 \cdot e^{-\frac{a_0}{\alpha} \cdot \frac{\varphi v}{m}\left(1 - e^{-\frac{\alpha V}{v}}\right)} \tag{20}$$

All the quantities in Equation (20) can be determined independently. The value of δ for a layer at rest is close to 0.3–0.4, while for a moving layer it may have a somewhat higher value, easily found experimentally. The value of v_0 can be found from the appropriate tables. If exact preliminary calculation of the value of φ is impossible, it can be determined from experimental data obtained in a unit with a moving catalyst. Moreover, sometimes it is possible to use the easily determined product $a_0 \cdot \varphi$ as a single constant.

We now consider the principal cases which may be met experimentally.

1) Constant catalyst feed rate (v) with a variable raw material feed rate (m).

We write Equation (20) in the form:

$$\ln \frac{C_0}{C_L} = \frac{a_0 \cdot \varphi \cdot v}{\alpha \cdot m}\left(1 - e^{-\frac{\alpha V}{v}}\right) = A \cdot \frac{\varphi}{m}, \tag{21}$$

where

$$A = \frac{a_0 v}{\alpha}\left(1 - e^{-\alpha \frac{V}{v}}\right). \tag{22}$$

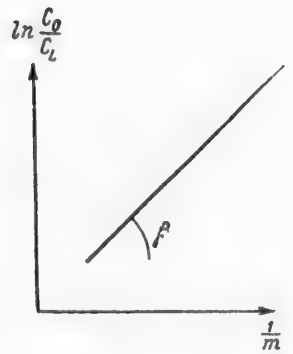

Fig. 2. Plot of $\ln \frac{C_0}{C_L}$ against $\frac{1}{m}$ for determination of φ; $\tan \beta = A \cdot \varphi$.

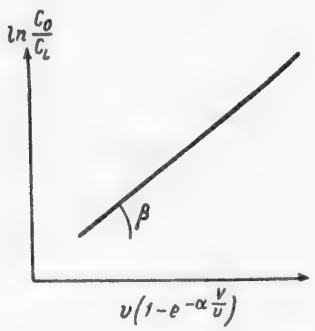

Fig. 3. Plot of $\ln \frac{C_0}{C_L}$ against $\underline{v}\left(1 - e^{-\alpha \frac{V}{v}}\right)$ for determination of φ; $\tan \beta = \frac{a_0}{\alpha m} \cdot \varphi$.

We use experimental data to plot a graph in $\ln\frac{C_0}{C_L}$ and $\frac{1}{m}$ coordinates (Fig. 2), and obtain a straight line of which the slope is given by

$$\tan\beta = A\cdot\varphi. \tag{23}$$

Since all the quantities in A are known, φ is calculated directly from Equation (23).

2) Variable catalyst feed rate (v) with a constant raw material feed rate (m).

Bearing in mind Equation (21), we use experimental data to plot a graph in $\ln\frac{C_0}{C_L}$ and $\underline{v}\left(1-e^{-\frac{\alpha V}{v}}\right)$. coordinates. The slope of the resultant straight line (Fig. 3) is given by

$$\tan\beta = \frac{a_0}{\alpha m}\cdot\varphi, \tag{24}$$

from which we calculate φ.

3) The catalyst feed rate (v) and the raw material feed rate (m) are both variable.

A straight line is plotted in $\ln\frac{C_0}{C_L}$ and $\frac{v\cdot\left(1-e^{-\alpha\frac{V}{v}}\right)}{m}$ coordinates; its slope is given by $\frac{a_0}{\alpha}\cdot\varphi$, and φ is calculated from this.

There are various ways of calculating a_0 (the initial catalyst activity) from experimental results obtained in a laboratory unit with a catalyst at rest.

The simplest method is to find $C_{L(init.)}$, corresponding to the initial activity a_0, by graphical extrapolation of the concentration C_L at the exit from the reactor to time $\underline{t} = 0$ (Fig. 4). If we know $C_{L(init.)}$, a_0 can be easily calculated from the usual equation for a 1st-order reaction

$$a_0 = \frac{1}{\tau}\ln\frac{C_0}{C_{L(init.)}}. \tag{25}$$

The more rigorous method is the more cumbersome. The experiment is continued over a considerable period, and samples of the reaction products are taken at different times t_1, t_2, etc., or during short time intervals Δt, corresponding to average times $t_1=(t'+\frac{\Delta t}{2})$, $t_2=(t'_2+\frac{\Delta t}{2})$ etc. where t'_1, t'_2 ... are the instants at which the sampling commences and Δt is the duration of sampling. We obtain a series of equations of the type of Equation (7).

Transformation gives:

$$\frac{a_0(e^{\alpha\tau}-1)}{\alpha} = \ln\frac{C_0}{C_{t_n}}\cdot e^{\alpha t_n}, \tag{26}$$

and hence

$$\ln\ln\frac{C_0}{C_{t_n}} = \ln\frac{a_0(e^{\alpha\tau}-1)}{\alpha} - \alpha t_n. \tag{27}$$

Experimental data are used to plot a graph in $\ln\ln\frac{C_0}{C_L}$ and $\underline{t}$ coordinates, which gives a straight line (Fig. 5) the the tangent of the slope of which is $-\alpha$, and the intercept cut off along the ordinate axis (b) is

$$b = \ln\frac{a_0(e^{\alpha\tau}-1)}{\alpha}. \tag{28}$$

We determine the numberical values of α and b and find a_0:

$$a_0 = \frac{\alpha\cdot e^b}{e^{\alpha\tau}-1}. \tag{29}$$

For use in calculations the value of a_0 must obviously be taken relative to unit bulk volume of the catalyst.

The author expresses his sincere gratitude to O.M. Todes for valuable advice and comments in discussion of this paper.

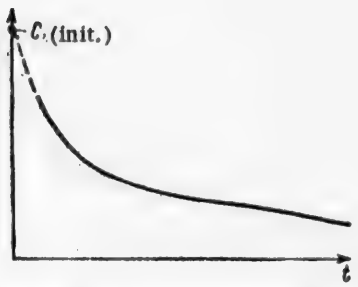

Fig. 4. Variation of the concentration of the substance at the exit from the reactor (C_L) with time (t) for determination of the initial activity (a_0).

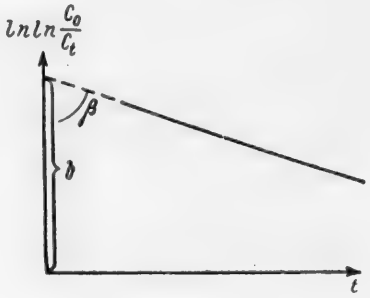

Fig. 5. Plot of $\ln \ln \frac{C_0}{C_L}$ against t for determination of a_0; $b = \ln \frac{a_0}{\alpha(e^{\alpha\tau} - 1)}$; $\tan \beta = -\alpha$.

SUMMARY

Particular solutions of kinetic equations for 1st-order processes on aging catalyst are given.

For a stationary catalyst layer, if its activity falls linearly with time until a certain constant activity (a_f) is reached:

$$C_{(x,t)} = C_0 \cdot e^{-\left(a_0 - \alpha t + \frac{\alpha\tau}{2}\right)\tau};$$

up to time t = t_0, after which

$$C_{(x,t)} = C_0 \cdot e^{-}$$

and if the activity falls exponentially with time:

$$C_{(x,t)} = C_0 \cdot e^{-\frac{a_0^2}{\alpha} \cdot e^{-\alpha t} \cdot (e^{\alpha\tau} - 1)}$$

For a moving catalyst layer, if its activity falls exponentially with time of use, in countercurrent flow of the catalyst and reacting substances:

$$C_L = C_0 \cdot e^{-\frac{a_0}{\alpha} \cdot \frac{\tau}{\vartheta}(1 - e^{-\alpha\vartheta})}$$

LITERATURE CITED

[1] O.M. Todes, Bull. Acad. Sci. USSR, Div. Chem. Sci. 5, 483 (1946).

Received September 17, 1955

KINETICS OF THE ABSORPTION OF NO BY $FeSO_4$ SOLUTIONS IN HIGH-SPEED MECHANICAL ABSORBERS

S.N. Ganz and L.I. Mamon

In earlier papers [1] we dealt with static aspects of the absorption of nitric oxide by solutions of $FeSO_4$ and other salts. It is clear from the published data that $FeSO_4$ solutions have fairly high chemical capacity, so that their practical utilization is feasible. Our investigations of the rate of absorption of NO by $FeSO_4$ solutions in laboratory and semiworks conditions in packed towers showed that the rate of absorption of NO by 10% aqueous $FeSO_4$ solution is approximately double the rate of absorption of N_2O_3 by 15% Na_2CO_3 solution under the same conditions. The semiworks scale experiments were carried out with continuous circulation of the liquid and gas feed, as shown in Fig. 1. The nitrose gas was fed into the tower (1) from below and left the tower through the

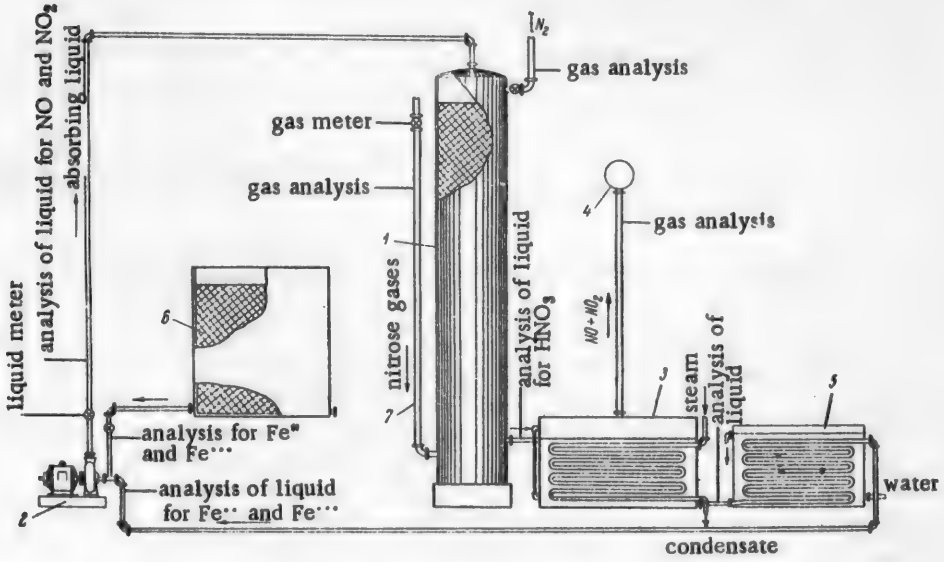

Fig. 1. Diagram of a semiworks unit for absorption of nitric oxide by $FeSO_4$ solution. 1) Absorption tower, 2) centrifugal pump, 3) regenerator, 4) collector, 5) cooler, 6) tank for $FeSO_4$ solution, 7) pipe for nitrose gas.

outlet pipe at the top. The $FeSO_4$ solution was fed into the tower by a centrifugal pump (2) and moved countercurrent to the gas, absorbing NO and NO_2. At the exit from the tower the solution containing NO was regenerated in the regenerator (3) at 90-100°. The degree of regeneration of the solution reached 98-100%, and the solution became light blue again after being dark brown. The concentrated nitrogen oxides liberated during the regeneration were conducted to the nitric acid absorption system through the collector (4). The solution

from the regenerator passed into the cooler (5), where it was cooled to 25-30°, and then returned to the tower (1) by the centrifugal pump (2). Fresh solution was fed into the system from the tank (6).

When the oxygen content of the gas was between zero and 2-3%, the solution could be used for a considerable time without renewal, and its absorbing power did not diminish. Increase of the oxygen content above 3% leads to gradual oxidation of $FeSO_4$ to $Fe_2(SO_4)_3$, the oxidation rate increasing with increasing contents of oxygen and NO_2 in the gas. The same experiments showed that the absorption of nitrogen oxides in packed towers proceeds at an adequate rate when their contents in the solution are 0.3% and over.

If the concentration of nitrogen oxides falls below 0.2-0.3% the absorption rate falls.

Since in practical conditions it is sometimes necessary to absorb nitrogen oxides at very low concentrations, we studied the rate of absorption of NO with the gas and liquid stirred vigorously in a high-speed mechanical absorber. The results of these experiments are given below.

EXPERIMENTAL

The apparatus shown schematically in Fig. 2 was used for absorption of nitrogen oxides by $FeSO_4$ solution.

The mechanical absorber (1) consisted of a horizontal cylinder, with a shaft bearing four disks lying along its axis. The ends of the absorber were closed by lids with packing glands for the shaft. The latter was joined to the motor (2) by an elastic coupling; the motor speed was variable between 200 and 5000 revolutions/minute with the aid of a rheostat.

The disks of the mechanical absorber were cut from the periphery along 1/3 of the diameter, the ends being bent over to form vanes, and the disk surfaces were perforated plates with holes 7 mm in diameter. The purpose of the holes was to allow the gas to pass freely. The diameter of the absorber was 47 mm, its length was 225 mm, its volume was 270 cc, and the disks were 42 mm in diameter.

The gas entered the absorber from below and moved countercurrent to the liquid, the speed of which was regulated by a stopcock. The gas was fed into the absorber from the mixing vessel (3). Nitric oxide was obtained by the action of a strong solution of $NaNO_2$ on $FeSO_4$ solution acidified with sulfuric acid.

After the absorber, the gas escaped into the atmosphere through a side tube and the liquid trap (4). The stopcocks (5) were used for taking the gas samples for analysis. The initial NO content of the gas (nitrogen) was determined in the gas holder (6).

The solution of $FeSO_4$ entered the absorber from the graduated supply vessel (7) through a lower inlet in the absorber wall, opposite to the gas inlet. The amount of solution was determined by means of a graduated scale on the vessel wall. The amount of liquid in the absorber was 25-30% of its volume.

The absorption coefficients were determined for different nitric oxide concentrations in the gas, volume flow rates, shaft speeds, and concentrations of $FeSO_4$ in the solution. The NO content of the gas at entry and exit was determined by the following method. Glass gas-sampling vessels 500 cc in volume were previously dried, evacuated, and filled with oxygen. Half the volume of oxygen from the sampling vessel was removed by means of a vacuum pump; this was checked with the aid of a contact manometer. The sampling vessel was then filled with the gas to be tested. Because of the considerable excess of oxygen, even very small amounts of NO were rapidly oxidized. After 60-80 seconds, 15-25 cc of 3% hydrogen peroxide solution was let into the sampling vessel, which was shaken mechanically for 3-4 hours; the NO became oxidized to HNO_3, the content of which was determined by titration with 0.1 N NaOH solution in presence of methyl red indicator.

Effect of peripheral disk speed. The rotation speed of the shaft (or the peripheral disk speed) largely determines the hydrodynamic conditions in the apparatus.

The experiments were carried out at a constant volume flow rate $\underline{w}$ = 500 $m^3/m^3 \cdot$ hour, with 0.9-1.15% nitric oxide in the gas, 20% $FeSO_4$ in the solution, and a temperature of 20-21°. The peripheral speed of the absorber disks was varied between 2.05 and 10.45 m/second. The experimental data are plotted in Figs. 3 and 4 and given in the Table.

Analysis of these data leads to the conclusion that the absorption coefficient k_v depends to a considerable extent on the peripheral disk speed.

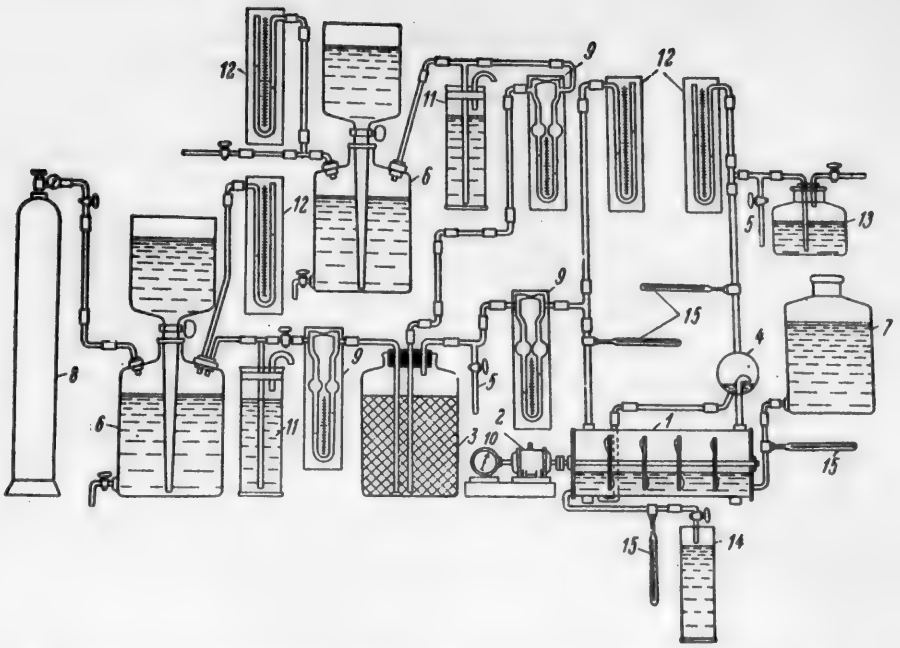

Fig. 2 Scheme of a laboratory assembly for absorption of NO by $FeSO_4$ solution in a high-speed mechanical absorber. 1) Absorber, 2) electric motor, 3) mixing vessel, 4) liquid trap, 5) stopcock for gas sampling, 6) gas holder, 7) supply vessel, 8) nitrogen cylinder, 9) rheometers, 10) tachometer, 11) manostats, 12) manometers, 13) water seal, 14) solution receivers, 15) thermometers.

Figure 3 shows that the absorption coefficient K_V first rises and then falls with increasing peripheral disk speed.

Variation of Absorption Coefficients with Hydrodynamic Conditions in the Absorber

Experiment No.	NO content of gas (in %)		ΔP_{av} (in atm.)	Shaft speed n_s (in rpm)	Absorption coefficient K_V (in kg/m³·hr atm)	Peripheral disk speed v_d (in m/sec.)
	before absorption	after absorption				
1	1.07	0.25	0.00575	2500	980	5.25
2	1.07	0.23	0.0055	3000	1080	6.28
3	0.91	0.22	0.00482	4000	972	8.4
4	0.91	0.21	0.00464	4000	1038	8.4
5	0.95	0.24	0.00515	4000	946	8.4
6	0.90	0.25	0.0051	5000	872	10.25
7	1.07	0.29	0.00595	5000	896	10.25
8	1.15	0.25	0.00593	3000	1040	6.28
9	1.15	0.535	0.0081	1000	522	2.05
10	1.15	0.314	0.00645	2000	892	4.1
11	0.97	0.47	0.00652	1000	526	2.05
12	0.98	0.64	0.0081	500	289	1.03
13	0.98	0.65	0.00825	500	274	1.03
14	0.93	0.72	0.0087	250	159	0.50
15	0.91	0.40	0.0062	1200	569	2.5
16	0.94	0.25	0.00522	2000	910	4.1

The most rapid absorption of NO occurs at n_s = 3000 revolutions/minute which corresponds to a peripheral disk speed of 6.5 m/second (for our absorber). The absorption of NO decreases with further increase of the shaft speed, probably because the liquid is forced against the absorber walls by centrifugal force and a space more or less free from liquid drops and foam is formed along the absorber axis. Gas-liquid contact in this axial space is less effective. Moreover, the effect noted by Kuzminykh [2] in a study of absorption on horizontal sieve plates

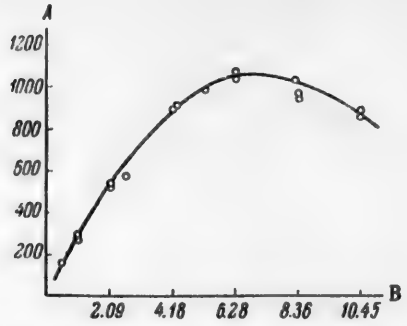

Fig. 3. Variation of absorption coefficient with peripheral disk speed. A) Absorption coefficient (in kg/m³·hr atm), B) peripheral disk speed (in m/sec)

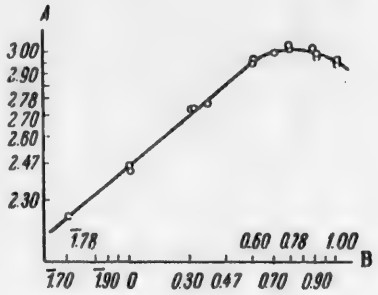

Fig. 4. Variation of absorption coefficient with peripheral disk speed. A) log K_V, B) log v_d.

is also found here. Kuzminykh reports that when the gas speed exceeds 0.3 m/second (for the effective cross section of the plate), the foam structure breaks down and the foam layer decreases, leading to a decrease of the phase contact area. In our case, when the peripheral disk speed exceeds 6.5-7 m/second, the foam layer also undergoes deformation, the liquid becomes denser at the absorber walls, and phase contact deteriorates. At peripheral disk speeds below 6-6.5 m/second the mixing of the liquid with the gas is less effective, and as a result the phase contact again deteriorates and the rate of absorption falls.

It follows from the above that there is an optimum hydrodynamic regime, determined by the appropriate shaft speed, at which the process is most rapid. If this shaft speed is exceeded or diminished, the absorption rate falls.

It may be concluded from this series of experiments that the relationship between the absorption coefficient and the peripheral disk speed can be represented by the general equation

$$K_V = A \cdot v_d^a, \quad (1)$$

since the plot of $K_V = f(v_d)$ in the logarithmic coordinates (log K_V, log v_d) is linear up to the point of inflection (Fig. 4). The region beyond the point of inflection is of no practical interest and is not represented by Equation (1).

Generalization of the experimental data yielded the following expression:

$$K_V = 276 \cdot v_d^{0.82}, \quad (2)$$

where v_d is the peripheral speed of the disks in the mechanical absorber (in m/second).

Variation of absorption rate with the partial pressure of NO in the gas. The experiments in this series were performed at a constant gas volume rate $\underline{w}$ = 500 m³/m³·hour, with 20% $FeSO_4$ solution at 20°.

The disk speed was varied in each group of experiments between 1000 and 5000 revolutions/minute, and the nitric oxide concentration in the gas, from 0.2 to 2.6%. Preliminary study of the process indicated that the rate of absorption of NO depends to a considerable extent on its concentration in the gas, and is represented by the equation

$$\frac{G}{\tau \cdot v_a} = K_V \cdot \Delta P_{av}, \quad (3)$$

where G is the amount of gas absorbed (in kg), v_a is the volume of the absorber (in m^3), τ is the duration of absorption (in hours), K_v is the coefficient of absorption (in $kg/m^3 \cdot hr.\ atm.$) and

$$\Delta P_{av} = \frac{(P'_g - P''_1) - (P''_g - P'_1)}{2.3 \log \frac{P'_g - P''_1}{P''_g - P'_1}},$$

where P_g is the initial pressure of nitric oxide in the gas, P''_1 is the pressure of nitric oxide over the liquid at the exit from the absorber, P''_g is the final pressure of nitric oxide in the gas, and P'_1 is the pressure of nitric oxide over the liquid at the entry into the absorber.

The results of this series of experiments are plotted in Figs. 5 and 6.

It may be concluded from these results that under given hydrodynamic conditions the rate of absorption of NO is proportional to the partial pressure of nitric oxide in the gas.

It is seen in Fig. 5 that the straight lines for the variation of the rate of absorption of NO with the partial pressure of nitric oxide pass through the coordinate origin. This indicates that in these hydrodynamic conditions and in this range of gas and liquid concentrations the partial pressure of NO is the entire motive force of the absorption process. Consequently, the above kinetic equation

$$\frac{G}{\tau \cdot v_a} = K_v \Delta P_{av}$$

correctly represents the process of nitric oxide absorption in these conditions.

The validity of this equation can be confirmed by plotting, on the basis of experimental data, the coefficients of absorption against the partial pressures of NO in the gas. This gives straight lines parallel to the

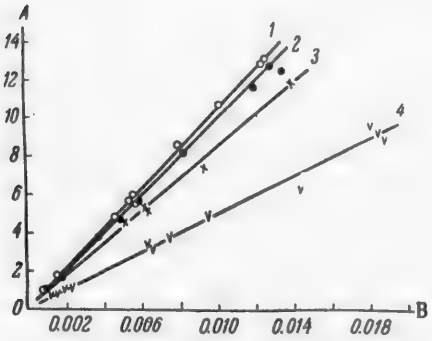

Fig. 5. Variation of absorption rate with the partial pressure of NO in the gas. A) Absorption rate (in $kg/m^3 \cdot$ hour), B) partial pressure of NO in the gas (in atm). Speed of the mechanical absorber shaft (in rpm): 1) 3000, 2) 4000, 3) 5000, 4) 1000.

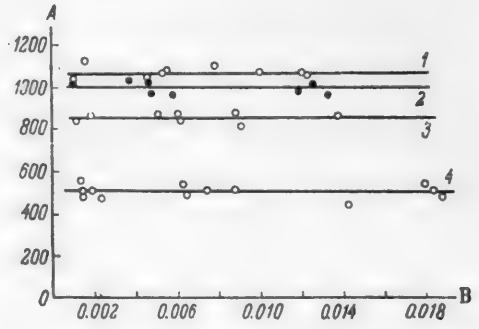

Fig. 6. Variation of absorption coefficient with the partial pressure of NO in the gas. A) Absorption coefficient (in $kg/m^3 \cdot$ hour-atm), B) partial pressure of NO in the gas (in atm). Speed of the mechanical absorber shaft (in rpm): 1) 3000, 2) 4000, 3) 5000, 4) 1000.

abscissa axis, as is seen in Fig. 6, and confirms that in our experimental conditions the rate of absorption depends on the partial pressure of NO in the gas, while the fact that the absorption coefficient K_v is constant confirms the validity of the kinetic Equation (3).

Consequently, the rate of absorption of NO depends both on the partial pressure of NO in the gas, and on the hydrodynamic conditions in the mechanical absorber, and the kinetic Equation (3), which represents this relationship, can be written in the form

$$\frac{G}{\tau \cdot v_a} = 276 \cdot v_d^{0.82} \cdot \Delta P_{av}. \qquad (4)$$

Variation of the degree of absorption with the volume rate of gas flow. The most important factor determining the efficiency of the process is the relationship between the degree and the rate of absorption under given temperature conditions. In our experiments the relationship between these two factors was studied under the following conditions: n_s = 3000 revolutions/minute, and NO concentrations in the gas 1.95, 1.22 and 0.46%. The volume flow rate was varied between 130 and 1300 $m^3/m^3 \cdot$ hour, corresponding to phase contact times between 30 and 2.8 seconds.

The experiments were carried out at 20° and 20% $FeSO_4$ in the solution. The results of this series of experiments are given in Fig. 7. Figure 8 gives the variation of the absorption coefficient with the volume flow rate, the NO concentration in the gas being 1.2%.

The direction of the curves in Fig. 7 shows that as the volume rate increases, the absorption rate rises rapidly at first, reaches a maximum, and begins to decrease.

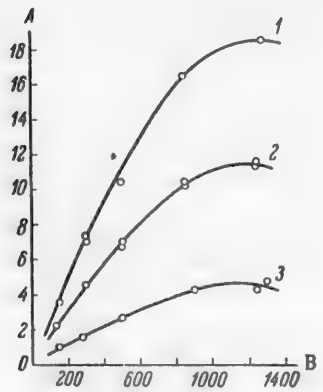

Fig. 7. Variation of the rate of absorption of nitric oxide by $FeSO_4$ solution with the volume rate of gas flow. A) Absorption rate (in $kg/m^3 \cdot$ hour), B) volume rate (in $m^3/m^3 \cdot$ hour). Concentration of NO in gas (in %): 1) 1.95, 2) 1.22, 3) 0.46.

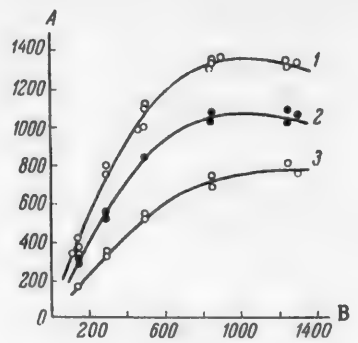

Fig. 8. Variation of the coefficient of absorption of NO by $FeSO_4$ solution with the volume rate of gas flow and the hydrodynamic conditions in the apparatus. A) Coefficient of absorption (in $kg/m^3 \cdot$ hour-atm.), B) Volume rate (in $m^3/m^3 \cdot$ hour). Peripheral disk speed in mechanical absorber (in m/second): 1) 6.28 2) 10.25, 3) 2.05.

The explanation of this course of the curves is that the rate of absorption depends mainly on the hydrodynamic process conditions. The absorption rate ($\frac{G}{\tau \cdot v_a}$) rose rapidly with increasing volume rate of gas flow, with a relatively small change of the motive force of absorption ΔP_{av} in our experiments.

The increase of the coefficient of absorption with increasing volume rate of gas flow is partially attributable to more vigorous pneumatic mixing of the gas and liquid as the linear gas speed increases up to a definite limit.

If the optimum volume rate is exceeded, the hydrodynamic conditions in the apparatus deteriorate. As was formerly noted by Kuzminykh [2], we found that when the linear gas speed exceeded 1.7 - 1.8 m/second (calculated on the free section of the absorber) the foam layer diminished, while with further increase of the gas speed the foam became detached, with deterioration of phase contact and decrease of the rate of absorption.

Thus, increase of the linear gas speed up to definite values plays a positive role, but beyond the optimum values the effect of this factor is reversed.

The results obtained were used to plot the relationship between the absorption coefficient K_w and the volume rate of gas flow $\underline{w}$ in logarithmic coordinates (log k_w, log $\underline{w}$) for each set of hydrodynamic conditions studied. This relationship is plotted in Fig. 9, and can be represented by the equation

$$K_w = A \cdot w^b, \qquad (5)$$

where K_w is the absorption coefficient (in kg/m^3 · hr-atm), $\underline{w}$ is the volume rate of gas flow (in m^3/m^3 · hour), and A and $\underline{b}$ are constants.

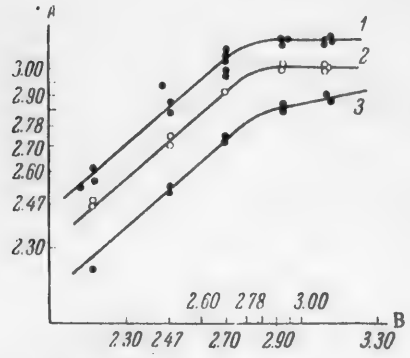

Fig. 9. Variation of the absorption coefficient with the volume rate and hydrodynamic conditions in the apparatus. A) log K_w, B) log $\underline{w}$. Peripheral disk speed (in m/sec): 1) 6.28, 2) 10.25, 3) 2.05.

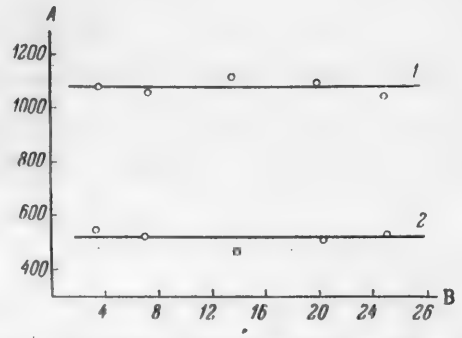

Fig. 10. Variation of the absorption coefficient with the $FeSO_4$ concentration. A) Absorption coefficient (in kg/m^3 · hour-atm), B) solution concentration (in %). Peripheral disk speed (in m/sec): 1) 6.28, 2) 2.05.

The experimental data gave the following expression for the absorption coefficient K_w as a function of the volume rate (w):

$$K_w = A \cdot w^{0.86} \qquad (6)$$

Here the constant A has the following values under different hydrodynamic conditions:

at v_d = 2.05 m/second A = 2.57,
at v_d = 6.28 m/second A = 5.3,
at v_d = 10.25 m/second A = 3.89.

Evidently Equation (6) is valid for volume rates not over 900 m^3/m^3 · hour.

Variation of the absorption coefficient with the $FeSO_4$ concentration in solution. These experiments were carried out at peripheral disk speeds v_d = 6.28 and 2.05 m/second, at a constant gas concentration of 1.5%, with volume rate $\underline{w}$ = 500 m^3/m^3 · hour, at 20°, with the $FeSO_4$ concentration varied from 3.4 to 25.2%.

The results of the experiments are plotted in Fig. 10, from which it follows that the absorption coefficient is practically independent of the $FeSO_4$ concentration, but depends on the hydrodynamic conditions in the apparatus.

The explanation is that in conditions of vigorous mixing of the gas and liquid phases the rate of hydrodynamic mass transfer and the coefficient of the rate of solution of the gas in the liquid phase are very considerable and do not control the absorption process.

SUMMARY

1. The absorption of nitric oxide by $FeSO_4$ solutions in conditions of vigorous mixing of the gas and liquid phases proceeds at a considerable rate, higher than the rate of absorption of nitrogen oxides by solutions of alkalies under the same conditions.

The results of the experiments show that absorption of NO by $FeSO_4$ solutions in high-speed mechanical absorbers can be effected fairly completely at volume rates of 500 - 900 m^3/m^3 · hour, which is many times more rapid than the absorption of nitrogen oxides by alkalies in packed towers.

2. If the gas and liquid are mixed vigorously, nitrogen oxides are rapidly absorbed at low concentrations; this is of great practical importance. This characteristic of the absorption process during vigorous mixing of the

phases makes it possible to absorb very low concentrations of nitrogen oxides, and thereby to improve sanitary and hygienic conditions in nitric acid, sulfuric acid, and other works. This is confirmed by data published by us earlier [3]. Therefore, low concentrations of nitrogen oxides can be removed from gases by means of weak spent pickling liquors from metal-treatment works, containing 1.5 -3% $FeSO_4$, the liquors being then discharged into effluent; or by means of concentrated solutions containing 17 -25% $FeSO_4$, with subsequent regeneration of the solution and recovery of the nitrogen oxides in concentrated form.

LITERATURE CITED

[1] S.N. Ganz and L.I. Mamon, J. Appl. Chem. 26, 10 (1953); 3 (1957).*

[2] I.N. Kuzminykh et al., J. Appl. Chem. 27, 2, 86 (1954).

[3] S.N. Ganz and S.B. Kravchinskays, J. Appl. Chem. 28, 2 (1955).

Received June 28, 1955

*Original Russian pagination. See C.B. Translation.

"SEPARATING LINES" OF DISTILLATION AND RECTIFICATION OF TERNARY SYSTEMS*

I.N. Bushmakin and I.N. Kish

The A.A. Zhdanov State University, Leningrad

Simple distillation and rectification processes in ternary systems often involve complications which may be attributed to separation of the triangular composition diagrams into distillation and rectification regions.

The question of the division of triangular diagrams into these regions is of practical and theoretical interest. This question has not been finally solved as yet. The purpose of the present paper is to discuss the still unsettled questions relating to separating lines of distillation and rectification.

Separating Lines of Distillation

The portion of the composition triangle occupied by a single family of distillation lines is termed a distillation region. A distillation line is a line representing the change of composition of the solution in simple distillation. Distillation lines originating from the same point in the composition triangle and terminating in another common point constitute a family.

Families of distillation lines are separated from each other by "separating lines of distillation", and the composition triangle is therefore divided into distillation regions. If we start with a solution belonging to one distillation region, we cannot obtain a solution belonging to another distillation region by means of distillation (in some instances the final solution compositions are the same for two adjacent distillation regions).

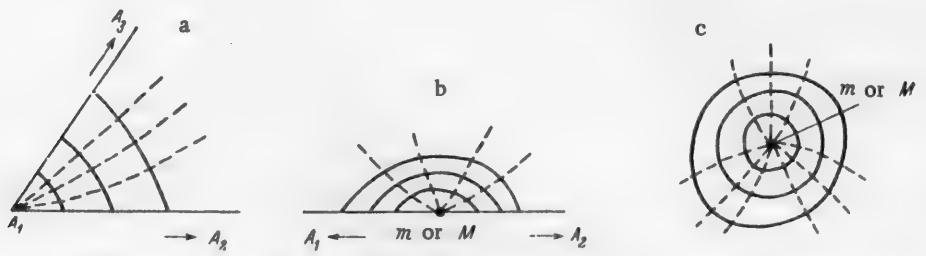

Fig. 1. Continuous lines—isotherm-isobars; dash lines—distillation lines. Explanation in text.

Schreinemakers [1] and others [2, 3] have shown that distillation lines can originate or terminate only in the vertices of the composition triangles or at azeotropic points. According to these authors, vertices and azeotropic points of the composition triangle are divided into two groups: 1) vertices or azeotropic points which are the extreme (initial or final) points of the distillation lines; 2) vertices or azeotropic points near which the distillation lines have a hyperbolic course.

*Paper III in the series on distillation and rectification processes in ternary systems.

It follows from the diagrams given by Schreinemakers and others [1, 2, 3] and ourselves [4] that a vertex or azeotropic point (binary or ternary) is an extreme point of a distillation line if it is a "point" isotherm-isobar. Such cases are illustrated in Fig. 1 (a, b, c). Here the continuous lines are isotherm-isobars, and the dash lines are distillation lines. Fig. 1,a represents the course of isotherm-isobars near the vertex A_1; Fig. 1,b — the course of isotherm-isobars close to the binary azeotrope of minimum (m) or maximum (M) boiling point; Fig. 1,c — the course of isotherm-isobars near the ternary azeotrope (m or M). The points A_1, m, or M can be regarded as degenerate isotherm-isobars; we term them "point" isotherm-isobars.

The distillation lines take a hyperbolic course near the vertices or azeotropic points if isotherm-isobars of finite length pass through the latter (Fig. 2). In Fig. 2,c the letter S represents the saddle-point.

It follows further from these considerations that a vertex of the composition triangle is a point isotherm-isobar if, in the immediate proximity of the vertex, the boiling point — concentration curves for two binary systems have slopes of the same sign (Fig. 3,a). An isotherm-isobar passes through the vertex of the triangle if the boiling point — concentration curves for two binary systems have slopes of opposite sign (Fig. 3,b).

Whether an azeotropic point is a point isotherm-isobar or whether an isotherm-isobar of finite length passes through it, depends on the relationships between the boiling points of the components of the system and of all the binary azeotropes. To determine this, it is necessary to start construction of the isotherm-isobars from the corners of the composition triangle, and extend this to the interior of the triangle, bearing in mind the boiling points of the binary azeotropes. By means of such a construction it is possible not only to determine the form of the isotherm-isobars near the binary azeotropic points, but also to find whether a ternary azeotrope or a saddle-point is present.

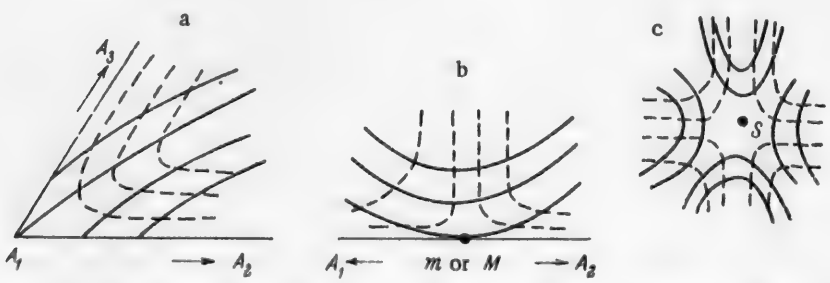

Fig. 2. Continuous lines — isotherm-isobars; dash lines — distillation lines. Explanation in text.

A ternary system which does not contain a binary azeotrope has one family of distillation lines. The opinion is very widely expressed in the literature that the presence of a binary azeotrope in a ternary system must inevitably be accompanied by the appearance of a second family of distillation lines and separation of the composition triangle into two distillation regions. As will be shown later, this is not correct. On the other hand, some authors doubt the existence of several distillation regions in cases when they must undoubtedly be present.

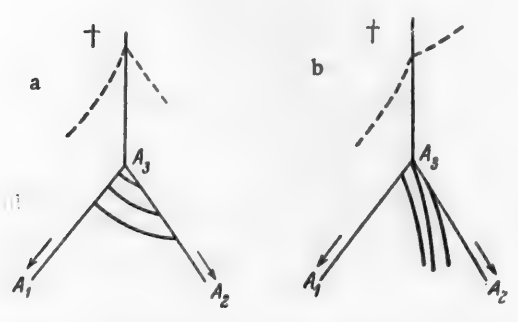

Fig. 3. Continuous lines — isotherm-isobars; dash lines — boiling point — concentration curves for binary systems. Explanation in text.

In our opinion, these incorrect views and doubts are the result of an insufficiently clear understanding of the relationship between the positions of the isotherm-isobars and the distillation lines in the composition triangle.

Consideration of the experimental data given in the literature shows that a necessary condition for the division of the composition triangle into distillation

regions is the existence of at least one azeotrope; however, not every azeotrope causes separation lines of distillation to appear. A separation line of distillation is only produced by an azeotrope through which passes an isotherm-isobar of finite length.

The explanation is that an azeotropic point divides an isotherm-isobar into two parts, and this leads to the appearance of a new family of isotherm-isobars. A family of distillation lines corresponds to each family of isotherm-isobars. The following reasoning shows that new families of distillation lines must arise by separation of isotherm-isobars into several families. It was shown by Schreinemakers [1] that distillation lines always run in the direction of rising boiling points; they cannot pass twice through an isotherm-isobar with the same temperature value. Therefore, when isotherm-isobars separate into families with the same boiling points, the distillation lines must also separate into the same number of families.

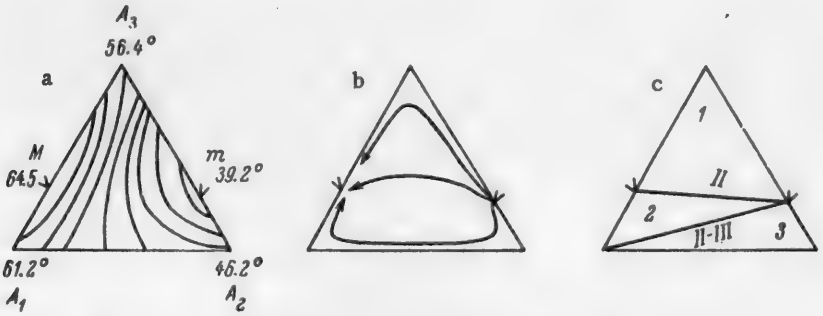

Fig. 4. The system chloroform (A_1) — carbon disulfide (A_2) — acetone (A_3). a) positions of isotherm-isobars; m, m_1, m_2, M) azeotropic points; S) saddle point; b) positions of distillation lines: discontinuous lines and thick continuous lines, separating lines of distillation corresponding to the depression and ridge of the boiling-point surfaces; c) rectification regions (1, 2, 3, etc.) and separating lines of rectification (of the types I, II, III and II–III). Designations apply to Figs. 4, 5, and 6.

Figure 4, a, b* shows the positions of the isotherm-isobars and distillation lines for the system chloroform — carbon disulfide — acetone, studied by Litvinov [5] in isothermal conditions. These diagrams have been transformed by us to correspond to isobaric conditions. The system has two azeotropic points, but as isotherm-isobars of finite length do not pass through them, these azeotropic points do not give rise to separating lines of distillation.

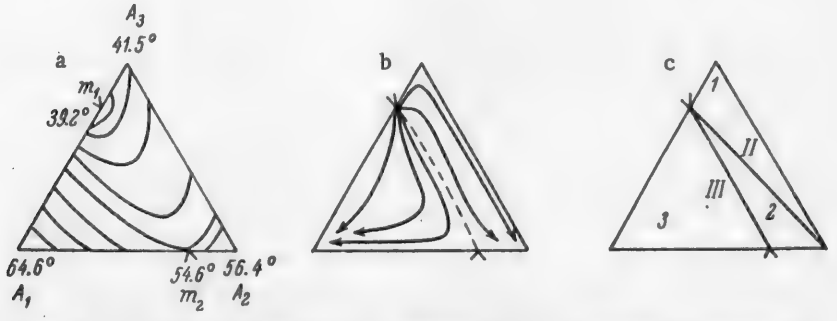

Fig. 5. The system methanol (A_1) — acetone (A_2) — methylene chloride (A_3).

Figure 5, a and b shows the positions of isotherm-isobars and distillation lines for the system methanol — acetone–methylene chloride, studied by Ewell and Welch [6]. These authors studied the system by means

*The compositions of the azeotropes in Figs. 4, 5, and 6 are in molar %.

of rectification experiments. We used their data to plot isotherm-isobars and distillation lines. The system has one azeotrope, through which passes an isotherm-isobar of finite length, and therefore a separating line of distillation passes through it also.

Our data on the system methyl acetate — chloroform — methanol [4] are represented in Fig. 6, a, b. Four isotherm-isobars pass through the saddle-point, and it is therefore the terminal point of four separating lines of distillation.

We thus reach the conclusion that a necessary condition for the appearance of a separating line of distillation is the presence of an azeotrope (binary or saddle-point) in the system, through which passes an isotherm-isobar of finite length. Each isotherm-isobar passing through the azeotropic point gives rise to a new separating line of distillation.

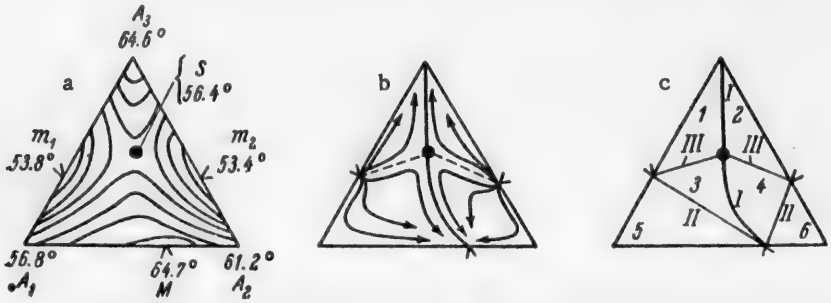

Fig. 6. The system methyl acetate (A_1) — chloroform (A_2) — methanol (A_3).

Two types of separating lines of distillation must be distinguished. 1) Lines which separate families of distillation lines having different starting points. Such separating lines correspond to the ridge of the boiling point surface of the system (Fig. 6, a, b). 2) Lines which separate families of distillation lines with different terminal points. Such separating lines correspond to the trough of the boiling point surface of the system (Figs. 5 and 6, a and b).

Schreinemakers [1] and Ostwald [7] held different views concerning the form of separating lines of distillation. Ostwald asserted that they must be straight lines. Schreinemakers proved theoretically that they can be straight in rare instances only. Experimental data show that in the general case the separating lines of distillation are curves.

Separating Lines of Rectification

The characteristic feature of the rectification region is that solutions corresponding to it yield the same fractions and in the same sequence during rectification, and only the relative amounts of the fractions vary according to the composition of the original solution.

The lines forming boundaries between rectification regions are known as separating lines of rectification.

In discussions of rectification processes in ternary systems much importance is attached to division of the composition triangle into rectification regions. Despite this, the problem of this division remains in an unsatisfactory state.

Reiders and de Minijer [2], and subsequently Haase [3] and Lang [8] considered that separating lines of rectification can only exist where separating lines of distillation are present. As will be shown below, this means that they ignored the middle fractions and only took into consideration the first fractions and bottoms in separating the composition triangle into rectification regions*.

*It is henceforth assumed that three-component solutions yield three fractions on rectification (including bottoms); special cases in which more than three fractions are obtained are not considered in this paper.

Ewell and Welch [6] took the middle fractions into account, and distinguished between three types of separating lines of rectification.

"1) Straight lines connecting binary minimum azeotropes with higher-boiling invariant compositions, which may or may not be associated with physical valleys in the vapor and liquid surfaces. 2) Straight lines connecting binary maximum azeotropes with low-boiling invariant compositions, which are always associated with physical ridges in the vapor and liquid surfaces. 3) Curves ridges connecting binary maximum azeotropes with other high-boiling invariant compositions."

This classification is obscure, it does not include certain types of separating lines, and, moreover, it does not indicate how the separated rectification regions differ from each other in rectification.

We propose the following types of separating lines of rectification.

A line of Type I separates rectification regions the solutions in which yield different first fractions on rectification (in Figs. 4, 5, and 6 the Arabic numerals represent the rectification regions, and the Roman numerals represent types of separating lines of rectification). A line of Type II separates rectification regions the solutions in which yield different second (middle) fractions. A line of Type III separates rectification regions the solutions in which give different third fractions (bottoms). A line of Type II–III separates rectification regions the solutions in which give different second and third fractions, the composition of the second fraction of one region being the same as the composition of the third fraction of the other region ("Different fractions" refers to rectification products of different constant compositions).

A line of Type I may be straight or curved, while lines of all the other types are always straight.

As is seen in Figs. 4–6, c, separating lines of different types may be found in one and the same system. Solutions belonging to different rectification regions differ in rectification by the fractions corresponding to the type of the separation line. For example, if there is a separating line of Type II between the compositions of the initial solutions on the Gibbs triangle, then rectification of these solutions will yield different second fractions (points in the rectification regions 1 and 2, Figs. 4 and 5, c). If there are separating lines of Type II and III between the compositions of the initial solutions, rectification of these solutions will yield different second and third fractions (points in the rectification regions 1 and 3, Fig. 5, c), and so on.

The separating lines of distillation and rectification are related as follows: a separating line of rectification of Type I is present if the system contains a separating line of distillation corresponding to the ridge of the boiling point surface; a separating line of rectification of Type II does not have a corresponding separating line of distillation; it always originates at some initial point of the distillation lines and ends at the terminal point of the same family; a separating line of rectification of Type III passes where there is a separating line of distillation corresponding to a trough of the boiling point surface.

A separating line of rectification of type II–III does not have a corresponding separating line of distillation. It originates in the starting point of some family of distillation lines and terminates in a vertex or an azeotropic point which is neither the initial or final point of the distillation lines.

Thus, Type I and III separating lines of rectification are found where the separating lines of distillation of types I and II are found. The other separating lines of rectification do not have corresponding separating lines of distillation.

If a separating line of distillation is curvilinear, the corresponding separating line of rectification is on its concave side; in rectilinear regions the separating lines of distillation and rectification coincide exactly.

It follows from the foregoing that the number of rectification regions may coincide with the number of distillation regions or may exceed it.

In systems with a curved separating line of rectification of Type I, an interesting effect is found in rectification — one of the fractions is a "fraction of variable composition", and its appearance is accompanied by a fall of the vapor temperature in the condenser of the rectifying column. The mechanism of this effect is discussed in our preceding paper [9].

SUMMARY

1. It is shown that a necessary condition for the existence of a separating line of distillation is the presence of an azeotrope (binary or saddle-point) in the system, with an isotherm-isobar of finite length passing through the azeotropic point.

2. A new classification of separating lines of rectification is proposed.

LITERATURE CITED

[1] F.A.H. Schreinemakers, Z. Phys. Ch., 36, 413 (1901).

[2] W. Reiders and C.H. de Minijer, Rec. trav. chim., 59, 207, 369, 392 (1940).

[3] R. Haase, Z. Naturfersch., 4/a, 342 (1949).

[4] I.N. Busmakin and I.N. Kish, J. Appl. Chem., 30, 2, 200 (1957).*

[5] N. D. Litvinov, J. Phys. Chem. 26, 1144 (1952).

[6] R. H. Ewell, and L.M. Welch, Ind. Eng. Ch., 37, 1224 (1945).

[7] W. Ostwald, Lehruch des allgemeinen Chemie. Leipzig (1896, 1902).

[8] H. Lang, Z. Eletrochem., 54, 438 (1950).

[9] I.N. Bushmakin and I.N. Kish, J. Appl. Chem., 30, 3 (1957).*

Received May 17, 1955

*Original Russian pagination. See C.B. Translation.

RECTIFICATION OF ETHANOL—METHANOL—WATER MIXTURE IN A COLUMN OF CONTINUOUS ACTION*

M.E. Aerov, G.L. Motina, and L.P. Golovanova

Calculations relating to the rectification of multicomponent mixtures have been frequently discussed in papers by Russian and foreign scientists—Lvov [1], Mikhailovsky [2], Fastovsky [3], Bogaturov [4], Chambers [5], and others, although there have been few publications dealing with experimental investigations of this question [6].

Our aim was to determine experimentally the distribution of components in a continuous-action rectifying column in rectification of a methanol—ethanol—water mixture.

EXPERIMENTAL

Laboratory perforated-plate rectifying column of continuous action. A column with the following characteristics is necessary for laborabory studies of continuous rectification: 1) the column output must be high enough for heat transfer to the surroundings to have no significant effect on the liquid—vapor ratio along the height of the column; a column in which the heat transfer into the condenser is 400-500 kcal/hour is desirable; 2) it should be possible to take intermediate samples of liquid along the height of the column in at least 6 points; the samples so taken must give the true average composition of the liquid for the given cross section of the column; 3) the nature and degree of vapor—liquid contact should not change with variations of phase composition; 4) it is desirable to be able to observe the bubbling process along the height of the column visually.

All these requirements are satisfied reasonably well by the laboratory perforated-plate rectifying column (Fig. 1) made and tested in our laboratory with the help of E.P. Darovskykh, a member of the laboratory staff.

Contact between vapor and reflux is effected on perforated disks (Fig. 2) with parallel grooves 2 mm wide cut in the surface. The open cross section of the slits constitutes 13.1% of the plate area. The total height of the column is about 2 m, with 20 plates 80 mm apart. Pieces of glass tubing 38 mm in diameter with ground ends are fitted on rubber washers between the plates. The still is made of stainless steel with five heating tubes, each containing a spiral electric heater; the total power of heaters is 3 kw**). The condenser is made of glass. The column is enclosed in a rectangular housing with two glass walls so that it is possible to observe the nature of the bubbling process on the plates. Alternate plates are equipped with devises for sampling the liquid.

The temperature of the cooling water before entering and after leaving the condenser was measured by mercury thermometers. The amount of cooling water was found from the time required to fill a measuring cylinder. It was therefore possible to determine fairly accurately the quantity of heat carried by the vapor into the condenser, and to find the amount of condensed vapor from the known latent heat of vaporization. The amounts of the liquid feed and distillate were controlled with the aid of dripcocks and measured by the fall and rise of the levels in graduated vessels. The level in the still was kept constant, excess liquid being let out through a hydraulic seal. The mixture was fed in at room temperature, and a correction was applied in the calculations for the heat required to raise the mixture to the boiling point.

*Communication I.

**The still is 280 mm in diameter and 460 mm wide; the heaters are 50 mm in diameter.

Starting materials, mixtures, methods of analysis. Liquid–vapor equilibrium data at 760 mm (abs.) for the system ethanol–methanol–water have been published in the literature [7, 8]. These sets of data were in agreement with each other, and were used in our analysis of the experimental results.

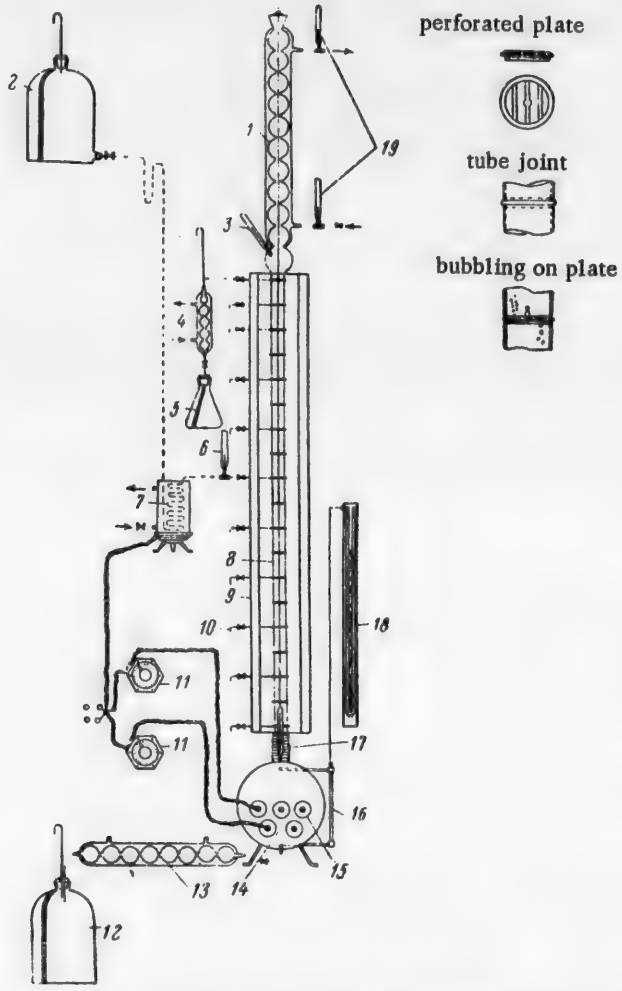

Fig. 1. Diagram of a perforated-plate laboratory rectifying column 38 mm in diameter. 1) Condenser, 2) feed vessel, 3) thermometer, 4) distillate condenser, 5) distillate receiver, 6) thermometer at feed entry, 7) feed preheater, 8) rectifying column, 9) housing for column, 10) sampling device, 11) laboratory autotransformers, 12) receiver for bottoms, 13) condenser for bottoms, 14) still, 15) cross section of heater, 16) gage glass, 17) thermometer in still, 18) U-shaped manometer, 19) thermometers at condenser entry and exit.

The following starting substances were used for the experiments: ethanol of 95.6% concentration, n_D^{20} = 1.3614, d_{20} = 0.790 g/cc; anhydrous methanol, n_D^{20} = 1.3289, d_{20} = 0.791; distilled water. Analysis of the ternary mixtures sampled from different plates along the height of the column presented the most difficulties. The analytical method described in the literature [9], based on the physical constants of the mixture: density boiling point, and refractive index, was found not to be accurate enough, especially for dilute solutions. Certain chemical and physicochemical methods require large volumes of samples and therefore could not be used [10]. A combined

method was used for analysis: the total alcohols were determined from the density of the mixture (because of their similar densities); methanol was determined by conversion into methyl formate followed by distillation at constant temperature with the use of an isothermal condenser [11]. The relative error of this analysis is ±1.5% (owing to formation and partial entrainment of ethyl formate). The ethanol content was found by difference. The refractive indices of the mixtures were determined by means of the Abbe refractometer.

Experiments on rectification of methanol–water mixtures. After several preliminary experiments on distillation of ethanol–water mixtures with total reflux, which showed that under steady-state conditions the alcohol concentrations along the height of the column remain fairly stable for a long time, experiments on the continuous rectification of the binary mixture methanol–water were carried out.

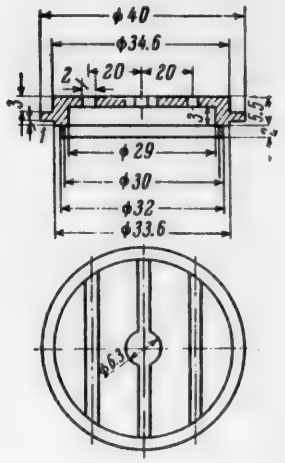

Fig. 2. Perforated plate.

The experimental procedure was as follows. A mixture of known concentration was put into a head vessel, and was fed from there through a rubber tube to plate No 9 in the initial experiments, and then to plate No 13, counting from the top. Arrangements were made at the same time for taking samples of distillate and bottoms. The samples were taken from the sampling tubes under constant conditions, usually after 4 - 5 hours, with uninterrupted feeding and withdrawal, and simultaneously from all the sampling tubes as far as possible.

The reflux ratios were calculated as follows: the total quantity of heat Q (kcal/hour) liberated in the condenser was calculated from the flow rate of water m (kg/hour) in the condenser and the difference between the water temperatures at the condenser entry and exit

$$Q = m \cdot c_p (t_2 - t_1);$$

the amount of vapor V (kg/hour) entering the condenser was determined by the equation

$$V = \frac{Q}{q},$$

where q (kcal /g) is the latent heat of condensation, calculated by the additivity rule for all the components of the mixture.

Heat losses in the column were estimated by calculations based on the measured temperature of the housing; they did not exceed 4% of the total heat liberated in the condenser.

The reflux ratio for the top of the column was determined by means of the equation

$$R = \frac{V - D}{D},$$

where D is the amount of distillate (in kg/hour).

For calculation of the reflux ratio of the exhausting part of the column, a correction was introduced for heat required to heat up the mixture.

The quantity of heat Q_h required to heat the feed to boiling point (in kcal /hour) was determined by the formula

$$Q_h = F \cdot c_p \cdot \Delta t,$$

where c_p is the specific heat of the mixture and Δt is the difference between the boiling point of the mixture and the temperature of the liquid in the feed vessel.

The total heat absorbed in the still is Q' (kcal /hour)

$$Q' = Q + Q_h$$

The quantity of vapor ascending in the lower part of the column is

$$V' = \frac{Q'}{q'},$$

where q' is the heat of vaporization, calculated by the additivity rule from the average molecular composition of the vapor between the still and the feed plate. The reflux ratio of the exhausting part of the column is

$$R' = \frac{V'}{w_0}.$$

Here w_0 is the amount of liquid taken from the still (in kg/hour).

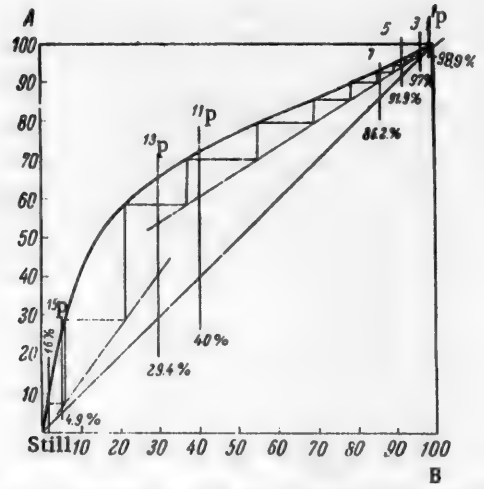

Fig. 3. Determination of the number of theoretical plates for the binary mixture methanol–water. A) Methanol content of vapor (molar %), B) methanol content of liquid (molar %). Efficiency 0.7, number of theoretical plates 14. $R_{upper} = 1.79$, $R_{lower} = 1.44$.

TABLE 1

Experiment No. 20. Liquid Composition on Intermediate Plates

Plate No. from top	Composition (molar %)		
	methanol	ethanol	water
1	95	5	—
3	81.1	12.5	6.4
5	70.2	16.8	13
7	58.6	15.8	25.6
11	39.0	13.4	47.6
15	17.4	3.8	78.8
Still . .	0.1	0.2	99.7

The following data were obtained for rectification of methanol–water mixture in Experiment 15. The number of theoretical plates in this experiment was found graphically (Fig. 3) to be 14 (with 20 actual plates). The concentrations in the distillate, still, and at individual plates are also shown in Fig. 3. The reflux ratio for the enriching part of the column is 1.79, and for the exhausting part, 1.44. The output of distillate from the column was 24.5 moles/hour.

Experiments on rectification of ternary mixtures. Experiments on the continuous rectification of ternary mixtures were performed with a methanol–ethanol–water mixture; ethanol was present in a small amount as an impurity of intermediate volatility between the principal components. The experimental procedure was the same as for methanol–water mixtures.

The most volatile component (methanol) was continuously distilled off in the experiments. The results of two experiments with identical reflux ratios and feed rates are given here. Table 1 gives analytical data for samples from individual plates in Experiment 20; the other data on the rectification process (for Experiments 20 and 21) are given in Table 2.

The calculation was based on combined graphical determinations of the number of theoretical plates from liquid–vapor diagrams for ethanol and methanol (Figs. 4 and 5).

Two diagrams were drawn for each experiment on the ternary system: in the first, the methanol content in the vapor was plotted against the methanol content in the liquid (Fig. 4), and in the second, the ethanol content in the vapor was plotted against the ethanol content in the liquid (Fig. 5). The operating lines were drawn through the final concentrations in the still and condenser in the same way as for binary mixtures. For the exhausting lines, corrections for the heat required to raise the mixture to the boiling point were introduced.

In constructions for the number of theoretical plates, the alcohol concentrations in the distillate were marked off from above in the respective diagrams for methanol and ethanol. From the points corresponding to these concentrations horizontal lines were drawn to meet the equilibrium lines. Verticals were then drawn from these intersection points to the operating lines.

The percentage contents of water at each plate were found by difference and taken into account in determination of the equilibrium concentrations at the next plate. The construction was continued until the component concentrations corresponding to the liquid in the still were reached.

It is seen in Fig. 5 that the calculated concentration of the component of intermediate volatility, ethanol, increases to a certain maximum at the middle of the column (in the region of the feed plate) and then falls.

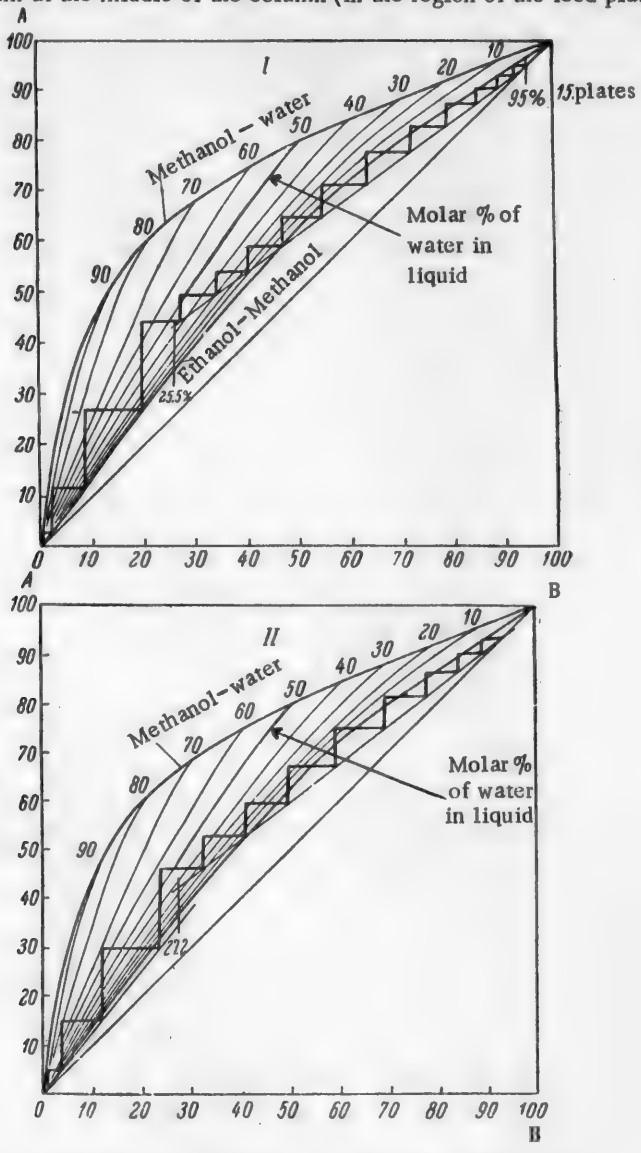

Fig. 4. Calculation of the number of theoretical plates from two diagrams for methanol. A) Methanol in vapor (molar %), B) methanol in liquid (molar %). I) Experiment 20, II) Experiment 21.

Experimental and calculated data on the concentration variations along the column are compared in Fig. 6. The plate efficiency along the column was assumed to be constant. The distribution of the components is similar in the two cases. The maximum ethanol concentration (calculated) is 20.2 molar % (Experiment 20), and experimental, 16.8 molar %; at plate No. 7 in the first case, and at plate No. 5 in second.

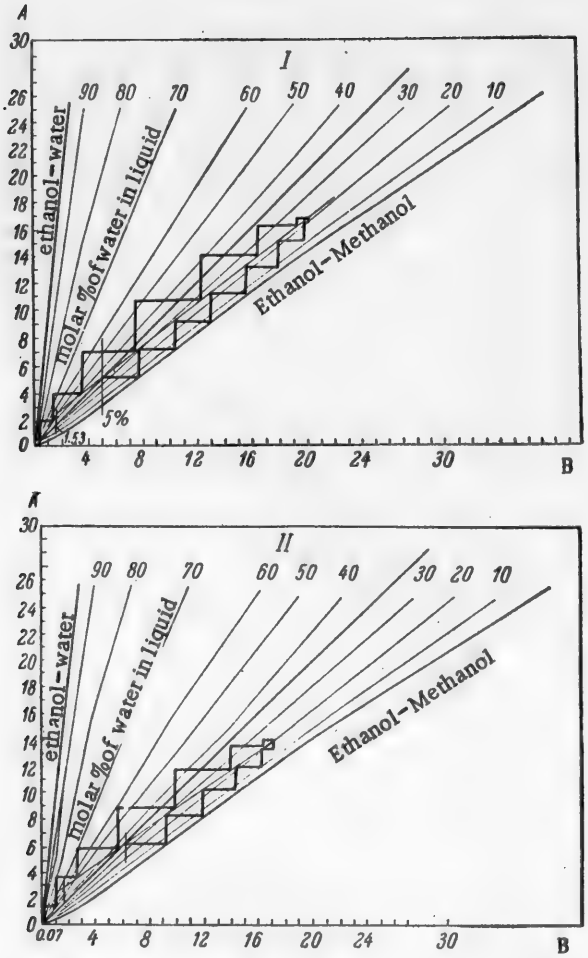

Fig. 5. Calculation of the number of theoretical plates from two diagrams for ethanol. A) Ethanol in vapor (molar %), B) ethanol in liquid (molar %). I) Experiment 20, II) Experiment 21.

TABLE 2

Continuous Rectification of the Ternary Mixture Methanol–Ethanol–Water

Experiment No.	Amount of mixture fed for separation (in g/hour)	Amount of distillate withdrawn (in g/hour)	Component concentrations in feed mixture (in molar %)			Component concentrations in distillate (in molar %)			Component concentrations in still (in molar %)			Reflux ratio		Ratio of theoretical (t) to actual (a) plates
			methanol	ethanol	water	methanol	ethanol	water	methanol	ethanol	water	enriching	exhausting	
20	1240	462	25.53	1.53	72.94	95	5	0	0.1	0.2	99.7	3.51	1.63	15t/20a
21	1303	510	27.2	1.64	71.16	93.4	6.2	0.4	0.2	0.5	99.3	3.05	1.67	13t/20a

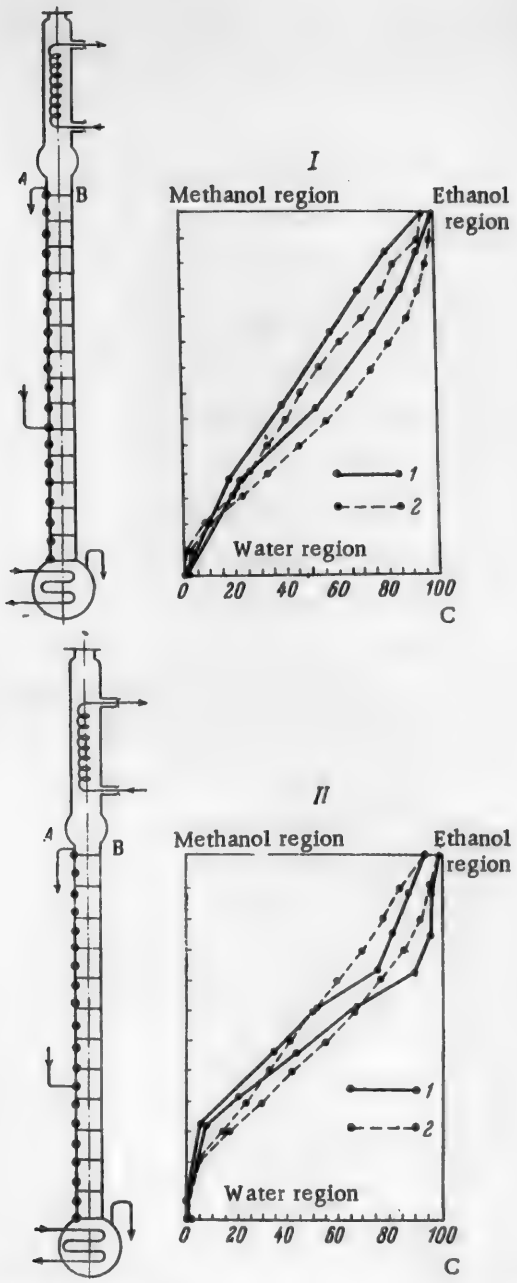

Fig. 6. Comparison of experimental and graphically calculated data on the distribution of the components of the mixture along the column for Experiments 20 (I) and 21 (II). A) Number of actual plates, B) number of theoretical plates, C) concentration (in molar %). 1) Experimental data, 2) data found by graphical calculation.

SUMMARY

1. A laboratory rectification column of continuous action, equipped with perforated plates, has been designed and tested; it was found that the intermediate component concentrations along the column determined by stepwise graphical construction are in fairly good agreement with the experimental data.

2. It is shown that if a mixture separated between the still and the distillate contains an additional component of intermediate volatility, this component is concentrated in the region of the feed plate, where the composition of the liquid may differ considerably from the composition of the mixture being separated.

LITERATURE CITED

[1] S.V Lvov, J. Chem. Ind. 6 (1947).

[2] B.N. Mikhailovsky, J. Chem. Ind. 4, 237 (1954).

[3] V.G. Fastovsky and Yu. V. Petrovsky, Petroleum Economy 10, 11 (1953).

[4] S.A. Bogaturov, Course on the Theory of Distillation and Rectification (State Fuel Tech. Press, 1954).

[5] I.M. Chambers, Chem. Eng. Progress, 47,555 (1951).

[6] I.P. Ishkin and P.Z. Burbo, Welding Ind. 8, 12–41 (1939).

[7] K.P. Andreev and S.N. Vorobyev, Hydrolysis Ind. USSR 2,6 (1949).

[8] I. Griswold and J.A. Dinwiddie, Ind. Eng. Ch., 2347 (1949).

[9] I. Macoun, J. Soc. Chem.Ind, Transact., 50, 281 (1931).

[10] E. Elvove, Ind. Eng. Ch., 9, 295 (1917).

[11] A.I. Gulyaeva, V.F. Polikarpova, and Z.K. Remiz, Analysis of the Products of Divinyl Production from Ethyl Alcohol by S.V. Lebedev's Process (Moscow, 1950).*

Received July 22, 1955

* In Russian.

STUDY OF THE INHIBITING PROPERTIES OF SOME INDUSTRIAL ADDITIVES

I.E. Titova

It is known that a number of industrial additives greatly retard the dissolution of metals in acids. It is of interest to determine what organic substances present in the additives give rise to the strong inhibiting effects.

The inhibiting properties of the following additives were studied in this work: "KS" (sulfonated slaughterhouse wastes), Luzina's additives ("peat," "sapropel," "brewery wastes") "ChM" (from oil industry wastes) in relation to the dissolution of iron in hydrochloric and sulfuric acids, and of aluminum in hydrochloric acid and alkali solutions; the composition and the inhibiting properties of the individual components of the most active inhibitor, "ChM," were also studied.

The apparatus and method were similar to those described previously [1]. Data on the inhibiting effects of the above additives are given in Table 1.

TABLE 1

Inhibiting Properties of Additives in Acid and Alkaline Media

Additive	System at 15°	Concentration of additive (in %)	Color of solution	Duration of experiment (in hours)	$Z^* = \frac{\rho_0 - \rho}{\rho_0} \cdot 100$
"ChM"	Fe — 1.2 N HCl	1	Red	214	99.62
	Fe — 11% H_2SO_4	1	Brownish orange	37	92.7
	Al — 1.6 N HCl	1	Red	37	99.95
	Al — 0.9 N HCl	0.1	Yellow	1	91.43
	Al — 0.9 N HCl	0.025	Pale yellow	1	88.57
	Al — 0.69 N KOH	1	Brown emulsion	1	64.78
	Al — 0.66 N KOH	1		1	58.52
"KS"	Fe — 1.2 N HCl	0.75	—	49	86.71
"Peat"		1	—	94	84.1
"Brewery wastes"		1	—	46	76.6
"Sapropel"		1	—	43	73.1
"KS"	Al — 1.2 N HCl	0.75	—	1	97.24
"Peat"		1	—	1	97.47
"Brewery wastes"		1	—	1	98.5
"Sapropel"		1	—	1	81.7
"Sapropel"		1	—	4	91.2
"KS"	Al — 0.64 N KOH	0.75	—	1	—51.33
"Peat"		1	—	1.5	24.5
"Brewery wastes"		2.2	—	1	94.4
"Sapropel"		1.2	—	1	94
"Sapropel"		1.2	—	19.5	86

*Z is the protective effect (in %), ρ_0 is the rate of solution of the metal in acid, ρ is the rate with added inhibitor.

The effects of "peat," "sapropel," and "brewery wastes" as additives on the solution rates of iron and steel in sulfuric acid were studied by Luzina [2]. Comparison of the data in Table 1 with Luzina's experimental data shows that these additives are more powerful inhibitors in sulfuric than in hydrochloric acid. Our polarization

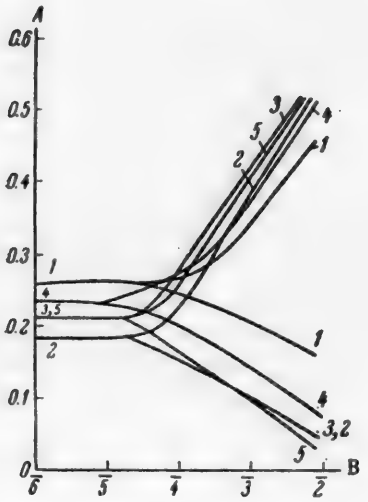

Fig. 1. Polarization curves for iron in hydrochloric acid containing additives. A)Potential I (in v), B)log i, where i is the current density. Hydrochloric acid concentration, 2N. Additives: 1)without additive, 2)"peat," 3)"brewery wastes," 4)"sapropel," 5)"KS." Concentrations of additives (as % on the weight of dry substance): 1) 0, 2)1, 3)1, 4)1, 5)0.75.

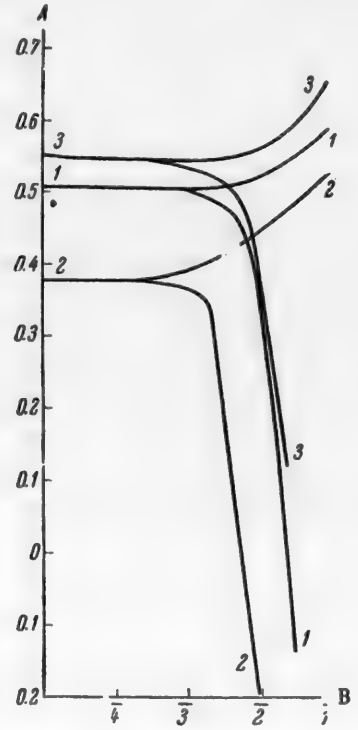

Fig. 2. Polarization curves for aluminum in 0.64 N KOH solution containing additives. A)Potential (in v), B)log i. Additives: 1)without additive, 2)"sapropel," 3)"KS." Concentrations of additives (in %): 1)0, 2)1, 3)1.

studies lead to the conclusion that the inhibiting action of the above-named additives, and also of "KS" additive, is of the same character in sulfuric as in hydrochloric acid. In both cases the cathodic and anodic processes are retarded, the latter to the greater extent, as the stationary potential is shifted in the positive direction. The results of investigations of these additives in hydrochloric acid are given in Fig. 1.

A similar shift of the polarization curves had been observed in solutions of nitrogenous substances yielding positively charged ions in acids [3]. The inhibiting action of these additives probably depends on the presence of protein decomposition products, as the latter are among the few compounds which are more powerful inhibitors in sulfuric acid than in hydrochloric [4].

It is seen in Table 1 that "sapropel" and "brewery wastes" have a fairly strong inhibiting effect on the dissolution of aluminum in caustic alkali. The polarization curves indicate that they produce a sharp shift of the stationary potential in the positive direction. "KS" additive accelerates the dissolution of aluminum (Fig. 2).

"ChM" additive is a more powerful inhibitor than the other additives in hydrochloric acid. Solutions containing "ChM" give polarization curves with a sharp ascent of the cathodic branch, as shown in Fig. 3.

At 0.25% concentration of "ChM" the limit of its inhibiting effect on the anode process is reached. Only the cathodic curve is shifted with further increase of "ChM" concentration.

It was of interest to study the most effective inhibitor in greater detail.

Study of the chemical composition of "ChM" additive. The "ChM" additive was an oily liquid with $d_4^{20} = 1.062$ g/cc; the nitrogen content was 6.71%. In hydrochloric acid, "ChM" yielded a red solution and an emulsion containing dark oily droplets. Metallic specimens became covered with an oily film when pickled in "ChM" solutions.

The composition of "ChM" additive was studied by means of steam distillation, whereby it was divided into two parts — a part volatile in steam, and a nonvolatile residue.

The volatile portion was termed "yellow oil" ($d_4^{20} = 1.0299$, $n_D^{20} = 1.59$), and it comprised about 50% of the total sample.

The "yellow oil" had a weaker inhibiting action than the original "ChM" additive toward iron and aluminum. Investigation of the "yellow oil" showed that about 70% of it consists of derivatives of quinoline and pyridine; in addition, naphthalene and phenol were isolated from it [5]. The latter compounds are the reason for the incomplete solubility of "ChM" in acids and the appearance of an oily film on the metal surface. The nitrogenous bases isolated from "yellow oil" had a stronger inhibiting action on the dissolution of the iron in acid than the "yellow oil" itself.

The nonvolatile part of the additive consisted of water-soluble substances and a tarry residue.

The tarry residue was extracted with hydrochloric acid; an intense red solution was obtained with a strong inhibiting action on iron, and especially on aluminum. Data on the inhibiting properties of the products obtained from "ChM" additive are given in Table 2 and Fig. 4.

TABLE 2

Inhibiting Properties of Products Obtained from "ChM" Additive

Products	Concentrations of products (in %)	System at 15°	Duration of experiment (in hours)	$Z = \frac{\rho_0 - \rho}{\rho_0} \cdot 100$
"Yellow oil" ("y.o.")	1	Al — 0.62 N KOH	1	12.1
	1	Al — 1 N HCl	1	91.6
	1	Al — 1N HCl	2	82.0
	1	Fe — 1N HCl	4	100
	1	Fe — N HCl	45	90.5
Nitrogenous bases from "y.o."	0.7	Al — 0.9 N HCl	1	11.0
	0.7	Fe — 0.9 N HCl	96	85.3
Hydrochloric acid extract of tar	0.06 (on the weight of dry substance)	Al — 0.9 N HCl	2	97.7
		Al — 0.9 N HCl	15.5	94.7
		Fe — 0.9 N HCl	15	92.5

The colored substances in the hydrochloric acid extract are easily extracted with ether after salting out with sodium acetate. After the ether and acetic acid have been distilled off, a "red oil," which partially crystallizes, is obtained. The crystalline portion had the appearance of a "brown powder" after separation. The "red oil" and "brown powder" have very strong inhibiting action, approximately ten times as strong as that of "ChM" itself, as is clear from Table 3 and Fig. 5.

It follows from Fig. 5 that the nature of the inhibiting effects of these substances on aluminum are the same as on iron — they cause a sharp ascent of the cathodic branch, in the same way as "ChM" additive itself (Figs. 3 and 4). According to approximate calculations, "ChM" additive contains about 10% of these substances [5]. Thus, the most active component of "ChM" additive, its "active principle," consists of the substances present in the part of the additive which is not volatile in steam (the tarry residue).

Nature of the active principle of "ChM" additive and the mechanism of its action. The method used for isolation of the "red oil" and of its crystallizable portion, which we term "brown powder," was similar to the method generally used for isolation of porphyrins from caustobiolites, in particular from petroleum [6]. Porphyrins are nitrogenous substances of complex structure, containing characteristic conjugate double bond systems in four

linked pyrrole rings. They are stable compounds with high melting points, with nitrogen contents between 9.5 and 11.7%, according to molecular weight (for example, mesoporphyrin has m.p. 292° and contained 9.49% nitrogen).

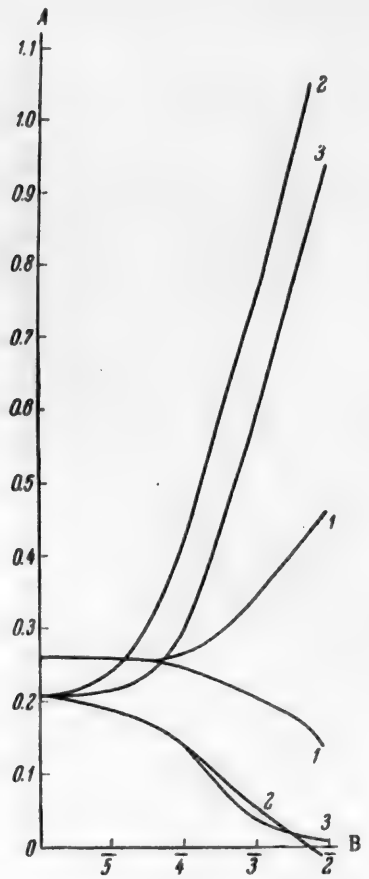

Fig. 3. Polarization curves for iron in 1.2 N hydrochloric acid containing "ChM" additive. A) Potential (in v), B) log i. Concentration of additive (in %): 1) 0, 2) 1, 3) 0.25.

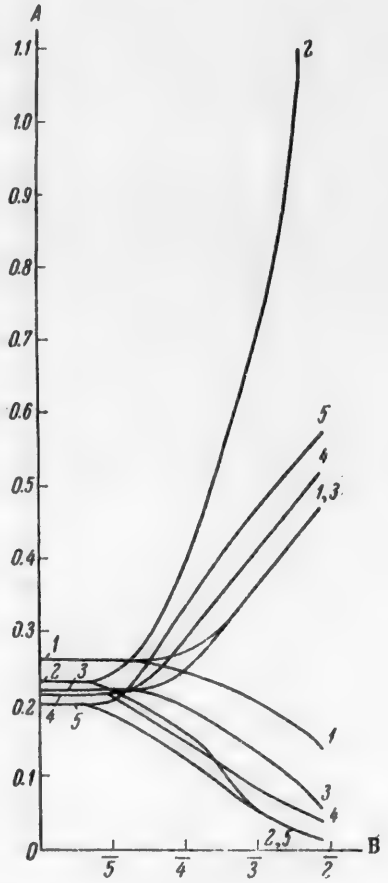

Fig. 4. Polarization curves for iron in 1.2 N HCl with additions of products isolated from "ChM" additive. A) Potential (in v), B) log i. Additives: 1) without additive, 2) hydrochloric acid extract of tar, 3) water-soluble, nonvolatile in steam, 4) alkaline extract of tar, 5) "yellow oil."

TABLE 3

Comparison of the Inhibiting Properties of "ChM" Additive and of Substances Isolated from it

System A1—0.9 N HCl

Inhibitor	Concentration of inhibitor (in %)	Color of solution	Duration of experiment (in hours)	$Z=\frac{\rho_0-\rho}{\rho_0}\cdot 100$
"Red oil"	0.025	Orange	1	99.8
"ChM"	0.025	Pale yellow	1	96.62
"Brown powder" . . .	0.009	yellow	1	97.43
"ChM"	0.1	yellow	1	97.4

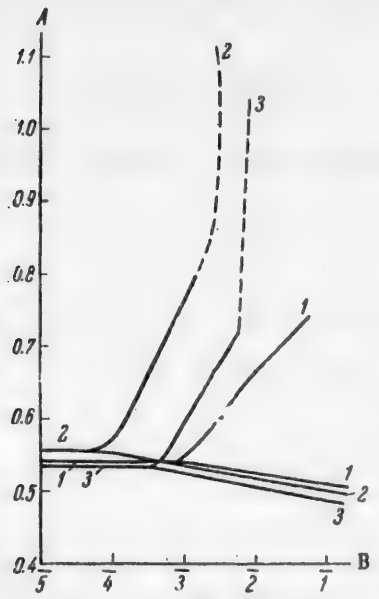

Fig. 5. Polarization curves for aluminum in 0.9 N HCl with additions of "ChM" and substances isolated from it. A) Potential (in v), B) log i. Additives: 1) without additive, 2) "ChM" 3) "brown powder." Concentrations of additives (in %): 1) 0, 2) 0.25, 3) 0.009.

The ether extract, obtained after salting out with sodium acetate of a hydrochloric acid extract of the portion of "ChM" additive nonvolatile in steam, had a red color characteristic of porphyrin solutions; spectroscopic investigation showed strong extinction in the violet region of the spectrum.

On irradiation by ultraviolet light (Hanau lamp), the ether solution exhibited a greenish yellow fluorescence with a bright yellow edge, which is characteristic of porphyrin solutions [7]. The crystalline portion ("brown powder") contained 10.58% total nitrogen, by the Kjeldahl method, and did not melt at 350°; it sublimed on further heating, with partial decomposition.

According to the above data, the substance isolated by us from "ChM" belongs to the substances of the porphyrin group.

The mechanism of interaction of these substances with the metal surface is probably the following. In substances of the porphyrin type the hydrogen atoms attached to adjacent nitrogen atoms acquire the nature of protons [8]. Depending on the structure of the compound, they may leave the nitrogen atoms to which they are attached, and approach another pair. The latter then acquire basic characteristics and may give rise to compounds with acids:

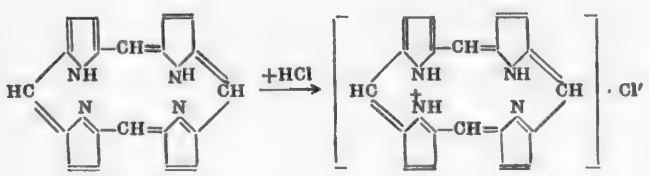

Such a saltlike compound has a plane configuration and, owing to absence of steric hindrances, comes close to the charged surface; electrons may be easily attracted from the latter to the hydrogen atoms within the molecule. The metal then becomes attached to nitrogen atoms by means of principal valences:

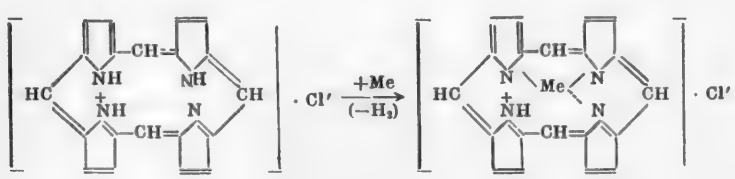

A surface compound is thus formed. Aluminum plates placed in hydrochloric acid solutions of these compounds become covered with an even red film, nonoily in character, which cannot be removed by simple rinsing but is easily rubbed off with filter paper.

SUMMARY

1. The inhibiting action of "KS," "peat," "sapropel," "brewery wastes," and "ChM" with respect to iron in acid media and to aluminum in acid and alkaline media has been studied and it is shown that the inhibiting action of "ChM" is due to the presence of nitrogen-containing substances.

2. The main active component of "ChM" additive consists of substances of the porphyrin group, which remain in the part of the additive which is not volatile in steam.

3. The "active principle" of "ChM" additive can be isolated; its inhibiting action in hydrochloric acid solutions is ten times that of "ChM" itself.

4. It is shown that the components which cause incomplete solubility of "ChM" in acids and adversely affect the properties of this additive are naphthalene and phenols.

LITERATURE CITED

[1] I.E. Titova and G.I. Chufarov, J. Phys. Chem. 29, 3, 502 (1955).

[2] G.S. Luzina, Candidate's Dissertation, Sverdlovsk Institute of Labor Protection (1951).

[3] V.A. Kuznetsov and Z.A. Iofa, J. Phys. Chem. 21, 202 (1947).

[4] S.A. Balezin, V.P. Barannik, and N.I. Putilova, Lenin MGPI 63, 119 (1951).

[5] I.E. Titova, Candidate's Dissertation, Urals State University (1951).

[6] H. Fischer and H. Orth, Die Chemie des Pyrrols, II, 579 (1937).

[7] I. Ya. Postovsky and V.B. Getsen, Chemistry of Solid Fuel 6, 459 (ONTI 1935).

[8] B.N. Stepanenko, Bull. Acad. Sci. USSR (Biol. Ser.) 3, 550 (1947).

Received September 22, 1955

METHOD OF USING DILUTE CATALYST SOLUTIONS

COMMUNICATION I. CONTINUOUS HYDROLYSIS OF LIGNOCELLULOSE RESIDUES FROM THE "WOOD SUGAR"* INDUSTRY

N.A. Sychev and V.L. Avtonomov

The modern technological processes used in the wood sugar industry are well known [1-7]. Fairly considerable amounts of residual raw materials are obtained in these processes; these can be subjected to further hexose hydrolysis in the same equipment by percolation. However, although this operation proceeds smoothly at first, difficulties soon arise; the digesters become "blocked" and flow of the hydrolyzed liquor ceases. This effect in the hydrolytic process, well known to specialists, is the result of a sharp change in the physical structure of the cellulose-containing material.

As the result of "blocking," saccharification of difficulty hydrolyzed polysaccharides does not exceed 50%, and the actual yield of hexoses reaches only about 40% of the theoretical.

In order to avoid this undesirable effect, which makes it difficult to obtain good yield of sugars by hydrolysis of straw, we tested, as long ago as 1936-1940, the use of a "diminishing" liquor ratio at the Bezenchuk Experimental Works, and recommended its adoption at other hydrolysis plants. The procedure consists of a systematic decrease of the volume of catalyst feed to the percolators, in accordance with the decreasing filtering power of the material in the course of hexose hydrolysis.

In this way we were able to obtain up to 60-70% saccharification of cellulose, with an actual yield of reducing sugars of up to 400-420 kg per ton of raw material.

Unfortunately, despite the progress achieved, the diminishing liquor ratio method was not free of disadvantages. Its use resulted in the loss of the "tail" fractions of the raw material, reaching 30% and over.

To avoid losses of sugar with the "tail" fractions, we have recently started work on the continuous hydrolysis of lignocellulose residues from straw by additional conversion into the so-called "technical hydrocellulose". This work is to some extent related to the method recently proposed by us for electrochemical delignification of plant materials [8, 9].

It is well known that x-ray investigations reveal a considerable degree of order in the structure of cellulose. Threadlike cellulose macromolecules may be arranged in parallel, but in some regions the orientation is less perfect, and in consequence crystalline oriented and nonoriented regions arise in cellulosic materials [10]. The amorphous regions have greater free energy and are more reactive than the crystalline. This is manifested in their higher hygroscopicity and relatively higher rate of hydrolysis.

The hydrolysis is at first a heterogeneous process at the surface of the solid phase. The subsequent conversion of the insoluble fragments of the cellulose macromolecules into a soluble state is accompanied by considerable hydration of the particles, which are attacked by the catalyst molecules. As a result of a homogeneous stepwise reaction these new particles are now gradually converted into glucose [11].

*In this translation "wood sugar" has been substituted for the original "xylose," which appears to be a misnomer — Publisher's note.

According to Sharkov, the hydrolysis of polysaccharides can be represented by the scheme A→ B→ C, with conversion of substance A into substance B, where A is the cellulose fiber, B represents water-soluble fragments of the native polysaccharide, and C represents the final hydrolysis products.

The above views lead us to the assumption that hydrolysis of our "tail" lignocellulose residues should be considerably accelerated if they are previously converted into technical hydrocellulose. It is known that in this case the process is inevitably accompanied by formation of cellodextrins, water-soluble intermediate compounds.

If the concentration of the catalyst, such as sulfuric acid, is increased to 72% and over it is easy to convert all the polysaccharides in the substrate into soluble cellodextrins and other polymers, the yields even being quantitative.

The following research scheme was planned on the basis of these theoretical considerations. The first stage was a study of the rate of continuous saccharification of the residues after careful treatment with small amounts of very dilute catalyst solution followed by rapid drying and grinding of the treated material. The second stage was a study of the behavior of the same raw material when treated with minimum amounts of 72–73% sulfuric acid both with and without the use of excess pressure (in the cold).

The first stage was investigated in detail in 1953–1954, and the second, in 1954–1955.

The results of our experiments are presented in the Experimental Section.

EXPERIMENTAL

Preliminary experiments showed that residues which had been washed with water can be "soured" with 1.5% sulfuric acid solution at 1:3 liquor ratio, followed by careful drying at 50–80° until the material turned slightly green. These residues contained up to 62% cellulose, 9% hemicelluloses, and 28–30% lignin.

The "technical hydrocellulose" obtained from the residues was then thoroughly ground and hydrolyzed. Preliminary grinding in hammer mills, burrstone mills, vertical cog mills, and finally in "coffee mills" was studied. The best method was found to be grinding to a powder in a coffee mill. The stability of aqueous acid suspensions of this material, with and without stabilizers (high-molecular fatty acids, propyl and butyl alcohols, etc.) was also studied. The experiments showed that satisfactory stability can probably be attained even without addition of stabilizers: suspensions of the finely ground material were found to be adequately stable in rapid and continuous flow through tubes.

The following results were obtained in a study of the behavior and yield of reducing substances (RS) in the hydrolysis of this material. Hydrolysis with 1% acid for 1 hour (without use of pressure) gave yields of between 6 and 8.7% of reducing substances, calculated on the original material. Before hydrolysis the material contained only about 3% free sugars*. Saccharification of the same material under pressure gave the results presented in Table 1.

TABLE 1

1st Hydrolysis of Residues. Liquor Ratio 1:10, Weight of Material 2 g

Process temperature (degree)	Acidity of solution (%)	Duration of hydrolysis (min.)	Actual yield of RS (% of starting material)
150	0.4	1	13.8
160			21.7
170			18.0
180			16.5
165	0.3	0.5	25.0
	0.6		22.5
	1.8		15.8
170	0.2	1	27.5
180			27.0
182			26.0

TABLE 2

2nd Hydrolysis of Residues. Liquor Ratio 1:10, Temperature 180°

Acidity of solution (%)	Duration of hydrolysis (min.)	Actual yield of RS (%) of starting material)
0.2	1	14.0
	2	10.0
	3	7.0
0.6	2	11.2
	5	7.0

*After boiling with water and determination by Bertrand's method.

Saccharification of the residues from the 1st hydrolysis gave the results presented in Table 2.

The lower actual RS yields obtained in the second hydrolysis are the consequence of a corresponding decrease of the cellulose content of the residues after first saccharification. In both cases (in the 1st and 2nd hydrolysis) the rate of the process is the same.

Subsequent experiments on the saccharification of residues after additional acid treatment were carried out with greater accuracy with new material (Tables 3 and 4).

TABLE 3

1st Hydrolysis of Residues. Liquor Ratio 1:10

Process temperature (degree)	Acidity of solution (%)	Duration of hydrolysis (min.)	Actual yield of RS (%) of starting material)
160	0.7	0.5	18.7
160	0.7	1.0	18.8
165	0.7	0.5	27.7
170	0.7	0.5	30.0
170	0.7	1.0	31.5
170	0.7	3.0	21.0
175	0.7	0.5	35.0
180	0.7	1.0	33.0
180	0.2	1.0	16.0
190	0.7	1.0	27.0

TABLE 4

2nd Hydrolysis of Residues. Liquor Ratio 1:10, Acidity of Solution 0.7%

Acidity of solution (%)	Duration of hydrolysis (min.)	Actual yield of RS (%) of starting material)
160	0.5	10.0
165	0.5	13.7
170	0.5	15.0
170	1.0	15.0
180	1.0	13.5

In our earlier investigations [12] autoclave hydrolysis of lignocellulose residues from straw after pentose hydrolysis, without additional acid treatment, gave the results presented in Table 5.

TABLE 5

Hydrolysis of Straw Residue Lignocelluloses. Temperature 170°

Experimental conditions	Sugar formation (%)		Sugar breakdown (%)		Actual yield of RS (% of starting material)	
	I*	II**	I	II	I	II
Acidity of solution 1%, hydrolysis time 1 hour	73.4	61.5	42.7	36.1	30.7	27.4
Acidity of solution 0.7%, hydrolysis time 0.5 hour . . .	35.9	26.1	8.8	5.03	27.1	21.1

SUMMARY

The foregoing data show that, as was to be expected, hydrolysis of ground residues proceeds unusually easily after suitable additional acid treatment. With 0.7% catalyst concentration up to 35% RS, calculated on the original raw material, can be obtained within 1 minute. It is evident that in a continuous process, with the

*Calculated by Luers–Scholler equation.

**Experimental data.

suspension flowing continuously through a tubular reactor, sugar breakdown can be reduced practically to zero. This leads to another conclusion of practical importance: by conversion of lignocellulose residues into technical hydrocellulose it is possible to accelerate considerably the subsequent hexose hydrolysis. It is then possible to use a "continuous" saccharification process, with the suspension passed through tubular hydrolyzers.

The fact that high RS yields (up to 28%) are obtained even at 0.2% catalyst concentrations and at relatively low temperatures makes the process all the more feasible.

LITERATURE CITED

[1] N.A. Sychev, J. Appl. Chem. 11, 4 (1938).

[2] N.A. Sychev, J. Appl. Chem. 12, 6 (1939).

[3] N.A. Sychev, Proc. Acad. Sci. USSR 29, 5–6 (1940).

[4] N.A. Sychev, J. Appl. Chem. 14, 4 (1941).

[5] N.A. Sychev, J. Appl. Chem. 21, 6 (1948).

[6] N.A. Sychev, Biochemical Technology of D-Xylose (Voroshilovgrad, 1952).*

[7] V.I. Sharkov, Hydrolysis Industry (1950).

[8] N.A. Sychev and V.N. Petrova, J. Appl. Chem. 27, 4 (1954).

[9] N.A. Sychev and V.N. Petrova, J. Appl. Chem. 28, 1127 (1955).

[10] A.E. Chichibabin, Principles of Organic Chemistry (1953) 5th edition, p. 621.

[11] V.I. Sharkov, Hydrolysis Industry (1945) 1, 23.

[12] N.A. Sychev, Dissertation: "Biochemical Technology of D-Xylose" (1952) 1, 241.

Received September 19, 1955

*Probably the same as Lit. Cit. 12 — Publisher's note.

INVESTIGATIONS OF CELLULOSE STRUCTURE BY THE ALCOHOLYSIS METHOD

I.I. Korolkov, V.I. Sharkov, and E.N. Garmanova

Various chemical and physical properties of cellulose indicate that its structure is heterogeneous; this is generally attributed to the existence of loose, disordered, so-called amorphous regions, and dense, ordered, so-called crystalline regions. Many different physical and chemical methods are now available for quantitative determinations of the heterogeneity of cellulose. They include the following.

Method based on the hydrolysis reaction. There are several variations of the determination of amorphous and crystalline regions of cellulose by hydrolysis with dilute acids [1, 2]. The principle of the method is that these portions of cellulose are hydrolyzed at different rates. Recently this method has been subjected to serious criticism [3 - 6], as it is believed that it gives low results owing to recrystallization of part of the amorphous cellulose during hydrolysis.

The method with the use of deuterium oxide [7] depends on the replacement of hydrogen in the cellulose hydroxyls by deuterium when the cellulose is exposed to heavy water, the replacement being considerably more rapid in the loose than in the dense regions. However, the readily accessible hydroxyls in cellulose consist not only of the hydroxyls in the amorphous regions, but also of the hydroxyls on the surface of the dense regions. Since there are at present no methods for the accurate determination of the latter surface area, the determination of the amorphous portion of cellulose by estimations of the accessible hydroxyls cannot be accepted as accurate.

Method based on treatment of cellulose with thallium ethylate [8]. As the result of such treatment, the readily accessible cellulose hydroxyls react to form thallium ethylate. The amount of the latter is found by replacement of thallium by methoxyl groups by the action of methyl iodide, with subsequent determination of the methoxyl content of the cellulose. This method has the same disadvantages as the deuterium method.

Methods based on determination of the amounts of sorbed moisture [9] depend on the assumption that cellulose binds water at the readily accessible hydroxyls. Its disadvantages are the same as for the preceding two methods.

Calorimetric method [10]. This is based on the assumption that the part of the water sorbed by the cellulose and bound to free hydroxyls by hydrogen bonds does not freeze when the cellulose sample is frozen. This method has the same disadvantages as all the above methods based on determinations of accessible hydroxyls. In addition, there is reason to believe that under these conditions the water present in fine capillaries does not freeze either.

Method based on measurement of the density of cellulose [11], in which use is made of the difference between the densities of the crystalline and amorphous modifications of cellulose. The method can give rise to error owing to the lack of exact data on the densities of crystalline and amorphous cellulose.

Methods of the diffuse scattering of x-rays [12 - 14] are based on the use of curves for the darkening intensity of the x-ray patterns given by the cellulose. The amount of amorphous fraction is estimated from the magnitude of the diffuse scattering. The method gives only a relative idea of the presence of heterogeneous regions, etc.

Results of determinations of the amorphous portions of several cellulose samples, obtained by different workers, are given in Table 1.

These data show that all the methods used indicate a heterogeneous structure in the cellulose samples, but quantitative estimations of this heterogeneity give variable results by different methods. Because of these variations, and also of the disadvantages inherent in principle in all these methods, it is at present difficult to draw quantitative conclusions concerning the heterogeneity of different celluloses.

In the present study an attempt was made to solve this problem by the use of a reaction in which cellulose is broken down in nonaqueous media, such as alcoholysis.

TABLE 1

Results of Determinations of the Amorphous Portion of Cellulose by Different Methods

Methods	Contents of amorphous portion (%) in different specimens					
	cotton cellulose	wood cellulose	mercerized wood cellulose	mercerized cotton cellulose	viscose rayon	
					without extr.	with extraction
X-Ray method [12, 15]	31	—	—	—	61	—
By density [9, 12]	42	47	—	60	75	68—76
By sorption of water [9]	22	35	57	—	65	82
Calorimetric [10]	13—19	—	—	23	48	—
By use of deuterium oxide [7]	22	37	—	—	—	80
By use of thallium ethylate [8]	0.4	—	—	17—22	—	—
By hydrolysis [2, 16]	5	10	—	11	21	—

It was to be expected that, when the cellulose is treated in a medium of low polarity, recrystallization of the amorphous regions should be greatly retarded or completely stopped, and therefore this method should give more correct results than the method based on the hydrolysis reaction.

EXPERIMENTAL

In order to choose the optimum alcoholysis conditions for determination of the heterogeneity of cellulose samples, the reactivities of two extreme modifications of cellulose in hydrolysis and alcoholysis in presence of dilute sulfuric acid were compared. The modifications used were native cotton cellulose, and a product obtained from it by dry grinding.

A vibratory mill designed by us jointly with Engineer L.M. Svedentsov was used for grinding the cotton cellulose. The mill had a spherical steel body 300 ml in volume, which was half filled with steel balls 15 mm in diameter. The body was vibrated mechanically in a vertical direction at frequencies of up to 1000 vibrations per minute, at an amplitude of 8 mm.

The optimum grinding time was found to be 60 minutes, after preliminary experiments on the grinding of thoroughly dried cellulose samples.

Such grinding yielded "amorphous" cellulose in the form of a very fine white powder, with degree of polymerization 330 and true sp. gr. 1.509. The x-ray patterns for both cellulose samples are given in Fig. 1; it is seen that the ground cellulose gives a very definite amorphous scattering pattern. Hydrolysis and alcoholysis of the samples were carried out in presence of 10% sulfuric acid in copper autoclaves heated in a boiling water bath. The results of the reactions were determined from the weight losses of the samples after washing with water, and from the yields of reducing substances (RS) in solution. For determination of the reducing substances in the solutions after alcoholysis, alcohol was distilled off and the residue was subjected to inversion in order to decompose the glucosides formed.

The alcoholysis reactions were carried out in methyl, ethyl, propyl, and butyl alcohols dried by means of copper sulfate and then metallic sodium, with subsequent distillation.

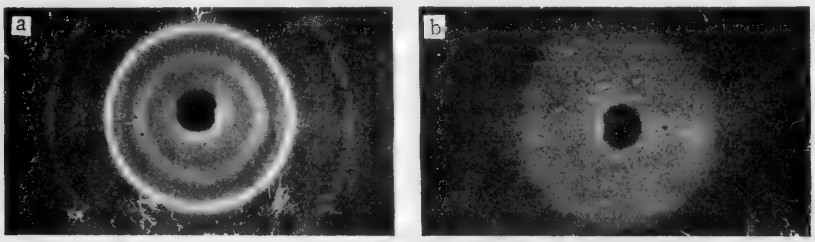

Fig. 1. X-ray patterns of cotton (a) and ground (b) cellulose.

Data on the reactivity of the native cotton cellulose are given in Table 2, and on that of ground cotton cellulose, in Table 3.

TABLE 2

Reactivity Characteristics of Native Cotton Cellulose (Reaction Time 180 minutes)

Reaction	Amount of cellulose dissolved (%)	Reaction rate constant $K_{min.}^{-1}$	Coefficient β
Hydrolysis	5.0	0.00028	1.0
Methanolysis	13.3	0.00079	2.8
Ethanolysis	9.1	0.00053	1.9
Propanolysis	8.3	0.00048	1.7
Butanolysis	3.4	0.00013	0.7

TABLE 3

Reactivity Characteristics of Ground Cotton Cellulose in Hydrolysis and Alcoholysis

Reaction	Reaction time (min.)	Amount of substance dissolved (% of sample)	RS yield (% of sample)	Reaction rate constant ($min.^{-1}$) for consecutive time intervals	Coefficient β
Hydrolysis	20	6.3	7.0	0.0034	12.6
	60	12.9	14.4	0.0018	6.7
	180	19.8	22.0	0.00069	2.5
Methanolysis	20	27.8	—	0.0162	60.0
	60	44.1	—	0.0064	23.7
	180	59.0	—	0.0026	9.6
Ethanolysis	20	24.0	20.6	0.0137	51.0
	60	48.0	45.8	0.0095	34.0
	180	63.2	61.4	0.0029	10.0
Propanolysis	20	10.6	—	0.0056	20.7
	60	20.5	—	0.0042	15.5
	180	43.7	—	0.0024	9.0
Butanolysis	20	4.8	—	0.0025	9.3
	60	7.7	—	0.00077	2.8
	180	15.6	—	0.00074	2.7

The data on the solubility of the cellulose samples were used to calculate the reaction rate constants by means of the first-order equation. The constants for ground cellulose were calculated for each consecutive reaction interval (for example, between 0 and 20 minutes, 20 and 60 minutes, etc.).

For clarity, the rate constants for the different reactions are expressed in terms of the coefficient β, which is the ratio of the constant found for a given reaction to the hydrolysis rate constant of the original native cellulose.

The data for the native cellulose samples containing a small proportion of amorphous material indicate that the reaction rates in alcohols differ from the rate of hydrolysis. It was found that the rates of methanolysis, ethanolysis, and propanolysis are 2-3 times as high as the rate of hydrolysis. In the case of butanolysis the reaction rate is lower, and here β is only 0.7.

According to the data for ground cellulose its hydrolysis rate during the first 20 minutes corresponds to a value of β equal to 12.6, but the rate then drops rapidly, and after 3 hours, when about 20% of the cellulose has passed into solution, the rate approximates to the hydrolysis rate of the native cellulose. The initial rates of methanolysis and ethanolysis of this sample correspond to values of β of the order of 50-60. The value of β gradually decreases with increasing reaction time, and after 3 hours the rate approximates to the rate of methanolysis and ethanolysis of native cellulose, when about 60% of the cellulose has passed into solution.

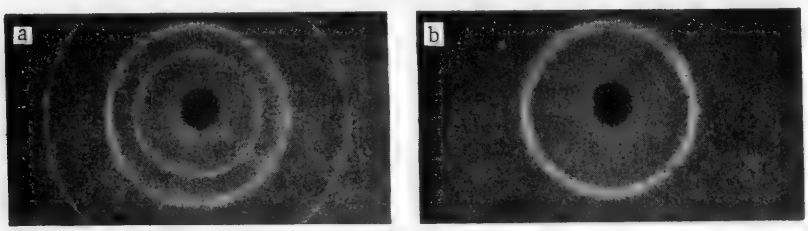

Fig. 2. X-ray patterns of ground cellulose after hydrolysis (a) and ethanolysis (b).

The x-ray patterns of ground cellulose residues after 20 minutes of hydrolysis and ethanolysis are given in Fig. 2. It is seen that the x-ray pattern of the sample after ethanolysis shows only some brightening of the diffuse ring for the original substance. Similar results were obtained for samples after alcoholysis in other alcohols.

In the case of the hydrolysis product, although its weight loss was considerably less than in ethanolysis, the x-ray pattern is similar to that of native cellulose.

Thus, the hydrolysis of ground cellulose samples is accompanied by a rapid decrease of the reaction rate, and this corresponds to the appearance of interference rings characteristic of the native fiber in the x-ray pattern. Methanolysis and ethanolysis of such samples are characterized by high rates of reaction with extensive dissolution of the material, and the x-ray patterns of the residues show only slight brightening of the original amorphous ring. Although methanolysis and butanolysis also cause some brightening of the amorphous ring in the x-ray pattern, the reaction rates in these cases are considerably lower than in methanolysis or ethanolysis.

These results lead to the conclusion that in alcoholysis, which is a reaction in a medium of low polarity, the amorphous structure of cellulose does not undergo a packing or recrystallization process, and therefore this reaction can be used for quantitative determination of the amorphous fraction in cellulose materials. The most suitable reaction from the practical aspect is ethanolysis. The possibility of avoiding recrystallization of cellulose in media of low dielectric constants was also verified by the hydrolysis of ground cellulose in pure dioxan containing 10% sulfuric acid; the dielectric constant of dioxan is less than that of ethyl alcohol. The experimental procedure was the same as in ethanolysis.

It is clear from the results, given in Table 4, that this cellulose sample dissolves in dioxan at a rate similar to its rate of solution in ethanolysis.

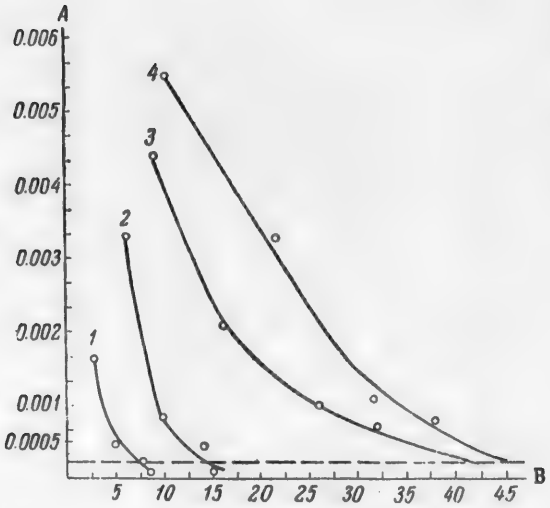

Fig. 3. Determinations of the amorphous fraction of different cellulose samples. A) Rate constant $K_{min^{-1}}$, B) amount of cellulose dissolved (%). 1) Cotton cellulose, 2) wood cellulose, 3) cellophane, 4) viscose rayon.

The fairly close agreement of the reaction rates in the two media confirms that absolute ethanol can be used as a reagent in which no appreciable recrystallization of amorphous cellulose occurs.

For determinations of the amorphous fraction in the cellulose samples, we calculated the ethanolysis rate constants for consecutive time intervals and plotted the constants against the amounts of substance dissolved (Fig. 3).

The amorphous fraction was taken to be the part of the cellulose which dissolved before the curve reached a point close to the ethanolysis rate constant for ordered or crystalline cellulose. This was taken as 0.002 $min.^{-1}$, double the ethanolysis rate constant for cotton hydrocellulose.

It must be pointed out that in determinations of the amorphous fraction by this method a correction must be applied for the amount of the crystalline cellulose dissolved at the same time. As the rate constant for this process is 0.0001 $min.^{-1}$, this correction will constitute about 1.5% of the weight of the sample, or less, depending on the amount of amorphous fraction present. This correction was not applied in our calculations.

This method was used for determinations of the amorphous fraction in various cellulose samples and for studies of a number of questions related to the structure and properties of polysaccharides.

Use of Ethanolysis for Determination of the Amorphous Fraction in Various Cellulose Samples

Samples of Cellophane, viscose rayon, and cotton and wood cellulose were used for the studies. These specimens were subjected to ethanolysis and, for comparison, to hydrolysis, for 20, 60, 180, and 300 minutes by the method described above.

Examination of the results in Table 5 shows that ethanolysis of different cellulose samples proceeds at different rates and that, as a rule, the degree of solution is considerably greater in ethanolysis than in hydrolysis. The ethanolysis rate constants are plotted against the amounts of substance dissolved in Fig. 5. The curves in this figure shows that cotton cellulose contains up to 7% of amorphous material, wood cellulose about 15%, cellophane about 42%, and viscose rayon about 45%. Thus, these specimens differ greatly in their contents of the reactive amorphous fraction. An interesting fact is that regenerated cellulose has a very high content of the amorphous fraction, up to 45% by weight.

TABLE 4

Results of "Hydrolysis" of Ground Cellulose in Dioxane

Reaction time (min.)	Amount of substance dissolved (% of sample)	
	in dioxan	in ethanol
20	20.2	24.0
60	50.7	53.6
180	67.0	63.2

The constants given in Table 5 were calculated from data on the solubilities of the whole cellulose samples, and they give only a relative idea of the rates of ethanolysis of the amorphous fraction itself. However, it is of interest to determine the order of magnitude of the ethanolysis rate constant for the amorphous fraction and to examine its variations for different cellulose samples. Such data can be derived from the quantitative contents of this fraction in the samples and the experimental data on their solubility given in Table 5.

TABLE 5

Results of Ethanolysis and Hydrolysis of Various Cellulose Samples

Sample	Reaction time (min.)	Ethanolysis		Hydrolysis	
		Amount of cellulose dissolved (% of sample)	$K_{min.}^{-1}$ for each time interval	Amount of cellulose dissolved (% of sample)	$K_{min.}^{-1}$ for each time interval
Cotton cellulose	20	3.2	0.00160	—	—
	60	5.0	0.00047	—	—
	180	7.7	0.00024	4.0	—
	300	8.7	0.0001	4.7	—
Wood cellulose	20	6.4	0.00330	—	—
	60	9.5	0.00085	2.0	0.00034
	180	14.0	0.00042	4.3	0.0002
	300	15.0	0.00010	5.6	0.0001
Cellophane	20	8.5	0.00440	3.3	0.00170
	60	15.9	0.00210	6.6	0.00086
	180	25.7	0.0010	12.5	0.00054
	300	31.8	0.0007	13.9	0.00013
Viscose rayon	20	10.5	0.0055	6.3	0.0032
	60	21.6	0.0033	9.3	0.00080
	180	31.5	0.0011	14.8	0.00052
	300	38.1	0.0008	18.2	0.00033

The results of such calculations for a reaction time of one hour are given in Table 6. These results show that the ethanolysis rate constants for the amorphous fraction of these samples lies in the approximate range of 0.01–0.02. They are therefore 50 to 100 times greater than the corresponding constants for the dense or crystalline fraction of cellulose.

TABLE 6

Calculated Ethanolysis Rate Constants for the Amorphous Fraction in Various Cellulose Samples (Reaction time 1 hour)

Sample	Amount of amorphous fraction (% of sample)		$K_{min.}^{-1}$
	before reaction	after reaction	
Ground cotton cellulose	68	48.0	0.0202
Cotton cellulose	7	2	0.0208
Wood cellulose	15	5.5	0.0167
Cellophane	42	26	0.0080
Viscose rayon	45	23.5	0.0110

Use of Ethanolysis in Studies of the Recrystallization of Cellulose

Samples of ground cotton and wood cellulose were used for studying the question of recrystallization of amorphous cellulose.

Recrystallization was brought about in these samples by soaking them in water at various temperatures. The soaked samples were washed with absolute alcohol to remove water and dried at 105°. Specimens of ground cotton cellulose were held in water for 1 hour at 20° and for 1 and 3 hours at 100°.

In the x-ray patterns for these samples interference rings were found similar to those found after hydrolysis.

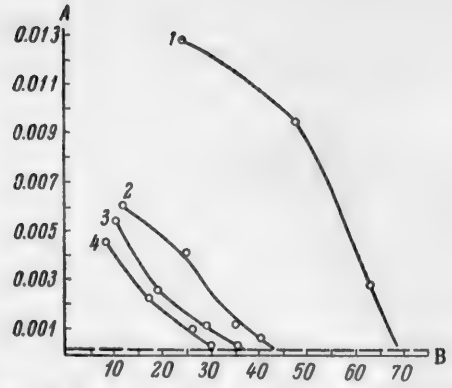

Fig. 4. Results of determination of the amorphous fraction in recrystallized samples of ground cotton cellulose. A)Rate constant $K_{min.}^{-1}$, B) amount of cellulose dissolved (%). Cellulose soaked in water: 1)original ground, 2) at 20° for 1 hour, 3) at 100° for 1 hour, 4) at 100° for 3 hours.

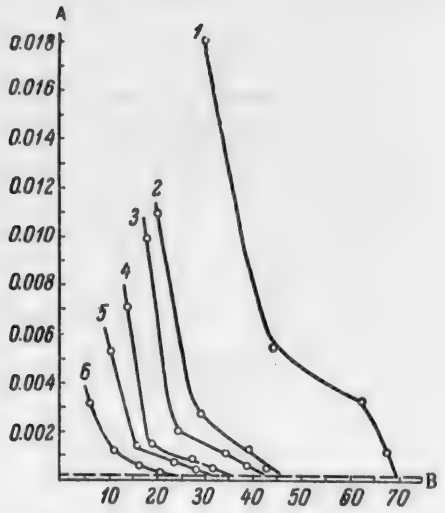

Fig. 5. Results of determination of the amorphous fraction in samples of ground wood cellulose recrystallized in water at various temperatures. A)Rate constant $K_{min.}^{-1}$, B) amount of cellulose dissolved (%). Temperature (degrees): 1)original cellulose, 2)1, 3)20, 4)100, 5)110, 6)180.

The results of ethanolysis of these samples, given in Table 7 and Fig. 4, show sharp changes in the reactivity of the samples. It is seen that the original sample of ground cellulose contains up to 68% of the amorphous fraction, the sample held in water for 1 hour at 20°, up to 43%, the sample held in water at 100° for 1 hour, up to 37%, and the sample held at 100° for 3 hours, up to 30%. These results therefore indicate that the amount of amorphous material in the samples falls rapidly with increase of temperature and soaking time. The influence of temperature on the recrystallization rate of the amorphous fraction was studied in greater detail for a sample of ground spruce sulfite cellulose. This sample was soaked in water at various temperatures for 30 minutes. Data on the contents of the amorphous fraction in the recrystallized cellulose samples, given in Table 8 and Fig. 5, show that at 1° the amount of amorphous fraction in the sample decreased from 68 to 45%. Increase of temperature produced a further decrease of the amount of amorphous material, which at 180° fell to 22% of the weight of the sample. It must be noted that during treatment with water, especially at high temperatures, part of the cellulose goes into solution; for example, at 180° up to 6% of the original sample is dissolved.

The ethanolysis rate constants for the amorphous fraction itself, calculated by the method described above, are given in Table 8. It is interesting to note that the values are in the range of 0.01–0.018, and are thus in the range found for different samples of native and regenerated cellulose. The constant decreases somewhat with decrease of the content of the amorphous fraction in the sample. Therefore the reactivity of the amorphous fraction is approximately the same in native, regenerated, degraded, and partially recrystallized samples of cellulose.

The amounts of the remaining amorphous cellulose are plotted against the soaking temperatures in Fig. 6. The plot is found to be linear. Since the hydrolysis rate of cellulose increases exponentially with temperature while the recrystallization rate increases linearly, it is to be expected that at high reaction temperatures the influence of recrystallization on the results of hydrolysis will be diminished considerably.

To verify this, experiments were carried out on the hydrolysis of ground wood cellulose at 140 and 160° in presence of 1% sulfuric acid, and at 200° in presence of 0.5% sulfuric acid. The results are plotted in Fig. 7 in the form of sugar yield curves. These results show that the mixiмum sugar yields at 140° reach 49% of the weight taken, at 160°, 63%, and at 200°, 76%. Thus, the sugar yield increased from 49 to 76%, i.e., by 27%, as the temperature increased from 140 to 200°. It is known, however, that in the hydrolysis of ordinary wood cellulose an increase of the reaction temperature from 140 to 200° increases the maximum yield of sugar only from

34.5 to 46.5%, that is, by 12%. Therefore the effect is considerably greater in the hydrolysis of ground cellulose, and this can be attributed to hydrolysis of the amorphous cellulose which does not have time to crystallize.

TABLE 7

Results of Ethanolysis of Recrystallized Samples of Ground Cotton Cellulose

Sample	Ethanolysis time (min.)	Amount of cellulose dissolved (% of sample)	Ethanolysis rate constant for each time interval $K_{min.}^{-1}$
Original ground cellulose	20	24.0	0.0137
	60	53.6	0.0123
	180	63.2	0.0019
Soaked in water at 18° for 1 hour	20	11.6	0.0063
	60	24.5	0.0039
	180	35.3	0.00128
	300	40.0	0.00063
Soaked in water at 100° for 1 hour	20	10.3	0.0054
	60	19.2	0.0026
	180	29.0	0.0011
	300	33.0	0.00044
Soaked in water at 100° for 3 hours	20	8.5	0.0048
	60	16.8	0.0024
	180	26.3	0.0010
	300	30.0	0.00042

Similar results were obtained in the hydrolysis of ground cotton cellulose and ground cellolignin. Experiments were also carried out on the recrystallization of viscose rayon by means of mild hydrolysis at 100° in 1% sulfuric acid for 30 minutes. 5.1% of the sample of viscose yarn passed into solution during this treatment. The amorphous fraction of the washed and dried residue was determined by the ethanolysis method. The results, given in Fig. 8, show that after hydrolysis of this rayon sample the content of its amorphous fraction fell from 45% to 32%, i.e., by 13%, with 5.1% weight loss in hydrolysis.

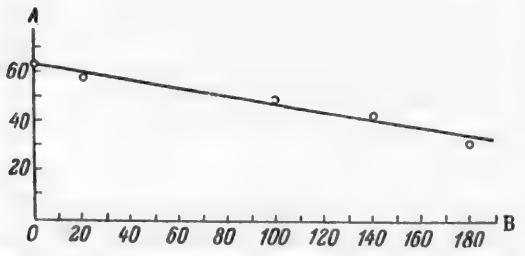

Fig. 6. Variations of the contents of the amorphous fraction in ground cellulose soaked in water at different temperatures. A) Amount of amorphous fraction (% of its content in original sample), B) temperature (degrees).

Thus, pronounced recrystallization occurs in this case also.

Use of the ethanolysis reaction for correction of the density values for amorphous cellulose

On the basis of x-ray data on the contents of the amorphous fraction in cellulose samples and of the densities of these samples, Hermans [12] found that the density of amorphous cellulose should be 1.505. It is evident that an error in determination of the amorphous fraction by the x-ray method must result in a corresponding error in the value found for the density. It is therefore of interest to calculate the density of amorphous cellulose with the aid of data obtained by the ethanolysis method.

The results obtained for ground cotton cellulose were used for this purpose. As stated earlier, this sample contained 68% amorphous fraction; its density, determined by the flotation method with carbon tetrachloride,

was 1.509. The density of the crystalline fraction was taken to be the value found by the flotation method [11]* for cotton cellulose after mild hydrolysis for removal of the amorphous fraction. This value was 1.550, which was near to the value of 1.558 found previously. The average of these two values, 1.554, was used by us for the calculations. Calculation of the density of amorphous cellulose gave a value of 1.488, which was considerably lower than the 1.505 found by Hermans.

TABLE 8

Results of Ethanolysis of Partially Recrystallized Samples of Ground Wood Cellulose

Recrystallization temperature (degrees)	Reaction time (min.)	Results of ethanolysis		Amount of amorphous fraction		Ethanolysis rate constant for amorphous fraction proper
		Amount of cellulose dissolved (% of sample)	$K_{min.}^{-1}$ for each time interval	as % of sample	as % of amorphous fraction in original sample	
Original cellulose sample	20	30.3	0.0180	—	—	—
	60	44.2	0.0056	—	—	—
	180	62.3	0.0032	—	—	—
	300	67.1	0.0011	70.0	100	0.0170
1	20	20.1	0.0110	—	—	—
	60	28.5	0.0028	—	—	—
	180	38.5	0.0012	—	—	—
	300	42.0	0.00049	45	64	0.0170
20	20	18.2	0.010	—	—	—
	60	24.5	0.0020	—	—	—
	180	33.8	0.0011	—	—	—
	300	38.4	0.0006	41	58	0.015
100	20	13.4	0.0072	—	—	—
	60	18.3	0.0015	—	—	—
	180	27.0	0.00095	—	—	—
	300	30.8	0.00044	35	50	0.012
140	20	10.3	0.0054	—	—	—
	60	15.4	0.0015	—	—	—
	180	24.0	0.0009	—	—	—
	300	28.1	0.0005	30	43	0.012
180	20	6.0	0.0030	—	—	—
	60	10.6	0.0012	—	—	—
	180	16.4	0.0006	—	—	—
	300	20.3	0.0004	22	31	0.011

The values found for the densities of the crystalline and amorphous fractions were used to determine the amorphous fraction in some cellulose samples, and the results were compared with data found by the ethanolysis method. The densities of partially recrystallized samples of ground cotton cellulose and viscose yarn were determined for this.

The amount of amorphous material in the cellulose was calculated by means of the formula

$$a = 100\,\frac{100 - (d_i - d_a)}{d_c - d_a}$$

where d_i is the density of the original material, d_c is the density of crystalline cellulose, and d_a is the density of amorphous cellulose.

The results, which are given in Table 9, show that determinations of the amount of amorphous material by the density method, with the use of our values for the densities of crystalline and amorphous cellulose, give results which are in better agreement than previously with the results found by the ethanolysis method.

*A.V. Krupnova assisted in the experimental work on density determination.

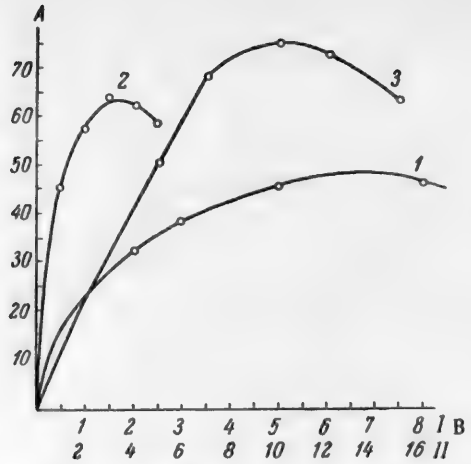

Fig. 7. Curves for sugar yields from ground wood cellulose hydrolyzed at different temperatures. A) Sugar yield (% of sample), B) reaction time (for 140 and 160°, in hours, I; for 200°, in minutes, II). Temperature (degrees): 1) 140, 2) 160, 3) 200.

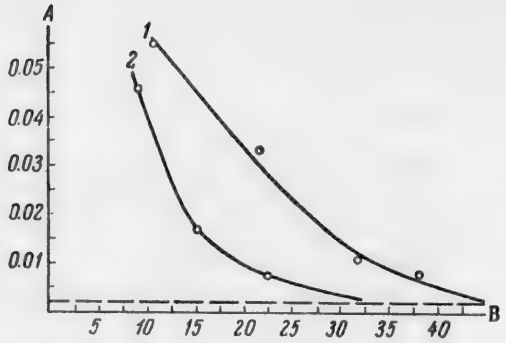

Fig. 8. Determination of the amorphous fraction of viscose rayon. A) Rate constant $K_{min.}^{-1}$, B) amount of cellulose dissolved (%). 1) Original fibers, 2) after mild hydrolysis.

TABLE 9

Determinations of the Amorphous Fraction of Cellulose from the Densities of Samples

Sample	Density at 20°	Content of amorphous fraction (in %)	
		by density	by ethanolysis
Ground cotton cellulose	1.509	68	68
Ground cotton cellulose soaked in water at 18°	1.517	56	43
Ground cotton cellulose soaked in water at 100° for 1 hour. . .	1.521	50	38
Cotton cellulose.	1.542	18	7
Viscose rayon	1.523	47	45

SUMMARY

1. In investigations of the reactivity of ground cellulose in alcoholysis in various alcohols it was shown that practically no recrystallization of the amorphous cellulose takes place.

2. It is shown that ethanolysis can be used as a method for the determination of the heterogeneity of cellulose.

3. The amounts of the amorphous fraction in different cellulose samples have been determined by the ethanolysis method.

4. The influence of temperature on the recrystallization rate of amorphous cellulose has been studied, and it is shown that by an increase of the hydrolysis temperature it is possible to diminish the influence of recrystallization on the hydrolysis rate of amorphous cellulose and on the yield of sugar formed in the process.

5. It is shown that hydrolysis of cellulose samples containing considerable amounts of amorphous cellulose is accompanied by rapid recrystallization of the latter.

6. The density of amorphous cellulose has been determined and it is shown that determinations of the amorphous fraction by the density method give results in agreement with ethanolysis data.

LITERATURE CITED

[1] V.I. Sharkov, O.A. Dobush, and G.D. Paramonova, Coll. Trans. All-Union Sci. Res. Inst. Hydrolysis and Sulfite Alcohol Ind. 3, 31 (1950).

[2] R. Nickerson, Ind. Eng. Chem., 33, 1022 (1941); 34, 85 (1942).

[3] F. Brenner, V. Frilette, H. Mark, J. Am. Chem. Soc., 70, 2, 877 (1948).

[4] H. Ingersoll, J. Appl. Phys., 17, 11, 924 (1946).

[5] O. Battista, Ind. Eng. Chem., 42, 3, 502 (1950).

[6] W.E. Roseveare, Ind. Eng. Chem., 44, 1, 168 (1952).

[7] V.I. Frilette, I. Hanle, H. Mark, J. Am. Chem. Soc., 70, 1107 (1948).

[8] A.G. Assaf, R.H. Haas, C.B. Purves, J. Am. Chem. Soc., 66, 1, 59 (1944).

[9] I.A. Howsman, Textile Research J., 19, 3, 152 (1949).

[10] F.C. Mayhes, H.I. Portas, H. Wakenam, J. Am. Chem. Soc., 69, 8, 1896 (1947).

[11] P.H. Hermans, I.I. Hermans, D.Vermaas, J. Polymer Sci. 1, 3, 162 (1946).

[12] P.H. Hermans, Contribution to the Physics of Cellulose Fibers (Amsterdam 1946).

[13] P.H. Hermans, A Weidinger, J. Am. Chem. Soc., 68, 12, 2547 (1946).

[14] P.H. Hermans, A. Weidinger, J. Polymer Sci. 1, 5, 533 (1951).

[15] P.H. Hermans, A. Weidinger, J. Appl. Phys., 19, 491 (1948).

[16] Nickerson, Habrle, Ind. Eng. Chem., 37, 1115 (1945); 38, 299 (1946).

Received March 5, 1956

THERMAL PROCESSING OF HYDROLYTIC LIGNIN

COMMUNICATION I. VACUUM — THERMAL DECOMPOSITION OF LIGNIN FROM WOOD HYDROLYSIS IN THE LIQUID PHASE

V.G. Panasyuk

The F.E. Dzerzhinsky Institute of Chemical Technology, Dnepropetrovsk

The processes now used for the thermal decomposition of plant tissues can be summarized as follows.

a) Dry distillation (or semicoking), performed in different modifications, such as continuous and discontinuous processes, distillation in vacuum or under pressure, distillation in inert gases or in vapors of various substances. All these modifications are intended to increase the yields of the most valuable chemical products.

b) Thermal liquefaction under pressure of solvent vapor. This has been used little as yet for plant materials.

In dry distillation, plant tissues are decomposed by the action of high temperatures.

The macromolecules in the plant materials become less stable under such conditions, and the forces binding atoms or groups of atoms together are disrupted under the action of thermal energy [1].

Scission of the molecules should occur at the weakest points in the chains. This may result in the formation either of substances of lower molecular weight, or of radicals. At high temperatures the molecules may combine with other molecules or with radicals. New substances are formed.

Secondary processes may then occur. Substances formed in the primary process undergo decomposition, the mechanism of which is not yet known. In dry distillation, secondary processes are induced by rapid rises of temperature caused by exothermic reactions [2], and also by overheating of the retort walls.

The aim in dry distillation is to reduce secondary processes to a minimum; this was achieved by some workers by the use of high vacuum [3], or by carrying out the process in various inert atmospheres [1].

In thermal liquefaction of substances under pressure of their own vapors [4], thermal decomposition of the molecules again occurs, and this is accompanied by decarboxylation, dehydration, and dehydrogenation reactions and by rupture of carbon chains; all this leads to formation of substances with different molecular weights. Up to 85% of the organic matter may be dissolved in the process. Dry distillation gives low yields of valuable chemical products.

In thermal liquefaction under pressure, higher yields are obtained, but the resulting solution requires further treatment—either hydrogenation or cracking. Moreover, this process must be carried out in equipment which withstands high pressures.

In our proposed process, dry distillation is combined with thermal liquefaction i.e., plant materials undergo heat treatment by vacuum—thermal decomposition in the liquid phase.

The procedure is as follows. The shredded plant material is mixed into a paste with tar, with a boiling point above 200°, and the mixture is gradually heated in a retort under a pressure of 40–60 mm Hg to 440–460°. This heating is continued for 90–120 minutes; the vapors of the tar and the vapors formed by decomposition of lignin are removed from the retort to a system of condensers.

In dry distillation the heat from the retort walls is transferred to the whole mass of plant material directly through the solid particles of this material; their heat conductivity is very low, and the process is therefore slow; the retort walls must be at a high temperature, and this favors the occurrence of secondary processes.

In the vacuum–thermal process heat transfer is much smoother, as the paste-former is heated at the retort walls and diffuses through the paste, transferring heat to it. The temperature in the retort is equalized rapidly, so that local overheating is prevented and secondary reactions thereby avoided.

In a large number of trials of the vacuum–thermal process we did not observe any sudden rise of temperature and increase of the yields of liquid distillate and gas such as take place when a definite temperature is reached in dry distillation; evidently no exothermic processes take place in this case.

The paste-forming tar plays a very important part in this process: it acts as a heat transfer medium and so assists the splitting of the molecules of plant material, decreasing the incidence of secondary processes considerably. The vaporized molecules are rapidly removed from the hot zone by the action of the vacuum, and are protected against cracking.

The yield of tar in this process is considerably higher than in dry distillation.

Vacuum–thermal decomposition is carried out in such a way that the tar used for making the paste can be returned to the process without addition of fresh tar. The additional tar formed by decomposition of the plant material, with b.p. up to 230°, is fairly valuable in composition and is processed.

The paste-forming tar must have a definite composition and properties. The tar used must boil out at a temperature close to the temperature at which the plant material begins to decompose, i.e., 280–340°, and must consist of substances with thermally stable molecules.

According to Tilicheev [5], aromatic substances, the rate of cracking of which is very low, are substances of this kind.

EXPERIMENTAL*

The vacuum-thermal decomposition of lignin from wood hydrolysis and cotton seed hulls was studied.

The thermal decomposition was carried out in high-boiling fractions of the tar obtained by dry distillation of the same materials, and also in anthracene oil which, as is known, is highly resistant to cracking.

TABLE 1

Yields Obtained in Vacuum–Thermal Decomposition of Wood Lignin

Experiment No.	Composition of paste	Yields (% on dry lignin)			
		carbon	tar	pyrolytic water	gas and losses
1	Lignin 1 part, dry-distillation tar 1.5 part	106.6	—	4.1	32.2
2	Lignin 1 part, tar 2 parts . . .	105.1	—	4.3	30.1
3	Lignin 1 part, tar 3 parts . . .	106.0	—	—	47.0
4	Lignin 1 part, tar 3 parts . . .	96.0	—	—	32.3
5	Lignin 1 part, heavy fractions from Experiments 3 and 4, 2 parts	87.8	—	7.0	33.0

*V.M. Mikhailenko took part in the experimental work.

At first, several experiments were carried out on the vacuum–thermal decomposition of wood lignin in high-boiling fractions of tar obtained by dry distillation of the same lignin. Light fractions were distilled off from the tar only up to 215°, as above this temperature the residue was too viscous. The paste was mixed at 100°.

The results of these experiments are given in Table 1.

All the experiments were carried out under the same conditions: final temperature 460°, pressure 60 mm Hg, duration 120 minutes.

The tar paste-former undergoes coking in these conditions, the amount of carbon formed being greater than the amount of lignin taken. Large amounts of gas are also evolved.

In Experiment No 5 the paste used was mixed with heavy tar fractions from Experiments 3 and 4. The process gave somewhat better results, but still was not good enough.

The only conclusion can be that the tar obtained by dry distillation of wood lignin cannot be used as paste-former for this process.

The process went considerably better in presence of anthracene oil, as Table 2 shows.

TABLE 2

Yields Obtained in Vacuum–Thermal Distillation of Wood Lignin in Anthracene Oil (Final temperature 460°, pressure 40 mm Hg)

Experiment No.	Composition of paste	Duration of process (min.)	Yields (% on dry lignin)			
			carbon	tar	pyrolytic water	gas and losses
1	Lignin 1 part, anthracene oil 2 parts	30	61.7	—	6.7	31.6
2	Lignin 1 part, oil 1.5 part. . .	60	55.0	17.5	10.0	17.5
3	Lignin 1 part, oil 2 parts . . .	90	56.2	28.3	5.0	10.5
4	Lignin 1 part, oil 1.5 part. . .	90	56.2	30.0	5.0	8.8
5	Lignin 1 part, oil 1.5 part. . .	90	56.0	28.2	6.2	9.6
6	Lignin 1 part, oil 1.5 part. . .	120	54.2	30.0	8.7	7.1

Examination of these data shows that excessively rapid decomposition (Experiment No. 1) leads to formation of much gas and gives a somewhat higher yield of carbon. Only the tar used in preparation of the paste was obtained.

If the process is carried out in 60 minutes, a fairly large amount of gas is formed, but the tar yield, after subtraction of the paste-former, is over 17%.

The subsequent temperature conditions, in Experiments Nos. 3, 4 and 5, were as follows: the temperature was raised at a rate of 4° per minute up to 300°, and after this at a rate of 7° per minute. It is seen that this had a favorable effect — the yields of tar increased considerably.

An increase of the duration of the process to 120 minutes did not raise the tar yield. The process was terminated at 420°. Above this temperature white smoke was given out, and deposited on the walls of the receiving flasks. The yields of water and gas showed that secondary processes were reduced to a minimum.

When anthracene oil was used as paste-former, it was necessary to determine how many times it can be returned into the process without addition of fresh anthracene oil. This was carried out as follows: all the tar

obtained in the first experiments was distilled up to 230°, the fractions below 230° were investigated, while the higher fractions were used for making the paste for the next series of experiments. The results of experiments with the tar recycled six times are given in Table 3.

These experiments were carried out under the optimum conditions in order to determine the yield of liquid substances from the organic part of the lignin: temperature 460°, duration 90 minutes, and pressure 40 mm Hg. It is seen that the heavy tar fractions obtained after the 1st run of the anthracene oil are less favorable to the process, as is shown by the higher yields of carbon and water and the lower tar yield.

After the 2nd run, under similar conditions, the yield of tar increased again, but did not reach the initial level; evidently the paste-former became stablized toward the action of high temperatures, after becoming somewhat enriched with lignin decomposition products. The subsequent yields of the tar fraction remained almost unchanged, apart from the experiments for the 5th run of the paste-former.

TABLE 3

Yields of Substances in Vacuum-Thermal Decomposition of Wood Lignin in Relation to the Number of Runs of the Tar

Paste-former	Yield (% on dry lignin)			
	carbon	tar	pyrolytic water	gas and losses
Anthracene oil.	55.6	29.1	6.2	9.0
Tar from 1st run.	60.4	21.6	9.3	8.7
Tar from 2nd run	57 1	25.4	7.5	10.0
Tar from 3rd run	60.0	26.3	7.5	6.2
Tar from 4th run	58.7	26.0	7.0	8.3
Tar from 5th run	57.4	30.5	8.4	3.7
Tar from 6th run	58.7	26.3	8.7	6.3

As is seen in Table 4, the paste-former changed both in fractional and in group composition.

The molecular weight changed little during the 6 runs. The molecular weight of the original anthracene oil was 200.0, and the molecular weight of the tar after the 6th run was 216.0. The density also showed little change. The anthracene oil had $d_4^{20} = 1.11$, and the tar after the sixth run, $d_4^{22} = 1.06$.

TABLE 4

Characteristics of Paste-Former Tars

Paste-former	Amounts of fraction (in %) at temperatures (deg)			Group composition (%)			
	up to 300	300—360	residue	acid substances	phenols	bases	neutral substances
Anthracene oil.	8.3	63.0	28.7	3.94	0.98	1.97	91.77
After 1st run	18.3	41.8	39.9	3.60	9.20	2.30	79.80
After 2nd run.	5.4	45.9	48.7	7.80	10.40	4.40	74.80
After 3rd run.	6.2	45.7	48.1	5.40	16.00	5.30	68.00
After 4th run.	5.0	50.9	44.1	7.50	21.80	5.20	65.50
After 5th run.	4.2	58.5	37.3	7.70	21.30	6.30	64.70
After 6th run.	3.2	52.5	44.5	7.70	18.00	6.30	64.00

Correlation of the fractional and group compositions of the tars with the degree of liquefaction of the lignin (as shown by the yield of liquids) indicates that the degree of decomposition of the lignin depends almost exclusively on the presence of the 300-360° fraction, which is the part of the paste-former in the boiling range of which the decomposition of lignin is most rapid. There is a direct relationship between the liquid distillate yield and the presence of the 300-360° fraction in the corresponding tar.

Anthracene oil is evidently a suitable medium for the liquid-phase vacuum-thermal decomposition of hydrolytic wood lignin.

The middle tar fraction (up to 230°) obtained in 25-30% yield on the weight of dry lignin by vacuum-thermal distillation is the product to be aimed at; phenols, their esters, and neutral substances (mainly hydrocarbons) can be isolated from it.

The group composition of the middle tar fraction (in % on the tar) is: acid substances 10.7, phenols 39.5, bases 6.5, neutral substances 43.3. It is seen that phenols and neutral substances predominate.

Up to 10-12% of phenols, on the weight of the dry lignin, can be obtained from this tar; wood lignin is therefore a valuable raw material for the production of light phenolic fractions.

SUMMARY

1. A new method for thermal conversion of hydrolytic lignin is proposed — vacuum-thermal decomposition in the liquid phase.

2. This process is ineffective if high-boiling fractions of tar obtained by dry distillation of wood lignin are used for paste making.

3. If anthracene oil is used as paste-former, a yield of up to 30%, calculated on the total lignin, of the middle tar fraction (up to 230°) can be obtained.

4. Anthracene oil can be repeatedly recycled for paste forming without losing its effectiveness in the process.

5. The middle tar fraction (up to 230°) yields 10-12% of light phenolic fractions, calculated on the weight of the lignin.

LITERATURE CITED

[1] N.I. Nikitin, Chemistry of Wood (1951).*

[2] V.N. Kozlov, Pyrolysis of Wood (1952).*

[3] P. Klason, J. prakt. Ch., 90, 413 (1914).

[4] M.K. Dyakova, Doctorate Dissertation, Institute of Mineral Fuels, Academy of Sciences USSR.

[5] M.D. Tilicheev, J. Appl. Chem. 12, 735 (1939).

Received July 23, 1955.

* In Russian.

REACTIONS OF STYRENE WITH VEGETABLE OILS

G.L. Yukhnovsky and R.R. Popanker

The V I. Lenin Polytechnic Institute, Kharkov

One important method of improving the film-forming properties of vegetable oils is by modification with polymerizable substances. This method has been extensively investigated abroad, and some copolymers of oils with polymerizable substances such as styrene and cyclopentadiene are extensively used. In our conditions, particular attention should be devoted to the possible applications of this method for improving the film-forming properties of semidrying oils, which hold the decisive position in our general vegetable oil economy. The subject of the present paper is an investigation of the conditions of copolymerization of sunflower seed oil with styrene.

Polystyrene gives very hard, water-resistant, light-resistant, chemically stable, colorless films with high dielectric properties. However, because of such defects as poor adhesion, brittleness poor compatibility with other film formers, etc., polystyrene cannot be used as a film former. Copolymerization of oil with styrene should yield a new product which combines the properties of both the starting materials.

A mechanism for the copolymerization of oils with styrene was postulated by Hewitt and Armitage [1] in 1946. In their opinion, the copolymerization mechanisms for oils with isolated double bonds and oils with conjugate double bonds are different. In the first instance the oil serves as a chain transfer agent, and plays the same part as a solvent. As is known [2], in presence of a solvent termination of a growing polymer chain may be caused by chain transfer effected by means of atoms of hydrogen, chlorine, or other mobile atoms of the solvent, which are attached to the free radical of the polymer and interrupt its growth. The free radical which is simultaneously formed from the rest of the solvent molecule can serve to initiate new chains. Chain transfer by solvent therefore lowers the molecular weight of the polymer. In presence of oils with isolated double bonds, polystyrene chain termination can take place by way of the mobile hydrogen of the methylene group in the α-position to the double bond; as a result, in the opinion of these authors, a product of the following type may be formed:

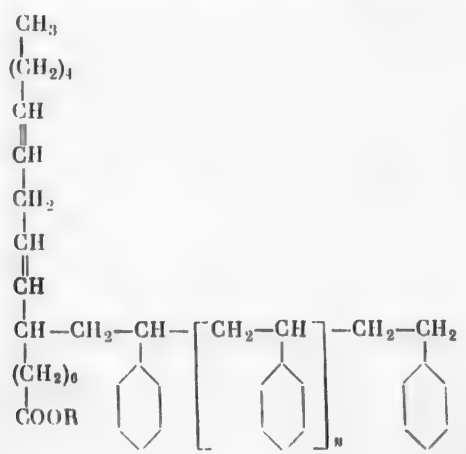

In copolymerization of styrene with fatty acids or their esters containing conjugate double bonds the reaction proceeds in the same way as in styrene–butadiene copolymerization, studied in detail by Alekseeva and Belitskaya [3]. According to their results, addition of styrene to butadiene occurs mainly in the 1, 4 position and the polystyrene chain growth is effected by way of the dienes. Copolymerization of styrene with fatty acids or their esters, which contain conjugate double bonds and which may be regarded as substituted butadienes, is represented by these authors as follows:

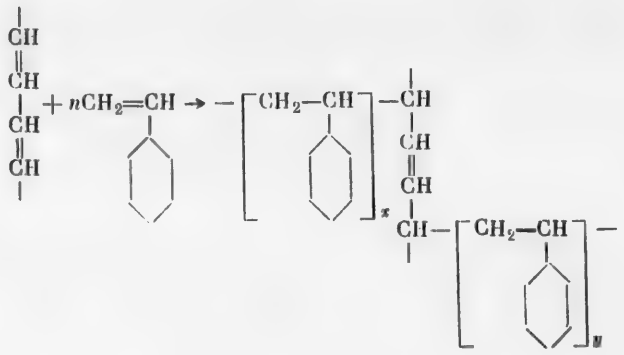

If the oils have high contents of double bonds, their copolymerization with styrene may easily result in gelation owing to formation of space polymers by cross linking between the fatty acid radicals.

Although there have been very many investigations of copolymerization of oils with styrene, sufficiently precise data on copolymerization conditions and the influence of individual factors on copolymerization have not been published, and studies of these questions and of the nature of the copolymerization products are of considerable interest. The present paper deals with the copolymerization of styrene with oil by the solution method.

EXPERIMENTAL

The experiments were carried out as follows. A mixture of the oil with styrene and xylene was boiled gently under reflux until the viscosity of natural drying oil was reached. Samples were taken at intervals for determinations of viscosity and of the dry residue (under vacuum); this quantity, and the saponification number of the dry residue, were used to calculate the contents of free and bound styrene in the copolymerization product.

Copolymerization of styrene with linseed, sunflower, or other "nonconjugated" oils under these conditions yields a product which leaves a turbid film after evaporation of the solvent. Copolymerization with tung oil yields a product giving a clear film, but this product has a strong tendency to gelation during heating or storage. Better results can be obtained by the use of an oil without conjugated bonds, with the addition of a certain amount (about 25%) of tung oil which, as is known, consists mainly of the triglyceride of eleostearic acid, with three conjugated double bonds. It is interesting to note that dehydrated castor oil, which also contains 20–25% of conjugated double bonds, is widely used abroad for copolymerization with styrene.

The results of the experiments are given in Table 1. In these experiments the proportions of oil: styrene: xylene were 1:1:2.

The data in Table 1 lead to the conclusion that the rate of viscosity increase, and hence the polymerization rate, depends on the degree of unsaturation of the oil — the slowest increase of viscosity was in the experiments with linseed oil (iodine number 185), and the most rapid was with olive oil (iodine number 81) and rape oil (iodine number 101). The explanation may be that highly unsaturated fatty acids contain more α-methylene groups, which give up their mobile hydrogens to the free radicals of the styrene polymer, terminating its growth. The molecular weight of the polymer and hence the viscosity increase is less in this case than if oils of a low degree of unsaturation are used. Sunflower oil (iodine number 125) occupies an intermediate position between

the above oils and therefore the duration of copolymerization has an intermediate value. The formation of an opaque product if olive oil is used may be attributed to the fact that the styrene polymers of higher molecular weight which are formed are less compatible with the oils, or with their styrene copolymers, than the low-molecular polymers formed when linseed oil is used.

Thus, in this case the oil acts as a molecular weight regulator of variable degree of activity, according to the number of double bonds and therefore the number of α-methylene groups.

Under the same conditions, styrene in presence of xylene, in 1:1 ratio without oil, quickly attains the viscosity of natural drying oil. When the copolymerization experiments were carried out under these conditions but in presence of benzoyl peroxide, the results did not differ greatly from those obtained without peroxide (Table 1).

TABLE 1

Results of Experiments on Copolymerization of Styrene with Oils

Composition of oil mixture (%)	Heating time to reach viscosity of natural drying oil (hours)	Dry residue (%)	Saponification number of copolymer (dry residue)	Amount of styrene reacted (%)	Appearance of dry residue	Film drying time (hours*)	Appearance of film
80 linseed + 20 tung	110	45	105	80	Transparent very viscous mass	1.5	Transparent
90 linseed + 10 tung	104	42	110	68		1.5	» »
70 sunflower + 30 tung	91	42.6	109	70		1	Opalescent
80 sunflower + 20 tung	62	50	95	100	Very viscous mass with slight opalescence	1	Slightly opalescent
90 sunflower + 10 tung	60	—	—	—	Turbid, very viscous mass	1.5	Turbid
95 sunflower + 5 tung	45	50	95	100		1.5	»
80 olive + 20 tung	36	—	—	—	White, almost solid dull mass	0.5	Dull white
100 tung	33	50	95	100	Transparent viscous mass	1	Transparent with glacial patterns
80 rape + 20 tung	25	45	99	80	White, almost solid opaque mass	—	Dull white
80 cottonseed + 20 tung	53	—	109	—	Dull mass	1	Dull
50 sunflower + 50 tung	46 Gels readily	—	—	—	Transparent mass	0.5	Transparent
Without oil (styrene: xylene = 1:1)	2	—	—	—	—	0.3	»

*The drying time was determined in presence of 0.1% cobalt linoleate, calculated on the metal.

In all the experiments given in Table 1 most of the styrene was combined within 25–40 hours. Further heating for tens of hours is needed to reach the required viscosity, as is seen from the graphs.

As will be shown later, the product formed in the polymerization of styrene with a mixture of nonconjugated and tung oils is a mixture of oil, copolymer, and polystyrene. Polystyrene is not compatible with oil, but has good compatibility with the copolymer, which aids the compatibility of polystyrene with oil. The copolymer in this instance was formed mainly from styrene and tung oil. Therefore if tung oil was absent or present in insufficient amounts, the product was an opaque or turbid mass, especially if oils of a low degree of unsaturation were used, as is seen in Table 1. With high contents of tung oil (sunflower:tung = 1:1) a transparent, rapidly drying film of high quality was obtained. However, the product is very unstable, and gels rapidly on keeping, and often even during preparation. The optimum oil ratio is sunflower:tung = 80:20.

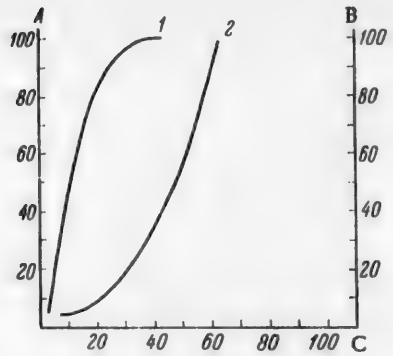

Effect of heating time on the reaction rate of styrene with oil (80% sunflower and 20% tung) (1), and the product (2). A) Amount of bound styrene (%), B) viscosity relative to natural drying oil (%), C) heating time (hours).

The relative proportions of the components — oil and styrene — have a considerable influence on the viscosity increase and on the properties of the product, as can be seen in Fig. 2.

The oil component in these experiments was a mixture of 80% sunflower and 20% tung oil. The rate of viscosity increase diminishes with increasing contents of oil (mainly nonconjugated) in the mixture; this is in agreement with the view advanced above that these oils act as solvents. At high oil contents (oil:styrene = 1:3 — 1:1 the molecular weight of the polymer is higher, the polymer is not compatible with the oil, and a dull product is obtained. With higher oil contents, the reaction product and the films made from it are transparent. The drying time increases sharply, and is similar to that for ordinary oil film formers.

TABLE 2

Effect of Component Ratio on Viscosity Increase

Composition of reaction mass (%)			Heating time reach viscosity of natural drying oil (hours)	Film drying time (hours)	Appearance of film	Saponification number of dry residue
oil	styrene	xylene				
—	50	50	2	0.25	Transparent	—
12.5	37.5	50	17	0.3	Dull	47
20	30	50	27	0.5	Dull	75
25	25	50	62	1	Slight opalescence	95
30	20	50	over 100	5	Transparent	—
35	15	50	over 120	5	Transparent	140
37.5	12.5	50	over 120	48	Transparent	149
37.5	37.5	25	15	1	Dull	100
30	30	40	30	1	Dull	96
20	20	60	over 100	1 (Remains tacky)	Transparent	95

The solvent content has a similar effect (Table 2). If the solvent content is low and the molecular weight of the product therefore higher, a dull film is obtained. With 60% xylene and a lower molecular weight, a clear film is obtained; the polymerization rate is very low and the required viscosity is not reached even after 100 hours of heating.

It follows from these results that, for formation of transparent films, the reaction mixture must contain not less than 25–30% oil (80% sunflower and 20% tung) and not less than 50% xylene. However, with these proportions of the components the viscosity increases very slowly, more than 60 hours being required before the viscosity of natural drying oil is reached. In order to shorten the process, we used previously polymerized oil. After numerous experiments, the following conditions were chosen. A 9:1 mixture of sunflower and tung oils (tung oil was added in order to raise the polymerization rate of the oil) was heated in an atmosphere of carbon dioxide at 280° for 12 hours, when the viscosity increased 35-fold. To this mixture 15% of tung oil was added; the molecular weight of the mixture of oils, determined cryoscopically in benzene, was 1429. This oil was heated with styrene and xylene, in the ratio 30 : 20 : 50. The required viscosity was reached after 45 hours. The dry residue in the product was 47%. According to its saponification number, this dry residue consisted of 66% of the oil and 34% of the styrene component. Its molecular weight was 1996. The properties of films made from this product were considerably superior to those of films from products made with nonpolymerized oil. The films dried within an hour. After 5 days the hardness by the pendulum apparatus was 0.4, the elasticity on the scale of the Scientific Research Institute for Lacquers and Paints was 1 mm, and the impact strength by the u–1 instrument was 50 kg/cm. The films have high resistance to water and oil and good adhesion (tested by the grid cutting test method). If the relative content of oil – either raw or polymerized – is decreased, the physicomechanical properties of the films decrease (impact strength, elasticity, and adhesion).

There are varied and highly contradictory views on the nature of the product. While the views of Hewitt and Armitage [1], given at the beginning of this paper, are to some extent supported by Powers [4], Schroeder [5], Bhow and Payne [6], and Drinberg [7], many workers, such as Falkenberg [8], Petit and Fournier [9], Brunner [10], and others, deny the formation of copolymers of oil and styrene and believe that the product is a mixture of polymers of moderately low molecular weight, mutually compatible with the unchanged oil. Petit and Fournier, and also Brunner and others, believe that this mutual compatibility is assisted by formation of a "monostyrenated" product (1 mole of styrene per 1 mole of fatty acid) from one molecule of acid with conjugated double bonds and one molecule of styrene, by the Diels – Alder reaction. Armitage and Kutt [11] demonstrated the presence of this product experimentally.

For our studies of the nature of the product we used the products of polymerization of styrene with acid isolated from oils. Acids of tung oil, sunflower oil, and of an 80 : 20 mixture of sunflower and tung oils were taken. The acids, styrene, and xylene in 1 : 1 : 2 ratio were boiled gently under reflux for 25 hours. As the data in Table 3 show 92–100% of the styrene became combined with the acids during this time.

TABLE 3

Results of Fractionation Experiments on the Copolymerization Products

Acids	Content of fatty acid component in dry residue (%)	Amount of combined styrene (%)	Fractionation results: fraction insoluble in alcohol		fraction soluble in alcohol*		fraction soluble in aqueous alcohol	
			% of dry residue	acid number	% of dry residue	acid number	% of dry residue	acid number
Tung oil	52.7	94.6	6	39.5	78	90	16	135.4
Sunflower oil	54	92	44	5.0	36	148	20	170
Mixture of sunflower and tung oils (80 : 20)	about 50	about 100	37	13	42	130	21	166

The products were fractionated; solutions in alcohol were treated with water by the following procedure, used in the case of the reaction product of styrene with tung oil fatty acids. The product was repeatedly extracted with boiling alcohol under reflux, with decantation of the alcoholic solutions. After each boiling and decantation the product must be thoroughly ground; therefore a Soxhlet extractor cannot be used in these

* This column gives the contents of the alcohol-soluble fraction after subtraction of the fraction soluble in aqueous alcohol.

conditions. After repeated extraction, the residue comprised 6% of the original weight taken, and had acid number 40. The alcoholic solution was treated with water in a separating funnel until slight turbidity appeared (29–30% of water must be added to 10% alcoholic solution for this). After standing, the product was extracted from both layers with benzene. 78% of the original sample consisted of an alcohol-soluble fraction with acid number 90, and 16%, of a fraction soluble in aqueous alcohol with acid number 135.4.

The reaction products of styrene with sunflower oil acids, and with a mixture of sunflower and tung oil acids (80 : 20) were fractionated similarly. The results are given in Table 3.

In investigations of the three fractions obtained from each copolymerization product we were primarily interested in determining whether a given product was a mixture of copolymers of different molecular weights or a mixture of polystyrenes of different molecular weights with unchanged acids. It is evident that if free non-styrenated acids are present in the product, they should first pass into the aqueous alcohol solution in fractionation. Free fatty acids of tung oil are readily detected spectrographically, as the eleostearic acid present in them has specific absorption in ultraviolet light in the 2680 A region. Eleostearic acid could not be detected spectrographically in the aqueous alcohol fraction of styrenated fatty acids from tung oil (with saponification number 135.4).

On the other hand, it would be interesting to establish the presence of pure polystyrene, which has specific absorption in the ultraviolet in the 2610 A region [12], in this product. Polystyrene could only be present in the fraction insoluble in alcohol; this fraction was studied spectrographically. No polystyrene was found.

Thus, the product formed by the reaction of styrene with tung oil fatty acids contains neither unchanged fatty acids nor polystyrene. The product is therefore a copolymer of styrene with the acids. On the basis of the work of Armitage and Kutt [11], who showed experimentally that a Diels — Alder product is formed when sorbic acid is treated with styrene, the presence of a compound of this type in our product may be expected. The acid number of such a compound, formed from one molecule of eleostearic acid and one molecule of styrene, is about 145. It seems likely that the fraction soluble in aqueous alcohol, with acid number 135.4, consists mainly of such a product.

Since 6% of the product consists of a fraction with acid number 39.5 (10–12 molecules of styrene to 1 molecule of acid), 78% consists of a fraction with acid number 90 (corresponding to one molecule of acid per 3–4 molecules of styrene), and only 16% is the fraction with acid number 135.4, it may be concluded that if a cyclic compound of the Diels — Alder type is present in the product, in any event the amount of it formed is relatively small; most of the product consists of a copolymer with average molecular weight 620, with 3–4 styrene units per one molecule of acid.

The polymerization product of sunflower oil acids with styrene has an entirely different composition. It contains 44% of a fraction insoluble in alcohol, with acid number 5.0. This fraction, like polystyrene, shows specific absorption in the ultraviolet in the 2610 A region. Comparison of the absorption maximum of polystyrene made by the solution method with the absorption maximum of the fraction insoluble in alcohol showed that the latter contained about 75% polystrene, so that 33% of the whole product consisted of polystyrene. The rest of the alcohol-insoluble fraction, or about 11% of the total product, had acid number 20. This means that 66% of the styrene taken for the reaction was converted into polystyrene and, as can be easily calculated from the acid number, about 20% of it was converted into a compound of polystyrene with fatty acids in which the fatty acids in which the fatty acid component comprises only about 10%. This may be a compound of the following type:

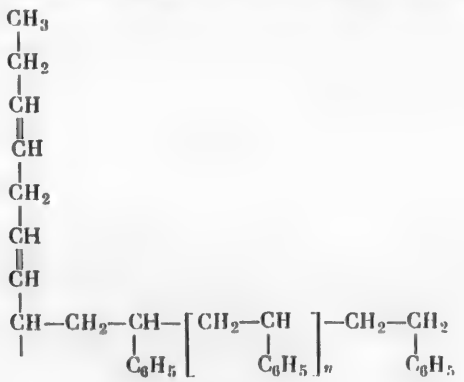

As was shown earlier in this paper, such a compound may be the result of chain termination by a free radical formed on removal of a mobile hydrogen atom from an α-methylene group.

The iodine number of the oil before and after its reaction with styrene shows that the polymeric radical is added to the methylene group and not at the double bond of the fatty acid molecule. Our determinations showed that after the reaction with styrene the iodine number of the dry residue corresponds almost exactly to the content of the oil component in it, and that the double bonds were not involved in the reaction.

Only 14% of the total styrene formed polymers of low molecular weight which, in combination with fatty acids, are soluble in alcohol and are even partially soluble in alcohol — water mixture. The acid number of the fraction soluble in aqueous alcohol (170), in which there are about 2 fatty acid molecules per styrene molecule, suggests that this fraction contains free acids. Shneiderova [13] also demonstrated, by means of molecular distillation, the presence of unreacted fatty acids after reaction of styrene with fatty acids containing isolated bonds. The styrene polymers of low molecular weight can dissolve in fatty acids and, together with the latter, in alcohol or even in water — alcohol mixture.

Thus the reaction product of styrene with fatty acids of sunflower oil differs sharply in nature from the reaction product of styrene with tung oil acids. The latter, as stated earlier, is a copolymer, whereas the former is a mixture of styrene polymer with fatty acids. Since polystyrene, apart from very low polymers, is insoluble in fatty acids, the product is opaque. It is obvious that if such a product is dissolved in an aromatic solvent the film formed after evaporation of the solvent is turbid.

As regards the reaction product of styrene with a mixture of the acids of sunflower and tung oils (80 : 20), analysis of the data in Table 3 leads to the conclusion that the contents and properties of individual fractions approximately correspond to the ratio between the nonconjugated and conjugated sunflower and tung oils. Spectrographic determination showed that the alcohol-insoluble fraction contained 51.7% polystyrene, so that 19% of the whole product was polystyrene. This means that 38% of all the styrene was converted into polystyrene. The rest of the alcohol-insoluble fraction, comprising about 18% of the total product, had, as can be easily calculated, acid number about 27, corresponding to a compound with molecular wight about 2100, so that a fatty acid molecule (of molecular weight 280) is combined with about 18 styrene molecules, and the compound contains about 82% of the styrene component. About 30% of the total styrene should take part in the formation of this product. The earlier data on the composition of the individual fractions of the reaction products of styrene with tung oil acids and styrene with sunflower oil acids indicate that the alcohol—insoluble fraction of the reaction product of styrene with a mixture of the acids of tung and sunflower oils is a mixture of polystyrene, a copolymer of eleostearic acid with styrene, and compounds of styrene with sunflower oil acids, of the type described above.

The remaining 32% of the styrene formed low-molecular products with the fatty acids; since the fraction soluble in aqueous alcohol has acid number 166, so that there is less than one molecule of styrene per molecule of acid, it may be concluded that free acids are present in the product.

All this complex mixture — fatty acids, polystyrene, copolymer of styrene with eleostearic acid, and compounds of styrene with sunflower oil acids — forms a transparent product owing to the mutual compatibility of a wide range of these compounds.

It seems likely that the reaction product of styrene with a mixture of tung and sunflower oils is of a similar nature.

As Petit and Fournier and others rightly stress, regardless of whether the reaction products of styrene with oils are pure copolymers or not, their coating properties are of very great interest to industry, and may give rise to extensive and varied applications.

LITERATURE CITED

[1] Hewitt and Armitage, J. Oil and Colour Chem. Ass., 29, 109 (1946).

[2] F.R. Mayo, J. Am. Chem. Soc., 65, 2324 (1943).

[3] E. Alekseeva and R. Belitskaya, J. Gen. Chem., 11, 358 (1941).

[4] Powers, Ind. Eng. Ch., 42, 2096 (1950).

[5] Schroeder, J. Am. Oil Chem. Soc., 26, 153 (1949).

[6] Bhow and Payne, Ind. Eng. Ch., 42, 700 (1950).

[7] A. Ya. Drinberg and B.M. Fundyler, J. Appl. Chem., 27, 618 (1954).

[8] Falkenberg, J. Am. Oil Chem. Soc., 29, 7 (1952).

[9] Petit and Fournier, Peinture, Pigments, Vernis, 26, 357 (1950).

[10] Brunner, Research, 42, 2 (1949).

[11] Armitage and Kutt, J. Oil and Colour Chem. Ass., 35, 195 (1952).

[12] Ahlers and O'Neill, J. Oil and Colour Chem. Ass., 37, 533 (1954).

[13] Schneiderova, Author's Summary of Dissertation, D.I. Mendeleev Inst. of Chemical Technology, (Moscow, 1954).

Received May 29, 1956

STUDIES OF DIENE COMPOUNDS

COMMUNICATION VI. POLYMERIZATION OF CHLOROHEXADIENOL

A.E. Akopyan and E. Kh. Khachatryan

The K. Marx Polytechnic Institute, Erevan

3-chloro-2, 4-hexadien-1-ol is obtained by hydrolysis of 1, 3-dichloro-2, 4-hexadiene [1].

Dichlorohexadiene has no tendency to spontaneous polymerization and does not enter into diene synthesis reactions, while chlorohexadienol polymerizes readily and enters into reactions of diene synthesis.

This great difference between the two compounds might be ascribed not only to the influence of the new substituent (OH), but also to changes in the structure of the diene compound during its preparation.

Normal hydrolysis of dichlorohexadiene should yield a primary chlorinated alcohol (I)

$$CH_2Cl-CH=CCl-CH=CH-\overset{HOH}{CH_3}\begin{cases}\nearrow CH_2OH-CH=CCl-CH=CH-CH_3 & (I)\\ \searrow CH_2=CH-CCl=CH-CH(OH)CH_3 & (II)\end{cases}$$

while hydrolysis accompanied by isomerization with diene rearrangement should give rise to a secondary chlorinated alcohol (II), which should be more reactive then (I).

To settle the question of the structure of chlorohexadienol, it was oxidized with potassium permanganate. Acetic and oxalic acids were isolated from the product, while formic acid was not found.

These results show that the structure of chlorohexadienol is represented by Formula (I).

However, in the oxidation of chlorohexadienol by potassium permanganate the possibility of isomerization with diene rearrangement of the diene compound is not excluded. Therefore, for more rigorous proof of the structure of chlorohexadienol it was hydrogenated over a nickel catalyst. Hydrogenation yielded n-hexyl alcohol.

The results obtained in diene synthesis reactions of (I) and the oxidation and hydrogenation of chlorohexadienol provide an adequate basis for assuming its structure to be 3-chloro-2, 4-hexadien-1-ol.

As far as we know there are no data in the literature on the polymerizability of chlorodienols. Therefore study of the polymerization of 3-chloro-2, 4-hexadien-1-ol is of definite theoretical interest, quite apart from the possible practical significance of the polymers formed.

Polymerization of chlorohexadienol to 60–70% conversion yields a polymer soluble in alcohol, while at greater degrees of conversion a gelatinous insoluble polymer is formed.

The polymerization of chlorohexadienol may be represented as

$$2n\left[\begin{array}{c}CH=CCl-CH=CH\\ |\qquad\qquad |\\ CH_2OH\qquad CH_3\end{array}\right]\rightarrow\left[\begin{array}{c}-CH-CCl=CH-CH-CH-CCl=CH-CH-\\ |\qquad\qquad |\quad |\qquad\qquad |\\ CH_2OH\qquad CH_3\ CH_2OH\qquad CH_3\end{array}\right]_n$$

since the principal decomposition product of the ozonide of the polymer is α-methylbutyrolactone-β-carboxylic acid, which is formed from the primary decomposition product of the ozonide, α-methyl-α'-methylolsuccinic acid, by loss of a water molecule

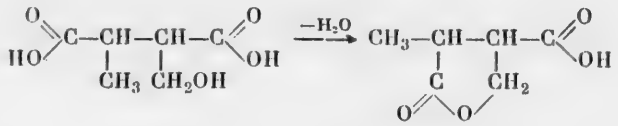

The gelatinous, insoluble polymer is probably the result of a branching reaction between the growing active radical and a polymer molecule

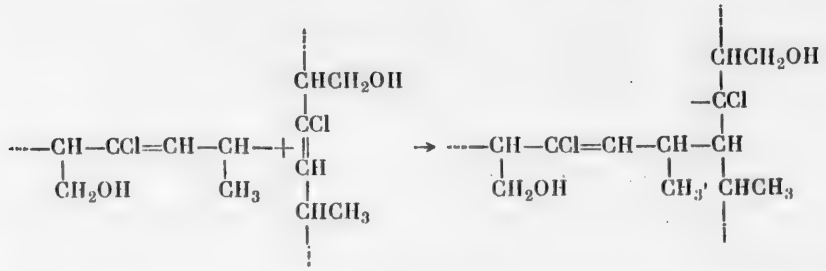

An alcoholic solution of chlorohexadienol polymer applied in a thin layer to a surface dries rapidly with formation of a transparent colorless (or faintly colored) film with satisfactory mechanical and chemical properties.

EXPERIMENTAL

Oxidation of chlorohexadienol with potassium permanganate. 350 ml of water was put into a three-necked flask fitted with a mechanical stirrer and thermometer, and 14.5 g of chlorohexadienol was then emulsified in this. 105 g of potassium permanganate was added during 7 hours with continuous vigorous stirring. The oxidation was carried out at 2–3°. The reaction medium was kept slightly alkaline by additions of small portions of potassium carbonate.

The manganese peroxide precipitate was filtered off by suction and washed with hot water; the filtrate was acidified with 10% sulfuric acid solution, and the organic acids were extracted with ether.

Fractionation of the ether solution, dried over anhydrous Na_2SO_4, gave two fractions and a crystalline residue.

The first fraction did not give the calomel reaction. The acid number of the second fraction was determined: 0.1972 g of substance took 32.5 ml of 0.1 N KOH, 0.1164 g took 19.0 ml of 0.1 N KOH. Acid numbers found: 923, 916; calculated for acetic acid, 935.

Acetic acid was identified by analysis of the silver salt, made by heating an aqueous solution of the acid with excess freshly precipitated silver oxide. The solution of silver salt was separated from the precipitate by filtration, the filtrate was evaporated on the water bath, and the silver salt so obtained was recrystallized and dried to constant weight.

The amount of silver in the salt was found gravimetrically

0.1582 g substance: 0.1031 g Ag
0.1742 g substance: 0.1122 g Ag
Found %: Ag 65.2, 64.5. CH_3COOA_g calculated %: Ag 64.7.

The crystalline residue from the distillation (somewhat contaminated with a tarry substance) melted at 98–99° after recrystallization from water (oxalic acid dihydrate melts at 100°). The oxalic acid was identified as its calcium salt, insoluble in acetic acid or water.

Hydrogenation of chlorohexadienol was carried out over a nickel catalyst at room temperature and under slight excess pressure. The duration of hydrogenation was 4 hours.

About 1 g of catalyst was put into a vessel about 200 ml in capacity. To the catalyst, 50 ml of ethyl alcohol (90%), containing 3.9 g of caustic soda and 11.5 g of chlorohexadienol, was added. Electrolytic hydrogen was used for hydrogenation. About 6 liters of hydrogen was absorbed. The first 4 liters of hydrogen was absorbed fairly rapidly (within 1 hour), and there was even some increase of temperature.

After absorption of hydrogen almost ceased, the alcoholic solution was separated from the precipitate by filtration, and the filter was washed with a small amount of alcohol which was added to the filtrate.

Ethyl alcohol was distilled off on a water bath from a flask fitted with a fractionating column, and the residue was washed three times with water (in 10 ml portions) to remove remaining ethyl alcohol; the oily layer was dried over calcium chloride and distilled. The distillate had the following properties; b.p. 153–154° at 730 mm, d_4^{20} 0.8285, n_D^{20} 1.4130; these are close to the corresponding values for n-hexyl alcohol.

Polymerization of chlorohexadienol. When the freshly distilled chlorohexadienol was kept at room temperature, its viscosity gradually increased. After 6 days it turned into a viscous faintly colored mass. After 8 days gelation of the mass took place. The gelatinous polymer is not soluble in common organic solvents, but partially swells in them. Gel formation usually occurs when 60–70% of the original monomer has been polymerized.

The gelatinous polymer (d = 1.175) obtained by complete polymerization of the monomer changes little when kept in air: it always remains soft, but is quite inelastic.

The product separated by precipitation with solvents (benzene) at up to 60% conversion of the chlorohexadienol is a soft and elastic polymer, soluble in alcohol. When this polymer is kept in air it is gradually converted into a hard dense mass, no longer soluble in alcohol.

Polymerization of chlorohexadienol is initiated by peroxides and by oxygen (from the air). The following experiments were performed in order to determine the variation of the polymerization rate with the amount of air present in the system: chlorohexadiene was polymerized in sealed tubes containing from 0 to 400% air (apart from the amount dissolved) on the volume of the chlorohexadienol, for 5 days at room temperature. The polymer contents in the samples were determined by vacuum distillation.

TABLE 1

Initiating Action of Oxygen

Amount of monomer (in g)	Ratio of air to monomer	Amount of polymer	
		in g	in %
10.25	0.00	0.98	7.8
9.78	0.25	1.81	18.5
10.64	0.50	2.83	26.6
9.84	1.00	3.14	32.1
10.45	4.00	3.60	34.5

The initiating effect of oxygen (atmospheric) is clear from the data in Table 1. Starting from 1:1 ratio of air to chlorohexadienol, the polymerized mass acquires a faint color, the intensity of which increases with the amount of air present.

The following series of experiments was performed in order to determine the effect of initiator concentration on the polymerization rate of chlorohexadienol: from 0.011 to 0.312 g of benzoyl peroxide and 9 ml of chlorohexadienol was put into each of a series of tubes. The air was displaced by nitrogen, the tubes were sealed, and kept at 40° for 12 hours. At the end of this time the tubes were opened, the polymers in them precipitated with benzene (20 ml), then washed with benzene (twice with 20 ml lots) and dried under vacuum at 50° to constant weight.

The results of these experiments are given in Table 2.

It is clear from the data in Table 2 that the polymerization rate of chlorohexadienol increases with increasing benzoyl peroxide concentration. At initial concentrations of 0.1115 and 3.02% of benzoyl peroxide the total polymerization rates correspond to the formation of 6.33 and 33.30% of polymer respectively.

The data in the penultimate column of the table show that the average polymerization rate is proportional to the square root of the original concentration of benzoyl peroxide ($w \approx 1.6\sqrt{\pi}$).

TABLE 2

Effect of Peroxide Concentration on the Polymerization Rate

No.	Amount of monomer (in g)	Peroxide concentration		Amount of polymer			$\frac{\eta}{c}$	Specific viscosity of solution
		in g	in %	in g	in %	in % per hour		
1	9.86	0.011	0.1115	0.624	6.33	0.527	1.59	0.170
2	9.75	0.019	0.1952	0.929	9.54	0.795	1.80	0.168
3	10.12	0.041	0.406	1.405	13.88	1.156	1.82	0.165
4	9.76	0.081	0.830	1.670	17.10	1.425	1.51	0.158
5	10.44	0.159	1.520	2.355	22.52	1.870	1.52	0.148
6	10.32	0.312	3.020	3.440	33.30	2.775	1.60	0.134

The effect of the initial benzoyl peroxide concentration on the molecular weight of the polymer formed was studied by measurement of the specific viscosity of dilute alcoholic solutions of the polymers. The results of these measurements, given in the last column of Table 2, are recalculated for 0.2% of the polymer in solution.

The data in the last column of the table show that the viscosity of the alcoholic solutions, and hence the molecular weight of the polymers, decreases with increasing concentration of benzoyl peroxide in the monomer.

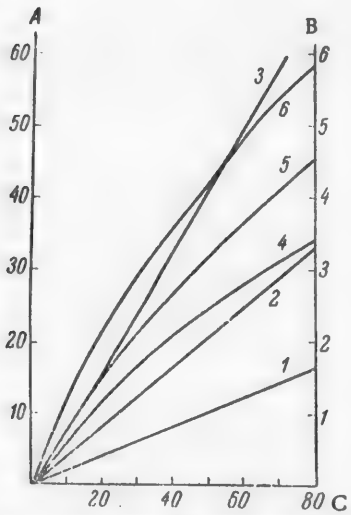

Polymerization curves. A) Polymer contents (%) obtained with initiator; B) polymer contents (%) obtained without initiator; C) time (hours). Curves: 1, 2, 3) polymerization without initiator at 30, 40, and 50° respectively; 4, 5, 6) the same, with initiator.

Effect of temperature. The polymerization of chlorohexadienol is accelerated by increase of temperature, both in presence and in absence of initiators. The temperature coefficient of the polymerization rate of chlorohexadienol is smaller in presence of initiators than in their absence.

Two series of experiments were carried out in order to determine the effect of temperature on the polymerization rate of chlorohexadienol.

In the first series of tubes the polymerization was carried out in absence of initiator, and in the second, in presence of 0.05 g of benzoyl peroxide. Parallel series of experiments were carried out at 30, 40, and 50°.

The polymer contents of the samples were determined by precipitation. The experimental results are given in the Figure.

Polymerization of chlorohexadienol in the 90–100° range yields colored polymers. Very small amounts of hydrogen chloride are liberated.

The polymers so formed differ in properties from the polymers obtained at lower temperatures. In distinction from low-temperature polymers, high-temperature polymers obtained in an atmosphere of air are soluble, if only slightly, in common organic solvents. The solubility of the high-temperature polymers in benzene is much lower if they are formed in a nitrogen or hydrogen atmosphere.

Ozonation of chlorohexadienol polymer. The polymer was made by polymerization of freshly distilled chlorohexadienol in presence of benzoyl peroxide (0.2%) at 40°. The polymer was precipitated with chloroform

at 35.8% conversion. The precipitated polymer was washed several times with chloroform and dried in a current of nitrogen under vacuum. The polymer (3.2 g), cut into thin shavings, was transferred to a reaction vessel which was then filled with chloroform.

To ozonize the polymer, ozonized oxygen containing about 3% ozone was passed through at 10 liters/hour. Because of its insolubility in chloroform, the polymer was very difficult to ozonize. The chloroform was distilled off under vacuum and the residue was dried to constant weight at 40° and 10 mm Hg. To the residue 60 ml of distilled water was added, and the liquid was boiled on the water bath for 3 hours. The aqueous solution of the ozonide decomposition products was filtered off, the water was distilled off under vacuum, and the residue (a crystalline mass) was dried at 50° to constant weight. The weight of the crystalline mass was 0.885 g. Recrystallization from ether gave long prisms with m.p. 103–103.5° (m.p. of 2-methylbutyrolactone-β-carboxylic acid is 104°) [2].

Attempts to isolate crystals of methylsuccinic acid from the mother liquor (ether solution) were not successful.

Tests of the mechanical properties of the films. The required amounts of the polymers were obtained by polymerization of chlorohexadienol in presence of benzoyl peroxide (0.5% on the weight of monomer) and air, at room temperature, in sealed tubes. The degree of conversion of the monomer was 59.5% in the first case and 32.5% in the second.

The polymers were isolated by precipitation and dissolved in alcohol to give 10% solutions. The alcoholic solutions were applied twice in thin layers to plates of glass and tin plate, which were then kept at room temperature.

The colorless clear films so formed were subjected to mechanical tests after 7 days. The results indicate that the presence or absence of initiator (peroxide) during polymerization of chlorohexadienol has no appreciable influence on the properties of the films obtained from the polymers.

The films had the following characteristics: drying time 0.5–2 hours, hardness, by the Clemens test, 150–300 g, elasticity 1 mm on the scale of the Scientific Research Institute for Lacquers and Paints, impact strength 30–50 cm.

Repeated tests (15 and 30 days after the first) showed no changes in the film properties. Little change was produced when the films were heated at 100° for 4–5 hours.

The films are resistant to the common organic solvents, dilute acids (sulfuric and hydrochloric), and water, but not to alkali solutions. These results were obtained by immersion of metal rods coated with the films in the reagents for 1.5–2 months. Polymerization of chlorohexadienol in presence of a small amount of air (2–3 times the volume of the polymer) yields faintly colored polymers, alcoholic solutions of which form elastic, strong films of a pleasant color (with a luster without polishing) on wood surfaces. Alcoholic lacquers made from chlorohexadienol polymer may prove suitable for treatment of furniture.

SUMMARY

1. Polymerization of 3-chloro-2, 4-hexadien-1-ol to 60–70% conversion yields a polymer soluble in alcohol, while at greater degrees of conversion gelatinous insoluble polymers are formed.

2. Polymerization of chlorohexadienol is accelerated in presence of initiators and oxygen (air).

3. Polymerization of chlorohexadienol at 90–100° yields colored polymers. The high-temperature polymers, in contrast to those obtained at low temperatures, are partially soluble in the common organic solvents.

4. Alcoholic solutions of chlorohexadienol polymer form elastic, strong films with satisfactory chemical and mechanical properties on wood, glass, and metal surfaces.

LITERATURE CITED

[1] A.E. Akopyan, J. Appl. Chem., 27, 562 (1954).

[2] Fichter, Rudin, Ber., 37, 1613 (1904).

Received for the second time, November 23, 1956

PRODUCTION OF FOAMING AGENTS BY CONDENSATION OF STARCH DEGRADATION PRODUCTS WITH AMINES AND AMINO ACIDS

V.P. Goguadze and G.M. Yashvili

The Tbilisi Scientific Research Chemicopharmaceutical Institute

The importance of substances which give mechanically and thermally stable foams is well known [1-4]. Among the numerous surface-active compounds suggested for this purpose, natural surface-active substances known as saponins have extensive practical uses, either in the form of extracts from saponin-containing plants such as licorice and sassafras [5], or as powders made by grinding separate portions of these plants. Mitkevich [6] recently reported successful experiments on the stabilization of foams, produced by licorice shoot extracts, by means of mineral additives.

The object of the present work was the synthesis of new types of foaming agents. Our attention was drawn to the possibility of making use of interactions between carbonyl groups and amino groups for combining the hydrophobic and hydrophilic parts of the molecule of a surface-active substance. We were therefore interested in the synthesis of foaming agents of the Schiff base type.

It has been stated [5] that the practical applicability of Schiff bases as foaming agents is limited owing to the weak surface-active properties of these substances. Nevertheless, we believed that if starch is used as the carbonyl-containing starting material in condensation of carbonyl compounds with amine and amino acids, effective foaming agents could be obtained. However, although this carbohydrate has a considerable hydrophilic group content, the difficulty of using it as a raw material lies in the fact that the carbonyl groups in starch are not free to react. This difficulty was overcome by the choice of special reaction conditions. In particular, use was made of the fact that when starch is heated its large molecules are broken down into smaller dextrin molecules, with formation of free carbonyl groups.

All the conditions necessary for condensation of carbonyl groups with amines should be present in most favorable form at the moment of dextrinization of the starch in presence of amino groups, when the molecules formed by dextrinization are at a high energy level.

There was another interesting aspect to the occurrence of this reaction in these peculiar conditions. The abundance of so-called potential carbonyl groups in the starch molecule made it possible to continue the condensation process to any desired limit by variations of the heating time of the reaction mixture, the temperature, and the relative proportions of the components.

Dextrinization of starch in presence of various amines was both of purely practical and of some general interest, as experiments on reactions of this type in such complex chemical conditions have not been described previously.

The typical representatives of amines and amino acids used for the experiments were aniline and o-aminobenzoic acid which, in our view, should give rise to the hydrophobic groups in the condensate molecules.

The condensation of these amines with starch degradation products was effected by the action of heat at 180°, for different periods, on mixtures of starch with the amine or amino acid in various proportions.

Exploratory experiments showed that aniline and o-aminobenzoic acid can yield, with starch degradation products, condensates of considerable foaming power, and that these condensates are most easily dissolved in boiling water.

It was also found that in dextrinization of starch in mixtures with aniline the mixture only retains a liquid consistency, which is very necessary for uniform heating of the reaction medium, if the ratio of starch to aniline in the reaction mixture does not exceed 1:10. With this ratio of the starting materials in the reaction medium, so much excess aniline remained if small amounts were condensed that the reaction mixture could be easily stirred and heated during the whole time of reaction. However, in experiments on a larger scale, with vigorous agitation, this ratio could be increased to 1:3. The experiments showed that the nitrogen contents of the reaction products increased with increasing boiling time of the reaction mixture. After 12 hours of boiling the nitrogen content of the reaction products reached 0.27%, and the foam produced by the condensate formed under these conditions had the greatest stability.

The condensation of starch degradation products with o-aminobenzoic acid was effected in a laboratory dextrinizer. It was found that, in addition to the heating time, the weight proportions of the starting materials are also significant for the course of the reaction. The experiments showed that for the production of a foaming agent yielding the most stable foam the weight ratio of starch to o-aminobenzoic acid should be 1:0.8. In these conditions the dextrinization of the mixture was adequate in 2.5 hours, and the nitrogen content of the condensate reached 2.87%. Further increase of the heating time and decrease of the component ratio invariably caused strong resinification of the reaction mass.

The complete investigation of all the surface properties of the condensates obtained was a separate task. However, for preliminary purposes we considered it sufficient to determine the stability of foams formed by aqueous solutions of the condendates, by a relatively simple method described in 1932 [7]. 10 ml lots of 2% aqueous solutions of the condensates were shaken in test tubes of standard size (150 mm long and 14 mm in diameter), and the stability of the forms was determined by observations for 24 hours after shaking.

The comparison standard in these experiments was an aqueous solution of a vigorous foaming agent — tea seed saponin [8] — of the same concentration, in a similar test tube.

The foaming power was indicated by the height of the foam formed when the tubes were shaken, and the foam stability, by the height retained by the foam for 24 hours.

For a final evaluation of the stability of the so-called chemical foam, the condensates were mixed with sodium bicarbonate and tested according to GOST [9]. The standard in these tests was a similar mixture of licorice root.

Because of the complex composition of the starch degradation products and of their condensation products with amines, the possibilities of isolating any individual compounds from the condensation products were very limited. It is therefore assumed, because of the formation of water in the reaction and the presence of nitrogen in the reaction products, that in the conditions of our experiments the condensation reaction leads to the formation of compounds of the Schiff base type.

Our experiments therefore confirmed that new foaming agents, equivalent to natural saponins, can be synthesized by condensation of aniline or o-aminobenzoic acid with starch degradation products.

EXPERIMENTAL

Condensation of starch degradation products with aniline. 15 g of starch dried at 115–120° and 150 g of freshly distilled aniline were put into a Wurtz flask, fitted with a dropping funnel and a Liebig condenser leading to a glass receiver. To protect the reaction medium against the action of atmospheric oxygen, the glass receiver was connected to a Tishchenko flask containing alkaline pyrogallol solution.

The reaction mixture was boiled on an oil bath. The mixture was boiled at the boiling point of aniline, which corresponded to the dextrinization temperature of starch. During the boiling aniline was distilled out of the reaction mixture, together with water formed in the condensation. As the aniline–water mixture was distilled off, equal amounts of freshly distilled aniline were continuously added from the dropping funnel.

At the end of the heating the reaction mixture was filtered, the residue was weighed, extracted with ether to remove aniline, and weighed again. The resulting condensate was a yellowish powder.

The experiment was repeated 8 times with different boiling times, 8 different condensates being obtained. The results given in Table 1 refer to experiments in which the proportions were 15 g of starch to 150 g of aniline.

10 ml lots of 2% aqueous solutions of the condensates listed in Table 1 were put into standard test tubes 14 mm in diameter and 150 mm long. The control tube contained, for comparison, 10 ml of a 2% aqueous solution of a known powerful foaming agent — tea seed saponin [8].

All the tubes were shaken vigorously and left at rest for 24 hours. It was found that the stability and degree of foam formation increase with increasing nitrogen contents in the condensates. With 1.29% nitrogen in the condensate the foaming power and foam stability were equivalent to those of tea seed saponin.

Large-scale experiment on the condensation of starch degradation with aniline. The reaction was carried out in a vertical tinplated cylinder, 40 cm in internal diameter and 83 cm high.

The reactor lid, which could be clamped down hermetically, was fitted with an electric motor connected to a stirrer which reached the bottom of the cylinder and which passed through the lid in a tight gland; the lid was also fitted with a thermometer, dropping funnel, and a Liebig condenser. The latter was joined, by means of an adapter, to a receiver, and the latter was connected by rubber tubing to a Tishchenko flask containing alkaline pyrogallol solution.

TABLE 1

Variation of Nitrogen Contents of Condensates with Time of Heating of the Reaction Mixture

Number of experiment (condensate No.)	1	2	3	4	5	6	7	8
Heating time (hours)	0.5	1	2	3	5	7	9	12
Amount of aniline distilled off	50	100	150	200	400	500	600	700
Nitrogen contents of condensate, by Kjeldahl (%) . .	Traces	Traces	Traces	0.51	0.93	1.09	1.29	1.29

16 liters of aniline was put into the reactor and 5 kg of starch, dried at 110–120° and sifted through a No. 3 sieve (32 threads per cm), was gradually added with constant stirring. The reactor was then hermetically closed, the electric stirrer was switched on, and the temperature of the mixture was gradually raised by means of a gas flame to the boiling point of aniline, which coincides with the dextrinization temperature of starch.

The reaction mixture was boiled for 12 hours. Water – aniline mixture was distilled off and collected in the receiver. Freshly distilled aniline was added during the whole time from the dropping funnel, in amounts equal to the volume of the distilled mixture. A total of 4.6 liters of water – aniline mixture was distilled off during the reaction, and the same amount of aniline was added. After 12 hours of heating the reaction mixture was cooled to room temperature and the condensate was purified as described for the previous experiment.

The yield was 6.75 kg of crude condensate moist with aniline, and 13.4 liters of technical aniline, suitable for recovery.

After extraction of excess aniline from 6.75 kg of the crude condensate (in an apparatus of the Soxhlet type) by means of 7 liters of dichloroethane for 44 hours, the extracted condensate was dried; the yield was 5.25 kg.

The elemental composition of the condensate was:

5.270 mg subst.: 8.539 mg CO_2; 3.00 mg H_2O.
5.375 mg subst.: 8.745 mg CO_2; 3.127 mg H_2O.
5.395 mg subst.: 0.059 ml N_2; 756 mm Hg, 22°.
6.401 mg subst.: 0.075 ml N_2; 756 mm Hg, 22°.
Found %: C 44.53, 44.39; H 6.37, 6.51; N 1.25, 1.34.

Condensation of starch degradation products with o-aminobenzoic acid. The experiments were carried out in a dextrinizer. A mixture of starch, dried at 115–120° and sifted through a No. 3 sieve, and o-aminobenzoic acid was placed in a horizontal duralumin cylinder with closely fitting lids. For mixing the reaction mixture, an iron shaft (5 mm in diameter) fitted with blades and driven by an electric motor passed through packing glands in the lids.

The reaction mixture in the dextrinizer was heated by means of an external cylindrical jacket filled with aniline and fitted with a reflux condenser. Aniline was heated to the boil in the outer jacket by means of a gas burner. This maintained a temperature of about 180° inside the dextrinizer.

TABLE 2

Variation of Nitrogen Contents of Condensates with Time of Heating and the Proportions of the Components in the Mixture

Experiment No.	Starch taken for reaction (kg)	Amount of aminobenzoic acid (%)	Heating time (hours)	Nitrogen contents of condensates, by Kjeldahl (%)
1	10	1	5	Traces
2	10	3	5	Traces
3	10	5	5	0.67
4	10	10	4	1.25
5	10	20	3.25	1.43
6	10	30	3.25	1.48
7	10	50	3	2.17
8	10	70	2.5	2.27
9	10	80	2.5	2.87

At the end of the prescribed time the reaction mixture was removed from the dextrinizer, weighed, extracted with alcohol — ether (1:1) mixture, dried, and weighed again. The product was a grayish powdery mass. A total of 9 experiments was performed;

The results of the individual experiments are given in Table 2.

Exploratory experiments on the foaming power and foam stability of the nine condensates were carried out in exactly the same way as the experiments described above, for determination of the properties of condensates of aniline with starch degradation products. As before, the comparison standard was 2% solution of tea seed saponin.

The experiments showed that No. 8 and 9 condensates of o-aminobenzoic acid with starch degradation products, containing 2.27–2.87% nitrogen, are equivalent to tea seed saponin in foaming power and and foam stability.

It was also found that increase of the heating time of the mixtures given in Table 2 in some cases led to unavoidable resinification of the reaction mixture.

Mixtures of Condensates No. 8 (Table 1), No. 9 (Table 2), and licorice root extract with sodium bicarbonate in 1:7.7 ratio were prepared. Tests of these mixtures by the GOST method [8] showed that the chemical foaming power of Condensates Nos. 8 and 9 is equal to that of licorice root extract, and "cutting" of the foam for both condensates took place after 6 minutes and 20 seconds.

Elemental analysis of Condensate No. 9 gave the following results:

6.185 mg subst.: 10.457 mg CO_2; 3.380 mg H_2O.
5.770 mg subst.: 9.497 mg CO_2; 3.130 mg H_2O.
4.389 mg subst.: 7.280 mg CO_2; 2.400 mg H_2O.
7.262 mg subst.: 0.176 ml N_2; 760 mm Hg, 22°.
7.756 mg subst.: 0.196 ml N_2; 756 mm Hg, 22°.
Found %: C 45.09, 44.26, 44.12; H 6.10, 6.07, 6.12; N 2.78, 2.91.

SUMMARY

Reaction of starch degradation products with typical amines and amino acids — aniline and o-aminobenzoic acid — yields foam-forming surface-active condensates. The foaming power and foam stability of these condensates are similar to those of tea seed and licorice root saponins.

LITERATURE CITED

[1] M.E. Pozin, I.P. Mukhlenov, E.S. Tumarkina, and E. Ya. Tarat, J. Appl. Chem., 27, 1, 12 (1954).

[2] V.N. Kozlov, V.B. Smolensky, and V.M. Arashkevich, J. Appl. Chem., 26, 9, 995 (1953).

[3] V.N. Kozlov, V.M. Arashkevich, and B.A. Sokolov, J. Appl. Chem., 27, 2, 223 (1954).

[4] J.W. McCutcheon, Synthetic Detergents (New York, 1950).

[5] A. Schwartz and J. Perry, Surface Active Agents (IL, Moscow, 1953).*

[6] G.M. Mitkevich, J. Appl. Chem., 26, 8, 873 (1953).

[7] Martin and Fischer, Soaps and Proteins (Leningrad – Moscow, 1932).*

[8] V.P. Goguadze, author's certif. 77057, June 6, 1949.

[9] GOST 182–53.

Received August 15, 1955

*In Russian.

REDUCTION OF p-NITROSALICYLIC ACID TO p-AMINOSALICYLIC ACID

L.A. Mikhailova, L.S. Solodar, E.A. Ovchinnikova, G.V. Kozyerva,
S.I. Samurova, and L.N. Efremova

Institute of Chemical Reagents

p-Aminosalicylic acid (PASA) in the form of its sodium salt is an important drug used in treatment of tuberculosis. The acid may be prepared in many different ways; production by reduction of p-nitrosalicylic acid gives a high yield and a product of good quality.

According to the literature, p-nitrosalicylic acid can be reduced by several methods; the reduction conditions are given in Table 1.

The data in the table show that the highest yields of p-aminosalicylic acid are obtained by catalytic reduction, in presence of Raney nickel catalyst, of the sodium salt of p-nitrosalicylic acid in 1:10 aqueous solution, at pH 8–7.5, under a pressure of 20–80 atm.

Reduction under high pressure involves the use of special autoclaves. Reduction under normal pressure may be effected in ordinary equipment.

The purpose of the present investigation was to find the conditions for reduction of p-nitrosalicylic acid under normal pressure.

Our investigations showed that reduction of aqueous solutions of the sodium and ammonium salts of p-nitrosalicylic acid under normal pressure in presence of nickel catalyst proceeds smoothly and at a high rate only at a definite pH value of the original solution.

The ammonium and sodium salts were prepared from pure p-nitrosalicylic acid and purified by crystallization from water.

The original p-nitrosalicylic acid had m.p. 235 -237° and was almost 100% pure (as shown by analysis for nitro group content and by potentiometric titration with 0.1 N NaOH solution in an alcoholic medium).

The ammonium salt was found to be 100% pure (by ammonia distillation after addition of NaOH); it crystallizes without water.

The sodium salt, which crystallizes with 1 molecule of water, was also 100% pure.

Before the reduction studies, the solubilities of the sodium and ammonium salts of p-nitrosalicylic acid in water in the 20–60° range were determined. The results are given in Table 2.

The percentage content of the ammonium salt in the weighed sample was determined by distillation of ammonia into standard hydrochloric acid. Caustic soda solution was first added to the ammonium salt solution.

To find the Na salt content in the solution, a weighed sample of the solution was evaporated to dryness, the residue was moistened with sulfuric acid, the liquid was evaporated, and the residue ignited. The content of sodium p-nitrosalicylate in the sample was calculated from the weight of Na_2SO_4.

TABLE 1

Conditions for the Reduction of p-Nitrosalicylic Acid, from Literature Data

Reducing agent	Temperature (deg)	Pressure (atm.)	Medium	Yield (%) PASA	Yield (%) hydrochloride	Literature source
Stannous chloride	90	Normal	Hydrochloric acid	Not stated		[1]
	60—70	»	ditto	—	77	[2]
		»	Concentrated hydrochloric acid	Not stated		[12]
Ferrous sulfate	100	»	Ammonia	60—70	—	[3,4]
	100	»		Not stated		[5]
Raney alloy	90	»	Caustic soda	60	—	[3]
	90	»	Na_2CO_3	65	—	[4]
Sodium sulfide	90	»	Water	25	—	[6]
Catalytic reduction: palladium catalyst	90	»	Absolute alcohol + NCl	20	—	[2]
platinum catalyst	90	»	Ethyl acetate	100	—	[3]
Raney nickel catalyst	80	30—80	Ethyl alcohol	Not stated		[7]
	40	70—80	ditto	66—72	—	[8]
	50—60	60—80		65	—	[4]
	50—60	20	Na salt, pH = 8.0*	90	—	[8]
	50—60	60—80	Na salt pH = 7.5	85	—	[4]
	Not stated	Not stated	Na salt pH = 7.5	95	—	[9]
	Room	80	Na salt pH = 8.0	90	—	[10]
Electrochemical reduction Sn cathode, D = 1.5—4 А/дм²	35—50	Normal	hydrochloric acid, ethyl alcohol	74	—	[11]

A 1:35 aqueous solution of the ammonium salt is saturated, at 20° and has pH = 5.92 (found by potentiometric titration). This solution is readily and quantitatively reduced (the amount of hydrogen absorbed is the theoretical amount required for reduction of NO_2 to NH_2) under normal pressure at 20–25° in presence of nickel catalyst.

The results of the reduction experiments are given below.

Reduction of Ammonium p-Nitrosalicylate under Normal Pressure

Yield (% of theoretical)		
PASA	hydrochloride	total
73.6	13.0	86.6
78.3	6.7	85.0

The resultant p-aminosalicylic acid, without additional purification, was almost white or slightly yellowish in color, and contained not less than 99% of the pure substance (from NH_2 and COOH group determinations).

*The p-nitrosalicylic acid was converted into the sodium salt in aqueous solution before reduction.

If the original solution of ammonium p-nitrosalicylate contains free ammonia, i.e., if the pH of the medium is above 5.9, then a complex nickel salt of the acid is precipitated during the reduction, and the reduction ceases. The composition of this precipitate was not studied.

TABLE 2

Solubility of Salts of p-Nitrosalicylic Acid in Water
pH of solutions: NH_4 salt 5.92, Na salt 8.20

Temperature (degrees)	Content of salt in solution (wt. %)	
	NH_4 salt	Na salt
20	2.90	5.80
30	3.75	10.0
40	5.74	13.5
50	7.70	18.3
60	11.30	23.6

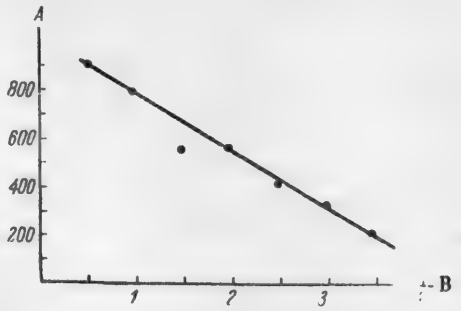

Variation of the rate of hydrogen absorption with time. A) Rate of hydrogen absorption (in ml), B) time (hours).

The nickel catalyst can be used repeatedly for normal reductions, with small additions of fresh catalyst for each successive reduction. Table 3 gives the results of 4 consecutive reductions of ammonium p-nitrosalicylate solution (1 : 35). At the 4th reduction a complex salt was precipitated. To complete the reduction it was necessary to filter off the precipitate and to add a fresh portion of catalyst to the filtrate.

TABLE 3

Conditions for the Reduction of Ammonium p-Nitrosalicylate

Amount of nitrosalicylic acid (g)	Amount of catalyst (g)	Amount of hydrogen (liters)	Duration of reduction	Yield (%)		
				PASA	hydrochloride	total
6	2	2.2	2 hr	62.6	15.6	78.2
6	0.5	2.2	2 hr	80.5	16.5	97.0
6	0.4	2·2	1hr 30 min	65.5	4.4	69.5
6	0.2g + 1.0g	1.5+0.201	2 hr 20 min	67.0	17.3	84.3
				Average yield from 4 experiments . . .		82.25

The experiments showed that to prevent the formation of precipitates the pH of the original solutions must be decreased to 5.5–5.45.

The yield of p-aminosalicylic acid greatly depends on the concentration of p-nitrosalicylic acid in the original solution before reduction.

At 1 : 35 concentration of the ammonium salt the direct yield of p-aminosalicylic acid is ~ 70% of the theoretical, when isolated by means of hydrochloric acid, at pH = 3 (weak blue spot on Congo red paper).

12–15% of p-aminosalicylic acid in the form of the hydrochloride can be precipitated from the mother liquor by excess hydrochloric acid.

It was found that, to increase the direct yield of p-aminosalicylic acid and to make better use of the equipment, the reduction can be performed in saturated solutions of the ammonium salt with pH 5.5 at 30–40°. The reduction proceeds smoothly even when part of the ammonium p-nitrosalicylate is present as a precipitate at the start of the reduction. As the reduction proceeds the amonium p-nitrosalicylate dissolves, while p-aminosalicylic acid may be precipitated. At the end of the reduction it should be dissolved by addition of ammonia.

The results of experiments with higher concentrations of ammonium p-nitrosalicylic acid (NSA) are given below:

Concentration of NSA salt in aqueous solution	Yield (%)		
	PASA	hydrochloride	total
1:15	72.2	17.06	89.26
1:15	72.2	6.3	85.5
1:10	77.8	15.0	92.8
1:10	78.2	11.9	90.1

During reduction of solutions of ammonium p-nitrosalicylate with pH 5.5, the solution pH increases as p-aminosalicylic acid is formed and at the end of the reduction the pH value reaches ~ 7.

The rate of hydrogen absorption decreases with increasing pH. This is illustrated by data on the hydrogen absorption rate in one of the experiments (see Figure).

The pH of the solution during reduction can also be regulated by addition of p-nitrosalicylic acid to the original solution of its ammonium salt.

As the reduction proceeds, p-aminosalicylic acid is precipitated, while p-nitrosalicylic acid passes into solution in the form of the ammonium salt, by displacement of the relatively weaker p-aminosalicylic acid. The amount of free p-nitrosalicylic acid necessary for smooth reduction without formation of an insoluble precipitate was determined experimentally. The amount of free acid must be not less than 20% of the amount of acid converted into the salt.

The yield of PASA was 78–81%, and of the hydrochloride, 7–4%.

Further investigations showed that a solution of sodium p-nitrosalicylate is also easily reduced if its pH is decreased to 5.5 by addition of acetic acid.

The effect of solution pH on the reduction of sodium p-nitrosalicylate is shown in Table 4.

TABLE 4

Effect of pH on the Reduction of Sodium p-Nitrosalicylate

Dilution	pH of initial solution	Amount of hydrogen absorbed (in liters)	Duration of reduction	Notes
1 : 17 (260 ml)	5.45	5.5	4 hr 20 min	Complete reduction
1 : 15.6 (234ml)	6.05	1.8	5 hr 30 min	Reduction not completed. Yellow precipitate formed, insoluble in ammonia or water.
1 : 15.6 (234ml)	6.95	1.3	5 hr 30 min	
1 : 15.5 (232ml)	7.95	1.0	7 hr	

The pH values of the solutions were determined potentiometrically. The results in Table 4 show that the reduction went to completion only in the solution with pH 5.45; the amount of hydrogen absorbed decreased w with increasing pH, and the higher the pH of the original solution, the earlier did the reduction stop.

EXPERIMENTAL

The optimum conditions for the production of p-aminosalicylic acid (in two variants) are given below.

1) to 10 g of p-nitrosalicylic acid 100 ml of water and 3.7 g of 25% ammonia solution was added, and the mixture stirred to convert the acid into the ammonium salt. The supernatant solution should be alkaline to bromocresol purple paper.

50 ml of water was added to the mixture, and the liquid was heated to 45–50°. The ammonium salt dissolved completely. The excess ammonia was neutralized with acetic acid to pH 5.5–5.8.

3 g of Raney nickel catalyst was added to the solution, and hydrogen was passed under normal pressure until absorption ceased (until nitro groups were no longer present). The reduction may be carried out in a jar placed in a mechanical shaker. Hydrogen was passed in from a calibrated holder.

The clear solution of ammonium p-aminosalicylate was siphoned off from the settled catalyst, a fresh portion of ammonium p-nitrosalicylate solution with pH 5.5–5.8 and 1 g of catalyst was added to the vessel, and the reduction was resumed.

The next two portions were reduced without addition of fresh catalyst. The catalyst consumption did not exceed 10% of the weight of p-nitrosalicylic acid. The solution of ammonium p-aminosalicylate was taken to pH 6–5.5 and treated with 30% sodium sulfide solution ($Na_2S \cdot 9H_2O$) at 35° until Ni^{++} was completely precipitated. This was tested after the liquid had stood for 9-10 hours.

After the nickel sulfide had been completely precipitated, sodium hydrosulfite and activated wood charcoal was added to the mixture. From the clear filtrate p-aminosalicylic acid was isolated by means of hydrochloric acid at pH 3.0. The yield was 79–80 of the theoretical. 5–11% (of the theoretical) of the hydrochloride of p-aminosalicylic acid was precipitated from the filtrate.

2) To a solution of ammonium p-nitrosalicylate (1:15) p-nitrosalicylic acid was added, the amount being not less than 20% of the weight of the acid converted into the salt, and the mixture was reduced at 30–35° in presence of nickel catalyst. During the reduction p-nitrosalicylic acid was dissolved while p-aminosalicylic acid was precipitated. At the end of the reduction all the acid was brought into solution as the ammonium salt, and treated as described above. The yield of PASA was 76–81% of the theoretical, and of PASA hydrochloride, 7–4%.

The p-aminosalicylic acid prepared by the 1st and 2nd methods is of high quality and does not require additional purification; its color is white or slightly yellow, and its purity is 99–99.5% as determined by amino group content (by diazotization) and by COOH group content (titration in alcohol with phenolphthalein indicator).

The high quality of p-aminosalicylic acid obtained by catalytic reduction of p-nitrosalicylic acid by our method, ensures 75–80% yields of the sodium salt* owing to the repeated use of the mother liquors in crystallization of the sodium salt.

SUMMARY

1. The conditions have been found for catalytic reduction of p-nitrosalicylic acid to p-aminosalicylic acid under normal pressure, with 80–85% yields. It is shown that under equal conditions the pH of the medium is of decisive importance for the reduction.

2. The reduction is carried out under normal pressure in aqueous solutions of ammonium p-nitrosalicylate at initial solution pH from 5.5 to 5.8.

3. The initial pH of the solution can be maintained at the required level by additions of free p-nitrosalicylic acid to its ammonium salt [13].

LITERATURE CITED

[1] H. Seidel and J.C. Bittner, M., 23, 432 (1902); Ber., 34, 432 (1901).

[2] E. Wenis and T.S. Gardner, J. Am. Pharm. Assoc., 9 (1949).

[3] D.J. Drain and D.D. Martin, J. Chem. Soc., 1498 (1949).

[4] Bull. Acad. Sci. Latvian SSR, 3 and 4 (1950).

*The sodium salt of PASA is the form in which it is supplied for medical purposes, prepared from pure PASA.

[5] J.F. McGhie, C. Morton et al. J. Soc. Chem. Ind., 68, 328 (1949).

[6] G. Ghilmetti, Farm. sci. e tec. (Pavia), 3, 652 (1948); C.A., 43, 2973 (1949).

[7] R. Justoni, Farm. sci. e tec. (Pavia), 3, 183 (1948); C.A., 42, 7273 (1948).

[8] R. Justoni, M. Ferruzzi and C. Pirola, Farm. sci. e tec. (Pavia), 3, 509 (1948); C.A., 43, 2189 (1949).

[9] D.S. Bhale and T.B. Panse, Proc. Indian Acad. Sci., 29A, 196 (1949), C.A. 44, 131 (1950).

[10] M.G. Sannie and M.H. Lapin, Bull. Soc. chim. France 322 (1950); C.A., 44, 8887 (1950).

[11] K. Honda, R. Jokouchi and S. Kikuchi, J. Electrochem. Soc. Japan, 20, 15 (1952); C.A., 46, 4930e (1952).

[12] D. Fontaine and Wm. Teh. Fu-Pan, C.A., 44, 5330i (1950).

[13] L.A. Mikhailova, L.S. Solodar, E.A. Ovchinnikova, G.N. Kozyreva, S.I. Samurova and L.I. Kravets, Soviet Authors' Certif. No.94585 (1952).

Received March 15, 1955

PRODUCTION OF CHLOROFORM AND CARBON TETRACHLORIDE BY CHLORINATION OF METHANE OVER A MOVING HEAT-TRANSFER MEDIUM

Ya. P. Choporov and O.A. Tishchenko

The extensive chlorination of methane over a moving heat-transfer medium has been studied at 390–500°, with chlorine — methane ratio 2.6–3.6 : 1. The reaction product consisted of the 3 highest chlorinated methane derivatives, the contents of which could be varied within considerable limits by variation of the component ratio. With increase of the chlorine — methane ratio within the above range, the methylene chloride and chloroform contents of the product fell from 11.0 to 6.0% and from 40.4 to 24.5% respectively; the carbon tetrachloride content increased from 42 to 64%. With increasing chlorine — methane ratio, chlorine breakthrough increased from 2.7 to 8.0%, and the consumption of chlorine per gram of product also increased, from 2.8 to 3.2 g; the reaction temperature was 460–480°.

Chlorinated methanes are widely used in many branches of industry. However, their production, especially of the higher substitution products, by chlorination of methane encounters considerable difficulties owing to the highly exothermic nature of the reaction, which is difficult to control.

In the production of methyl chloride and methylene chloride by chlorination of methane, the reaction heat is controlled by the use of excess methane, which also serves as a means for regulating the degree of chlorination. By combined use of the effects of these two factors, with the use of a chlorine — methane ratio of about 0.25 : 1, an industrial process for the production of methylene chloride and methyl chloride has been developed. However, in extensive chlorination of methane for production of carbon tetrachloride as the main product the chlorine — methane ratio must be about 3.5 : 1, and the problem of temperature regulation must be solved differently.

For temperature regulation in the chlorination of methane for production of chloroform and carbon tetrachloride, the methods used included the use of inert diluents such as nitrogen, carbon dioxide, steam, carbon tetrachloride, hydrogen chloride, and fused salts as heat-transfer media [1-5], and the use of multistage volume chlorination [6]. However, none of these methods, which proved effective in laboratory conditions, could lead to a commercial process for extensive chlorination of methane, as none provided a practical solution of the problem of removal of the heat of reaction in large-scale production.

The industrial development of the production of chloroform and carbon tetrachloride from methane has had to be based on the use of a 2-stage process [7, 8], consisting of volume chlorination of methane with predominant formation of methylene chloride, and liquid-phase photochemical chlorination of methylene chloride with formation of chloroform and carbon tetrachloride.

One new trend in the search for a solution to this problem is the use of moving heat-transfer media. For example, Johnson [9] used a finely ground inert material in fluidized form in three reactors in series, without circulation, for chlorination of a mixture of methane and hydrogen with predominant formation of chloroform and carbon tetrachloride.

Meissner and Thode [10] refer to the use of a fluidized catalyst as a means for the most effective regulation of the reaction temperature. Gorin et al. [5] also found in work on chlorination of methane in fused salts that a fluidized catalyst layer is more convenient, and demonstrated this [11, 12].

The present paper deals with the results of experiments on the production of chloroform and carbon tetrachloride by direct chlorination of methane over a moving granulated heat-transfer medium [13], in an experimental unit similar to that used earlier for pyrolysis of dichloroethane for the production of vinyl chloride [14].

EXPERIMENTAL

A diagram of the experimental unit with a moving heat-transfer medium is given in Fig. 1. The heat-transfer medium moves under gravity from the separator through the regenerator and reactor at a rate which depends on the output rate of the screw feeder; from the screw feeder the heat-transfer medium enters the funnel of a pneumatic suction conveyor, which conveys it to the separator. This completes the cycle of the heat-transfer medium. The carbon deposited on the heat-transfer medium during chlorination was burned out by means of flue gases entering the regenerator from the furnace. Hydrogen was used as fuel. The temperature of the heat-transfer medium was measured by means of thermocouples in the regenerator, at the exit from the regenerator, and at the reactor entry and exit. The reactor was made of concrete consisting of a mixture of high-alumina cement and rubble, sodium fluosilicate, and water glass; the diameter of the reactor was 50 mm and its effective capacity, 1 liter. The regenerator was made of high-alumina bricks with a casing of carbon steel. The rest of the equipment was made from stainless steel. The heat-transfer medium consisted of crushed high-alumina brick, with 3-5 mm grains. The reagents — methane and chlorine — were fed into the lower part of the reactor. The chlorine was fed in stepwise; 20% of the total was fed in with all the methane in the first step, 30% in the second, and 50% in the third. This stepwise distribution of the chlorine was calculated to give approximately the same chlorine — methane ratio at the first stage, as the ratio of chlorine to the reaction products, including hydrogen chloride, at the other stages. The reaction product was drawn out of the top of the reactor through a ball condenser, where the heaviest fraction was condensed, through a water spray tower for removal of hydrogen chloride, and through a tower sprayed with 20% caustic soda solution to absorb free chlorine. The vapor scrubbed free from hydrogen chloride and chlorine was then drawn through wash bottles containing potassium iodide solution and sulfuric acid, and through condensers immersed in a freezing mixture of acetone and solid carbon dioxide. The amount of methane feed was measured by means of a fluid meter, the chlorine feed was regulated with the aid of flow meters.

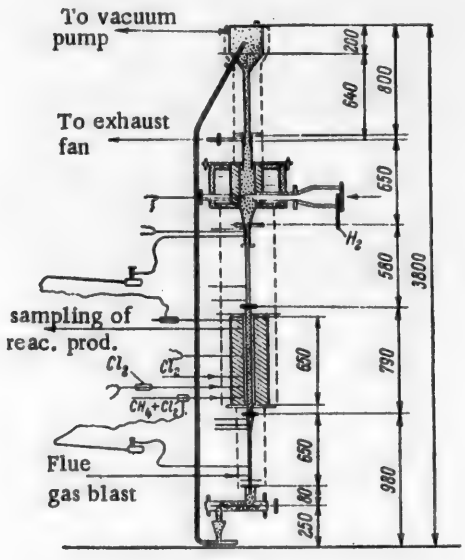

Fig. 1. Diagram of experimental unit.

The flow conditions in the reactor were regulated, on the one hand, by a blast of flue gas from the regenerator into the lower end of the reactor, and on the other, by withdrawal of the reaction product by suction; the blast and suction, which determined the direction of the gas streams in the reactor, were regulated according to the readings of differential manometers fitted at the top and bottom seals. The amount of heat-transfer medium, which passed through the reactor and the whole system at a constant rate, with the screw feeder running at the same speed throughout, varied between 16 -17 kg/hour; this was checked by weighing of samples taken at intervals. Hydrogen chloride and unreacted chlorine were determined by titration of the wash water and the alkali solution. The condensate formed before removal of hydrogen chloride was washed with caustic alkali solution and water, dried over calcium chloride, and combined with the deep-cooled condensate. The combined reaction product was then fractionated.

Methane of biological origin was used for chlorination; after removal of carbon dioxide its composition was (in %): CH_4 92–93, CO_2 0–0.2, O_2 1.3, N_2 5–6. The chlorine had the following composition (in %): Cl_2 93–94, H_2 1.0, CO_2 1.3, O_2 0.8–1.0, N_2 3–4. The regenerator flue gas used for the blast contained 13–14% oxygen.

RESULTS AND DISCUSSION

The first part of the work consisted of a study of the flow conditions of the heat-transfer medium in the equipment under conditions of methane chlorination, and a determination of the general chlorination picture based on the principal data.

In the subsequent experiments, the effects of reaction temperature between 390 and 500°, methane feed rate between 1 and 2 moles per liter of heat-transfer medium per hour, and molar ratio of chlorine to methane in the range 2.6 – 3.6:1 on the yield and composition of the product were studied. The average temperature of the heat-transfer medium between the reactor entry and exit was taken as the reaction temperature. The results of experiments on the effect of temperature on the yields of reaction products are given in Table 1.

TABLE 1

Effect of Reaction Temperature on Yields

Temperature (deg)	CH_4 feed (in mole/hour)	Molar ratio of C_{12} to CH_4	Contents of chlorinated methanes in residue in reaction products (in wt. %)				Yield of reaction products (% of theoretical)
			CH_2Cl_2	$CHCl_3$	CCl_4	residue	
390	0.95	3.10	12.9	30.2	49.5	7.4	45
410	0.95	3.10	11.7	30.6	50.0	7.7	53
440	1.04	2.90	7.9	31.4	52.0	8.7	56
470	1.01	2.90	6.6	27.1	56.0	10.3	57
480	1.00	3.06	5.4	20.5	57.7	16.4	56
498	1.00	3.00	5.0	21.5	56.1	17.4	51

The effect of temperature on the reaction yield is also shown in Fig. 2. It follows from the data in Table 1 and Fig. 2 that the optimum reaction temperature is in the 440–480° range. However, increase of temperature results in an increase of the residue by formation of C_2 polychlorides, including tetrachloroethylene, of which over 40% was present in the residue. The lower yields at temperatures below 410° are attributable to the inhibiting action of oxygen which enters the reactor together with the flue gases in the blast, the amount being about 5% of the amount of chlorine; the chlorine breakthrough then rose to 16–18%. At higher temperatures, when the

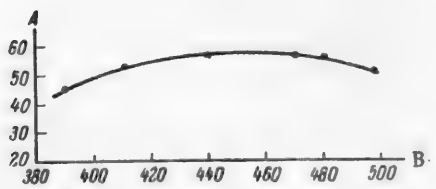

Fig. 2. Effect of reaction temperature on the yield. A) Yield (in wt. %), B) temperature (degrees).

TABLE 2

Methane Feed Rate and Yield of Product

Temperature (degrees)	CH_4 feed rate (in moles/hr.	Molar ratio of Cl_2 to CH_4	Yield (%)
470	1.0	2.9	57
480	1.0	3.0	56
467	1.5	3.0	57
478	1.5	3.0	55.8
480	2.0	3.0	58.0

bimolecular reaction [15, 16] predominates over the reaction proceeding by a chain mechanism, the inhibiting effects of oxygen disappeared. As the reaction temperature increases there is an appreciable increase of the carbon tetrachloride content owing to decomposition of chloroform, which is the least thermostable of the chloromethanes.

The methane feed rate between 1 and 2 moles per liter of heat-transfer medium per hour had practically no influence on the yield, as can be seen from the data in Table 2. The fact that the yield remains constant when the methane feed rate is increased is evidently attributable to the reliable regulation of the reaction temperature by the moving heat-transfer medium.

At a feed rate of 2 moles of methane per hour, the yield of product per liter of heat-transfer medium is 160 g. Table 3 shows the influence of the chlorine – methane ratio on the contents of chlorinated methanes in the reaction products.

The composition of the chloromethanes isolated from the reaction products is shown in Fig. 3.

TABLE 3

Variations of Chlorinated Methane Contents with the Chlorine — Methane Ratio

Reaction temperature (deg)	CH_4 feed rate (in moles/hour)	Molar ratio of C_{12} to CH_4	Contents of chlorinated methanes (in wt. %)				Yield of product (%)
			CH_3Cl_2	$CHCl_3$	CCl_4	Residue	
460	1.7	2.59	11.0	40.4	42.0	6.6	60.0
468	1.6	2.77	8.3	34.3	50.0	7.4	57.7
467	1.5	3.07	6.8	28.0	57.0	8.2	57.0
478	1.5	3.02	5.1	31.1	56.0	7.8	55.8
475	1.6	3.14	5.9	27.7	57.4	9.0	53.5
468	1.4	3.46	7.4	28.4	57.4	6.8	54.8
480	1.4	3.64	5.6	24.5	64.2	5.7	56.2

The chlorine and methane consumption per 1 g of product, and the chlorine balance, are given in Table 4.

TABLE 4

Consumption of Reagents and Chlorine Balance (Reaction temperature 460–480°, methane feed rate 1.4–1.7 moles/hour)

Experiments	Molar ratio of C_{12} to CH_4	Chlorine balance						Molar ratio of Cl in the form of HCl to Cl in product	C_{12} breakthrough (%)	Consumption per 1 g of product	
		Consumption of C_{12} (in g)	chlorine found							C_{12} (in g)	CH_4 (in liters)
			combined in product (in g)	as HCl (in g)	free (in g)	total					
						in g	as % of consumption				
55	2.59	479	152	226	28	406	85	1.50	—	2.86	0.35
56	2.77	479	144	243	13	400	84	1.67	2.7	2.98	0.32
58	3.07	495	145	215	23	383	76	1.48	4.6	3.26	0.32
59	3.02	524	149	229	41	419	80	1.53	7.8	3.20	0.32
60	3.14	543	149	251	39	439	81	1.67	7.2	3.11	0.33
62	3.46	525	147	261	47	455	86	1.77	8.0	3.20	0.30
61	3.64	543	154	245	38	437	81	1.60	7.0	3.21	0.30

It follows from the data in Table 4 that when the chlorine—methane ratio is raised from 2.59 to 3.64 the consumption of chlorine per 1 g of reaction product increased by only 10%; the methane consumption remains practically unchanged.

The methane balance is given below.

Methane balance per 100 g of product from data for Experiment 61

Methane consumption	liters	%
For formation of chlorinated methanes	14.6	48.8
In residue after distillation of product	2.2	7.4
Combustion in reactor	1.0	3.4
Losses in pyrolysis	9.8	32.4
Losses with product in disturbances of flow conditions in reactor	2.4	8.0
Total	30.0	100.0

The contact time in the reaction zones, the number of which is determined by the number of steps in which the chlorine is added, varied; it depended, on the one hand, on the distance between the points at which the chlorine was introduced, and on the other, on the increasing amounts of the reaction products as a result of the stepwise introduction of chlorine. With the flue gases drawn in with the blast, amounting to 25–30% relative to the methane, which passed through the reactor together with the product as far as the withdrawal point, the contact time was 1.3 second in the 1st zone, 0.8 second in the 2nd zone, and 4.1 seconds in the 3rd. The total contact time was 6.2 seconds.

As is seen from the data in Table 4 (Columns 8 and 9), losses of the reaction product occurred during the experiments, with pyrolysis resulting in formation of excess hydrogen chloride and carbon. This is attributable to the defects of the small experimental unit with a moving heat-transfer medium; because of the low heat load, the reactor seals must inevitably be short and temperature drops must occur in the heat-transfer medium in the reactor. Because of the short length of the seals, the withdrawal of the reaction product was regulated with the aid of differential manometer readings in the range of 0.2 – 0.4 mm water column, to avoid excessive leakages. With such a low pressure difference, the slightest resistance in the product withdrawal system resulted in escape of gases from the reactor into the seals. Because of the pressure drop in the medium in the reactor it was necessary to maintain the temperature in the upper part of the reactor, from which the product was withdrawn, at about 520°, and this led to pyrolysis. These defects are easily avoidable in larger units.

However, even in the existing conditions the results of these experiments on the chlorination of methane over a moving heat-transfer medium show that selective production of carbon tetrachloride directly from methane is possible by this method. The moving heat-transfer medium acting as a cooling agent, and stepwise introduction of chlorine into the reactor are evidently the decisive factors in ensuring that the reaction takes a normal course in such extensive chlorination of methane. Extensive chlorination of methane with production of the higher chloromethanes, including methylene chloride, occurs without recycling of the gases owing to the total conversion of methane and of the intermediate reaction product methyl chloride. This allows the use of methane of any concentration. At the same time, extensive chlorination of methane can yield chloroform of better quality than that obtained as a by-product of methylene chloride production, owing to the simultaneous more exhuastive chlorination of C_2–C_5 hydrocarbons, which usually accompany natural methane. The conversion of C_2–C_5 hydrocarbons into trichloroderivatives, which is ensured by the presence of free chlorine at these high reaction temperatures, makes it possible to obtain not only chloroform but also carbon tetrachloride by ordinary rectification. The higher chlo chlorides of ethane and other higher hydrocarbons, which boil at higher temperatures than the chloromethanes, will remain in the still bottoms.

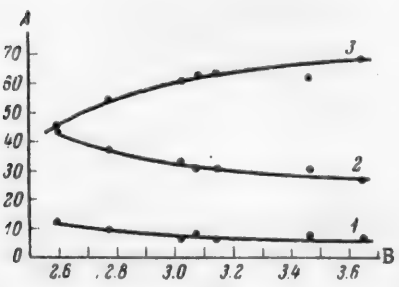

Fig. 3. Composition of chlormoethanes as a function of the chlorine–methane ratio. A) Contents of chloromethanes (wt. %), B) molar $Cl_2 : CH_4$ ratio. Chloromethanes: 1) CH_2Cl_2, 2) $CHCl_3$, 3) CCl_4.

The production cost of chloroform and carbon tetrachloride is considerably lower if they are made directly from methane. Especially favorable conditions for the production of these compounds by extensive chlorination of methane arise if the process is carried out in conjunction with recovery of chlorine from hydrogen chloride by one of the known processes [17].

If a moving heat transfer medium is used, the reactor for extensive chlorination of methane can be lined, and can be of any desired dimensions, close to the dimensions of reactors used for catalytic cracking of petroleum over flowing catalysts. In this way it is possible to devise a highly productive process for the production of chloroform and carbon tetrachloride directly from methane, with a considerable decrease of capital costs.

Carbon tetrachloride and chloroform are becoming increasingly important as intermediates, owing to recent progress in syntheses based on free-radical reactions [18, 19].

The demand for chloroform for the production of fluorine compounds: plastics, lubricants, acids, and esters [20], in the synthesis of which it is the primary starting material, may become considerable.

SUMMARY

1. It is shown that methane can be exhaustively chlorinated with predominant formation of carbon tetrachloride, with the use of a chemically inert moving heat-transfer medium as cooling agent.

2. The effect of the molar chlorine—methane ratio on the composition of the product has been determined.

3. The chlorine and methane balances have been determined for an experimental unit, and the consumptions of these materials per unit amount of product have been found.

4. The reliability of a moving heat-transfer medium for heat removal and temperature regulation has been demonstrated by variations of the methane feed into the reactor.

5. Suitable materials for the reactor and heat-transfer medium have been found.

LITERATURE CITED

[1] J.J. Crebe, J.H. Reily and R.M. Milly, U.S. patent, 2 034 292; Z. II, 2611 (1936).

[2] J.H. Reily, U.S. patent, 2 140 548; Ch. A., 2540 (1939).

[3] J.H. Reily, U.S. patent, 2 140 550; Ch. A., 2541 (1939).

[4] J.H. Reily, U.S. patent, 2 140 551; Ch. A., 2540 (1939).

[5] E. Gorin, C.M. Fontana and G.A Kidder, Ind. Eng. Ch., 1, 2128 (1948).

[6] E.T. McBee, H.B. Hass, C.M. Neher and H. Strickland, Ind. Eng. Ch., 3, 298 (1942).

[7] W. Hirschkind, Ind. Eng. Ch., 12, 2749 (1949).

[8] Petr. Refiner, 11, 124 (1953).

[9] P.R. Johnson, U.S. patent, 2 585 496; Ch. A., 8143 (1952).

[10] H.P. Meissner and E.F. Thode, Ind. Eng. Ch., 1,129 (1951).

[11] C.M. Fontana and E. Gorin, U.S. patent, 2 575 167; Ch. A., 5072 (1952).

[12] E.W. Kilgran and E. Gorin, U.S. patent, 2 498 552; Ch. A., 5575 (1950).

[13] Ya. P. Choporov, Author's Certif. 102541, November 23, 1954.

[14] Ya. P. Choporov and M.D. Trikhanov, Authors' Certif. 437556 (1950).

[15] W.E. Vaughan and F.F. Rust, J. Org. Chem., 449 (1940).

[16] E.T. McBee and H.B. Hass, Ind. Eng. Ch., 2, 137 (1941).

[17] I. Gordon, Chem. Eng., 5, 187 (1953).

[18] G.A. Razuvaev and N.S. Vasileiskaya, Progr. Chem., 1, 37 (1953).

[19] I. Cadogan and D.H. Hey, Quart. Rev., 8, 3, 308 (1954).

[20] I.O. Hendricks, Ind. Eng. Ch., 1, 99 (1953).

Received October 1, 1955

BRIEF COMMUNICATIONS

INFLUENCE OF THE ACIDITY OF THE ORIGINAL SOLUTION ON THE LIGHT FASTNESS OF LEAD CHROMATE

A.V. Pamfulov and R. Ya. Mushiy

Laboratory of Physical Chemistry, Chernovits University

In a continuation of our work on the light fastness of lead chromate [1], we studied the light fastness of lead chormates formed from solutions of lead nitrate and acetate with different hydrogen ion concentrations in the solutions from which the precipitates were formed.

It is known that variations of the acidity of a lead salt solution result in the formation of precipitates with different ratios of chromic anhydride to lead oxide [2]. The color of the precipitates also varies [3]. It has been reported that the light fastness of lead chromate increases if it is precipitated from inorganic lead salts and if the pigment is dried at 60–120° [4].

The ratio of lead salt to potassium dichromate in the solutions was 3.21, as in the previous investigation. The pH of the medium was varied by additions of acid or alkali.

The hydrogen ion concentration of the lead salt solution was measured by means of the quinhydrone electrode, and the chromate was then precipitated by addition of potassium dichromate. For strongly acid solutions calculated pH values were used, as at high nitric acid concentrations the quinhydrone electrode cannot be used for pH determinations. According to Ernst [3], the glass electrode is unsuitable for pH determinations of lead salt solutions, as it gives high pH values.

The washed precipitate was dried at 80–100° or 40–50°. We did not find any appreciable difference between the light fastness of samples dried at 80–100° and at 40–50°.

The color of the lead chormate varies with the solution pH from a dull dark orange in very acid media (pH from about 0.5 to 0) to light orange at pH 1.5–5.5. With further increase of pH the color of the precipitates becomes orange with progressively increasing depth of color, which passes into red (Table 1).

TABLE 1

pH Values of Solutions in Precipitation of Lead Chromate

Nos. of samples formed from $Pb(CH_3COO)_2$ solution	pH of solution	Nos. of samples formed from $Pb(NO_3)_2$ solution	pH of solution
1	(—0.5)	6	(—0.7)
2	0	7	(—0.2)
3	1.6	8	1.4
4	1.9	9	3.1
5	5.6	10	5.0
		11	7.3

For the light fastness tests the lead chromate powder was put onto a glass plate. The surface was smoothed out. The samples were exposed to the light of a 500 w lamp at a distance of 35 cm. The samples were covered with cellophane to protect them from dust. The temperature rise of the samples did not exceed 40–50°. Darkening of the samples was measured by means of the FM Pulfrich photometer [5]. Three light filters—red (λ_{eff} = 633 mμ), green (λ_{eff} = 541 mμ), and blue (λ_{eff} = 478 mμ) were used in measurements of the reflection coefficient of each sample before and after irradiation. The comparison standard was a barite plate with a reflection coefficient of 85%.

Three parallel determinations of the reflection coefficient were carried out, after which the sample and standard were changed over and the determinations were repeated. The arithmetic mean of each six determinations was taken. This was taken as the reflection coefficient of the specimen. The sum of the reflection coefficients Σ_0 of the sample before irradiation represents the total light reflected before irradiation. The corresponding sum for a sample irradiated for τ hours (Σ_τ) expressed as a percentage of Σ_0 : $\frac{\Sigma_\tau}{\Sigma_0} \cdot 100$ % provides a measure of the change in the amount of light reflected by the sample, i.e., in this case, its darkening.

We were mainly concerned with the change in the color as the result of radiation rather than with the color of lead chromate. Light filters Nos. 1-8 of the instrument have a very narrow transmission region and transmit a beam of light of very low intensity. Therefore the results of parallel determinations of reflection coefficients, carried out with the aid of these filters show variations of 10–15% and cannot be used for measuring small changes in the color of the samples. Nevertheless, the results of the determinations carried out with the aid of the three above-mentioned light filters provide a fairly complete characterization of the color changes.

The results of measurements of the darkening of lead chromate samples, obtained from lead acetate solutions of different pH, with different irradiation times are given in Fig. 1. Similar results for samples from lead nitrate solutions are given in Fig. 2. Examination of Figs. 1 and 2 shows that all the samples become darker in the course of irradiation. This is accompanied by considerable changes in the spectral composition of the reflected light. This is illustrated by the data in Table 2. This table contains data for Sample No. 11 precipitated from nitrate solution (pH = 7.3).

TABLE 2

Light Fastness of Sample No. 11, pH = 7.3

Irradiation time (hours)	Reflection coefficient at λ_{eff} (in mμ)			Σ_τ	$\frac{\Sigma_\tau}{\Sigma_0} \cdot 100\%$
	633	541	478		
0	94.5	29.2	5.0	128.7	100
26	77.1	27.2	5.6	109.9	85
80	62.2	24.4	5.2	91.8	71.3
117	59.9	23.8	5.2	88.9	69.1
168	54.9	21.6	5.1	81.6	63.5
246	53.0	22.6	5.4	81.0	63.0
292	51.9	22.5	6.4	80.0	62.7

The amounts of red and green light reflected by the sample decrease in the course of irradiation, whereas the amount of blue light reflected remains practically unchanged. Thus, the sample turns greed during irradiation.

It follows from Figs. 1 and 2 that the darkening of lead chromate proceeds irregularly during irradiation. For most of the samples studied the amount of light reflected by the sample decreased by 15–20% during the first 10–30 hours of irradiation. The subsequent changes in the amount of light reflected by the sample and of its spectral composition are small. Samples irradiated for 180–200 hours do not darken on further exposure and do not change color.

The pH of the solution from which the chromate was precipitated has an appreciable influence on the light fastness of the chromates precipitated from lead acetate solutions; the light fastness decreases with increasing pH. It follows from Fig. 2 that variations of solution pH from −0.7 to 5 have no appreciable effect on the light fastness of chromates precipitated from lead nitrate solutions. The difference in the light fastness of samples made from lead acetate and nitrate solutions is attributable to differences in the size of the lead chromate crystals, as was shown earlier [1].

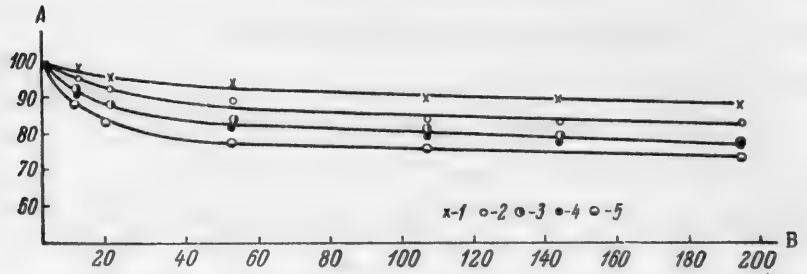

Fig. 1. Effect of irradiation time on the color of lead chromate samples made from lead acetate solutions. A) value of $\frac{\Sigma \tau}{\Sigma_0} \cdot 100$ (in %), B) irradiation time (hours). Solution pH: 1)(−0.5), 2)0, 3)1.6, 4)1.9, 5)5.6.

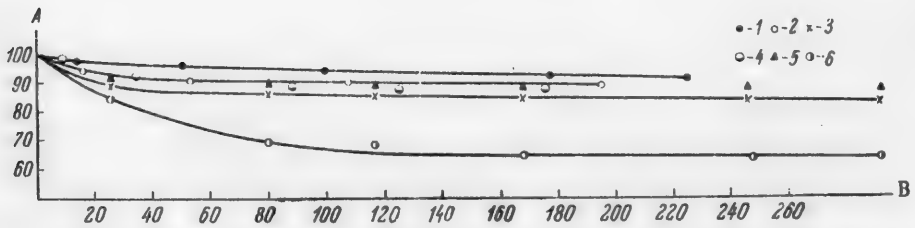

Fig. 2. Effect of irradiation time on the color of lead chromate samples made from lead nitrate solutions. A) Value of $\frac{\Sigma \tau}{\Sigma_0} \cdot 100$ (in %), B) irradiation time (hours). Solution pH: 1)(−0.7), 2)(−0.2), 3)1.4, 4)3.1, 5)5.0, 6)7.3.

According to Guiter's data [2], as the solution pH changes from −0.6 to +5.2, the composition of the lead chromate precipitate changes from $PbO \cdot 3CrO_3$ at pH −0.6 to $2PbO \cdot CrO_3$ at pH 5.2. Therefore variations of the composition of lead chromate within these limits have no effect on the light fastness.

This is confirmed by the results of our experiments in which the relative amounts of lead nitrate and potassium dichromate were varied in preciptation, without change of pH value.

If the pH of the solution is raised to 7.3, the light fastness of the precipitates diminishes appreciably. This is probably the consequence of the formation of basic lead chromates. According to Guiter's data, when lead chromate is precipitated from lead nitrate at pH 4.6 there is already a certain excess of lead oxide above the stoichiometric ratio for $PbO \cdot CrO_3$.

This corresponds to an appreciable decrease in the light fastness of samples obtained at pH above 5, while the light fastness of samples from solutions of pH below 5 is practically constant. It is therefore likely that the decreased light fastness is the consequence of the presence of excess lead oxide in the precipitates.

SUMMARY

1. The light fastness of lead chromate samples precipitated from solutions with pH between −0.7 and 5 is independent of the solution pH.

2. When the pH is increased from 6 to 7, the light fastness of the precipitates formed decreases appreciably. This decrease of light fastness is greater in samples precipitated from acetate solutions, which have lower light fastness than samples precipitated from lead nitrate solutions.

LITERATURE CITED

[1] A.V. Pamfilov and A.D. Bochkov, J. Appl. Chem., 26, 681 (1953).

[2] M.H. Guiter, Bull. Soc. Chim., 60 (1946).

[3] R.C. Ernst, E. Pragoff and E.E. Litkenhous, Ind. Eng. Ch. Anal. Ed., 3, 174 (1931).

[4] H. Wagner, M. Zippel, G. Heitz and R. Haug, Farbenzeit., 38, 932 (1933).

[5] Gmelin, Gruss, Sauer and Kronert, Physicochemical Analysis in Industry (GNTIU, Kiev, 1936) p. 183.*

Received October 22, 1955

* In Russian.

KINETICS OF SOLUTION OF IRON AND IRON—CADMIUM ELECTRODES IN ALKALINE SOLUTIONS

Ya. E. Gindelis

The question of the mechanism and kinetics of the solution of iron in alkaline solutions is closely associated with the problem of the mechanism of self-discharge of iron and iron – cadmium electrodes in alkaline secondary cells.

Platonova and Levina [1] have shown that the loss of capacity by self-discharge of a pure iron electrode is equivalent to the amount of hydrogen liberated owing to the corrosion of the iron.

The foregoing facts formed the basis of the present investigation, in which a study was made of the rate of hydrogen liberation on iron—cadmium and iron electrodes in 4.6 N KOH solution, used as electrolyte in alkaline secondary cells.

EXPERIMENTAL

The iron and iron – cadmium electrodes were made as follows. The active powders of the corresponding compositions were formed into briquettes 72 mm × 12 mm.

The briquets were enclosed in cases made from perforated low-carbon steel ribbon. These were placed in steel vessels lined with perforated vinyl plastic and covered with 4.6 N KOH solution. They were then formed by the following procedure: charge — at a current strength of 250 ma for 12 hours; discharge at 200 ma down to 0.65 v potential for iron electrodes, and 0.70 v for iron—cadmium electrodes.

The potentials were measured against amalgamated zinc electrodes in the same solution.

At these potentials the anodic dissolution of iron and cadmium practically ceases.

The walls of the steel vessel acted as the opposite electrode during the forming process. This process was stopped when constant capacity was reached. The electrodes were then charged for 6 hours at 250 ma. The steel vessels containing the electrodes covered with alkali were firmly closed with rubber bungs. Hydrogen was withdrawn through glass tubes passing through the bungs and connected to eudiometers. Mercury was used as the sealing liquid. The volume of hydrogen liberated during the dissolving process was reduced to normal conditions (760 mm, 0°).

RESULTS

The following electrodes were studied: 1) electrodes in which the active mass consisted of iron – cadmium sponge made electrolytically with the combined use of cadmium and iron anodes; 2) electrodes made from mass obtained by mixing of CdO and Fe_3O_4 with cadmium—iron ratios of 2.6 : 1 and 0.5 : 1 by weight respectively; 3) electrodes made from Fe_3O_4 powders with different amounts of extraneous impurities.

Experiments on the solution of type 1 electrodes were continued 7720 hours at temperatures from 18 to 27°. Solution of type 2 electrodes was studied in experiments lasting 720 hours at temperatures between 24 and 30°. Finally, type 3* electrodes were studied at 25 ± 0.5° for 2160 hours.

*Type 3 electrodes were tested by V.I. Aksenova.

The experimental results are plotted in Fig. 1.

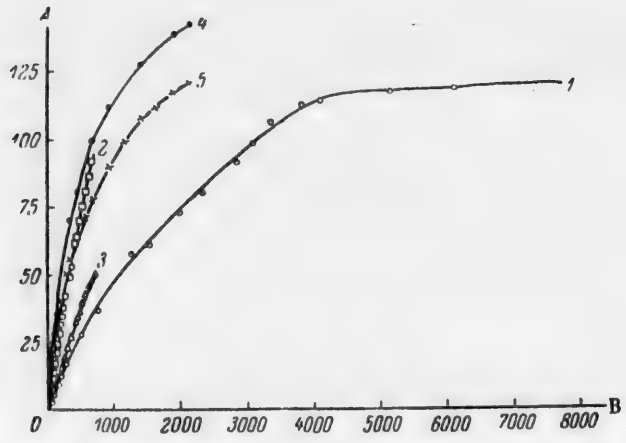

Fig. 1. Increase of the volume of hydrogen liberated in the course of solution of iron in 4.6 N KOH. A) Average volume of hydrogen liberated (in ml H_2 per g Fe), B) time τ (hours. 1) Cd–Fe mass made by electrolysis; 2) Cd–Fe mass made by mixing of CdO with Fe_3O_4; 3) the same, with Cd : Fe = 0.5 : 1; 4, 5) Fe mass made from Fe_3O_4.

Here the average volumes of hydrogen obtained in tests of several electrodes for each powder of given composition and method of preparation, relative to the total contents of the electrodes, are taken along the ordinate axis. The total iron contents of the electrodes were determined by the permanganate method. The time from the start of the test is taken along the abscissa axis.

The resultant curves are asymptotic in character, so that if the time of the solution process is long enough the amount of hydrogen liberated per unit weight of iron becomes practically constant. In the initial stages of the experiment, on the other hand, the amount of hydrogen liberated is proportional to the time. The course of the curves in Fig. 1 is adequately represented by an equation of the type

$$V = \frac{\tau}{a\tau + b}, \qquad (1)$$

where V is the volume of hydrogen (ml) liberated per 1 g of total iron, τ is the time (hours), and a and b are constants which depend on the composition and method of preparation of the electrode, and the composition and temperature of the electrolyte. Equation (1) is easily transformed into

$$\frac{1}{V} = a + b \cdot \frac{1}{\tau}. \qquad (2)$$

Figure 2 shows that this equation is in good agreement with the experimental data; the constant a is inversely proportional to the maximum volume of hydrogen obtainable from 1 g of total iron (at $\tau \longrightarrow \infty$).

DISCUSSION OF RESULTS

From this relationship a number of conclusions can be drawn concerning the kinetics of the solution of iron in alkaline solutions. The starting point is the fact that the potential of iron–cadmium and iron electrodes remains practically unchanged during the solution process, while the liberation of hydrogen is accompanied by a decrease of the amount of metallic iron in the electrode and by formation of the hydroxide $Fe(OH)_2$. This

suggests that the hydrogen liberation rate $\frac{dV}{d\tau}$ is at any given instant proportional to the metallic iron content of the electrode, i.e.

$$\frac{dV}{d\tau} = kp \tag{3}$$

where p is the amount of metallic iron per 1 g total iron, and k is a constant factor with the dimensions ml H_2/g Fe_{total} · hour. In the general case the factor k should depend on the composition and method of preparation of the electrode, and also on the electrolyte composition and temperature. Since, in the solution reaction

$$Fe + 2H_2O \rightarrow Fe(OH)_2 + H_2$$

1 mole of hydrogen is liberated per gram-atom of iron oxidized, it may be assumed that the metallic iron content at any instant (p) is related to the metallic iron content at the initial instant (p_0) by the equation

$$p = p_0 - cV, \tag{4}$$

where c = 0.00249 g Fe per ml H_2, the iron equivalent of the liberated hydrogen.

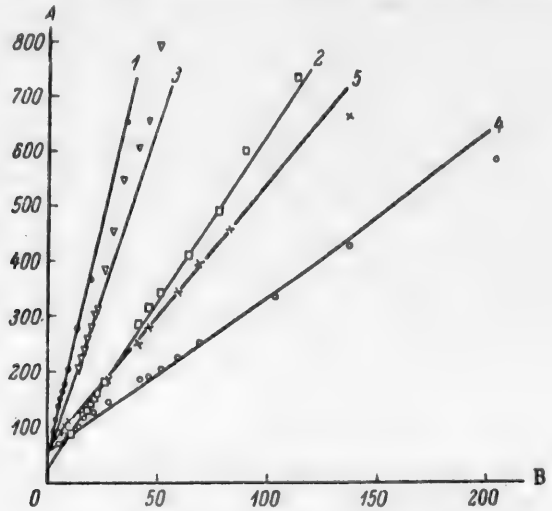

Fig. 2. Applicability of Equation (2) to experimental data. A) $\frac{1}{V} \cdot 10^4$, B) $\frac{1}{\tau} \cdot 10^4$. The numbering of the curves is the same as in Fig. 1.

From Equations (3) and (4) we have:

$$\frac{dV}{d\tau} = k(p_0 - cV). \tag{5}$$

After integration, on the condition that when $\tau = 0$, $V = 0$, we have

$$V = \frac{p_0}{c}(1 - e^{-ck\tau}). \tag{6}$$

If $\tau \rightarrow 0$, then $p \rightarrow p_0$, and evidently in this case, in agreement with experimental data

$$V \approx kp_0\tau. \tag{7}$$

If $\tau \rightarrow \infty$, it can be easily shown that

$$V \approx \frac{p_0}{c} = \text{const}, \tag{8}$$

which is also confirmed experimentally.

It is also easy to derive the empirical Equation (1) from Equation (6). Resolution of the exponential term into series gives

$$V \approx \frac{p_0}{c}\left(1 - \frac{1}{1 + ck\tau}\right) = \frac{p_0 k\tau}{1 + ck\tau} \qquad (9)$$

or

$$V \approx \frac{\tau}{\frac{c}{p_0} + \frac{1}{kp_0}} \qquad (10)$$

thus, with the earlier notation, we have

$$a = \frac{c}{p_0}$$

$$b = \frac{1}{kp_0} \qquad (11)$$

It follows directly from the curves in Fig. 2 that, for example, for an iron–cadmium electrode with the ratio Cd : Fe = 2.6 : 1 the value of $\underline{a}$ is 0.002 g/ml, which is close to the theoretical value of $\underline{c}$ (0.00249 g/ml). Therefore, for the iron component of this electrode mass, $p_0 = 0.80$. For the second iron–cadmium electrode (Cd : Fe = 0.5 : 1), $p_0 = 0.62$. For iron electrodes p_0 is considerably lower. It seems that the low values of p_0 are the consequence not only of the low content of metallic iron in the charged electrode, but also of its passivation during the solution process [2].

It seems likely that study of spontaneous solution processes in the light of the above relationships and determinations of the values of $\underline{k}$, p_0, and $\underline{a}$ will assist in future objective studies of such processes as self-discharge and passivation of iron and iron–cadmium electrodes.

It must be remembered, however, that data obtained in experiments with single electrodes cannot be applied completely to the dissolution of such electrodes in alkaline cells, as such factors as the presence of oxygen in the electroyte as the result of gas evolution at the nickel oxide electrode become of great significance.

SUMMARY

1. A kinetic equation for gas evolution on iron and iron–cadmium electrodes has been derived, and shown to be in satisfactory agreement with experimental data.

2. It is shown that in iron–cadmium electrodes the metallic iron content decreases with decreasing cadmium–iron ratio in the electrode mass.

LITERATURE CITED

[1] I. Platonova and S. Levina, J. Phys. Chem., 21, 331 (1947).

[2] B.N. Kabanov and D.I. Leikis, J. Phys. Chem., 20, 995 (1946); Proc. Acad. Sci. USSR 58, 1685 (1948).

Received December 29, 1955

THE SURFACE STATE AND ANODE POTENTIALS OF COPPER AND NICKEL IN ELECTROCHEMICAL POLISHING

N.P. Fedotyev and S. Ya. Grilikhes

As was shown earlier [1, 2], metal passivation effects in electrolysis play an important part in the electrochemical polishing of steel. This might be expected to be generally applicable to the polishing of other metals. To elucidate this question, the electrochemical polishing of nickel and copper in various electrolytes has been studied.

Nickel was polished in a solution of the following composition (in %): H_3PO_4 65, H_2SO_4 15, CrO_3 6, H_2O 14. The anode current density was 40 amp./dm^2, the solution temperature was 20°, and the plishing time was 2 minutes.

Copper was polished in an electrolyte containing (in %): H_3PO_4 74, CrO_3 6, H_2O 14. The anode current density was 40 amp/dm^2, the electrolyte temperature was 20°, and the polishing time was 2 minutes.

The variations of the surface state of the metals as the result of electrochemical polishing were studied by measurement of the capacity and contact resistance of the electric double layer. The method of measurement was described in detail earlier [1]. The results obtained in the capacity and contact resistance measurements in 1 N K_2SO_4 solution are tabulated below.

Effects of Surface Treatment of Copper and Nickel on the Capacity and Contact Resistance at the Metal–Solution Boundary

Details of specimens	Capacity (in μF/cm^2)	Contact resistance (in ohms/dm^2)	Surface state of metal
Rolled nickel	20.4	350	Dull
Electrochemically polished nickel	17.7	665	Bright
Rolled copper	33.2	5.5	Dull
Electrochemically polished copper	16.2	12.4	Bright

As in the previously examined case of the electrochemical polishing of steel, electrochemical polishing of copper and nickel is accompanied by a decrease of capacity and an increase of the contact resistance, indicating the formation of an oxide film on the metal. The differences in the absolute values of the capacity and contact resistance for the different metals depend on the different composition and physicochemical characteristics of the films formed on them.

Figure 1 shows anodic polarization curves for chrome steel (12 × 14 A), nickel (Nl) and carbon steel (St 45) in an electrolyte containing (in %): H_3PO_4 65, H_2SO_4 15, CrO_3 6, H_2O 14 at 80°.

The potentials of these metals in the electrolyte without current have larger positive values than the normal potentials. All the curves have two limiting current regions. The anodic polarization curve for chrome steel

only differs from the curve for carbon steel by a somewhat higher positive value of the potential corresponding to the start of dissolution of iron in the form of $Fe^{\cdots}$, and a higher second limiting current region. The anode potential curve for nickel is close in configuration and values of the potentials to the curve for chrome steel. All this shows that the anode processes occurring in the electrochemical polishing of nickel and steel have much in common.

In the case considered above, passivation of the anode and the polishing effect – increase of the reflecting power of the metal – depend on the presence of an oxidizing agent, sexivalent chromium, in the electrolyte. It is known, however, that a number of metals can be electropolished in electrolytes without chromic anhydride. Such metals include nickel, which can be polished in concentrated sulfuric acid solutions.

The anodic polarization curve for the treatment of nickel in an electrolyte containing 730 g H_2SO_4 per liter has two limiting current regions (Fig. 2).

The first limiting current plateau is probably the consequence of the formation of a salt film on the anode. Such a film may be formed because nickel sulfates have limited solubility in sulfuric acid. It is known, for example, that nickel sufate is deposited in the polishing bath in the course of use. The film covering the anode is fairly porous, as it allows current to pass. After most of the anode surface has become covered with the salt film, the current density at the regions of the pores increases so much that oxidation of the metal becomes possible and liberation of oxygen begins at its surface. The formation of an oxide film on the metal is marked by a second limiting current region on the anode potential curve.

The possibility of the use of electrolytes of different composition for the polishing of nickel depends on the electrochemical properties of the metal. It is known that nickel is more prone to passivation than iron. This is probably the reason why an oxide film is formed on a nickel anode during electrolysis in sulfuric acid, even in absence of active oxidants such as CrO_3.

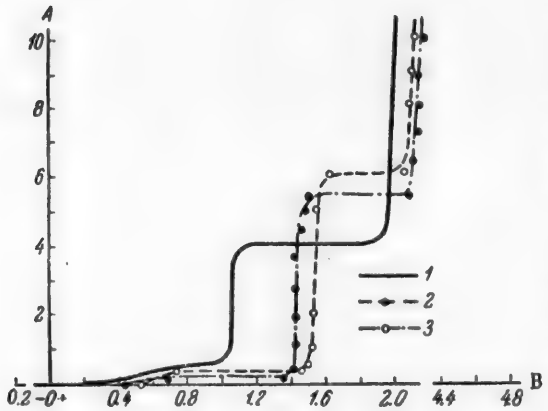

Fig. 1. Effect of current density on anode potentials of steel and nickel in electrochemical polishing. A) Anode current density (in amp/dm^2), B) anode potential (in v). Anode materials: 1) carbon steel, 2) nickel, 3) chrome steel.

Polishing of nickel in sulfuric acid is effected at potentials exceeding the oxygen evolution potential for a given solution. In this case, as in the treatment of steel, the electrochemical polishing process in associated with anode passivation.

The course of electrochemical polishing of copper in orthophosphoric acid solution, which is widely practised, is somewhat different. In contrast to the polishing of steel and nickel as examined above, the electrochemical polishing of copper in H_3PO_4 occurs under limiting current conditions and is not accompanied by evolution of oxygen. Analysis of the black film which covers the copper anode in electrolysis shows it to consist of copper oxide [3]. The metal surface under the film is polished.

Fortunatov and Finkelshtein [3] believe that the anode potential reaches values at which discharge of water molecules is possible. The intermediately formed singly charged oxygen ions react with the copper forming the oxide of the metal, and this subsequently dissolves in the orthophosphoric acid. All this indicates that the electrochemical polishing of copper under limiting current conditions in an electrolyte without oxidizing agents nevertheless depends on formation of a passive oxide film on the anode.

Increase of the anode current density above the limiting value results in deterioration of the surface quality – small blisters appear, caused by retention of oxygen bubbles on the metal surface.

The situation changes if CrO_3 is added to the orthophosphoric acid solution. In such an electrolyte (H_3PO_4 74%, CrO_3 6%, H_2O 14%) polishing takes place at potentials exceeding the potential of oxygen evolution in the given solution. The gas bubbles are not retained on the passivated anode surface. It seems that the oxide films

formed on copper anodes during polishing in H_3PO_4 solutions differ in composition and structure depending on whether CrO_3 is present. These differences are reflected in the course of the anode potential curves.

Figure 3 shows anode potential curves for electrolytes of the following composition (in %): 1) H_3PO_4 74, H_2O 26; 2) H_3PO_4 74, CrO_3 6, H_2O 20. The solution temperature was 20° in both cases. The anode potential curve for the electrolyte without CrO_3 has one limiting current region, and the curve for the electrolyte with CrO_3 has two such regions.

At a current density of 0.07 amp/dm^2, i.e., before the limiting current density is reached, the current efficiency in Electrolyte 1 is 95% (calculated for Cu^{++}), and in Electrolyte 2 it is 116%. At 5 amp/dm^2, above the limiting current density, the current efficiency is 62% in Electrolyte 1, and 47% in Electrolyte 2.

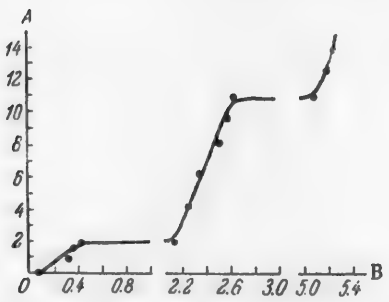

Fig. 2 Effect of current density on anode potential in electrochemical polishing of nickel in sulfuric acid solution. A) Anode current density (in amp./dm^2), B) anode potential (in v).

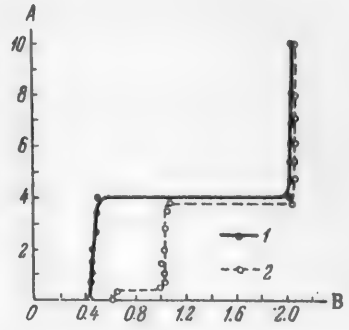

Fig. 3. Effect of current density on anode potential in electrochemical polishing of copper in electrolytes of different composition. A) Anode current density (in amp/dm^2), B) anode potential (in v). Electrolyte composition (in wt. %): 1) H_3PO_4 74, H_2O 26; 2) H_3PO_4 74, CrO_3 6, H_2O 20.

The high current efficiency in Electrolyte 2 in electrolysis at low current densities must be ascribed to chemical dissolution of copper in presence of an oxidizing agent. Formation of Cu^{+}, which might also result in increased current efficiency, is hardly possible in this case.

In electrolytes containing CrO_3 at low current densities the solution of copper is accompanied by reduction of sexivalent to trivalent copper. The anode surface becomes coated with a passive oxide film, in the formation of which chromium compounds take part. The presence of the passive film is confirmed by the results of capacity and contact resistance determinations given above. Literature data also indicate that when copper is treated in solutions containing CrO_3 a passive film is formed on the metal surface [4].

SUMMARY

1. Measurements of capacity and contact resistance at the metal – solution boundary have demonstrated the presence of passive oxide films on the surfaces of electrochemically polished copper and nickel specimens.

2. Analysis of current density – anode potential curves for the electrochemical polishing of copper and nickel in electrolytes of different composition confirm the formation of oxide films on the metal surfaces during anodic treatment.

3. A polishing effect – increase of the reflecting power of the metal – is produced by electrolysis in conditions which ensure the formation of passive oxide films on copper and nickel surfaces.

LITERATURE CITED

[1] N.P. Fedotyev, S. Ya. Grilikhes, and V.L. Kheifets, J. Appl. Chem., 29, 12 (1956).*

[2] N.P. Fedotyev and S. Ya. Grilikhes, J. Appl. Chem., 30, 2 (1957).*

[3] A.V. Fortunatov and A.V. Finkelshtein, Proc. Acad. Sci. USSR 90, 5 (1953).

[4] G. Akimov and A. Golubev, J. Appl. Chem., 12, 11 (1939).

Received September 16, 1955

*Original Russian pagination. See C.B. Translation.

POLYTHERM FOR THE TERNARY SYSTEM UREA—PHOSPHORIC ACID—WATER

V.P. Blidin, A.Ya. Malakhova, and S.M. Aslanov

Studies of the interaction of urea with various salts and acids are of both theoretical and applied importance in relation to the production of mixed fertilizers. Urea is the best concentrated nitrogenous fertilizer. Unfortunately, it has not been used in practice as a bulk fertilizer, owing to the great demand for it in a number of industries (plastics, etc.) and its relatively high cost. There is no doubt that in the near future it will become considerably cheaper and will become widely used in agriculture both as an independent fertilizer and in conjunction with other fertilizers.

Interactions of urea with other substances have been considered in a number of papers [1 - 5]. The solubility of urea in presence of phosphoric acid has been studied for the first time.

According to literature data [2], the cryohydric point for the system $CO(NH_2)_2$—H_2O is at −11.0° and corresponds to a composition of 32.9% urea and 67.1% water. Two breaks were found on the crystallization curve for urea – the first at +1.1°, with 40.7% urea, and the second at 24.4°, with 54.5% urea. Thus, urea exists in α, β, γ, modifications.

The cryohydric point for the system H_3PO_4—H_2O, according to our data, corresponds to −68° and 61.5% H_3PO_4. Starting from the eutectic point, phosphoric acid crystallizes as $2H_3PO_4 \cdot H_2O$, and then at +23.5° it passes into H_3PO_4, as was first reported by Ross and Jones [6].

EXPERIMENTAL

Chemically pure grade reagents were used for the work. The investigations were carried out by the visual polythermal method, which consists of determinations of the temperatures at which the crystals disappear and first new crystals appear. The degree of accuracy of the determinations was within ± 0.1°.

TABLE 1

30% $CO(NH_2)_2$

Point No.	Temperature (deg)	Contents (wt. %)			Total salts	Solid phase
		$CO(NH_2)_2$	H_3PO_4	H_2O		
1	— 9.8	30	—	70	30	Ice
2	—10	27.3	4.5	68.2	31.8	
3	—10.5	26.8	9.6	63.6	36.4	
4	—11.5	25.5	14.4	60.1	39.9	Ice + $mCO(NH_2)_2 \cdot nH_3PO_4$
5	—9	24.8	15.5	59.7	40.3	$mCO(NH_2)_2 \cdot nH_3PO_4$
6	—5	24.3	16.6	59.1	40.9	
7	3.7	22.8	21.5	55.7	44.3	
8	15.5	20.6	28.3	51.1	48.9	
9	24	18.8	33.7	47.5	52.5	
10	30	17.7	37.0	45.3	54.7	

The difficulty in the work lay in the high viscosities of the solutions, especially at high concentrations of phosphoric acid.

7 internal sections of the diagram for the ternary system were investigated. The data for the sections are given in Tables 1-7 and plotted in Fig. 1.

The directions of the sections are given below:

Section I (30% $CO(NH_2)_2$ + 70% H_2O) → H_3PO_4,
Section II (40% $CO(NH_2)_2$ + 60% H_2O) → H_3PO_4,
Section III (50% $CO(NH_2)_2$ + 50% H_2O) → H_3PO_4,
Section IV (22.5% H_3PO_4 + 77.5% H_2O) → $CO(NH_2)_2$,
Section V (40.5% H_3PO_4 + 59.5% H_2O) → $CO(NH_2)_2$,
Section VI (58.5% H_3PO_4 + 41.5% H_2O) → $CO(NH_2)_2$,
Section VII (67.5% H_3PO_4 + 32.5% H_2O) → $CO(NH_2)_2$.

TABLE 2

40% $CO(NH_2)_2$

Point No.	Temperature (deg)	Contents (wt. %)			Total salts	Solid phase
		$CO(NH_2)_2$	H_3PO_4	H_2O		
1	— 3	40.0	—	60	40	$CO(NH_2)_2$
2	— 7.5	37.1	6.4	56.5	43.5	
3	—11	35.3	10.6	54.1	45.9	
4	—14.2	34.8	12.5	52.7	47.3	
5	—17.5	33.5	16.3	50.2	49.8	$CO(NH_2)_2 + mCO(NH_2)_2 \cdot nH_3PO_4$
6	—15	32.4	17.9	49.7	50.3	
7	—10.5	30.4	20.2	49.4	50.6	
8	— 6.0	29.7	21.5	48.8	51.2	
9	+ 5	29.0	24.2	46.8	53.2	
10	10	28.3	25.5	46.2	53.8	
11	14	27.6	26.3	46.1	53.9	
12	20	27.0	27.1	45.9	54.1	
13	30	26.2	29.8	44.0	56.0	

TABLE 3

50% $CO(NH_2)_2$

Point No.	Temperature (deg)	Contents (wt. %)			Total salts	Solid phase
		$CO(NH_2)_2$	H_3PO_4	H_2O		
1	12.5	50	—	50	50	$CO(NH_2)_2$
2	5.5	47.2	5	47.8	52.2	
3	— 1	44.8	9.4	45.8	54.2	
4	— 6	42.8	13.0	44.2	55.8	
5	—12	40.2	17.6	42.2	57.8	$CO(NH_2)_2 + mCO(NH_2)_2 \cdot nH_3PO_4$
6	— 6	38.6	20.7	40.7	59.3	$mCO(NH_2)_2 \cdot nH_3PO_4$
7	0	37.9	21.8	40.3	59.7	
8	7	36.6	24.1	39.3	60.7	
9	18	35.4	26.3	38.3	61.7	
10	26	33.7	29.3	37.0	63.0	

TABLE 4

22.5% H_3PO_4

Point No.	Temperature (deg)	Contents (wt. %)			Total salts	Solid phase
		$CO(NH_2)_2$	H_3PO_4	H_2O		
1	— 6	—	22.5	77.5	22.5	Ice
2	— 5.7	2.8	21.9	75.3	24.7	Ice
3	— 5.6	5.0	21.3	73.7	26.3	Ice
4	— 5.5	6.0	21.2	72.8	27.2	Ice + $mCO(NH_2)_2 \cdot nH_3PO_4$
5	— 4	6.8	21.0	72.2	27.8	$mCO(NH_2)_2 \cdot nH_3PO_4$
6	+10	8.8	20.5	70.7	29.3	$mCO(NH_2)_2 \cdot nH_3PO_4$
7	25	11.2	20.1	68.7	31.3	$mCO(NH_2)_2 \cdot nH_3PO_4$

TABLE 5

40.5% H_3PO_4

Point No.	Temperature (deg)	Contents (wt. %)			Total salts	Solid phase
		$CO(NH_2)_2$	H_3PO_4	H_2O		
1	—21	—	40.5	59.5	40.5	Ice
2	—22	1.2	40.2	58.6	41.4	Ice + $mCO(NH_2)_2 \cdot nH_3PO_4$
3	—16	2.5	39.5	58.0	42.0	$mCO(NH_2)_2 \cdot nH_3PO_4$
4	—10.5	4.2	38.8	57.0	43.0	$mCO(NH_2)_2 \cdot nH_3PO_4$
5	— 1.0	6.7	37.8	55.5	44.5	$mCO(NH_2)_2 \cdot nH_3PO_4$
6	+ 5.5	8.5	37.1	54.4	45.6	$mCO(NH_2)_2 \cdot nH_3PO_4$
7	7.1	9.7	36.6	53.7	46.3	$mCO(NH_2)_2 \cdot nH_3PO_4$
8	12.5	11.5	35.9	52.6	47.4	$mCO(NH_2)_2 \cdot nH_3PO_4$
9	15.5	13.4	35.1	51.5	48.5	$mCO(NH_2)_2 \cdot nH_3PO_4$
10	18.5	15.4	34.3	50.3	49.7	$mCO(NH_2)_2 \cdot nH_3PO_4$
11	20.5	16.8	33.5	49.7	50.3	$mCO(NH_2)_2 \cdot nH_3PO_4$
12	22.5	18.3	33.1	48.6	51.4	$mCO(NH_2)_2 \cdot nH_3PO_4$
13	26.3	21.7	31.7	46.6	53.4	$mCO(NH_2)_2 \cdot nH_3PO_4$

TABLE 6

58.5% H_3PO_4

Point No.	Temperature (deg)	Contents (wt. %)			Total salts	Solid phase
		$CO(NH_2)_2$	H_3PO_4	H_2O		
1	—65	—	58.5	41.5	58.5	Ice
2	—66	0.7	58.0	41.3	58.4	Ice + $mCO(NH_2)_2 \cdot nH_3PO_4$
3	—47	1.6	57.40	41.0	59.0	$mCO(NH_2)_2 \cdot nH_3PO_4$
4	—19	3.2	56.6	40.2	59.8	$mCO(NH_2)_2 \cdot nH_3PO_4$
5	+ 4	4.1	56.1	39.8	60.2	$mCO(NH_2)_2 \cdot nH_3PO_4$
6	+24	5.3	55.4	39.3	60.7	$mCO(NH_2)_2 \cdot nH_3PO_4$

TABLE 7

67.5% H_3PO_4

Point No.	Temperature (deg)	Contents (wt. %)			Total salts	Solid phase
		$CO(NH_2)_2$	H_3PO_4	H_2O		
1	—53	—	67.5	32.5	67.5	$mCO(NH_2)_2 \cdot nH_3PO_4$
2	—46	2.5	65.8	31.7	68.3	
3	—35	3.8	64.9	31.3	68.7	
4	0	5.2	64.0	30.8	69.2	
5	14	6.4	63.2	30.4	69.6	
6	25	7.5	62.5	30.0	70.0	

The composition data for the intersection points of the solubility curves are given in the tables. In sections running in the direction of urea, increased solubility of the latter in phosphoric acid is found, with formation of fine homogeneous crystals corresponding to a solid solution of the type m $CO(NH_2)_2$ n H_3PO_4. The regions of the curves corresponding to crystallization of ice in these sections diminish with increasing H_3PO_4 concentration. No branches corresponding to crystallization of phosphoric acid are found. The sections running in the directionof phosphoric acid show the reverse effect, i.e., H_3PO_4 has less tendency to form solid solutions in concentrated solutions of urea.

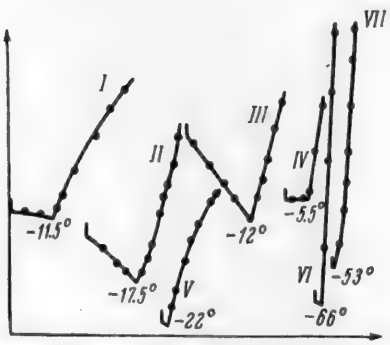

Fig. 1. Sections for ternary system.

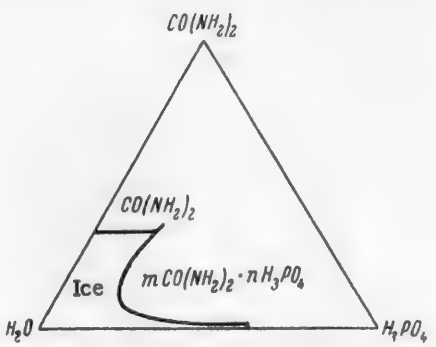

Fig. 2. Polythermal diagram.

Sections II and III show considerable branches of urea crystallization, confirming the above conclusion. The crystallization branches of the solid solution ascend sharply with increase of temperature in all the sections. The explanation is that temperature has little effect on increase of the solubility of the solid solution, which has lower solubility than phosphoric acid and higher solubility than urea.

The data in the sections were used to plot the polythermal diagram (Fig. 2).

This diagram contains a region of ice crystallization with a projection in the phosphoric acid direction, a urea region, and the largest region of crystallization of a solid solution of the type m $CO(NH_2)_2$ n · H_3PO_4.

The system contains one triple point at − 18.5° for the composition 19.2% H_3PO_4, 34.4% $CO(NH_2)_2$ and 46.5% H_2O.

We did not detect any differences due to the α, β, and γ forms of urea in presence of phosphoric acid.

SUMMARY

1. The system urea − phosphoric acid − water has been studied by a visual polythermal method and it was found that solid solutions of the restricted type are formed in the system.

2. A triple eutectic point has been determined, corresponding to the composition 19.2% H_3PO_4, 34.3% $CO(NH_2)_2$, 46.5% H_2O and $-18.5°$.

LITERATURE CITED

[1] V.P. Blidin, J. Gen. Chem., 11, 887 (1941).

[2] V.A. Polosin and A.G. Treshchov, J. Phys. Chem., 20, 1 (1953).

[3] V.A. Sokolov, J. Gen. Chem., 9, 753 (1939).

[4] A.G. Bergman and M.N. Kuznetsova, J. Gen. Chem., 9, 631 (1939).

[5] V.P. Blidin, J. Gen. Chem., 17, 1381 (1947).

[6] W.H. Ross and R.M. Jones, J. Am. Chem. Soc., 47, 2167 (1925).

Received August 25, 1955

INSECTOFUNGIDICAL ACTION OF ORGANIC, ORGANOSILICON, AND INORGANIC THIOCYANATES

M.Ya. Marova, M.G. Voronkov, and B.N. Dolgov

Institute of Silicate Chemistry, Academy of Sciences USSR, and Laboratory for the Preservation and Restoration of Documents, Academy of Sciences USSR

We found in a study of the insectofungicidal and bactericidal properties of various classes or organosilicon compounds that some thiocyano – substituted silanes (alkyl isothiocyanosilanes [1], $R_nSi(NCS)_{4n}$, where n = 1–3) have appreciable insectofungicidal and bactericidal action. The results of a study of the effects of a number of organosilicon thiocyanates on Macrosporium and Cladosporium fungi are given in Table 1. These results show that additions of 1–3% of $C_4H_9Si(NCS)_2$, $(CH_3)_2Si(NCS)_2$, $(C_2H_5)_2Si(NCS)_2$ or $(C_2H_5)_3SiNCS$ to nutrient media infected with cultures of these fungi strongly suppress or even completely inhibit their development for a year or more, and also prevent the growth of molds or bacteria from the surrounding air on these media.

TABLE 1

Suppression of the Growth of Macrosporium and Cladosporium Fungi and Bacteria by Thiocyanate-Substituted Silanes $R_nSi(NCS)_{4-n}$

Compound	Time (days) before start of growth of molds or bacteria on nutrient media infected with cultures of Macrosporium and Cladosporium and containing additions of $RnSi(NCS)_{4-n}$				
	0.1	0.2	0.3	0.5	1.0
Pure medium	5	5	5	5	5
$CH_3Si(NCS)_3$	5	5	5	5	8
$C_2H_5Si(NCS)_3$	5	5	5	5	8
n-$C_3H_7Si(NCS)_3$	5	5	5	5	8
n-$C_4H_9Si(NCS)_3$	5	10	105	185	240
$(CH_3)_2Si(NCS)_2$	5	15	105	115	150
$(C_2H_5)_2Si(NCS)_2$	5	15	150	150	180
$(n\text{-}C_4H_9)_2Si(NCS)_2$	5	5	5	5	8
$(CH_3)_3SiNCS$	5	5	5	5	8
$(C_2H_5)_3SiNCS$	5	5	15	105	365
$(n\text{-}C_4H_9)_3SiNCS$	5	5	5	5	8

It is rather difficult to establish any strict correlation between the toxic action and the structure of alkylisothiocyanosilanes from the data in Table 1. There is no doubt, however, that the toxic action of these compounds does not depend on thiocyanic acid, HSCN, formed from them by hydrolysis. This is shown, first, by the fact that there is no definite connection between the number of NCS groups in the molecule and the toxicity of a particular compound. Second, the most easily hydrolyzed alkylisothiocyanosilanes $CH_3Si(NCS)_3$ and $C_2H_5Si(NCS)_3$, are the least effective. However, the least easily hydrolyzed compounds, such as $(n-C_4H_9)_3SiNCS$ and $(n-C_4H_9)_2Si(NCS)_2$, are nontoxic. Neither is there any definite connection between the toxicity of a compound

and the structure of the alkyl radical in it. It is interesting to note that, as we have shown, alkylisocyanosilanes of analogous structure to the thiocyano compounds studied do not have fungicidal or bactericadal action.

Alkylisothiocyanosilanes also have an appreciable fungicidal action in the vapor phase. For example, the most volatile of the four most effective compounds listed above, $(CH_3)_2Si(NCS)_2$ and $(C_2H_5)_3SiNCS$, suppress the growth of Cladosporium, Macrosporium, and Torula fungi even at concentrations of 0.2 g per liter of air. Dimethyldiisothiocyanosilane has considerable fumigant action. In particular, exposure of 6–15 hours to an atmosphere containing a relatively low concentration of $(CH_3)_2Si(NCS)_2$ causes 100% mortality in agricultural insect pests of the Pentatomidae family*.

Having demonstrated the insectofungicidal action of organosilicon thiocyanates, which must be attributed to the presence of the isothiocyano group NCS, we decided to study certain organic and inorganic derivatives of isothiocyanic and thiocyanic acids from this aspect. As a result of these investigations we found a new class of compounds with very effective fungicidal and bactericidal action, as is clearly demonstrated by the data in Table 2. For comparison, the same table gives data on the commonly used effective insectofungicides – thiophos (parathion), sodium pentachlorophenate, and also of corrosive sublimate and sodium fluosilicate.

TABLE 2

Suppression of the Development of Cladosporium and Macrosporium Fungi and of Bacteria by Organic and Inorganic Derivatives of Thiocyanic and Isothiocyanic Acids

Compound	Time (days) before start of growth of molds or bacteria on nutrient media infected with cultures of Cladosporium and Macrosporium and containing additions of thiocyanates or isothiocyanates (in %):					
	0.05	0.1	0.2	0.3	0.5	1.0
Pure medium	5	5	5	5	5	5
$NCSCH_2SCN$ (MT-2)	10	>365	>365	>365	>365	—
$NCSCH_2CH_2SCN$ (ET-2)	10	>365	>365	>365	>365	—
$NCSCH_2CH(SCN)CH_2SCN$ (PT-3)	10	>365	>365	>365	>365	—
C_6H_5NCS	7	9	15	45	90	180
$CH_2CH{=}CHNCS$	5	5	5	5	5	8
$Cu(SCN)_2$	5	5	15	105	180	240
NH_4SCN	5	5	5	5	5	8
$(C_2H_5O)_2P(=S)OC_6H_4NO_2$	10	150	>365	>365	>365	—
Cl_5C_6ONa	7	21	150	>365	>365	—
$HgCl_2$	7	>365	>365	>365	>365	—
Na_2SiF_6	8	14	21	>365	>365	—

The data in Table 2 demonstrate the very powerful fungicidal and bactericidal effects of dithiocyanomethane $CH_2(SCN)_2$ (MT-2), 1,2-dithiocyanoethane $NCSCH_2CH_2SCN$ (ET-2), and 1,2,3-trithiocyanopropane $NCSCH_2CH(SCN)CH_2SCN$ (PT-3), which are even more powerful than thiophos and other most commonly used insectofungicides. Compounds of this type can therefore be recommended for such purposes as the protection of glues and paints against molds and bacteria, especially as these compounds were found during our prolonged experiments to be less toxic to warm-blooded animals than such substances as thiophos or corrosive sublimate. Moreover, polythiocyanoalkanes are stable on keeping, are colorless, and do not cause color changes (such as are caused, for example, by thiophos of sodium pentachlorophenate) or deterioration of the physical and mechanical properties of the medium to which they are added. Our tests of the mechanical properties of filter paper and newsprint paper impregnated with glue containing 0.5% of MT-2, ET-2, or PT-3 showed that the breaking length, extensibility, and flexing strength of the paper are practically unchanged, and the color is also unaffected.

* According to G.A. Chigarev's data, certain alkylisocyanosilanes have a considerable fumigant action on Pentatomidae pests.

A great advantage of the polyisothiocyanoalkanes over many of the insectofungicides now in use is their cheapness owing to the readily available raw materials (olefins, halogenated hydrocarbons, and sodium or amonium thiocyanate) and to the simplicity of preparation.

It follows from the data in Table 2 that not all the compounds containing the thiocyano group have fungicidal and bactericidal action. For example, ammonium thiocyanate does not have this action. The toxicity of copper thiocyanate is more likely due to the Cu ion than to the SCN group. In contrast to the organic thiocyanates, the organic analogs of the alkylisothiocyanosilanes, RNCS, and in particular allylisothiocyanate have low activity.

It is not possible to establish a correlation between toxicity and structure of polythiocyanoalkanes from the preliminary data given here; further investigations are required for this. However, as in the case of the organosilicon thiocyanates, it seems that an increase of the number of thiocyano groups in the molecule does not lead to an increase of toxicity. The presence of two thiocyano groups attached to the same or different carbon atoms likewise has no practical influence on the fungicidal and bactericidal properties.

EXPERIMENTAL

Starting materials. Alkylisothiocyanosilanes were prepared by the interaction of the corresponding alkylchlorosilanes with anhydrous ammonium thiocyanate in dry benzene. Products described earlier [1] were used in the present work.

Dithiocyanomethane (MT-2), 1,2-dithiocyanoethane (ET-2), and 1,2,3-trithiocyanopropane (PT-3) were obtained by reactions of the corresponding bromides with ammonium or sodium thiocyanate in boiling alcohol, and were recrystallized from hot water or alcohol. Their melting points were 102, 90, and 126° respectively, in agreement with the literature [2-4]. Polythiocyanoalkanes are colorless crystalline substances, soluble in boiling water, alcohol, ether, and acetone. They are almost insoluble in cold water. Their vapors have an irritant action.

The other compounds studied were commercial chemically pure reagents.

Method of investigation. A 10% paste made from wheat flour or gelatin was used as the nutrient medium for the molds. The nutrient medium was poured into Petri dishes, and the respective compounds, dissolved in acetone, were added (in weight concentrations of 0.05, 0.1, 0.2, 0.3, 0.5, and 1% on the weight of the medium). For each concentration of a given compound 4-6 parallel experiments were carried out. The medium was seeded with pure cultures of Macrosporium and Cladosporium. The growth of bacteria or of other mold species was determined by the appearance of colonies on the medium caused by infection from the outside air, as sterile conditions were deliberately not maintained. The dishes were placed in a compartment at 80-90% relative humidity and kept at 18-20° until the medium showed mold growth or became covered with colonies of bacteria. The experiments were continued for up to 12 months. Compounds which prevented the appearance of molds and bacteria for a year (i.e., >365 days, as shown in Table 2) were not tested further.

Control experiments were started simultaneously in the same conditions (with medium seeded with the pure culture with addition of the same amount of acetone). In the control experiments the molds generally developed after 3-5 days, bacteria appeared after 4-5 days, and other species of molds from the air (Penicillium, Mucor, Aspergillus, etc.) appeared after 8-12 days.

Tests of the fumigant action of the thiocyanates were carried out as follows. Into a flat-bottomed liter flask were placed short test tubes containing different species of molds (Cladosporium, Macrosporium, etc.) grown on agar, and test tubes with strips of paper seeded with the molds. 0.2g of the compound under test was placed on the bottom of the flask, which was then sealed. After 24 hours at room temperature the experimental cultures were transferred to sterile agar; absence of mold growth was a sign of a positive fungicidal action.

SUMMARY

It is shown that polythiocyanoalkanes (dithiocyanomethane, 1,2-dithiocyanoethane, 1,2,3-trithiocyanopropane) are very effective fungicides and bactericides. Certain alkylisothiocyanosilanes also have appreciable insectofungicidal action.

LITERATURE CITED

[1] M.G. Voronkov and B.N. Dolgov, J. Gen. Chem., 24, 1082 (1954).*

[2] Yu. Lermontova, Ber. 7, 1282 (1874).

[3] Glutz, Lieb. Ann., 153, 313 (1870).

[4] L. Henry, Ber., 2, 637 (1869).

Received March 28, 1956

*Original Russian pagination. See C.B. Translation.

THE ISOLATION OF LAGOCHILIN

M.M. Abramov

Chair of Chemistry, the V.V. Kuibyshev Institute of Soviet Trade, Samarkand

The wild Central Asian plant Lagochilus inebrians (fam. Labiatae) contains in its leaves an active principle, lagochilin, which has powerful general hemostatic action [1].

The lagochilin content of L. inebrians may be up to 3% of the total weight of the air-dry plant mass [2].

Lagochilin consists of snow-white needlelike crystals. It crystallizes from hot water or aqueous alcohol (1 : 1) with one molecule of water. M.p. of the hydrate is 115-116°. Anhydrous lagochilin melts at 154–154.5° It is optically inactive. It is easily soluble in alcohol, pyridine, dioxan and acetone, and with more difficulty in water, chloroform, dichloroethane, and anisole, It dissolves in concentrated acids, and is insoluble in dilute acids, alkalies, ether, carbon tetrachloride, and benzene. From analytical data, the empirical formula of lagochilin is $C_{24}H_{44}O_6$ [3].

Lagochilin was formerly extracted by the method used for isolation of alkaloids [4]. The dried and shredded plant was moistened with ammonia solution and covered with dichloroethane. After prolonged infusion the dichloroethane was decanted off and washed with dilute acid. The acid solution was made alkaline; lagochilin was then extracted with ether from the alkaline solution.

The method described above did not give complete extraction of lagochilin even after repeated treatment of the dichloroethane extract (yield 0.03%). After removal of dichloroethane by distillation and trituration of the residue with 15% hydrochloric acid, followed by addition of alkali to the acid solution, the yield could be raised to 0.5%. However, it was later found that in this method of extraction the concentrated acid caused considerable decomposition of the lagochilin, while if dilute acid was used the yield was considerably reduced.

Because of the high content of lagochilin in the plant (up to 3%) and of its great medicinal value, we sought a simpler and more productive method for isolation of lagochilin, which could be recommended for production purposes. Our searches in this direction proved successful.

We were able to extract up to 3% lagochilin on the weight of the air-dry mass by means of hot extraction with dichloroethane without alkaline or acid treatment of the plant material. The method is essentially as follows. The dried and shredded plant stems and leaves are boiled with dichloroethane for 2-3 hours. The hot extract is decanted from the main residue, filtered to remove suspended particles, and the filtrate is left for 24 hours. The crystalline precipitate is filtered off under suction and washed on the funnel with cold dichloroethane to remove resins and colored impurities. After the washing the residue is almost pure lagochilin. This is then purified by crystallization from hot water or 50% aqueous alcohol. In the dichloroethane extraction the loss of lagochilin is 0.08%, and in recrystallization from water, 0.066%.

The above method gave a yield of 297 g of lagochilin from 10 kg of the air-dry mass, which is 2.97%.

It was found that a single treatment of the plant material with hot dichloroethane results in complete extraction of lagochilin without any signs of decomposition of the latter. The used dichloroethane can be utilized for three more extractions of fresh portions of plant material without detriment to the lagochilin yield. Twofold recrystallization from hot water, of the lagochlin isolated from dichloroethane, gives a fairly pure product.

SUMMARY

A method has been developed for isolation of lagochilin from the Lagochilus inebrians plant by extraction of the dry plant material with dichloroethane; the distinctive feature of the method is that the air-dry plant leaves and stems are extracted with hot dichloroethane for 3 hours, and the extract is then filtered and cooled; the crystals of lagochilin are then washed with cold dichloroethane to remove impurities and the product is recrystallized from hot water or solvent.

The proposed method is simpler, and gives higher yields of lagochilin (3% on the weight of the dry plant material, as against 0.5% given by the known acid method).

LITERATURE CITED

[1] M.M. Abramov, I.E. Akopov and I.I. Ibragimov, Bull. Exp. Biol. Med. Acad. Med. Sci. USSR, 11, 37 (1953).

[2] M.M. Abramov, Proc. Acad. Sci. Uzbek SSR 10, 25 (1954).

[3] M.M. Abramov, Trans. Uzbek State University, 56, 41 (1955).

[4] M.M. Abramov and G.V. Lazuryevsky, Proc. Acad. Sci. Uzbek SSR 10, 7 (1948).

Received October 26, 1955

PRODUCTION OF ISOQUINOLINE FROM COAL-TAR BASES

M.M. Potashnikov and P.N. Gorelov

Eastern Scientific Research Institute of Coal Chemicals

In the production of quinoline from coal-tar bases [1], an isoquinoline fraction boiling in the 242–245° range can be isolated. Polarographic investigation [2] of this fraction showed that it contains about 35% isoquinoline and 50-55% quinoline. The rest of the isoquinoline fraction consists mainly of quinaldine, which can be easily removed in the form of quinophthalone by condensation with phthalic anhydride.

After removal of quinaldine from the isoquionoline fraction the latter can be regarded as a binary mixture consisting of about 40% isoquinoline and 60% quinoline. Thus, the problem of production of isoquinoline from the isoquinoline fraction essentially reduces to the separation of the binary quinoline – isoquinoline mixture.

Owing to the close similarity of the chemical and physical properties of quinoline and of its isomer, isoquinoline, direct separation of the two either by physical or by chemical methods is practically impossible. Some chemical methods for isolation of isoquinoline from its mixtures with quinoline and quinaldine are described in the literature.

Weissgerber [3] proposed a method for extraction of isoquinoline from the mixed bases, in which its somewhat higher basicity as compared with quinoline and quinaldine is used. In this method the mixture of bases is treated stepwise with small portions of sulfuric acid; isoquinoline is the first to be combined as the sulfate. The isoquinoline sulfate formed after treatment with each portion of sulfuric acid is separated from the rest of the mass and decomposed with alkali, the layer of bases which separates out being fractionated. The precipitation of isoquinoline sulfate is repeated many times, and at each successive step the amounts of the sulfates of other bases in the precipitated isoquinoline sulfate increase. Because of the laborious nature of the process and the negligible yield of isoquinoline, Weissgerber's method has not been adopted in practice.

Tartarini and Samaja [4] described a method for isolation of quinoline in the form of the tetraisoquinoline–nickel thiocyanate complex, $(C_9H_7N)_4 \cdot Ni(CNS)_2$. A test of this method by the present authors failed to confirm that isoquinoline can be separated from quinoline in the form of the tetraisoquinoline – nickel thiocyanate complex. Synthetic quinoline, in which no isoquinoline is present, also forms a complex salt with nickel thiocyanate.

Neither can the rectification method give effective separation of quinoline – isoquinoline mixtures owing to the low relative volatility of the system $\alpha = 1.143$. Since isoquinoline is the higher-boiling component, it should be concentrated in the still residue during rectification. Therefore, to obtain isoquinoline in maximum yield and concentration by rectification, quinoline as the low-boiling component must be distilled off as completely as possible. The following equations [5] were used for the calculations:

$$n = \frac{\log\left[\frac{X_n}{1-X_n} \cdot \frac{1-X_0}{X_0}\right]}{\log \alpha},$$

$$R = \frac{1}{\alpha - 1}\left(\frac{X_n}{X_0} - \alpha \frac{1-X_n}{1-X_0}\right),$$

where n is the minimum number of theoretical plates, R is the minimum reflux ratio, X_n is the concentration of the low-boiling component in the distillate, X_0 is the concentration of the component in the still residue, and α is the relative volatility.

Table 1 contains the values calculated for the minimum number of theoretical plates and minimum reflux ratios for separation of a mixture consisting of 40% isoquinoline and 60% quinoline, to give a still residue containing 95% isoquinoline.

TABLE 1

Calculated Numbers of Theoretical Plates and Reflux Ratios for Separation of Isoquinoline – Quinoline Mixtures

Amount of residue (in % of charge)	Composition of residue (%)		Amount of isoquinoline in residue (as % of the amount in charge)	Minimum	
	isoquinoline	quinoline		theoretical plates	reflux ratio
40	95	5	95	46	120
30	95	5	71	34	111
20	95	5	47	30	97
10	95	5	24	27	86
5	95	5	12	26	82

It follows from the data in Table 1 that separation of quinoline – isoquinoline mixtures requires enormous reflux ratios with a relatively large number of theoretical plates, and consequently rectification must be regarded as ineffective in this case.

For fairly effective separation of quinoline – isoquinoline mixtures use may be made of the different solubilities of their acid sulfates in ethyl alcohol. This was the subject of a special study by the present authors [6], who studied the solubilities of the acid sulfates of quinoline and isoquinoline in ethyl alcohol of different concentrations, and at various temperatures. Results of this work, given in Table 2, show that it is possible to find

TABLE 2

Solubility of Quinoline and Isoquinoline Bisulfates in Ethyl Alcohol

Concentration of alcohol (in vol. %)	Solubilities (in g/100 ml) of the bisulfates of quinoline (A) and isoquinoline (B), and ratios of the solubilities (C) at temperatures (deg)																	
	0			10			20			30			40			50		
	A	B	C	A	B	C	A	B	C	A	B	C	A	B	C	A	B	C
95	4.44	1.61	2.8	5.92	2.31	2.6	10.39	3.18	3.3	16.39	4.44	3.7	17.71	6.38	2.8	25.28	8.42	3.0
90	12.99	4.02	3.2	19.91	6.08	3.3	26.75	8.46	3.1	36.25	11.81	3.1	40.91	16.99	2.5	51.57	22.23	2.3
85	28.35	8.27	3.4	36.72	13.06	2.8	44.01	18.19	2.4	52.15	25.23	2.1	60.50	31.34	1.9	69.29	36.84	1.9
80	36.22	13.11	2.8	43.87	19.24	2.3	51.78	25.83	2.0	59.32	33.03	1.8	66.05	40.97	1.6	79.82	50.35	1.6
75	44.88	20.53	2.2	54.63	29.42	1.9	61.93	35.33	1.8	68.16	—	—	74.73	—	—	81.98	—	—

conditions in which the solubility of quinoline bisulfate is more than three times the solubility of isoquinoline bisulfate. In this case, when equilibrium is reached the bisulfates in the liquid phase will be in 3:1 ratio, while the solid phase will be richer in the less soluble component, isoquinoline bisulfate.

If a mixture contains a% isoquinoline, because of the difference between the solubilities of the acid sulfates it is possible to obtain, in the solid phase, practically pure isoquinoline (as the acid sulfate) in the following yield (as % of the original mixture):

$$B = 100 - (100 - a) \quad 1 + \frac{K_{isoquin.}}{K_{quin.}} ,$$

where $K_{isoquin.}$ and $K_{quin.}$ are the solubilities of isoquinoline and quinoline bisulfates.

It follows from the above expression that if the original mixture contains 40% isoquinoline and if the solubility ratio of the bisulfates is 3:1 it is possible to extract 20% isoquinoline from the mixture, corresponding to 50% of the total amount available. At this solubility ratio of the bisulfates isoquinoline can only be extracted from mixtures containing over 25% isoquinoline.

EXPERIMENTAL

The raw material used for isolation of isoquinoline from coal tar was the isoquinoline fraction obtained in the rectification of heavy bases from coal tar in a semiworks unit.

The isoquinoline fraction had the following characteristics: specific gravity at 20°, 1.080, start of boiling 242.7°, distillation range 50% 243.5°, — 95% 244.7°, isoquinoline content 38.0%.

The freshly distilled isoquinoline fraction was dissolved in 85% methyl alcohol in 1:1 ratio. To the solution 95% sulfuric acid was slowly added in the cold from a separating funnel in the amount necessary to form the acid sulfates. The temperature of the reaction mass was kept at 22-25° during the addition of sulfuric acid. The precipitated bisulfates were filtered off on a Buchner funnel, washed once with a small amount of 85% alcohol, and purified by recrystallization. For this, the bisulfates were transferred from the Buchner funnel into a wide-necked thick-walled Erlenmeyer flask standing in a water bath; 85% ethyl alcohol was introduced into the flask in small portions through a reflux condenser until the precipitate dissolved completely at 65-70°. When the precipitate was dissolved the flask was heated to 70-75° and then cooled slowly on the water bath with gentle stirring. When the temperature in the flask had fallen by 4-5°, 2-3 large crystals of pure isoquinoline bisulfate were introduced into the solution to accelerate crystallization and to prevent supercooling of the solution. Stirring was continued throughout the crystallization period, to prevent the formation of a solid block, undesirable not only because it is difficult to remove from the flask, but also because it retains solvent with impurities, which is hard to remove. The precipitated bisulfate was filtered off on a paper filter in a Buchner funnel. The filtrate was easily and rapidly separated in all cases.

The results of the experiments are given in Table 3.

TABLE 3

Results of Experiments on Extraction of Isoquinoline

Amt. of isoquinoline fraction taken (g)	Isoquinoline content in fraction (%)	Obtained								
		After 1st recrystallization			After 2nd recrystallization			After 3rd recrystallization		
		bases in bisulfate (g)	Yield (%)*	mp of isoquinoline sulfate	bases in bisulfate (g)	Yield (%)*	mp of isoquinoline sulfate	bases in bisulfate (g)	Yield (%)*	mp of isoquinoline sulfate
35.8	38.0	11.8	86.7	175.2—192.6	6.9	50.0	204.9	—	—	—
50.0	38.0	20.0	105.2	168.1—190.0	10.1	53.0	200.0—204.4	—	—	—
10.0	38.0	14.1	92.7	180.0—192.5	6.9	45.1	199.0—203.4	—	—	—
300.0	38.0	114.3	100.0	180.0—190.0	66.3	58.2	196.2—202.0	50.2	44.0	205.5—206.5
100.0	38.0	—	—	181.0—193.5	18.7	49.0	200.0—204.1	16.3	43.0	204.8—206.3
800.0	38.0	—	—	176.0—193.5	155.2	51.0	197.1—203.7	12.2	40.0	204.9—206.9

*On the available isoquinoline in the fraction.

It follows from these results that even after the 2nd recrystallization the isoquinoline bisulfate formed melted at temperatures close to the melting point of pure isoquinoline bisulfate (207-208°). The products obtained by decomposition of this isoquinoline bisulfate contain from 90 to 95% pure isoquinoline.

After the 3rd recrystallization the isoquinoline bisulfate melted over a 1.0-2.0° range at a temperature which differed only slightly from the melting point of pure isoquinoline bisulfate. The bisulfate obtained after the 3rd recrystallization contained from 40 to 44% of the available isoquinoline in the original fraction. Decomposition of the bisulfate after the 3rd recrystallization yielded isoquinoline which, after drying with solid alkali (KOH) and distillation, crystallized in the form of colorless platelets with m.p. 24.0-24.5°.

Polarographic investigation [2] of the product showed that it contains only isoquinoline, other bases being absent. The melting point and the results of polarographic analysis indicate that the product is pure isoquinoline.

SUMMARY

1. A method is proposed for isolation of isoquinoline from the isoquinoline fraction of coal-tar heavy bases; the method depends on the different solubilities of quinoline and isoquinoline bisulfates.

2. A fraction containing 38% isoquinoline yielded, after twofold recrystallization of the bisulfate (without removal of quinaldine), technical isoquinoline in 90-95% concentration in an average yield of 51% on the isoquinoline present in the fraction, while after threefold recrystallization pure isoquinoline was obtained, with m.p. 24.0-24.5° and in 40-44% yield calculated on the isoquinoline present in the original fraction.

LITERATURE CITED

[1] M.M. Potashnikov, Author's Certif. No. 77953 (1949).

[2] T.M. Markacheva and A.G. Stromberg, Factory Labs. 6, 676 (1952).

[3] R. Weissgerber, Ber. 47, 3175 (1914).

[4] G. Tartarini and T. Samaja, Ann. Chim. Appl., 23, 351 (1933).

[5] N.I. Gelperin, Distillation and Rectification (Goskhimizdat, 1947).*

[6] M.M. Potashnikov and P.N. Gorelov, J. Appl. Chem., 30, 3, 482 (1957).**

Received August 29, 1955

*In Russian.

**Original Russian pagination. See C.B. Translation.

CHANGES IN THE COMPOSITION OF ENGINE OILS DURING USE

G.V. Vinogradov, L.Ya. Semechkin and N.T. Pavlovskaya

Considerable progress has been made during the past decade in detailed studies of the chemical composition of high-molecular petroleum products, and especially lubricating oils. The method, proposed by Tarasov as long ago as the 1920's [1], for the use of silica gel for separating aromatic hydrocarbons from naphthenic paraffins has become widely used for lubricating oils as the result of the work of Velikovsky and Boguslavskaya [2]. The investigations of Krein and Borovaya [3] have demonstrated the effectiveness of this method for establishing a relationship between the composition and properties of engine oils. Separation of engine oils into their components by any one method (by means of adsorbents, selective solvents, etc.) is, of course, imperfect and arbitrary. Despite this obvious defect, undoubted interest attaches to comparative studies of changes in the chemical composition of engine oils in course of use.

In this investigation tests were carried out on two samples of MS-14 oil (GOST 1013-49) from best Emba oils, and also SU engine oil (GOST 1707-51) from Balakhany oil. These oils were tested in several engines. A 12-cylinder V-2 Diesel engine of about 500 horse power ran on MS-14 oil for 60 hours without topping up. The test was carried out in bench conditions, and the load on the engine was 85-90% of its maximum power, with a fuel consumption of about 70 kg/hour. In addition, MS-14 oil was used for 50 hours without topping up in a 6-cylinder "Hercules" Diesel engine (model DFXE, 200 horse power) installed in a tractor. The same "Hercules" engine,

TABLE 1

Characteristics of the Original and Used Oils

Oil data	MS-14 oil, 1st sample		MS-14 oil, 2nd sample		SU oil		
	before use	used, from V-2 engine	before use	used, from tractor engine	before use	used, from tractor engine	used, from bus engine
Viscosity at 100° (sst)	15.8	13.9	15.5	—	8.81	9.00	9.50
Viscosity at 50° (sst)	98.5	82.5	91.5	91.7	50.4	52.2	56.6
Flash point, Brekenn (deg)	207	182	203	222	230	222	230
Acid number (in mg KOH per 1 g oil)	0.09	0.30	0.11	0.28	0.11	0.24	0.32
Conradson coke value	0.40	0.56	0.42	0.58	0.72	—	—
Solidification point	—28	—33	—30	—22	—35	—31	—15
Mechanical impurities (%)	Absent	0.150	Absent	0.180	Absent	0.210	5.4
Ash (%)	0.002	0.026	0.003	0.040	0.002	0.086	0.33
Iron content (%)	Absent	0.0032	Absent	0.087	Absent	0.0210	0.112

under the same conditions, ran for 50 hours on SU oil without topping up. Finally, SU oil was used for 60 hours (2000 km) without topping up in a 6-cylinder Mercedes-Benz engine (120 horse power) driving a bus. Brief details of the original and used oils are given in Table 1. It should be noted that the analytical results for the used oils, given in Tables 1 and 2, represent average data for three series of experiments.

TABLE 2

Yields and Characteristics of the Fractions

Characteristics	Density d_{20}^{4}	Refractive index n_D^{20}	Molecular weight	Average number of rings in molecule	Yield in separation on silica gel (%)
MS-14 oil, original					
Naphthenic paraffins	0.8712	1.4865	402	2.6	84.1
Ist aromatic fraction (isooctane)	0.9126	1.5206	394	1.7	7.9
IInd aromatic fraction (benzene)	0.9696	1.5549	524	3.2	6.3
Tars	—	—	—	—	1.2
Used MS-14 oil (from V-2 motor)					
Naphthenic paraffins	0.8729	1.4840	437	2.5	82.5
Ist aromatic fraction (isooctane)	0.9374	1.5226	273	1.5	9.1
IInd aromatic fraction (benzene)	0.9882	1.5590	532	3.4	4.9
Tars	—	—	—	—	2.4
MS-14 oil, original (2nd sample)					
Naphthenic paraffins	—	1.4805	—	—	84.7
Ist aromatic fraction (isooctane)	—	1.5158	—	—	7.1
IInd aromatic fraction (benzene)	—	1.5460	—	—	6.2
Tars	—	—	—	—	1.4
MS-14 oil (2nd sample) from tractor					
Naphthenic paraffins	—	1.4819	—	—	84.6
Ist aromatic fraction (isooctane)	—	1.5210	—	—	5.2
IInd aromatic fraction (benzene)	—	1.5520	—	—	5.3
Tars	—	—	—	—	2.3
Industrial 50 (SU) oil, fresh*					
Naphthenic paraffins	0.8923	1.4821	305	2.2	70.9
Ist aromatic fraction (isooctane)	0.9590	1.5236	332	1.6	12.3
IInd aromatic fraction (benzene)	1.0400	1.5828	417	3.4	12.5
Tars	—	—	—	—	1.3
Used SU oil from tractor ("Hercules" engine)					
Naphthenic paraffins	0.8874	1.4792	392	2.2	77.1
Ist aromatic fraction (isooctane)	0.9451	1.5130	350	1.7	13.0
IInd aromatic fraction (benzene)	0.9698	1.5850	392	3.3	8.0
Tars	—	—	—	—	4.2
Used SU oil from bus ("Mercedes-Benz" engine)					
Naphthenic paraffins	0.8840	1.4828	312	2.3	72.0
Ist aromatic fraction (isooctane)	0.9488	1.5302	—	—	15.5
IInd aromatic fraction (benzene)	—	1.5971	—	—	9.5
Tars	—	—	—	—	2.8

*During separation of the fresh oil on silica gel, intermediate fractions between the naphthenic paraffin and isooctane aromatic fractions (3%) and between the isooctane and benzene aromatic fractions (3.4%) were isolated.

A metal column 2500 mm high was used for separation of the oils into their components. The internal diameter of the column was 25 mm. ASK silica gel was used. The silica gel was washed with water and dried at 150° for 6 hours. The dried adsorbent was poured into the aluminum column in a continuous stream, the column being tapped the whole time. The volume ratio of the silica gel to the oil to be separated was 5:1. 100 g of the oil was diluted with isooctane in 1:6 ratio. The isooctane solution was slowly poured into the silica gel column. After all the solution had been poured in, pure isooctane was poured in, in order to displace the naphthenes. The filtrate was collected in 100 ml portions. Its refractive index was determined and it was tested by the formolite reaction. The appearance of a weak formolite rection corresponded to elution of a low-cyclic, so-called isooctane-aromatic fraction which probably consists of aromatic naphthene hydrocarbons. The elution with isooctane was stopped when pure isooctane began to leave the column. A total of 4 liters of isooctane was used for elution. The aromatic fraction was then displaced with benzene, which was passed through the adsorbent until it ran through pure. The amount of benzene used was about 1.5 liters. Tars were displaced from the adsorbent by alcoholic benzene (with alcohol to benzene in 1:1 ratio). When the filtrate (alcoholic benzene) became colorless, acetone was passed through to displace tars. About 950 ml of alcoholic benzene and 1000 ml of acetone was used for washing the adsorbent.

The yields of the fractions into which the oils were separated, and the characteristics of these fractions, are given in Table 2. It should also be noted that the naphthenic paraffin fractions had a negative formolite reaction and did not contain sulfur compounds.

The group-structural (ring) composition of the fractions was calculated by the method proposed by Hersh et al. [4].

The present investigation has demonstrated for the first time that the chemical group composition of engine oils remains practically unchanged for many hours (up to 60) during use in piston engines. Prolonged trials are necessary, probably lasting about 100 hours without topping up, in order to detect appreciable changes in the chemical composition of the oils and to determine the direction of the processes taking place.

LITERATURE CITED

[1] B.N. Tarasov, Azerbaijan Petroleum Economy 10, 47 (1926).

[2] M.S. Boguslavskaya and A.S. Velikovsky, Petroleum Economy 3, 52 (1947).

[3] S.E. Krein and M.S. Borovaya, Trans. All-Union Sci. Res. Inst. Petroleum IV (State Fuel Tech. Press, 1954) p. 211.

[4] R.E. Hersh et al., J. Inst. Petroleum 36, 324, 624 (1950).

Received March 1, 1956

UTILIZATION OF HIGHER PHENOLS FROM COAL TAR

COMMUNICATION II. INVESTIGATION OF THE ANTISEPTIC PROPERTIES OF HIGHER PHENOLS

M.B. Goftman and G.D. Kharlampovich

The S.M. Kirov Polytechnic Institute of the Urals

It was stated in our previous paper [1] that, according to the literature, higher phenols should have good antiseptic effects. We have now studied the activity of phenols toward domestic fungi.

The reason for this choice was the great importance of the struggle against organisms which attack wood, and which cause damage costing the state many millions of rubles annually.

The most widely used antiseptics include sodium fluoride and coal-tar oils, especially anthracene oil.

Searches for new highly effective antiseptics for impregnation of wood are continuing. Among the most effective new antiseptics which have been proposed are o-phenylphenol, β-naphthol, tetra- and pentachlorophenols, and a number of other phenols and their derivatives [2, 3]. Thus it is seen that investigations of higher phenols for the production of antiseptics are of definite interest, as this source may provide new highly effective antiseptics.

We studied the antiseptic activity of the following phenols: No. 1 phenol, No. 2 o-cresol, No. 3 phenol-cresol fraction, No. 4 xylenol fraction, No. 5 polyalkylphenol fraction, No. 6 β-naphthol, No. 7 p-phenylphenol, No. 8 α-naphthol wastes, No. 9 β-naphthol wastes, No. 10 methylnaphthols, No. 11 dimethylnaphthols, No. 12 methylphenylphenols, No. 13 heavy phenols, and No. 14 pitch phenols (the numbers represent specimen numbers).

The antiseptic activity of most of these had not been studied before.

The experiments were carried out with pure cultures of Coniophora cerebella and Merulius domesticus fungi. These are the commonest and most harmful wood-destroying fungi, which grow rapidly. They are often recommended as standards for tests of this type [4].

The tests were carried out in wide-necked conical flasks 0.75 liter in capacity. Nutrient medium (20 g) consisting of pine sapwood sawdust, oatmeal, and water, in 10 : 5 : (200–300) ratio was put into each flask. The flasks were closed by cotton wool plugs and sterilized by steam three times in an autoclave. The duration of each sterilization was 45 minutes. The sterilized nutrient media were seeded with the fungal cultures. After the whole surface of the nutrient medium became overgrown with the fungal mycelium (20-25 days after infection), pieces of wood impregnated with the antiseptic and control pieces were introduced into the flasks.

Specimens 20 × 20 × 10 mm cut from pine sapwood were taken for the experiments. The specimens were weighed and their moisture contents and dry weights were determined. They were then impregnated with benzene solutions of the antiseptics. The impregnation was performed under vacuum at a residual pressure of 40–50 mm Hg, the vacuum being released and renewed several times during the impregnation. The total impregnation time was 10 minutes. The concentrations of the benzene solutions were 0.5, 1.0, 3.0, 5.0%. The contents of antiseptics in the wood were found by weighing an impregnated specimen dried to constant weight at 105°, and subtraction of the weight of the specimen before impregnation from the result. Before the specimens were put into the flasks they were moistened with boiled distilled water to 20-30% moisture content and sterilized by the light of a quartz lamp for one minute. This sterilization was quite adequate. The control specimens were treated similarly.

Four parallel specimens were used in each experiment. The average results for all the parallel tests are given in the tables.

The wood was kept in the flasks for 60 days, after which the samples were removed, cleaned to remove mycelium and sawdust, dried at 105° to constant weight, and weighed. The growth of mycelium on the specimens was examined at intervals of three or four days. The phenolic products were distilled under vacuum before the impregnation, to remove any oxidation products.

The degree of mycelium growth on the specimens was estimated on the following arbitrary scale: – no growth, +mycelium seen on the specimen, ++mycelium covers 35-45% of the specimen surface, +++mycelium covers over 80% of the surface, ++++completely overgrown, +++++completely overgrown, sporophores appear on the specimen.

In the first series of experiments the antiseptic activity of a number of phenols at a high concentration (2.5% on the weight of dry substance) was investigated. The results are given in Table 1.

It follows from the data in Table 1 that most phenols at 2.5% concentration ensure complete preservation of the wood. Phenol itself is a low-quality antiseptic in this concentration. Although polyalkylphenols prevent the destruction of wood by fungi, they do not prevent the growth of mycelium over the specimens. It is possible that this effect is due to the high vapor pressures of these antiseptics, so that they evaporate from the specimen surface and render it harmless to the fungi. Xylenols, like phenol and polyalkylphenols, also fail to prevent growth. It must be noted that around some of the specimens (Nos 6, 7, 8, 9, 11) the fungal mycelium on the

TABLE 1

Investigation of the Antiseptic Activity of Phenols Used in 2.5% Concentrations (Series I)

Fungus	Specimen No.	Growth (days)					Weight loss (%)	Notes
		+	++	+++	++++	+++++		
Coniophora cerebella	Control	2		5		8	48	Specimen very soft and moist. Disintegrates under pressure
	1	12	28	35	40	50	3—6	Very strong growth, but destruction slight and only on the surface
	4	25	35	45	50		—	Strong growth, but practically no destruction
	5	43	50	55			0.0	Specimen covered with fungus, mycelium easily removed
	6 7 8 11 13 14 (3.5%)	No growth					0.0	
	Pure benzene	2	—	—	—	5	52	Very strong destruction
Merulius domesticus	Control	5	7	9	12	14	35	Specimen soft, easily penetrated by needle
	1	25	36	50	53	60	3	Very strong growth, but destruction only on surface
	4	45	60				0.0	
	5 6 11 13 (3.5%) 14	No growth					0.0	

sawdust surface was subdued in growth, and became dark or even disappeared. The experiments in the series showed that the benzene used as solvent does not influence the results.

We did not consider it necessary to study the antiseptic properties of phenol and xylenols any further. With regard to the other phenols it was decided to test their antiseptic activity at lower concentrations and to determine the optimum conditions for their use.

In the second series of experiments we studied the low-boiling and high-boiling phenols (heavy and pitch phenols, polyalkylphenols, and o-cresol). The results of this series of experiments are given in Table 2.

TABLE 2

Antiseptic Activity of Phenols (Series II)

Fungus	Specimen No.	Concentration of antiseptic (%)	Growth (days)					Weight loss (%)
			+	++	+++	++++	+++++	
Coniophora cerebella	Control	0.0	1	3	5	—	8	49.2
	2*	1.5	14	25	40	50	—	13.5
	3	1.5	30	45	—	50	—	0.0
	5	1.0	20	35	40	—	45	9.3
	14	2.0	20	35	40	—	50	13.0
	13	0.6	9	18	30	—	40	23.0
	13	1.0	9	28	40	60	—	6.0
	13	1.5	No growth					0.0
Merulius domesticus	Control	0.0	3	6	9	12	16	35.0
	2	1.5	18	25	30	40	42	8.5
	3	1.5	30	30	38	43	—	6.0
	13	0.6	9	14	18	30	35	15.8
	13	1.0	30	46	—	52	—	2.0
	14	1.5	20	35	40	56	—	10.3

It follows from the data in Table 2 that o-cresol and the phenol–cresol fraction, like phenol and the xylenol fraction, are unsatisfactory antiseptics. Their critical concentration is over 1.5%. Polyalkylphenols protect wood against destruction fairly well (critical concentration 1-1.5%) but they do not prevent the spread of mycelium over the wood surface, and therefore they cannot be classed with the active antiseptics. Heavy phenols are active at concentrations above 1.0%. A very important fact is that wood specimens containing 1.5% of heavy phenols have no odor and almost no color. Pitch phenols, as expected, proved to be weak antiseptics.

In the third series of experiments naphthols and phenylphenols and their homologs were studied; i.e., the group of phenols which, in our view, should be the most active antiseptics. The results of these experiments are given given in Table 3.

It follows from the data in Table 3 that naphthols and their derivatives are very active antiseptics. Methyl- and dimethylnaphthols, β-naphthol wastes, and p-phenylphenol have especially powerful fungicidal action.

The antiseptic activity of α-naphthol wastes and methylphenylphenols is somewhat lower. In the case of α-naphthol wastes this can be ascribed to a high content of relatively inactive polyalkylphenols, and in the case of methylphenylphenols to an increase of the complexity and weight of the molecule. A similar effect was found by Melnikov, Rakitskaya, and Bekker [5] for ethyl- and butylphenylphenols.

Table 4 gives data on the minimum critical concentrations of the different phenols with respect to Coniophora cerebella fungus.

A very important characteristic of the most active phenols from the antiseptic aspect is their weak odor. This makes it possible to use higher phenols as antiseptics even for wood used for domestic purposes.

*Considerable growth, no destruction.

TABLE 3

Antiseptic Activity of Phenols (Series III)

Fungus	Specimen No.	Concentration of antiseptic (%)	Growth (days)					
			+	++	+++	++++	+++++	
Merulius domesticus	Control	0.0	4	7	9	—	12	43.0
	11	0.6	No growth					0.0
	7	0.6	No growth					0.0
	12	0.6	12	15	18	—	21	13.0
	8	0.6	15	21	27	30	38	6.0
	8	1.5	No growth					0.0
Coniophora cerebella	Control	0.0	—	3	6	—	9	36.5
	7	0.3	4	9	30	41	—	11.2
	7	0.6	No growth					0.0
	7	1.6	No growth					0.0
	8	0.6	12	18	30	50	—	17.5
	8	1.0	No growth					0.0
	6	0.75	No growth					0.0
	Control	0.0	3	—	6	—	9	45.0
	9	0.6	No growth					0.0
	9	4.0						
	10	1.0						
	12	0.6	9	30	39	46	—	14.8
	12	1.0	No growth					0.0
	Control	0.0	5	8	8	—	12	41.0
	11	0.3	8	12	15	21	—	18.6
	11	0.6	No growth					0.0
	11	1.5	No growth					0.0

TABLE 4

Critical Concentrations of Various Phenols with Respect to Coniophora Cerebella Fungus

Phenols	Concentration (% on weight of wood)	Phenols	Concentration (% on weight of wood)
Phenol	2.5	β-Naphthol wastes	0.3—0.6
o-Cresol	1.5	Methylnaphthols	0.3—0.6
β-Naphthol	0.75	Dimethylnaphthols	0.3—0.6
p-Phenylphenol	0.3—0.6	Methylphenylphenols	0.6—1.0
Polyalkylphenol fraction	1.0—1.5	Heavy phenols	1.0—1.5
"Pitch phenols"	0.6—1.0	α-Naphthol wastes	2.0—3.5

LITERATURE CITED

[1] M.B. Goftman and G.D. Kharlampovich, J. Appl. Chem. 30, 3, 463 (1957).*

[2] A.T. Vakin, Trans. Forestry Inst. 6, 401 (1950).

[3] S.N. Gorshin, Trans. Forestry Inst. 6, 401 (1950).

[4] Z.A. Demidova, Trans. Inst. Biology, Ural Branch Acad. Sci. USSR 3, 31 (1949).

[5] N.N. Melnikov, M.S. Rakitskaya and Z.E. Bekker, Proc. Acad. Sci. USSR 31, 125 (1947).

*Original Russian pagination. See C.B. Translation.

Received August 13, 1955

BOOK REVIEW

N.A. TOROPOV, CHEMISTRY OF CEMENTS. Industrial Construction Press, Moscow, 1956, 271 pp. Price 10 r 55 k.

The rapid development of the building materials industry in our country demands an increasingly deep scientific approach to the fundamental principles of the technological processes used for their production. Generalization of scientific data in appropriate monographs compiled at the level of present-day physical chemistry is very valuable. The book "Chemistry of Cements" by N.A. Toropov differs in principle from the "Chemistry of Binding Materials" by V.F. Zhuravlev, published in 1951. The material in N.A. Toropov's book is presented from an entirely different angle, more in accordance with the present status of the physical chemistry of silicates.

The book is divided into 12 chapters, in which the most important advances in cement chemistry are reviewed; in full accord with its practical significance, principal attention is devoted to Portland cement.

N.A. Toropov has drawn extensively on original work by Soviet and foreign scientists, and has devoted most attention to phase equilibria, the kinetics of formation of cement compounds, and crystal chemistry of cement; i.e., to the composition, conditions of formation, and properties of cement materials, which constitute the basis of the modern cement industry. In addition, questions of hydration, plasticization, hydrophobization and a number of other subjects are discussed in the book, and also questions relating to slag and alumina cements.

The scientific editing of the book was done by the well-known specialist in cement technology, M.I. Strelkov.

The book is not without faults. First, it should be pointed out that the title of the book demands the inclusion not only of water-hardened cements, but of air-hardened binding materials. However, even the group of water-hardened cements is not fully represented. The book contains nothing about pozzolana cements, in the development of which an important part was played by the extensive researches of Russian scientists. Nothing is said about high-strength, quick-hardening, and low-expansion cements.

Further, some of the sections are presented in very compressed form. For example, fundamental problems of hardening (the work of Le Chatelier, Michaelis, N.A. Baikov, V.F. Zhuravlev, P.A. Rebinder, and others) should have been discussed more fully. Methods for studying cements are described too briefly. For example, only a few lines are devoted to radioactive tracers, which are becoming increasingly important, while in the discussion of the thermochemical method the available data on the thermodynamics of cement systems are not even mentioned. The solid phase reactions taking place during clinker burning are also presented incompletely.

The size of the section dealing with slag cements is not appropriate to the role of the latter in the cement economy of the USSR (about 35%). The section on corrosion must also be expanded.

Finally, the author's views on the questions discussed are not always clearly expressed.

It follows from the above that the treatment of different questions of cement chemistry in the book is uneven. Therefore the author should be advised not to be content with the extensive work already done, but to revise the book as soon as possible with suitable additions so that, with the most detailed treatment of questions of cement chemistry possible, the book is transformed from a collection of essays on cement chemistry into an exhaustive monograph on the subject.

N.A. Toropov's book is a valuable contribution to our literature on cement chemistry and is of considerable interest to specialists in the fields of silicate chemistry and technology.

P.P. Budnikov and O.P. Mchedlov-Petrosyan

JOURNAL OF APPLIED CHEMISTRY OF THE U.S.S.R. IN ENGLISH TRANSLATION

April, 1957

TABLE OF CONTENTS

(continued on inside back cover)

TABLE OF CONTENTS (continued)